

Changes in temperature also affect SERs. Hypothermia causes increases in latency and decreases in amplitude of cortical and subcortical SERs after all types of stimulation.²⁷³⁻²⁷⁵ Hyperthermia also alters SERs, with increases in temperature leading to decreases in amplitude in SSEPs and loss of SSEPs at 42°C during induced hyperthermia.²⁷⁶

Changes in arterial blood gas tensions can alter SERs, probably in relation to changes in blood flow or oxygen delivery to neural structures.^{277,278} Hypoxia produces SSEP changes (decreased amplitude) similar to the changes seen with ischemia.²⁷⁸ Decreased oxygen delivery associated with anemia during isovolemic hemodilution results in progressive increases in latency of SSEPs and VEPs that become significant at hematocrit values lower than 15%. Changes in amplitude were variable until very low hematocrit values (approximately 7%) were reached, at which point the amplitude of all waveforms decreased.²⁷⁹

Summary

Regardless of the type of intraoperative neurologic monitor, several principles must be observed for neurologic monitoring to provide potential benefit to the patient. First, the pathway at risk during the surgical procedure must be amenable to monitoring. Second, if evidence of injury to the pathway is detected, some intervention must be possible. If changes in the neurologic monitor are detected, and no intervention is possible, although the monitor may be of

prognostic value, it does not have the potential to provide direct benefit to the patient from early detection of impending neurologic injury. Third, the monitor must provide reliable and reproducible data. If the data have a high degree of variability in the absence of clinical interventions, their utility for detecting clinically significant events is limited.

This chapter reviews the most common clinically used intraoperative neurologic monitors. Ideally, clinical studies would provide outcome data on the efficacy of a neurologic monitor in a given procedure to improve neurologic outcome. Although there is a wealth of clinical experience with many of these monitoring modalities, there is little in the way of randomized prospective studies evaluating the efficacy of neurologic monitoring. Based on clinical experience with neurologic monitoring and nonrandomized clinical studies in which neurologic monitoring is used and generally compared with historical controls, practice patterns for use of neurologic monitoring have developed. In certain procedures, neurologic monitoring is recommended and used by most centers; in other procedures, monitoring is used almost routinely in some centers, but not in others; and in some procedures, no clear clinical experience or evidence indicates that monitoring is useful at all (experimental use). Finally, there are procedures in which monitoring is used selectively for patients believed to be at higher-than-usual risk for intraoperative neurologic injury. Table 39.5 provides a summary of current clinical practice.

 Complete references available online at expertconsult.com.

TABLE 39.5 Current Practices in Neurologic Monitoring

Procedure	Monitors	Current Practice
Carotid endarterectomy	Awake patient neurologic examination, EEG, SSEP, TCD	NIH recommends use of one of these four available monitors
	CO	Threshold value not determined, inadequate normative population data
Scoliosis surgical treatment	SSEP	Monitoring recommended and may substitute for wake-up testing
	Wake-up test	Largely abandoned in centers using electrophysiologic monitoring; monitoring is not continuous, and false-negative monitoring patterns reported
	MEP	Increased clinical use now that transcranial electrical stimulation is FDA approved; useful in combination with SSEP
Acoustic neuroma	Facial nerve monitor	Facial nerve monitoring recommended
	BAEP	BAEP showing some clinical evidence of improved outcome in some procedures
Intracranial aneurysm clipping	SSEP, EEG, tcMEP	Used routinely in some centers; limited clinical data on outcome, but appears clinically useful during anterior circulation procedures
Cranial nerve V decompression	BAEP	Used in some centers; reduces hearing loss
Cranial nerve VII decompression	BAEP, facial nerve monitor	Data from small series showing improved hearing preservation
Supratentorial mass lesions	SSEP, tcMEP	Used in some centers in selected high-risk procedures
Infratentorial mass lesions	BAEP, SSEP, tcMEP	BAEP to detect retractor-related cranial nerve VIII injury; SSEP and tcMEP in rare, high-risk lesions adjacent to ascending sensory or descending motor pathways
Decompression of spinal stenosis	SSEP, tcMEP	Used in some centers in high-risk procedures (more often cervical)
Spinal cord trauma	SSEP, MEP	Used in some centers in high-risk procedures
Cardiopulmonary bypass	EEG, TCD, Sjvo ₂ , CO	Used routinely in some centers; actively studied, but no outcome data yet
Aortic coarctation	SSEP	Used routinely in a few centers; no widespread acceptance
Aortic aneurysm repair	SSEP, MEP	Used routinely in a few centers; no widespread acceptance

BAEP, Brainstem auditory-evoked potential; CO, cerebral oximetry; EEG, electroencephalogram; FDA, U.S. Food and Drug Administration; MEP, motor-evoked potential; NIH, National Institutes of Health; Sjvo₂, jugular bulb venous oxygen saturation; SSEP, somatosensory-evoked potential; TCD, transcranial Doppler; tcMEP, transcranial motor-evoked potential.

References

1. Skinner SA, et al. *J Clin Monit Comput*. 2014;28:103. 2014.
2. Martin NA, Doberstein C. *Neurosurg Clin North Am*. 1994;5:607. 1994.
3. Kety SS, Schmidt CF. *Am J Physiol*. 1945;143:53. 1945.
4. Udes R, et al. *J Ultrasound Med*. 2017;36:621. 2017.
5. Bass A, et al. *J Vasc Surg*. 1989;10:549. 1989.
6. Manno EM. *Crit Care Clin*. 1997;79. 199713.
7. White H, Baker A. *Can J Anaesth*. 2002;49:623. 2002.
8. Hongo K, et al. *Neurol Res*. 1995;17:89. 1995.
9. Davie SN, Grocott HP. *Anesthesiology*. 2012;116:834. 2012.
10. Zheng F, et al. *Anesth Analg*. 2013;116:663. 2013.
11. Bickler P, et al. *Anesth Analg*. 2017;124:72–82. 2017.
12. Samra SK, et al. *Anesthesiology*. 2000;93:964. 2000.
13. Rigamonti A, et al. *J Clin Anesth*. 2005;17:426. 2005.
14. Dings J, et al. *Neurosurgery*. 1998;43:1082. 1998, PMID: 9620000.
15. Vajkoczy P, et al. *J Neurosurg*. 2003;98:1227. 2003.
16. Lang EW, et al. *Neurosurg Rev*. 2007;30:99. 2007.
17. Vajkoczy P, et al. *J Neurosurg*. 2000;93:265. 2000.
18. Clark LC. *Trans Am Soc Artif Int Org*. 1956;2:41. 1956.
19. Ngwenya LB, et al. *Respir Care*. 2016;61:1232. 2016.
20. Menzel M, et al. *J Neurosurg Anesthesiol*. 1999;11:240. 1999.
21. Gopinath SP, et al. *Crit Care Med*. 1999;27:2337. 1999.
22. Valadka AB, et al. *Crit Care Med*. 1998;26:1576. 1998.
23. Sarrafzadeh AS, et al. *Acta Neurochir Suppl (Wien)*. 1998;71:186. 1998.
24. Rosenthal G, et al. *Crit Care Med*. 2008;36:1917. 2008.
25. Menzel M, et al. *J Neurosurg*. 1999;91(1). 1999.
26. Menzel M, et al. *J Neurosurg Anesthesiol*. 1999;11:240. 1999.
27. Carney N, et al. *Neurosurgery*. 2017;80(6). 2017.
28. Gloor P, In: Wieser HG, Elger CE, eds. *Presurgical Evaluation of Epileptics*. Berlin: Springer; 1987.
29. Hughes JR. *EEG in clinical practice*. Newton, Mass: Butterworth-Heinemann; 1994. 1994.
30. Vitek JL, et al. *J Neurosurg*. 1998;88:1027.
31. Garonzik IM, et al. *Mov Disord*. 2002;17(suppl 3):S135. 2002.
32. Martin JT, et al. *Anesthesiology*. 1959;20:359. 1959.
33. Sharbrough FW, et al. *Stroke*. 1973;4:674. 1973.
34. Craft RM, et al. *J Neurosurg Anesthesiol*. 1994;6:301. 1994.
35. Spackman TN, et al. *Anesthesiology*. 1987;66:229. 1987.
36. Billard V, et al. *Clin Pharmacol Ther*. 1997;61:45. 1997.
37. Schmidt GN, et al. *Anesthesiology*. 2003;99:1072. 2003.
38. Willmann K, et al. *J Clin Monit Comput*. 2002;17:345. 2002.
39. Drover DR, et al. *Anesthesiology*. 2002;97:82. 2002.
40. Levy WJ. *Anesthesiology*. 1987;66:489. 1987.
41. Grundy BL. *Neurosurgery*. 1982;11:556. 1982.
42. Greenberg RP, Ducker TB. *J Neurosurg*. 1982;56(1). 1982.
43. Cohen AR, et al. *Neurosurgery*. 1981;9:157. 1981.
44. York DH. *Progr Neurobiol*. 1985;25(1). 1985.
45. Bundo M, et al. *Stroke*. 2002;33:61. 2002.
46. Symon L. *Br J Anaesth*. 1985;57:34. 1985.
47. Brainston NM, et al. *J Cereb Blood Flow Metab*. 1984;4:68. 1984.
48. Lopez JR, et al. *J Neurol Neurosurg Psychiatry*. 1999;66:189. 1999.
49. Guerit JM, et al. *Electroencephalogr Clin Neurophysiol*. 1997;104:459. 1997.
50. Chiappa KH, Ropper AH. *N Engl J Med*. 1982;306:1140. 1982.
51. Ganes T. *Electroencephalogr Clin Neurophysiol*. 1980;49:446. 1980.
52. Chiappa KH, Ropper AH. *N Engl J Med*. 1982;306:1140. 1982.
53. Grundy BL, et al. *J Neurosurg*. 1982;57:674. 1982.
54. Raudzens PA, Shetter AG. *J Neurosurg*. 1982;57:341. 1982.
55. Duncan PG, et al. *Can Anaesth Soc J*. 1979;26:492. 1979.
56. Sasaki T, et al. *J Neurosurg*. 2010;112:273. 2010.
57. Levy WJ, et al. *Neurosurgery*. 1984;15:287. 1984.
58. Legatt AD. *J Clin Neurophysiol*. 2002;19:454. 2002.
59. MacDonald DB, et al. *Spine*. 2003;28:194. 2003.
60. Szelényi A, et al. *J Neurosurg*. 2003;99:575. 2003.
61. Meylaerts S, et al. *Ann Surg*. 1999;230:742. 1999.
62. Pelosi L, et al. *Clin Neurophysiol*. 2002;113:1082. 2002.
63. Skinner SA, et al. *J Clin Monit Comp*. 2008;22:131. 2008.
64. Harner SG, et al. *Mayo Clin Proc*. 1987;62:92. 1987.
65. Harper CM, Daube RJ, In: Desmedt JE, ed. *Neuromonitoring in Surgery*. New York: Elsevier Science; 1989:275–297. 1989.
66. Skinner S, et al. *J Clin Neurophysiol*. 2017;34:477. 2017.
67. Freedman WA, et al. *Neurosurgery*. 1991;29:98. 1991.
68. Lokuge K, et al. *Br J Surg*. 2018;105:26. 2018.
69. De Rango P, et al. *Stroke*. 2015;46:3423. 2015.
70. Sundt TW Jr, et al. *Mayo Clin Proc*. 1981;56:533. 1981.
71. Bond R, et al. *Eur J Vasc Endovasc Surg*. 2002;23:117. 2002.
72. Kalkman CJ. *J Cardiothorac Vasc Anesth*. 2004;18:381. 2004.
73. Plestis KA, et al. *J Vasc Surg*. 1997;25:620. 1997.
74. Halsey JH Jr. *Stroke*. 1992;23:1583. 1992.
75. Roseborough GS. *J Cardiothorac Vasc Anesth*. 2004;18:375. 2004.
76. Schneider JR, et al. *J Vasc Surg*. 2002;35:1114. 2002.
77. Woodworth GF, et al. *Neurosurgery*. 2007;61:1170. 2007.
78. Chongruksut W, et al. *Cochrane Database Syst Rev*. 2014;6:CD000190. 2014.
79. Lam AM, et al. *Anesthesiology*. 1991;75(15). 1991.
80. Ackerstaff RG, van de Vlasakker CJ. *J Cardiothorac Vasc Anesth*. 1998;12:341. 1998.
81. AbuRahma AF, et al. *J Vasc Surg*. 2011;54:1502. 2011.
82. Thirumala PD, et al. *Neurol Res*. 2016;38:698. 2016.
83. Ackerstaff RG, et al. *Stroke*. 2000;31:1817. 2000.
84. Ogasawara K, et al. *Stroke*. 2008;39:3088. 2008.
85. Mueller M, et al. *Acta Neurol Scand*. 1998;97:110. 1998.
86. Abbott AL, et al. *Cerebrovasc Dis*. 2007;23:362. 2007.
87. Dunne VG, et al. *J Clin Neurosci*. 2001;8:140. 2001.
88. Spencer MP. *Stroke*. 1997;28:685. 1997.
89. Gaunte ME. *Ann R Coll Surg Engl*. 1998;80:377. 1998.
90. Calderon-Arnulphi M, et al. *J Neurosurg*. 2007;106:283. 2007.
91. Friedland ML, et al. *J Vasc Surg*. 2008;48:601. 2008.
92. Friedman WA, et al. *Neurosurgery*. 1991;29:83. 1991.
93. Mizoi K, Yoshimoto T. *Neurol Med Chir (Tokyo)*. 1991;31:318. 1991.
94. Mizoi K, Yoshimoto T. *Neurosurgery*. 1993;33:434. 1993.
95. Holland NR. *J Clin Neurophysiol*. 1998;15:439. 1998.
96. Schramm J, et al. *Neurol Res*. 1994;16:20. 1994.
97. Wiedemayer H, et al. *J Neurosurg*. 2002;96:255. 2002.
98. Manninen PH, et al. *Can J Anaesth*. 1994;41:92. 1994.
99. Manninen PH, et al. *Can J Anaesth*. 1990;37:S23. 1990.
100. Friedman WA, et al. *Neurosurgery*. 1987;20:678.
101. Little JR, et al. *Neurosurgery*. 1987;20:421. 1987.
102. Sasaki T, et al. *J Neurosurg*. 2007;107:60. 2007.
103. Hemmer LB, et al. *World Neurosurg*. 2014;81:99. 2014.
104. Thomas B, Guo D. *World Neurosurg*. 2017;103:829. 2017.
105. Meng L, et al. *Can J Anaesth*. 2017;64:517. 2017.
106. Stevanovic A, et al. *PLoS One*. 2016;11:e0156448. 2016.
107. West S, et al. *Epileptic Disord*. 2016;18:113. 2016.
108. Ryvlin P, et al. *Lancet Neurol*. 2014;13:1114.
109. Ramnarayan R, Mackenzie I. *Neurol India*. 2006;54:250. 2006.
110. Sindou MP. *Acta Neurochir (Wien)*. 2005;147:1019. 2005.
111. Brock S, et al. *Stereotact Funct Neurosurg*. 2004;82:199. 2004.
112. Sindou M, et al. *Laryngoscope*. 1992;102:678. 1992.
113. Friedman WA, et al. *J Neurosurg*. 1985;62:552. 1985.
114. Thirumala PD, et al. *J Clin Neurophys*. 2011;28:56. 2011.
115. Khrais T, Sanna M. *J Laryngol Otol*. 2006;120:366. 2006.
116. Vivas EX, et al. *Neurosurgery*. 2018;82:E44. 2018.
117. Sala F, et al. *Childs Nerv Syst*. 2015;31:1791. 2015.
118. McCallum JE, Bennett MH. *Surg Forum*. 1975;26:469. 1975.
119. Maccabee PJ, et al. *Electroencephalogr Clin Neurophysiol*. 1982;53: P32. 1982.
120. Lueders H, et al. *Spine*. 1982;7:110. 1982.
121. Raudzens PA. *Ann N Y Acad Sci*. 1982;388:308. 1982.
122. Grundy BL, In: Nodar RH, Barber C, eds. *Evoked potentials II*. Boston: Butterworth; 1984:624. 1984.
123. Deutsch H, et al. *J Neurosurg*. 2000;92(suppl 2):155. 2000.
124. Ben-David B, et al. *Spine*. 1987;12:536. 1987.
125. Szilagyi DE, et al. *Surgery*. 1978;83:38. 1978.
126. Edmonds HL, et al. *Spine*. 1989;14:683. 1989.
127. Boyd SG, et al. *J Neurol Neurosurg Psychiatry*. 1986;49:251. 1986.
128. Sloan TB, et al. *Curr Opin Anesthesiol*. 2008;21:560. 2008.
129. Padberg AM, et al. *Spine*. 1998;23:1392. 1998.
130. Schwartz DM, et al. *J Bone Joint Surg Am*. 2007;89:2440. 2007.
131. MacDonald DB, et al. *Spine*. 2003;28:194. 2003.
132. MacDonald DB, et al. *Clin Neurophysiol*. 2013;124:2291. 2013.
133. Elmore JR, et al. *J Vasc Surg*. 1991;14:131. 1991.
134. Reuter DG, et al. *J Thorac Cardiovasc Surg*. 1992;104:262. 1992.
135. Conrad MF, et al. *J Vasc Surg*. 2011;53:1195. 2011.
136. Weigang E, et al. *Ann Thorac Surg*. 2006;82:1679. 2006.
137. Etz CD, et al. *Ann Thorac Surg*. 2006;82:1670. 2006.
138. Skinner SA, Vodusek DB. *J Clin Neurophysiol*. 2014;31:313. 2014.
139. Raynor BL, et al. *Spine*. 2007;32:2673. 2007.
140. Shi YB, et al. *Spine*. 2003;28:595. 2003.
141. Isley MR, et al. *Neurodiagn J*. 2012;52:100. 2012.
142. Shin AY, et al. *J Am Acad Orthop Surg*. 2005;13:382. 2005.

143. Kline DG, et al. *J Neurosurg*. 1998;89(13). 1998.
144. Kim DH, et al. *J Neurosurg*. 2003;98:1005. 2003.
145. Cornelissen L, et al. *Elife*. 2015;23(4):e06513. 2015.
146. Levy WJ. *Anesthesiology*. 1984;60:291. 1984.
147. Levy WJ, et al. *Anesthesiology*. 2003;98:53. 2003.
148. Chabot RJ, et al. *Clin Electroencephalogr*. 1997;28:98. 1997.
149. Edmonds HL Jr, et al. *J Thorac Cardiovasc Surg*. 1992;103:555. 1992.
150. Miller G, et al. *Pediatr Neurol*. 1994;10:124. 1994.
151. Hirsch JC, et al. *Am Thorac Surg*. 2012;94:1365. 2012.
152. Doblar DD. *Semin Cardiothorac Vasc Anesth*. 2004;8:127. 2004.
153. Rodriguez PA, et al. *Stroke*. 2010;41:2229. 2010.
154. Sakamoto T, et al. *J Cardiothorac Vasc Anesth*. 2004;18:293. 2004.
155. Kussman BD, et al. *Anesth Analg*. 2005;101:1294. 2005.
156. Murkin JM, et al. *Anesth Analg*. 2007;104:51. 2007.
157. Zheng F, et al. *Anesth Analg*. 2013;116:663. 2013.
158. Ono M, et al. *Br J Anaesth*. 2012;109:391. 2012.
159. Colak Z, et al. *Eur J Cardiothorac Surg*. 2015;47:447. 2015.
160. Brady K, et al. *Stroke*. 2010;41:1951. 2010.
161. Gopinath SP, et al. *J Neurol Neurosurg Psychiatry*. 1994;57:717. 1994.
162. Fandino J, et al. *J Clin Neurosci*. 2000;7:226. 2000.
163. Cormio M, et al. *J Neurosurg*. 1999;90(9). 1999.
164. Hilkman DM, et al. *Curr Opin Anaesthesiol*. 2017;30:192. 2017.
165. Herman ST, et al. *J Clin Neurophysiol*. 2015;32:87. 2015.
166. Herman ST, et al. *J Clin Neurophysiol*. 2015;32:96. 2015.
167. Cremer OL, et al. *Crit Care Med*. 2005;33:2207. 2005.
168. Stiefel MF, et al. *J Neurosurg*. 2006;105:568.
169. Fortune JB, et al. *J Trauma*. 1995;39:1091. 1995.
170. Skippen P, et al. *Crit Care Med*. 1997;25:1402. 1997.
171. Imberti R, et al. *J Neurosurg*. 2002;96:97. 2002.
172. Coles JP, et al. *Crit Care Med*. 2002;30:1950. 2002.
173. van den Brink WA, et al. *Neurosurgery*. 2000;46:868. 2000.
174. Stiefel MF, et al. *J Neurosurg*. 2005;103:805. 2005.
175. Suarez JI, et al. *Crit Care Med*. 2002;30:1348. 2002.
176. Topcuoglu MA, et al. *Curr Treat Options Cardiovasc Med*. 2002;4:3731. 2002.
177. Jarus-Dziedzic K, et al. *Neurol Res*. 2002;24:5822. 2002.
178. Aaslid R. *Eur J Ultrasound*. 2002;16(3). 2002.
179. Mascia L, et al. *Intensive Care Med*. 2003;29:1088. 2003.
180. Sloan MA, et al. *Neurology*. 1989;39:1514. 1989.
181. Sekhar LN, et al. *Neurosurgery*. 1988;22:813. 1988.
182. Vespa PM, et al. *J Clin Neurophysiol*. 1999;16(1). 1999.
183. Bricolo A, et al. *Electroencephalogr Clin Neurophysiol*. 1978;45:211. 1978.
184. Gutling E, et al. *Neurology*. 1995;45:915. 1995.
185. Alexandre A, et al. *Acta Neurochir Suppl (Wien)*. 1979;28:188. 1979.
186. Bergamasco B, et al. *Electroencephalogr Clin Neurophysiol*. 1968;24:374. 1968.
187. Winer JW, et al. *Neurosurgery*. 1991;29:739. 1991.
188. Koenig MA, Kaplan PW. *J Clin Neurophysiol*. 2015;32:472. 2015.
189. Facco E, et al. *Neurophysiol Clin*. 1993;23:237. 1993.
190. Pohlmann-Eden B, et al. *Intensive Care Med*. 1997;23:301. 1997.
191. Ruiz-Lopez MJ, et al. *Crit Care Med*. 1999;27:412. 1999.
192. Goodwin SR, et al. *Crit Care Med*. 1991;19:518. 1991.
193. Morgalla MH, et al. *Anaesthetist*. 2006;55:760. 2006.
194. Nuwer MR. *Neurosurg Clin North Am*. 1994;5:647. 1994.
195. Lew HL, et al. *J Head Trauma Rehabil*. 2006;21:350. 2006.
196. Carter BG, Butt W. *Crit Care Med*. 2001;29:178. 2001.
197. Carter BG, Butt W. *Intensive Care Med*. 2005;31:765. 2005.
198. Fischer C, Luata J. *Neuropsychol Rehabil*. 2005;15:372. 2005.
199. Petty GW, et al. *Neurology*. 1990;40:300. 1990.
200. Rosen I, Hagerdal M. *Acta Anaesthesiol Scand*. 1976;20:32. 1976.
201. Akeju Oluwaseun, et al. *Clin Neurophysiol*. 2016;127:2414. 2016.
202. McGuire G, et al. *Br J Anaesth*. 2003;91:651. 2003.
203. La Marca S, et al. *Psychopharmacology (Berl)*. 1995;120:426. 1995.
204. Sebel PS, et al. *Anesthesiology*. 1981;55:203. 1981.
205. Hyypponen E, et al. *Acta Anaesthesiol Scand*. 2008;52:289. 2008.
206. Maksimow A, et al. *Acta Anaesthesiol Scand*. 2007;51:22. 2007.
207. Kasuya Y, et al. *Anesth Analg*. 2009;109:2009. 1811.
208. Yamamura T, et al. *Anesth Analg*. 1981;60:283. 1981.
209. Clark DL, et al. *Anesthesiology*. 1973;39:261. 1973.
210. Artru AA, et al. *Anesth Analg*. 1997;85:587. 1997.
211. Komatsu H, et al. *Anesthesiology*. 1994;81:1535. 1994.
212. Jaaskelainen SK, et al. *Neurology*. 2003;61:1073. 2003.
213. Endo T, et al. *J Neurosurg Anesthesiol*. 2002;14:59. 2002.
214. Rampil IJ, et al. *Anesthesiology*. 1991;74:434. 1991.
215. Sharpe MD, et al. *Anesthesiology*. 2002;97:261. 2002.
216. Hoffman WE, Edelman G. *Anesth Analg*. 1995;81:811. 1995.
217. Banoub M, et al. *Anesthesiology*. 2003;99:716. 2003.
218. Peterson DO, et al. *Anesthesiology*. 1986;65:35. 1986.
219. McPherson RW, et al. *Anesthesiology*. 1985;62:626. 1985.
220. Pathak KS, et al. *Anesthesiology*. 1989;70:207. 1989.
221. Samra SK, et al. *Anesthesiology*. 1987;66:29. 1987.
222. Haghghi SS, et al. *J Neurosurg Anesthesiol*. 1996;8:148. 1996.
223. Bernard JM, et al. *Anesthesiology*. 1996;85:1013. 1996.
224. Boisseau N, et al. *Br J Anaesth*. 2002;88:785. 2002.
225. Vaughan DJ, et al. *Br J Anaesth*. 2001;86:59. 2001.
226. Manninen PH, et al. *Anesth Analg*. 1985;64:43. 1985.
227. Thornton C, et al. *Br J Anaesth*. 1983;55:479. 1983.
228. Matsushita S, et al. *J Clin Monit Comput*. 2015;29:621. 2015.
229. Chi OZ, Field C. *Anesthesiology*. 1986;65:328. 1986.
230. Sofrin EM, et al. *J Clin Monit Comput*. 2017.
231. Uribe AA, et al. *Clin Neurophysiol*. 2017;128:2006. 2017.
232. Sebel PS, et al. *Br J Anaesth*. 1984;56:1403. 1984.
233. Liu EH, et al. *Br J Anaesth*. 2005;94:193. 2005.
234. Boisseau N, et al. *Br J Anaesth*. 2002;88:785. 2002.
235. Taniguchi M, et al. *Neurosurgery*. 1992;31:891. 1992.
236. Chassard D, et al. *Br J Anaesth*. 1989;62:522.
237. Purdie JA, Cullen PM. *Anaesthesia*. 1993;48:192. 1993.
238. Drummond JC, et al. *Anesthesiology*. 1985;63:249. 1985.
239. Shimoji K, et al. *Anesthesiology*. 1974;40:234. 1974.
240. Ganes T, Lundar T. *J Neurol Neurosurg Psychiatry*. 1983;46:509. 1983.
241. Sutton LN, et al. *J Neurosurg*. 1982;57:178. 1982.
242. Koht A, et al. *Anesth Analg*. 1988;67:435. 1988.
243. Sloan TB, et al. *Anesth Analg*. 1988;67:582. 1988.
244. Heneghan CPH, et al. *Br J Anaesth*. 1985;57:554. 1985.
245. Doring WH, Daub D. *Arch Otorhinolaryngol*. 1980;227:522. 1980.
246. Grundy BL, et al. *Anesthesiology*. 1979;53:197951.
247. Pathak KS, et al. *Anesth Analg*. 1984;63:833. 1984.
248. Schubert A, et al. *Anesth Analg*. 1986;65:S136. 1986.
249. Grundy BL, Brown RH. *Electroencephalogr Clin Neurophysiol*. 1980;50:177. 1980.
250. Samra SK, et al. *Anesthesiology*. 1984;61:261. 1984.
251. Bala E, et al. *Anesthesiology*. 2008;109:417. 2008.
252. Mahmoud M, et al. *Anesthesiology*. 2010;112:1364. 2010.
253. Zentner J, et al. *Neurosurgery*. 1989;24:253. 1989.
254. Jellinek D, et al. *Neurosurgery*. 1991;29:551. 1991.
255. Taniguchi M, et al. *Neurosurgery*. 1993;33:407. 1993.
256. Ubags LH, et al. *J Neurosurg Anesthesiol*. 1997;9:228. 1997.
257. Kalkman CJ, et al. *Neurosurgery*. 1994;35:1066. 1994.
258. Sloan TB, Heyer EJ. *J Clin Neurophysiol*. 2002;19:430. 2002.
259. Zentner J, et al. *Spine*. 1997;22:1002. 1997.
260. Nathan N, et al. *Br J Anaesth*. 2003;91:493. 2003.
261. Ghaly RF, et al. *Neurol Res*. 2001;23:881. 2001.
262. Scheufler KM, Zentner J. *J Neurosurg*. 2002;96:571.
263. Pechstein U, et al. *Electroencephalogr Clin Neurophysiol*. 1998;108:175. 1998.
264. Pelosi L, et al. *Clin Neurophysiol*. 2001;112:1076. 2001.
265. Ubaga LH, et al. *Neurosurgery*. 1998;43:90. 1998.
266. Stockard JJ, Bickford RG. In: Gordon E, ed. *A Basis and Practice of Neuroanesthesia*. New York: Elsevier; 1981;3. 1981.
267. Kraaijer V, et al. *Electroencephalogr Clin Neurophysiol*. 1988;70:377. 1988.
268. Clowes GHA, et al. *Ann Surg*. 1953;138:558. 1953.
269. Eng DY, et al. *Anesthesiology*. 1980;53:S92. 1980.
270. Kobrine AI, et al. *J Neurol Sci*. 1980;45:65. 1980.
271. Bunegin L, et al. *Anesthesiology*. 1981;55:A232. 1981.
272. Grundy BL, et al. *Anesthesiology*. 1981;54:249. 1981.
273. Russ W, et al. *Anesthesiology*. 1984;61:207. 1984.
274. Stockard JJ, et al. *Ann Neurol*. 1978;3:368. 1978.
275. Spetzler RF, et al. *J Neurosurg*. 1988;68:868. 1988.
276. Dubois M, et al. *Electroencephalogr Clin Neurophysiol*. 1981;52:157. 1981.
277. Nakagawa Y, et al. *Stroke*. 1984;25:275. 1984.
278. Grundy BL, et al. *Anesth Analg*. 1981;60:437. 1981.
279. Nagao S, et al. *J Surg Res*. 1978;25:530. 1978.

References

1. Skinner SA, Cohen BA, Morledge DE. Practice guidelines for the supervising professional. Intraoperative neurophysiological monitoring. *J Clin Monit Comput.* 2014;28:103–111. PMID:24022172.
2. Martin NA, Doberstein C. Cerebral blood flow measurement in neurosurgical intensive care. *Neurosurg Clin North Am.* 1994;5:607–618. PMID:7827473.
3. Kety SS, Schmidt CF. The determination of cerebral blood flow in man by the use of nitrous oxide in low concentrations. *Am J Physiol.* 1945;143:53–66.
4. Udes R, Natarajan P, Thiagarajan K. Transcranial Doppler monitoring in carotid endarterectomy. A systematic review and meta-analysis. *J Ultrasound Med.* 2017;36:621–630. PMID:28127789.
5. Bass A, Krupski WC, Schneider PA, et al. Intraoperative transcranial Doppler. Limitations of the method. *J Vasc Surg.* 1989;10:549–553. PMID:2681842.
6. Manno EM. Transcranial Doppler ultrasonography in the neurocritical care unit. *Crit Care Clin.* 1997;13:79–104. PMID:9012577.
7. White H, Baker A. Continuous jugular venous oximetry in the neurointensive care unit. A brief review. *Can J Anaesth.* 2002;49:623–629. PMID:12067878.
8. Hongo K, Kobayashi S, Okudera H, et al. Noninvasive cerebral optical spectroscopy. Depth-resolved measurements of cerebral haemodynamics using indocyanine green. *Neurol Res.* 1995;17:89–93. PMID:7609855.
9. Davie SN, Grocott HP. Impact of extracranial contamination on regional cerebral oxygen saturation. A comparison of three cerebral oximetry technologies. *Anesthesiology.* 2012;116:834–840. PMID:22343469.
10. Zheng F, Sheinberg R, Yee MS, Ono M, Zheng Y, Hogue CW. Cerebral near-infrared spectroscopy monitoring and neurologic outcomes in adult cardiac surgery patients. A systematic review. *Anesth Analg.* 2013;116:663–676. PMID:23267000.
11. Bickler P, Feiner J, Rollins M, Meng L. Tissue oximetry and clinical outcomes. *Anesth Analg.* 2017;124:72–82. PMID:27308951.
12. Samra SK, Dy EA, Welch K, et al. Evaluation of a cerebral oximeter as a monitor of cerebral ischemia during carotid endarterectomy. *Anesthesiology.* 2000;93:964–970. PMID:11020747.
13. Rigamonti A, Scandroglio M, Minicucci F, et al. A clinical evaluation of near-infrared cerebral oximetry in the awake patient to monitor cerebral perfusion during carotid endarterectomy. *J Clin Anesth.* 2005;17:426–430. PMID:16171662.
14. Dings J, Meixensberger J, Jager A, et al. Clinical experience with 118 brain tissue oxygen partial pressure catheter probes. *Neurosurgery.* 1998;43:1082–1095. PMID:9802852.
15. Vajkoczy P, Horn P, Thome C, et al. Regional cerebral blood flow monitoring in the diagnosis of delayed ischemia following aneurysmal subarachnoid hemorrhage. *J Neurosurg.* 2003;98:1227–1234. PMID:12816269.
16. Lang EW, Mulvey JM, Mudaliar Y, et al. Direct cerebral oxygenation monitoring. A systematic review of recent publications. *Neurosurg Rev.* 2007;30:99–107. PMID:17221264.
17. Vajkoczy P, Roth H, Horn P, et al. Continuous monitoring of regional cerebral blood flow. Experimental and clinical validation of a novel thermal diffusion microprobe. *J Neurosurg.* 2000;93:265–274. PMID:10930012.
18. Clark LC. Monitor and control of blood and tissue oxygen tensions. *Trans Am Soc Artif Int Org.* 1956;2:41–45.
19. Ngwenya LB, Burke JF, Manley GT. Brain tissue oxygen monitoring and the intersection of brain and lung. A comprehensive review. *Respir Care.* 2016;61:1232–1244. PMID:27435860.
20. Menzel M, Doppenberg EM, Zauner A, et al. Cerebral oxygenation in patients after severe head injury. Monitoring and effects of arterial hyperoxia on cerebral blood flow, metabolism and intracranial pressure. *J Neurosurg Anesthesiol.* 1999;11(4):240–251. PMID:28137548.
21. Gopinath SP, Valadka AB, Uzura M, Robertson CS. Comparison of jugular venous oxygen saturation and brain tissue PO_2 as monitors of cerebral ischemia after head injury. *Crit Care Med.* 1999;27:2337–2345. PMID:10579245.
22. Valadka AB, Gopinath SP, Contant CF, et al. Relation of brain tissue PO_2 to outcome after severe head injury. *Crit Care Med.* 1998;26:1576–1581. PMID:18766094.
23. Sarrafzadeh AS, Kiening KL, Bardt TF, et al. Cerebral oxygenation in contused vs. Nonlesioned brain tissue. Monitoring of PtO_2 with Licox and Paratrend. *Acta Neurochir.* 1998;71(suppl):186–189. PMID:9779180.
24. Rosenthal G, Hemphill JC, Sorani M, et al. Brain tissue oxygen tension is more indicative of oxygen diffusion than oxygen delivery and metabolism in patients with traumatic brain injury. *Crit Care Med.* 2008;36:1917–1924. PMID:18496376.
25. Menzel M, Doppenberg EM, Zauner A, et al. Increased inspired oxygen concentration as a factor in improved brain tissue oxygenation and tissue lactate levels after severe human head injury. *J Neurosurg.* 1999;91:1–10. PMID:10389873.
26. Menzel M, Doppenberg EM, Zauner A, et al. Cerebral oxygenation in patients after severe head injury. Monitoring and effects of arterial hyperoxia on cerebral blood flow, metabolism and intracranial pressure. *J Neurosurg Anesthesiol.* 1999;11:240–251. PMID:10527142.
27. Carney N, Totten AM, O'Reilly C, et al. Guidelines for the management of severe traumatic brain injury. 4th ed. *Neurosurgery.* 2017;80:6–15. PMID:27654000.
28. Gloor P. Volume conductor principles. Their application to the surface and depth electroencephalogram. In: Wieser HG, Elger CE, eds. *Presurgical Evaluation of Epileptics.* Berlin: Springer; 1987.
29. Hughes JR. *EEG in Clinical Practice.* 2nd ed. Newton, MA: Butterworth-Heinemann; 1994.
30. Vitek JL, Bakay RAE, Hashimoto T, et al. Microelectrode-guided pallidotomy. Technical approach and its application in medically intractable Parkinson's disease. *J Neurosurg.* 1998;88:1027. PMID:9609298.
31. Garonzik IM, Hua SE, Ohara S, et al. Intraoperative microelectrode and semi-microelectrode recording during the physiological localization of the thalamic nucleus ventral intermediate. *Movement Disord.* 2002;17:S135. PMID:11948768.
32. Martin JT, Faulconer A, Bickford RG. Electroencephalography in anesthesiology. *Anesthesiology.* 1959;20:359. PMID:13650223.
33. Sharbrough FW, Messick JM, Sundt TM. Correlation of continuous electroencephalograms with cerebral blood flow measurements during carotid endarterectomy. *Stroke.* 1973;4:674. PMID:4723697.
34. Craft RM, Losasso TJ, Perkins WJ, et al. EEG monitoring for cerebral ischemia during carotid endarterectomy (CEA). How much is enough? *J Neurosurg Anesthesiol.* 1994;6:301. Abstract oral session, no DOI/PMID.
35. Spackman TN, Faust RJ, Cucchiara RF, et al. A comparison of a periodic analysis of the EEG with standard EEG and cerebral blood flow for detection of ischemia. *Anesthesiology.* 1987;66:229. PMID:3813085.
36. Billard V, Gambus PL, Chamoun N, et al. A comparison of spectral edge, delta power, and bispectral index as EEG measures of alfentanil, propofol, and midazolam drug effect. *Clin Pharmacol Ther.* 1997;61:45. PMID:9024173.
37. Schmidt GN, Bischoff P, Standl T, et al. Narcotrend and bispectral index monitor are superior to classic electroencephalographic parameters for the assessment of anesthetic states during propofol-remifentanil anesthesia. *Anesthesiology.* 2003;99:1072. PMID:1492640.
38. Willmann K, Springman S, Rusy D, et al. A preliminary evaluation of a new derived EEG index monitor in anesthetized patients. *J Clin Monit Comput.* 2002;17:345. PMID:12885178.
39. Drover DR, Lemmens HJ, Pierce ET, et al. Patient state index. titration of delivery and recovery from propofol, alfentanil, and nitrous oxide anesthesia. *Anesthesiology.* 2002;97:82. PMID:12131107.
40. Levy WJ. Effect of epoch length on power spectrum analysis of the EEG. *Anesthesiology.* 1987;66:489. PMID:3565814.
41. Grundy BL. Monitoring of sensory evoked potentials during neurosurgical operation. Methods and applications. *Neurosurgery.* 1982;11:556. PMID:6755296.
42. Greenberg RP, Ducker TB. Evoked potentials in the clinical neurosciences. *J Neurosurg.* 1982;56:1. PMID:7054401.
43. Cohen AR, Young W, Ransohoff J. Intrapinal localization of the somatosensory evoked potential. *Neurosurgery.* 1981;9:157. PMID:7266814.
44. York DH. Somatosensory evoked potentials in man. Differentiation of spinal pathways responsible for conduction from the forelimb vs. hindlimb. *Prog Neurobiol.* 1985;25:1. PMID:3909220.

45. Bundo M, Inao S, Nakamura A, et al. Changes of neural activity correlate with the severity of cortical ischemia in patients with unilateral major cerebral artery occlusion. *Stroke*. 2002;33:61. PMID:11779890.
46. Symon L. Flow thresholds in brain ischaemia and the effects of drugs. *Br J Anaesth*. 1985;57:34. PMID:3881114.
47. Brainston NM, Ladds A, Symon L, et al. Comparison of the effects of ischaemia on early components of the somatosensory evoked potential in brainstem, thalamus, and cerebral cortex. *J Cereb Blood Flow Metab*. 1984;4:68. PMID:6693514.
48. Lopez JR, Chang SD, Steinberg GK. The use of electrophysiological monitoring in the intraoperative management of intracranial aneurysms. *J Neurol Neurosurg Psychiatry*. 1999;66:189. PMID:10071098.
49. Guerit JM, Witdoeck C, de Tourtchaninoff M, et al. Somatosensory evoked potential monitoring in carotid surgery. I. Relationships between qualitative SEP alterations and intraoperative events. *Electroencephalogr Clin Neurophysiol*. 1997;104:459. PMID:9402888.
50. Chiappa KH, Ropper AH. Evoked potentials in clinical medicine. *N Engl J Med*. 1982;306:1205. PMID:6280049.
51. Ganes T. A study of peripheral, cervical, and cortical evoked potentials and afferent conduction times in the somatosensory pathway. *Electroencephalogr Clin Neurophysiol*. 1980;49:446. PMID:6158426.
52. Chiappa KH, Ropper AH. Evoked potentials in clinical medicine. *N Engl J Med*. 1982;306:1140. PMID:7040957.
53. Grundy BL, Jannetta PJ, Procopio PT, et al. Intraoperative monitoring of brain-stem auditory evoked potentials. *J Neurosurg*. 1982;57:674. PMID:7131068.
54. Raudzens PA, Shetter AG. Intraoperative monitoring of brain-stem auditory evoked potentials. *J Neurosurg*. 1982;57:341. PMID:7097329.
55. Duncan PG, Sanders RA, McCollough DW. Preservation of auditory-evoked responses in anaesthetized children. *Can Anaesth Soc J*. 1979;26:492. PMID:526876.
56. Sasaki T, Itakura T, Suzuki K, et al. Intraoperative monitoring of visual evoked potential. Introduction of a clinically useful method. *J Neurosurg*. 2010;112:273–284. PMID:2199497.
57. Levy WJ, York DH, McCaffrey M, et al. Motor evoked potentials from transcranial stimulation of the motor cortex in humans. *Neurosurgery*. 1984;15:287. PMID:6090972.
58. Legatt AD. Current practice of motor evoked potential monitoring. Results of a survey. *J Clin Neurophysiol*. 2002;19:454. PMID:12477990.
59. MacDonald DB, Al Zayed Z, Khoudeir I, et al. Monitoring scoliosis surgery with combined multiple pulse transcranial electric motor and cortical somatosensory-evoked potentials from the lower and upper extremities. *Spine*. 2003;28:194. PMID:12544939.
60. Szelenyi A, Bueno de Camargo A, Flamm E, et al. Neurophysiological criteria for intraoperative prediction of pure motor hemiplegia during aneurysm surgery. Case report. *J Neurosurg*. 2003;99:575. PMID:12959448.
61. Meylaerts S, Jacobs MJ, van Iterson V, et al. Comparison of transcranial motor evoked potentials and somatosensory evoked potentials during thoracoabdominal aortic aneurysm repair. *Ann Surg*. 1999;230:742. PMID:10615928.
62. Pelosi L, Lamb J, Grevitt M, et al. Combined monitoring of motor and somatosensory evoked potentials in orthopaedic spinal surgery. *Clin Neurophysiol*. 2002;113:1082. PMID:12088704.
63. Skinner SA, Transfeldt EE, Savik K. Surface electrodes are not sufficient to detect neurotonic discharges. Observations in a porcine model and clinical review of deltoid electromyographic monitoring using multiple electrodes. *J Clin Monit Comput*. 2008;22:131. PMID:18335318.
64. Harner SG, Daube JR, Beatty CW. Improved preservation of facial nerve function with use of electrical monitoring during removal of acoustic neuromas. *Mayo Clin Proc*. 1987;62:92. PMID:3807440.
65. Harper CM, Daube RJ. Surgical monitoring with evoked potentials. The Mayo Clinic experience. In: Desmedt JE, ed. *Neuromonitoring in Surgery*. New York: Elsevier Science; 1989:275. ISBN. 0444810137.
66. Skinner S, Holdefer R, McAuliffe JJ, Sala F. Medical error avoidance in intraoperative neurophysiological monitoring. The communication imperative. *J Clin Neurophysiol*. 2017;34:477–483. PMID:29023306.
67. Freedman WA, Chadwick GM, Verhoeven JS, et al. Monitoring of somatosensory evoked potentials during surgery of middle cerebral artery aneurysms. *Neurosurgery*. 1991;29:98. PMID:1870692.
68. Lokuge K, de Waard DD, Halliday A, Gray A, Bulbulia R, Mihaylova B. Meta-analysis of the procedural risks of carotid endarterectomy and carotid artery stenting over time. *Br J Surg*. 2018;105:26–36. PMID:29205297.
69. De Rango P, Brown MM, Chaturvedi S, et al. Summary of evidence on early carotid intervention for recently symptomatic stenosis based on meta-analysis of current risks. *Stroke*. 2015;46:3423–3436. PMID:26470773.
70. Sundt TW, Sharbrough FW, Piepgras DG, et al. Correlation of cerebral blood flow and electroencephalographic changes during carotid endarterectomy. With results of surgery and hemodynamics of cerebral ischemia. *Mayo Clin Proc*. 1981;56:533. PMID:7266064.
71. Bond R, Warlow CP, Naylor AR, Rothwell PM. European Carotid Surgery Trialists' Collaborative Group. Variation in surgical and anesthetic technique and associations with operative risk in the European Carotid Surgery Trial. Implications for trials of ancillary techniques. *Eur J Vasc Endovasc Surg*. 2002;23:117–126. PMID:11863328.
72. Kalkman CJ. Con. Routine shunting is not the optimal management of the patient undergoing carotid endarterectomy, but neither is neuromonitoring. *J Cardiothorac Vasc Anesth*. 2004;18:381–383. PMID:15232822.
73. Plestis KA, Loubser P, Mizrahi EM, et al. Continuous electroencephalographic monitoring and selective shunting reduces neurologic morbidity rates in carotid endarterectomy. *J Vasc Surg*. 1997;25:620. PMID:9129616.
74. Halsey JH. Risks and benefits of shunting in carotid endarterectomy. The International Transcranial Doppler Collaborators. *Stroke*. 1992;23:1583–1587. PMID:1440706.
75. Roseborough GS. Pro. Shunting is the optimal management of the patient undergoing carotid endarterectomy. *J Cardiothorac Vasc Anesth*. 2004;18:375–380. PMID:15232821.
76. Schneider JR, Drost JS, Schindler N, et al. Carotid endarterectomy with routine electroencephalography and selective shunting. Influence of contralateral internal carotid artery occlusion and utility in prevention of postoperative strokes. *J Vasc Surg*. 2002;35:1114–1122. PMID:12042721.
77. Woodworth GF, McGirt MJ, Than KD, et al. Selective versus routine intraoperative shunting during carotid endarterectomy. A multivariate outcome analysis. *Neurosurgery*. 2007;61:1170–1177. PMID:18162895.
78. Chongruksut W, Vaniyapong T, Rerkasem K. Routine or selective carotid artery shunting for carotid endarterectomy (and different methods of monitoring in selective shunting). *Cochrane Database Syst Rev*. 2014;6:CD000190. PMID:24956204.
79. Lam AM, Manninen PH, Ferguson GG, et al. Monitoring of electrophysiologic function during carotid endarterectomy. A comparison of somatosensory evoked potentials and conventional electroencephalogram. *Anesthesiology*. 1991;75:15. PMID:2064043.
80. Ackerstaff RG, van de Vlasakker CJ. Monitoring of brain function during carotid endarterectomy. An analysis of contemporary methods. *J Cardiothorac Vasc Anesth*. 1998;12:341. PMID:9636921.
81. AbuRahma AF, Mousa AY, Stone PA. Shunting during carotid endarterectomy. *J Vasc Surg*. 2011;54:1502–1510. PMID:21906905.
82. Thirumala PD, Natarajan P, Thiagarajan K, et al. Diagnostic accuracy of somatosensory evoked potential and electroencephalography during carotid endarterectomy. *Neurol Res*. 2016;38:698–705. PMID:27342607.
83. Ackerstaff RG, Moons KG, van de Vlasakker CJ, et al. Association of intraoperative transcranial Doppler monitoring variables with stroke from carotid endarterectomy. *Stroke*. 2000;31:1817–1823. PMID:10926940.
84. Ogasawara K, Suga Y, Sasaki M, et al. Intraoperative microemboli and low middle cerebral artery blood flow velocity are additive in predicting development of cerebral ischemic events after carotid endarterectomy. *Stroke*. 2008;39:3088–3091. PMID:18688007.
85. Mueller M, Behnke S, Walter P, et al. Microembolic signals and intraoperative stroke in carotid endarterectomy. *Acta Neurol Scand*. 1998;97:110–117. PMID:9517861.
86. Abbott AL, Levi CR, Stork J, et al. Timing of clinically significant microembolism after carotid endarterectomy. *Cerebrovasc Dis*. 2007;23:362–367. PMID:17268167.
87. Dunne VG, Besser M, Ma WJ. Transcranial Doppler in carotid endarterectomy. *J Clin Neurosci*. 2001;14:140–145. PMID:11484664

88. Spencer MP. Transcranial Doppler monitoring and causes of stroke from carotid endarterectomy. *Stroke*. 1997;28:685–691. PMID:9099179.
89. Gaunte ME. Transcranial Doppler. Preventing stroke during carotid endarterectomy. *Ann R Coll Surg Engl*. 1998;80:377–387. PMID:10209403.
90. Calderon-Arnulphi M, Alaraj A, Amin-Janjani S, et al. Detection of cerebral ischemia in neurovascular surgery using quantitative frequency-domain near-infrared spectroscopy. *J Neurosurg*. 2007;106:283–290. PMID:17410713.
91. Friedell ML, Clark JM, Graham DA, et al. Cerebral oximetry does not correlate with electroencephalography and somatosensory evoked potentials in determining the need for shunting during carotid endarterectomy. *J Vasc Surg*. 2008;48:601–606. PMID:18639412.
92. Friedman WA, Chadwick GM, Verhoeven FJ, et al. Monitoring of somatosensory evoked potentials during surgery for middle cerebral artery aneurysms. *Neurosurgery*. 1991;29:83. PMID:1870692.
93. Mizoi K, Yoshimoto T. Intraoperative monitoring of the somatosensory evoked potentials and cerebral blood flow during aneurysm surgery. Safety evaluation for temporary vascular occlusion. *Neur Med Chir (Tokyo)*. 1991;31:318. PMID:1724295.
94. Mizoi K, Yoshimoto T. Permissible temporary occlusion time in aneurysm surgery as evaluated by evoked potential monitoring. *Neurosurgery*. 1993;33:434. PMID:8413875.
95. Holland NR. Subcortical strokes from intracranial aneurysm surgery. Implications for intraoperative neuromonitoring. *J Clin Neurophysiol*. 1998;15:439. PMID:9821071.
96. Schramm J, Zentner J, Pechstein U. Intraoperative SEP monitoring in aneurysm surgery. *Neurol Res*. 1994;16:20. PMID:7913523.
97. Wiedemayer H, Fauser B, Sandalcioglu IE. The impact of neurophysiological intraoperative monitoring on surgical decisions. A critical analysis of 423 cases. *J Neurosurg*. 2002;96:255. PMID:11838799.
98. Manninen PH, Patterson S, Lam AM, et al. Evoked potential monitoring during posterior fossa aneurysm surgery. A comparison of two modalities. *Can J Anaesth*. 1994;41:92. PMID:8131241.
99. Manninen PH, Cuillerier DJ, Gelb AW, et al. Monitoring of brain stem function during posterior fossa surgery. *Can J Anaesth*. 1990;37(4 Pt 2):S23. PMID:2361284.
100. Friedman WA, Kaplan BL, Day AL. Evoked potential monitoring during aneurysm operation. Observations after fifty cases. *Neurosurgery*. 1987;20:678. PMID:3601013.
101. Little JR, Lesser RP, Luders H. Electrophysiological monitoring during basilar aneurysm operation. *Neurosurgery*. 1987;20:421. PMID:3574618.
102. Sasaki T, Kodama N, Matsumoto M, et al. Blood flow disturbance in perforating arteries attributable to aneurysm surgery. *J Neurosurg*. 2007;107:60–67. PMID:17639875.
103. Hemmer LB, Zeeni C, Bebawy JF, et al. The incidence of unacceptable movement with motor evoked potentials during craniotomy for aneurysm clipping. *World Neurosurg*. 2014;81:99–104. PMID:23043993.
104. Thomas B, Guo D. The diagnostic accuracy of evoked potential monitoring techniques during intracranial aneurysm surgery for predicting postoperative ischemic damage. A systematic review and meta-analysis. *World Neurosurg*. 2017;103:829–840. PMID:28433839.
105. Meng L, McDonagh DL, Berger MS, Gelb AW. Anesthesia for awake craniotomy. A how-to guide for the occasional practitioner. *Can J Anaesth*. 2017;64:517–529. PMID:2818184.
106. Stevanovic A, Rossaint R, Veldeman M, Bilotta F, Coburn M. Anesthesia management for awake craniotomy. Systematic review and meta-analysis. *PLoS One*. 2016;11:e0156448. PMID:27228013.
107. West S, Nolan SJ, Newton R. Surgery for epilepsy. A systematic review of current evidence. *Epileptic Disord*. 2016;18:113–121. PMID:27193634.
108. Ryvlin P, Cross JH, Rheims S. Epilepsy surgery in children and adults. *Lancet Neurol*. 2014;13:1114–1126. PMID:25316018.
109. Ramnarayan R, Mackenzie I. Brain-stem auditory evoked responses during microvascular decompression for trigeminal neuralgia. predicting postoperative hearing loss. *Neurol India*. 2006;54:250–254. PMID:16936382.
110. Sindou MP. Microvascular decompression for primary hemifacial spasm. Importance of intraoperative neurophysiological monitoring. *Acta Neurochir (Wien)*. 2005;147:1019–1026. PMID:16094508.
111. Brock S, Scaioli V, Ferroli P, Broggi G. Neurovascular decompression in trigeminal neuralgia. Role of intraoperative neurophysiological monitoring in the learning period. *Stereotact Funct Neurosurg*. 2004;82:199–206. PMID:15583464.
112. Sindou M, Fobé JL, Ciriano D, Fischer C. Hearing prognosis and intraoperative guidance of brainstem auditory evoked potential in microvascular decompression. *Laryngoscope*. 1992;102:678–682. PMID:1602916.
113. Friedman WA, Kaplan BJ, Gravenstein D, Rhonan AL. Intraoperative brain-stem auditory evoked potentials during posterior fossa microvascular decompression. *J Neurosurg*. 1985;62:552–557. PMID:3973725.
114. Thirumala PD, Shah AC, Nikanow TN, et al. Microvascular decompression for hemifacial spasm. evaluating outcome prognosticators including the value of intraoperative lateral spread response monitoring and clinical characteristics in 293 patients. *J Clin Neurophys*. 2011;28:56–66. PMID:21221005.
115. Khrais T, Sanna M. Hearing preservation surgery in vestibular schwannoma. *J Laryngol Otol*. 2006;120:366–370. PMID:16556349.
116. Vivas EX, Carlson ML, Neff BA, et al. Congress of neurological surgeons systematic review and evidence-based guidelines on intraoperative cranial nerve monitoring in vestibular schwannoma surgery. *Neurosurgery*. 2018;82:E44–E46. PMID:29309641.
117. Sala F, Coppola A, Tramontano V. Intraoperative neurophysiology in posterior fossa tumor surgery in children. *Childs Nerv Syst*. 2015;31:1791–1806. PMID:26351231.
118. McCallum JE, Bennett MH. Electrophysiologic monitoring of spinal cord function during intraspinal surgery. *Surg Forum*. 1975;26:469. PMID:1216195.
119. Maccabee PJ, Pinkhasov EI, Tsairis P, et al. Spinal and short latency scalp derived somatosensory evoked potentials during corrective spinal column surgery. *Electroencephalogr Clin Neurophysiol*. 1982;53:32.
120. Luederes H, Gurd A, Hahn J, et al. A new technique for intraoperative monitoring of spinal cord function. Multichannel recording of spinal cord and subcortical evoked potentials. *Spine*. 1982;7:110. PMID:7089686.
121. Raudzens PA. Intraoperative monitoring of evoked potentials. *Ann N Y Acad Sci*. 1982;388:308. PMID:6953874.
122. Grundy BL. Intraoperative monitoring of sensory evoked potentials. In: Nodar RH, Barber C, eds. *Evoked Potentials I*. Boston: Butterworth; 1984:624.
123. Deutsch H, Arginteanu M, Manhart K, et al. Somatosensory evoked potential monitoring in anterior thoracic vertebrectomy. *J Neurosurg*. 2000;92(suppl 2):155–161. PMID:10763685.
124. Ben-David B, Haller G, Taylor P. Anterior spinal fusion complicated by paraplegia. A case report of a false-negative somatosensory-evoked potential. *Spine*. 12:536–539. PMID:3660079.
125. Szilagyi DE, Hageman JH, Smith RF, et al. Spinal cord damage in surgery of the abdominal aorta. *Surgery*. 1978;83:38. PMID:619471.
126. Edmonds HL, MPJ Paloheimo, Backman MH, et al. Transcranial magnetic motor evoked potentials for functional monitoring of motor pathways during scoliosis surgery. *Spine*. 1989;14:683. PMID:2772715.
127. Boyd SG, Rothwell JC, Cowan JMA, et al. A method of monitoring function in corticospinal pathways during scoliosis surgery with a note on motor conduction velocities. *J Neurol Neurosurg Psychiatry*. 1986;49:251. PMID:3958738.
128. Sloan TB, Janik D, Jameson L. Multimodality monitoring of the central nervous system using motor-evoked potentials. *Curr Opin Anesthesiol*. 2008;21:560–564. PMID:18784479.
129. Padberg AM, Wilson-Holden TJ, Lenke LG, Bridwell KH. Somatosensory and motor evoked potential monitoring without a wake-up test during idiopathic scoliosis surgery. An accepted standard of care. *Spine*. 1998;23:1392–1400. PMID:9654631.
130. Schwartz DM, Auerbach JD, Dormans JP, et al. Neurophysiologic detection of impending spinal cord injury during scoliosis surgery. *J Bone Joint Surg Am*. 2007;89:2440–2449. PMID:17974887.
131. MacDonald DB, Al Zayed Z, Khoudeir I, Stigsby B. Monitoring scoliosis surgery with combined multiple pulse transcranial electric motor and cortical somatosensory-evoked potentials from the lower and upper extremities. *Spine*. 2003;28:194–203. PMID:12544939.

132. MacDonald DB, Skinner S, Shils J, Yingling C. Intraoperative motor evoked potential monitoring. A position statement by the American Society of Neurophysiological Monitoring. *Clin Neurophysiol*. 2013;124:2291–2316. PMID:24055297.
133. Elmore JR, Głowiczki P, Harper CM, et al. Failure of motor evoked potentials to predict neurologic outcome in experimental thoracic aortic occlusion. *J Vasc Surg*. 1991;14:131. PMID:1861323.
134. Reuter DG, Tacker WA, Badylyak SF, et al. Correlation of motor-evoked potential response to ischemic spinal cord damage. *J Thorac Cardiovasc Surg*. 1992;104:262. PMID:1495288.
135. Conrad MF, Ergul EA, Patel VI, et al. Evolution of operative strategies in open thoracoabdominal aneurysm repair. *J Vasc Surg*. 2011;53:1195–1201. PMID:21315544.
136. Weigang E, Hartert M, Siegenthaler MP, et al. Perioperative management to improve neurologic outcome in thoracic or thoracoabdominal aortic stent grafting. *Ann Thorac Surg*. 2006;82:1679–1687. PMID:17062227.
137. Etz CD, Halstead JC, Spielvogel D, et al. Thoracic and thoracoabdominal aneurysm repair. Is reimplantation of spinal cord arteries a waste of time. *Ann Thorac Surg*. 2006;82:1670–1677. PMID:17062225.
138. Skinner SA, Vodúšek DB. Intraoperative recording of the bulbocavernosus reflex. *J Clin Neurophysiol*. 2014;31:313–322. PMID:25083842.
139. Raynor BL, Lenke LG, Bridwell KH, et al. Correlation between low triggered electromyographic thresholds and lumbar pedicle screw malposition. Analysis of 4857 screws. *Spine*. 2007;32:2673–2678. PMID:18007243.
140. Shi YB, Binette M, Martin WH, et al. Electrical stimulation for intraoperative evaluation of thoracic pedicle screw placement. *Spine*. 2003;28:595–601. PMID:12642768.
141. Isley MR, Zhang XF, Balzer JR, Leppanen RE. Current trends in pedicle screw stimulation techniques. Lumbosacral, thoracic, and cervical levels. *Neurodiag J*. 2012;52:100–175. PMID:22808751.
142. Shin AY, Spinner RJ, Steinmann SP, Bishop AT. Adult traumatic brachial plexus injuries. *J Am Acad Orthop Surg*. 2005;13:382–396. PMID:16224111.
143. Kline DG, Kim D, Midha R, et al. Management and results of sciatic nerve injuries. A 24-year experience. *J Neurosurg*. 1998;89:13. PMID:9647167.
144. Kim DH, Cho YJ, Tiel RL, et al. Outcomes of surgery in 1019 brachial plexus lesions treated at Louisiana State University Health Sciences Center. *J Neurosurg*. 2003;98:1005. PMID:12744360.
145. Cornelissen L, Kim SE, Purdon PL, Brown EN, Berde CB. Age-dependent electroencephalogram (EEG) patterns during sevoflurane general anesthesia in infants. *Elife*. 2015;4:e06513. PMID:26102526.
146. Levy WJ. Quantitative analysis of EEG changes during hypothermia. *Anesthesiology*. 1984;60:291. PMID:6703384.
147. Levy WJ, Pantin E, Mehta S, et al. Hypothermia and the approximate entropy of the electroencephalogram. *Anesthesiology*. 2003;98:53. PMID:12502979.
148. Chabot RJ, Gugino LD, Aglio LS, et al. QEEG and neuropsychological profiles of patients after undergoing cardiopulmonary bypass surgical procedures. *Clin Electroencephalogr*. 1997;28:98. PMID:9137873.
149. Edmonds HL, Griffiths LK, van der Laken J, et al. Quantitative electroencephalographic monitoring during myocardial revascularization predicts postoperative disorientation and improves outcome. *J Thorac Cardiovasc Surg*. 1992;103:555. PMID:1545555.
150. Miller G, Rodichok LD, Baylen BG. EEG changes during open heart surgery on infants aged 6 months or less. Relationship to early neurologic morbidity. *Pediatr Neurol*. 1994;10:124. PMID:8024660.
151. Hirsch JC, Jacobs ML, Andropoulos D, et al. Protecting the infant brain during cardiac surgery. A systematic review. *Ann Thorac Surg*. 2012;94:1365–1373. PMID:23006704.
152. Doblar DD. Intraoperative transcranial ultrasonic monitoring for cardiac and vascular surgery. *Semin Cardiothorac Vasc Anesth*. 2004;8:127–145. PMID:15247999.
153. Rodriguez PA, Rubens FD, Wozny D, Nathan HJ. Cerebral emboli detected by transcranial Doppler during cardiopulmonary bypass are not correlated with postoperative cognitive deficits. *Stroke*. 2010;41:2229–2235. PMID:20724717.
154. Sakamoto T, Duebener LF, Laussen PC, Jonas RA. Cerebral ischemia caused by obstructed superior vena cava cannula is detected by near-infrared spectroscopy. *J Cardiothorac Vasc Anesth*. 2004;18:293–303. PMID:15232808.
155. Kussman BD, Wypij D, DiNardo JA, et al. An evaluation of bilateral monitoring of cerebral oxygen saturation during pediatric cardiac surgery. *Anesth Analg*. 2005;101:1294–1300. PMID:16243983.
156. Murkin JM, Adams SJ, Novick RJ, et al. Monitoring brain oxygen saturation during coronary bypass surgery. A randomized prospective study. *Anesth Analg*. 2007;104:51–58. PMID:17179242.
157. Zheng F, Sheinberg R, Yee MS, Ono M, Zheng Y, Hogue CW. Cerebral near-infrared spectroscopy monitoring and neurologic outcomes in adult cardiac surgery patients. A systematic review. *Anesth Analg*. 2013;116:663–676. PMID:23267000.
158. Ono M, Joshi B, Brady K, et al. Risks for impaired cerebral autoregulation during cardiopulmonary bypass and postoperative stroke. *Br J Anesth*. 2012;109:391–398. PMID:22661748.
159. Colak Z, Borojevic M, Bogovic A, Ivancan V, Biocina B, Majeric-Kogler V. Influence of intraoperative cerebral oximetry monitoring on neurocognitive function after coronary artery bypass surgery. A randomized prospective study. *Eur J Cardiothorac Surg*. 2015;47:447–454. PMID:24810757.
160. Brady K, Joshi B, Zweifel C, et al. Real-time continuous monitoring of cerebral blood flow autoregulation using near-infrared spectroscopy in patients undergoing cardiopulmonary bypass. *Stroke*. 2010;41:1951–1956. PMID:20651274.
161. Gopinath SP, Robertson CS, Contant CF, et al. Jugular venous desaturation and outcome after head injury. *J Neurol Neurosurg Psychiatry*. 1994;57:717–723. PMID:8006653.
162. Fandino J, Stocker R, Prokop S, et al. Cerebral oxygenation and systemic trauma related factors determining neurological outcome after brain injury. *J Clin Neurosci*. 2000;7:226–233. PMID:10833621.
163. Cormio M, Valadka AB, Robertson CS. Elevated jugular venous oxygen saturation after severe head injury. *J Neurosurg*. 1999;90:9–15. PMID:10413150.
164. Hilkman DM, van Mook WN, van Kranen-Mastenbroek VH. Continuous electroencephalographic-monitoring in the ICU. An overview of current strengths and future challenges. *Curr Opin Anaesthesiol*. 2017;30:192–199. PMID:28151826.
165. Herman ST, Abend NS, Bleck TP, et al. Critical Care Continuous EEG Task Force of the American Clinical Neurophysiology Society. Consensus statement on continuous EEG in critically ill adults and children, Part I. Indications. *J Clin Neurophysiol*. 2015;32:87–95. PMID:25626778.
166. Herman ST, Abend NS, Bleck TP, et al. Critical Care Continuous EEG Task Force of the American Clinical Neurophysiology Society. Consensus statement on continuous EEG in critically ill adults and children, Part II. Personnel, technical specifications, and clinical practice. *J Clin Neurophysiol*. 2015;32:96–108. PMID:25626777.
167. Cremer OL, van Dijk GW, van Wensen E, et al. Effect of intracranial pressure monitoring and targeted intensive care on functional outcome after severe head injury. *Crit Care Med*. 2005;33:2207–2213. PMID:16215372.
168. Stiebel MF, Udoetuk JD, Spiotta AM, et al. Conventional neurocritical care and cerebral oxygenation after traumatic brain injury. *J Neurosurg*. 2006;105:568–575. PMID:17044560.
169. Fortune JB, Feustel PJ, Graca L, et al. Effect of hyperventilation, mannitol, and ventriculostomy drainage on cerebral blood flow after head injury. *J Trauma*. 1995;39:1091. PMID:7500400.
170. Skippen P, Seear M, Poskitt K, et al. Effect of hyperventilation on regional cerebral blood flow in head-injured children. *Crit Care Med*. 1997;25:1402. PMID:9267957.
171. Imberti R, Bellinzona G, Langer M. Cerebral tissue PO₂ and SjVO₂ changes during moderate hyperventilation in patients with severe traumatic brain injury. *J Neurosurg*. 2002;96:97. PMID:11794610.
172. Coles JP, Minhas PS, Fryer TD, et al. Effect of hyperventilation on cerebral blood flow in traumatic head injury. Clinical relevance and monitoring correlates. *Crit Care Med*. 2002;30:1950. PMID:12352026.
173. van den Brink WA, van Santbrink H, Steyerberg EW, et al. Brain oxygen tension in severe head injury. *Neurosurgery*. 2000;46:868–876. PMID:10764260.
174. Stiebel MF, Spiotta A, Gracias VH, et al. Reduced mortality rate in patients with severe traumatic brain injury treated with brain tissue oxygen monitoring. *J Neurosurg*. 2005;103:805–811. PMID:16304983.
175. Suarez JI, Qureshi AI, Yahia AB, et al. Symptomatic vasospasm diagnosis after subarachnoid hemorrhage. Evaluation of transcranial Doppler ultrasound and cerebral angiography as related to compromised vascular distribution. *Crit Care Med*. 2002;30:1348. PMID:12072693.

176. Topcuoglu MA, Pryor JC, Ogilvy CS, et al. Cerebral vasospasm following subarachnoid hemorrhage. *Curr Treat Options Cardiovasc Med*. 2002;4:3731. PMID:12194810.
177. Jarus-Dziedzic K, Juniewicz H, Wronski J, et al. The relation between cerebral blood flow velocities as measured by TCD and the incidence of delayed ischemic deficits. A prospective study after subarachnoid hemorrhage. *Neurol Res*. 2002;24:5822. PMID:12238625.
178. Aaslid R. Transcranial Doppler assessment of cerebral vasospasm. *Eur J Ultrasound*. 2002;16:3. PMID:12470845.
179. Mascia L, Fedorko L, ter Brugge K, et al. The accuracy of transcranial Doppler to detect vasospasm in patients with aneurysmal subarachnoid hemorrhage. *Intensive Care Med*. 2003;29:1088. 12774157.
180. Sloan MA, Haley EC, Kassell NF, et al. Sensitivity and specificity of transcranial Doppler ultrasonography in the diagnosis of vasospasm following subarachnoid hemorrhage. *Neurology*. 1989;39:1514. PMID:2682350.
181. Sekhar LN, Wechsler LR, Yonas H, et al. Value of transcranial Doppler examination in the diagnosis of cerebral vasospasm after subarachnoid hemorrhage. *Neurosurgery*. 1988;22:813. PMID:3288899.
182. Vespa PM, Nenov V, Nuwer MR. Continuous EEG monitoring in the intensive care unit. Early findings and clinical efficacy. *J Clin Neurophysiol*. 1999;16:1–13. 10082088.
183. Bricolo A, Turazzi S, Faccioli F, et al. Clinical application of compressed spectral array in long-term EEG monitoring of comatose patients. *Electroencephalogr Clin Neurophysiol*. 1978;45:211–225. PMID:78831.
184. Gutling E, Gonser A, Imhof HG, Landis T. EEG reactivity in the prognosis of severe head injury. *Neurology*. 1995;45:915–918. PMID:7746406.
185. Alexandre A, Rubini L, Nertempi P, Farinello C. Sleep alterations during post-traumatic coma as a possible predictor of cognitive defects. *Acta Neurochir Suppl (Wien)*. 1979;28:188–192. PMID:225934.
186. Bergamasco B, Bergamini L, Doriguzzi T, Fabiani D. EEG sleep patterns as a prognostic criterion in post-traumatic coma. *Electroencephalogr Clin Neurophysiol*. 1968;24:374–377.
187. Winer JW, Rosenwasser RH, Jimenez F. Electroencephalographic activity and serum and cerebrospinal fluid pentobarbital levels in determining the therapeutic end point during barbiturate coma. *Neurosurgery*. 1991;29:739–741. PMID:1961405.
188. Koenig MA, Kaplan PW. Clinical applications for EPs in the ICU. *J Clin Neurophysiol*. 2015;32:472–480. PMID:26629757.
189. Facco E, Munari M, Baratto F, et al. Multimodality evoked potentials (auditory, somatosensory and motor) in coma. *Neurophysiol Clin*. 1993;23:237–258. PMID:8326933.
190. Pohlmann-Eden B, Dingethal K, Bender HJ, Koelfen W. How reliable is the predictive value of SEP (somatosensory evoked potentials) patterns in severe brain damage with special regard to the bilateral loss of cortical responses? *Intensive Care Med*. 1997;23:301–308. PMID:9083233.
191. Ruiz-Lopez MJ, Martinez de Azagra A, Serrano A, Casado-Flores J. Brain death and evoked potentials in pediatric patients. *Crit Care Med*. 1999;27:412–416. PMID:10075069.
192. Goodwin SR, Friedman WA, Bellefleur M. Is it time to use evoked potentials to predict outcome in comatose children and adults? *Crit Care Med*. 1991;19:518–524. PMID:2019138.
193. Morgalla MH, Bauer J, Ritz R, Tatagiba M. Coma. The prognostic value of evoked potentials in patients after traumatic brain injury. *Anaesthesia*. 2006;55:760–768. PMID:16718461.
194. Nuwer MR. Electroencephalograms and evoked potentials. Monitoring cerebral function in the neurosurgical intensive care unit. *Neurosurg Clin North Am*. 1994;5:647–659. PMID:7827476.
195. Lew HL, Poole JH, Castaneda A, et al. Prognostic value of evoked and event-related potentials in moderate to severe brain injury. *J Head Trauma Rehabil*. 2006;21:350–360. PMID:16915010.
196. Carter BG, Butt W. Review of the use of somatosensory evoked potentials in the prediction of outcome after severe brain injury. *Crit Care Med*. 2001;29:178–186. PMID:11176182.
197. Carter BG, Butt W. Are somatosensory evoked potentials the best predictor of outcome after severe brain injury? A systematic review. *Intensive Care Med*. 2005;31:765–775. PMID:15846481.
198. Fischer C, Luuante J. Evoked potentials for the prediction of vegetative state in the acute stage of coma. *Neuropsychol Rehabil*. 2005;15:372–380. PMID:16350978.
199. Petty GW, Mohr JP, Pedley T, et al. The role of transcranial Doppler in confirming brain death. *Neurology*. 1990;40:300. PMID:2405294.
200. Rosen I, Hagerdal M. Electroencephalographic study of children during ketamine anesthesia. *Acta Anaesthesiol Scand*. 1976;20:32. PMID:1266554.
201. Akeju O, Song AH, Hamilos AE, et al. Electroencephalogram signatures of ketamine-induced unconsciousness. *Clin Neurophysiol*. 2016;127:2414–2422. PMID:27178861.
202. McGuire G, El-Beheiry H, Manninen P, et al. Activation of electrocorticographic activity with remifentanil and alfentanil during neurosurgical excision of epileptogenic focus. *Br J Anaesth*. 2003;91:651–655. PMID:14570785.
203. La Marca S, Lozito RJ, Dunn RW. Cognitive and EEG recovery following bolus intravenous administration of anesthetic agents. *Psychopharmacol (Berl)*. 1995;120:426. PMID:8539323.
204. Sebel PS, Bovill JG, Wauquier A, et al. Effects of high dose fentanyl anesthesia on the electroencephalogram. *Anesthesiology*. 1981;55:203. PMID:7270948.
205. Huupponen E, Maksimow A, Lapinlampi P, et al. Electroencephalogram spindle activity during dexmedetomidine sedation and physiological sleep. *Acta Anaesthesiol Scand*. 2008;52:289–294. PMID:18005372.
206. Maksimow A, Snapir A, Sarkela M, et al. Assessing the depth of dexmedetomidine-induced sedation with electroencephalogram (EEG)-based spectral entropy. *Acta Anaesthesiol Scand*. 2007;51:22–30. PMID:17073855.
207. Kasuya Y, et al. The correlation between bispectral index and observational sedation scale in volunteers sedated with dexmedetomidine and propofol. *Anesth Analg*. 2009;109:1811–1815. PMID:19923507.
208. Yamamura T, Fukuda M, Takeya H, et al. Fast oscillatory EEG activity induced by analgesic concentrations of nitrous oxide in man. *Anesth Analg*. 1981;60:283. PMID:7194592.
209. Clark DL, Hosick EC, Neigh JL. Neural effects of isoflurane (Forane) in man. *Anesthesiology*. 1973;39:261. PMID:4145825.
210. Artru AA, Lam AM, Johnson JO, et al. Intracranial pressure, middle cerebral artery flow velocity, and plasma inorganic fluoride concentrations in neurosurgical patients receiving sevoflurane or isoflurane. *Anesth Analg*. 1997;85:587. PMID:9296414.
211. Komatsu H, Taie S, Endo S, et al. Electrical seizures during sevoflurane anesthesia in two pediatric patients with epilepsy. *Anesthesiology*. 1994;81:1535. PMID:7997923.
212. Jaaskelainen SK, Kaisti K, Suni L, et al. Sevoflurane is epileptogenic in healthy subjects at surgical levels of anesthesia. *Neurology*. 2003;61:1073. PMID:14581667.
213. Endo T, Sato K, Shamoto H, et al. Effects of sevoflurane on electrocorticography in patients with intractable temporal lobe epilepsy. *J Neurosurg Anesthesiol*. 2002;14:59. PMID:11773826.
214. Rampil IJ, Lockhart SH, Eger EI, et al. The electroencephalographic effects of desflurane in humans. *Anesthesiology*. 1991;74:434. PMID:2001021.
215. Sharpe MD, Young GB, Mirsattari S, et al. Prolonged desflurane administration for refractory status epilepticus. *Anesthesiology*. 2002;97:261. PMID:12131129.
216. Hoffman WE, Edelman G. Comparison of isoflurane and desflurane anesthetic depth using burst suppression of the electroencephalogram in neurosurgical patients. *Anesth Analg*. 1995;81:811. PMID:7574015.
217. Banoub M, Tetzlaff JE, Schubert A. Pharmacologic and physiologic influences affecting sensory evoked potentials. *Anesthesiology*. 2003;99:716. PMID:12960558.
218. Peterson DO, Drummond JC, Todd MM. Effects of halothane, enflurane, isoflurane, and nitrous oxide on somatosensory evoked potentials in humans. *Anesthesiology*. 1986;65:35. PMID:3014922.
219. McPherson RW, Mahla M, Johnson R, et al. Effects of enflurane, isoflurane, and nitrous oxide on somatosensory evoked potentials during fentanyl anesthesia. *Anesthesiology*. 1985;62:626. PMID:3994028.
220. Pathak KS, Amadio BS, Scoles PV, et al. Effects of halothane, enflurane, and isoflurane in nitrous oxide on multilevel somatosensory evoked potentials. *Anesthesiology*. 1989;70:207. PMID:2643892.
221. Samra SK, Vanderzant CW, Domer PA, et al. Differential effects of isoflurane on human median nerve somatosensory evoked potentials. *Anesthesiology*. 1987;66:29. PMID:3800031.

222. Haghghi SS, Sirintrapun SJ, Johnson JC, et al. Suppression of spinal and cortical somatosensory evoked potentials by desflurane anesthesia. *J Neurosurg Anesthesiol*. 1996;8:148. PMID:8829563.
223. Bernard JM, Pereon Y, Fayet G, et al. Effects of isoflurane and desflurane on neurogenic motor- and somatosensory-evoked potential monitoring for scoliosis surgery. *Anesthesiology*. 1996;85:1013. PMID:8916817.
224. Boisseau N, Madany M, Staccini P, et al. Comparison of the effects of sevoflurane and propofol on cortical somatosensory evoked potentials. *Br J Anaesth*. 2002;88:785. PMID:12173194.
225. Vaughn DJ, Thornton C, Wright DR, et al. Effects of different concentrations of sevoflurane and desflurane on subcortical somatosensory evoked responses in anaesthetized, non-stimulated patients. *Br J Anaesth*. 2001;86:59. PMID:11575411.
226. Manninen PH, Lam AM, Nicholas JF. The effects of isoflurane-nitrous oxide anesthesia on brainstem auditory evoked potentials in humans. *Anesth Analg*. 1985;64:43. PMID:3966651.
227. Thornton C, Catley DM, Jordan C, et al. Enflurane anaesthesia causes graded changes in the brainstem and early cortical auditory evoked response in man. *Br J Anaesth*. 1983;55:479. PMID:6407493.
228. Matsushita S, Oda S, Otaki K, et al. Change in auditory evoked potential index and bispectral index during induction of anesthesia with anesthetic drugs. *J Clin Monit Comput*. 2015;29:621–626. PMID:25427598.
229. Chi OZ, Field C. Effects of isoflurane on visual evoked potentials in humans. *Anesthesiology*. 1986;65:328. PMID:3752582.
230. Soffin EM, Emerson RG, Cheng J, et al. A pilot study to record visual evoked potentials during prone spine surgery using the SightSaver™ photic visual stimulator. *J Clin Monit Comput*. 2017. PMID:29264762.
231. Uribe AA, Mendel E, Peters ZA, et al. Comparison of visual evoked potential monitoring during spine surgeries under total intravenous anesthesia versus balanced general anesthesia. *Clin Neurophysiol*. 2017;128:2006–2013. PMID:28837906.
232. Sebel PS, Flynn PJ, Ingram DA. Effect of nitrous oxide on visual, auditory, and somatosensory evoked potentials. *Br J Anaesth*. 1984;56:1403. PMID:6498051.
233. Liu EH, Wong HK, Chia CP, et al. Effects of isoflurane and propofol on cortical somatosensory evoked potentials during comparable depth of anaesthesia as guided by bispectral index. *Br J Anaesth*. 2005;94:193–197. PMID:15516356.
234. Boisseau N, Madany M, Staccini P, et al. Comparison of the effects of sevoflurane and propofol on cortical somatosensory evoked potentials. *Br J Anaesth*. 2002;88:785–789. PMID:12173194.
235. Taniguchi M, Nadstawek J, Pechstein U, Schramm J. Total intravenous anesthesia for improvement of intraoperative monitoring of somatosensory evoked potentials during aneurysm surgery. *Neurosurgery*. 1992;31:891–897. PMID:1436413.
236. Chassard D, Joubaud A, Colson A, et al. Auditory evoked potentials during propofol anaesthesia in man. *Br J Anaesth*. 1989;62:522–526. PMID:2786421.
237. Purdie JA, Cullen PM. Brainstem auditory evoked response during propofol anaesthesia in children. *Anaesthesia*. 1993;48:192–195. PMID:8460794.
238. Drummond JC, Todd MM, Sang H. The effect of high dose sodium thiopental on brain stem auditory and median nerve somatosensory evoked responses in humans. *Anesthesiology*. 1985;63:249. PMID:4025886.
239. Shimoji K, Kano T, Nakashima H, et al. The effects of thiamyl sodium on electrical activities of the central and peripheral nervous systems in man. *Anesthesiology*. 1974;40:234. PMID:1962176.
240. Ganes T, Lundar T. The effect of thiopentone on somatosensory evoked responses and EEGs in comatose patients. *J Neurol Neurosurg Psychiatry*. 1983;46:509. PMID:6875584.
241. Sutton LN, Frewen T, Marsh R, et al. The effects of deep barbiturate coma on multimodality evoked potentials. *J Neurosurg*. 1982;57:178. PMID:7086510.
242. Koht A, Schutz W, Schmidt G, et al. Effects of etomidate, midazolam, and thiopental on median nerve somatosensory evoked potentials and the additive effects of fentanyl and nitrous oxide. *Anesth Analg*. 1988;67:435. PMID:3364762.
243. Sloan TB, Ronai AK, Toleikis JR, et al. Improvement of intraoperative somatosensory evoked potentials by etomidate. *Anesth Analg*. 1988;67:582. PMID:3132058.
244. Heneghan CPH, Thornton C, Navaratnarajah M, et al. Effect of etomidate on the auditory evoked response in man. *Br J Anaesth*. 1985;57:554–561. PMID:3890909.
245. Doring WH, Daub D. Akustisch evozierte Hirnstamm und Rindenpotentiale bei sedierung mit diazepam. *Arch Otorhinolaryngol*. 1980;227:522.
246. Grundy BL, Brown RH, Greenbergh BA. Diazepam alters cortical potentials. *Anesthesiology*. 1979;51:538.
247. Pathak KS, Brown RH, Cascorbi HF, et al. Effects of fentanyl and morphine on intraoperative somatosensory cortical-evoked potentials. *Anesth Analg*. 1984;63:833. PMID:6465579.
248. Schubert A, Peterson DO, Drummond JC, et al. The effect of high-dose fentanyl on human median nerve somatosensory evoked responses. *Anesth Analg*. 1986;65:S136. PMID:3829283.
249. Grundy BL, Brown RH. Meperidine enhances somatosensory cortical evoked potentials. *Electroencephalogr Clin Neurophysiol*. 1980;50:177.
250. Samra SK, Lilly DJ, Rush NL, et al. Fentanyl anesthesia and human brain-stem auditory evoked potentials. *Anesthesiology*. 1961;261. PMID:6476433.
251. Bala E, Sessler DI, Nair DR, McLain R, Dalton JE, Farag E. Motor and sensory evoked potentials are well-maintained in patients given dexmedetomidine during spine surgery. *Anesthesiology*. 2008;109:417–425. PMID:18719439.
252. Mahmoud M, Sadhasivam S, Salisbury S, et al. Susceptibility of transcranial electric motor-evoked potentials to varying targeted blood levels of dexmedetomidine during spine surgery. *Anesthesiology*. 2010;112:1364–1373. PMID:20460997.
253. Zentner J, Kiss I, Ebner A. Influence of anesthetics—nitrous oxide in particular—on electromyographic response evoked by transcranial electrical stimulation of the cortex. *Neurosurgery*. 1989;24:253. PMID:2918976.
254. Jellinek D, Jewkes D, Symon L. Noninvasive intraoperative monitoring of motor evoked potentials under propofol anesthesia. Effects of spinal surgery on the amplitude and latency of motor evoked potentials. *Neurosurgery*. 1991;29:551. PMID:1944835.
255. Taniguchi M, Nadstawek J, Langenbach U, et al. Effects of four intravenous anesthetic agents on motor evoked potentials elicited by magnetic transcranial stimulation. *Neurosurgery*. 1993;33:407. PMID:8413871.
256. Ubags LH, Kalkman CJ, Been HD, et al. The use of ketamine or etomidate to supplement sufentanil/N₂O anesthesia does not disrupt monitoring of myogenic transcranial motor evoked responses. *J Neurosurg Anesthesiol*. 1997;9:228. PMID:9239584.
257. Kalkman CJ, Drummond JC, Patel PM, et al. Effects of droperidol, pentobarbital and ketamine on myogenic motor evoked responses in humans. *Neurosurgery*. 1994;35:1066. PMID:7885550.
258. Sloan TB, Heyer EJ. Anesthesia for intraoperative neurophysiologic monitoring of the spinal cord. *J Clin Neurophysiol*. 2002;19:430. PMID:1247988.
259. Zentner J, Thees C, Pechstein U, et al. Influence of nitrous oxide on motor-evoked potentials. *Spine*. 1997;22:1002. PMID:9152450.
260. Nathan N, Tabaraud F, Lacroix F, et al. Influence of propofol concentrations on multipulse transcranial motor evoked potentials. *Br J Anaesth*. 2003;91:493. PMID:14504148.
261. Ghaly RF, Ham JH, Lee JJ. High-dose ketamine hydrochloride maintains somatosensory and magnetic motor evoked potentials in primates. *Neuro Res*. 2001;23:881. PMID:11760882.
262. Scheufler KM, Zentner J. Total intravenous anesthesia for intraoperative monitoring of the motor pathways. An integral view combining clinical and experimental data. *J Neurosurg*. 2002;96:571. PMID:11883843.
263. Pechstein U, Nadstawek J, Zentner J, et al. Isoflurane plus nitrous oxide versus propofol for recording of motor evoked potentials after high frequency repetitive electrical stimulation. *Electroencephalogr Clin Neurophysiol*. 1998;108:175. PMID:9566630.
264. Pelosi L, Stevenson M, Hobbs GJ, et al. Intraoperative motor evoked potentials to transcranial electrical stimulation during two anaesthetic regimens. *Clin Neurophysiol*. 2001;112:1076. PMID:11377268.
265. Ubaga LH, Kalkman CJ, Been HD. Influence of isoflurane on myogenic motor evoked potentials to single and multiple transcranial stimuli during nitrous oxide/opioid anesthesia. *Neurosurgery*. 1998;43:90. PMID:9657194.

266. Stockard JJ, Bickford RG. The neurophysiology of anaesthesia. In: Gordon E, ed. *A Basis and Practice of Neuroanesthesia*. New York: Elsevier; 1981:3.
267. Kraaier V, van Huffelen AC, Wieneke GH. Changes in quantitative EEG and blood flow velocity due to standardized hyperventilation. A model of transient ischaemia in young human subjects. *Electroencephalogr Clin Neurophysiol*. 1988;70:377. PMID:2460311.
268. Clowes GHA, Kretchmer HE, McBurney RW, et al. The electroencephalogram in the evaluation of the effects of anesthetic agents and carbon dioxide accumulation during surgery. *Ann Surg*. 1953;138:558. PMID:13092786.
269. Eng DY, Dong WK, Bledsoe SW, et al. Electrical and pathological correlates of brain hypoxia during hypotension. *Anesthesiology*. 1980;53:S92.
270. Kobrine AI, Evans DE, Rizzoli HV. Relative vulnerability of the brain and spinal cord to ischemia. *J Neurol Sci*. 1980;45:65. PMID:6766991.
271. Bunegin L, Albin MS, Helsel P, et al. Evoked responses during trimethaphan hypotension. *Anesthesiology*. 1981;55:A232.
272. Grundy BL, Nash CL, Brown RH. Arterial pressure manipulation alters spinal cord function during correction of scoliosis. *Anesthesiology*. 1981;54:249. PMID:7469108.
273. Russ W, Kling D, Loesevitz A, et al. Effect of hypothermia on visual evoked potential (VEP) in humans. *Anesthesiology*. 1984;61:207. PMID:6331776.
274. Stockard JJ, Sharbrough FW, Tinker JA. Effects of hypothermia on the human brainstem auditory response. *Ann Neurol*. 1978;3:368. PMID:666280.
275. Spetzler RF, Hadley MN, Rigamonti D, et al. Aneurysms of the basilar artery treated with circulatory arrest, hypothermia, and barbiturate cerebral protection. *J Neurosurg*. 1988;68:868. PMID:3373282.
276. Dubois M, Loppola R, Buchsbaum MS, et al. Somatosensory evoked potentials during whole body hyperthermia in humans. *Electroencephalogr Clin Neurophysiol*. 1981;52:157. PMID:6167425.
277. Nakagawa Y, Ohtsuka T, Tsura M, et al. Effects of mild hypercapnia on somatosensory evoked potentials in experimental cerebral ischemia. *Stroke*. 1984;25:275. PMID:6422587.
278. Grundy BL, Heros RC, Tung AS, et al. Intraoperative hypoxia detected by evoked potential monitoring. *Anesth Analg*. 1981;60:437. PMID:7195166.
279. Nagao S, Roccaforte P, Moody RA. The effects of isovolemic hemodilution and reinfusion of packed erythrocytes on somatosensory and visual evoked potentials. *J Surg Res*. 1978;25:S30. PMID:102873.

EMERY N. BROWN, PATRICK L. PURDON, OLUWASEUN AKEJU, and KEN SOLT

KEY POINTS

- Anesthesiologists rely extensively on physiologic signals and anesthetic dosing strategies to infer and to track states of the brain and central nervous system under general anesthesia.
- Heart rate and systemic arterial blood pressure changes are the principal physiologic signals used to monitor the anesthetic state of patients receiving general anesthesia.
- Use of the neurologic examination during induction of and emergence from general anesthesia can provide information regarding loss and recovery of consciousness.
- Electroencephalogram (EEG)-based indices are used to track the level of unconsciousness of patients receiving general anesthesia. The most commonly used EEG-based indices are the bispectral index (BIS), the Patient Safety Index (PSI), Narcotrend, and Entropy.
- Real-time analysis of the unprocessed EEG and the spectrogram (density spectral array) is a highly informative way to monitor the level of unconsciousness of patients receiving general anesthesia.
- Use of the unprocessed EEG and spectrogram for real-time monitoring of the level of unconsciousness is made possible by the fact that the EEG oscillations of anesthetized patients change systematically with anesthetic dose, with anesthetic class (mechanism of action), and patient age.
- Anesthetic-induced oscillations are one of the primary mechanisms through which these agents induce altered arousal states such as sedation and unconsciousness. Therefore, real-time monitoring of the unprocessed EEG and the spectrogram provide a scientifically based, practical, and patient-specific way to track sedation and unconsciousness in the operating room.
- Normalized symbolic transfer entropy (NSTE) is an approach for quantifying how changes in frontoparietal functional connectivity relate to anesthesia-induced changes in consciousness.
- In the future, closed-loop anesthetic delivery (CLAD) systems may provide highly accurate ways to control states of general anesthesia, medical coma, and sedation.
- Obtaining reliable quantitative markers of nociception is an active area of investigation.

General anesthesia is a drug-induced reversible condition composed of four behavioral and physiologic states: antinociception, unconsciousness, amnesia, immobility; and stability of the physiologic systems, including the autonomic, cardiovascular, respiratory, and thermoregulatory systems.¹⁻³ Continuously monitoring the status of the patient during general anesthesia is crucial for safe and proper delivery of anesthesia care. The physiologic state of the patient under general anesthesia is commonly monitored using the electrocardiogram and an arterial blood pressure cuff, or an arterial catheter, to monitor the cardiovascular system. In more complex cases, a central venous catheter can be used to monitor central venous pressures, and a pulmonary artery catheter can be placed to monitor cardiac output and pressures in the heart and pulmonary circulation. Transesophageal echocardiography can be used intermittently to gain direct visual information about the anatomy and function of the heart. The capnogram provides a continuous readout of the level of expired carbon dioxide and respiration. In intubated patients, more detailed

information about the state of the lungs can be acquired from the pressure and volume tracings on the ventilator. The pulse oximeter estimates the level of hemoglobin saturation in the arterial blood, and the thermometer tracks body temperature. Muscle relaxation, or immobility, is monitored primarily using a train-of-four stimulation device, and more grossly by observing changes in muscle tone or movement.

Monitoring the behavioral states is more challenging. During general anesthesia, amnesia is not monitored directly but implicitly by the extent to which unconsciousness is achieved. If the patient is unconscious and not simply conscious but unresponsive, the patient will likely have amnesia. In this chapter, we discuss approaches for monitoring unconsciousness and analgesia, or more accurately stated antinociception, and each of the three phases of general anesthesia: induction, maintenance, and emergence. This chapter's focus is on physiologic signs and neurologic examination findings, and the electroencephalogram (EEG)-based measures, used to track these states of general anesthesia.

Induction of General Anesthesia

Monitoring of a patient's level of consciousness begins at induction of general anesthesia. Induction is usually achieved by an intravenous bolus dose of a hypnotic drug such as propofol, a barbiturate, ketamine, or etomidate. Unconsciousness usually occurs in 10 to 30 seconds. The brain state of the patient, which in this case is the transition into unconsciousness, is tracked by monitoring the patient's physiologic signs and the EEG-based index.

PHYSIOLOGIC SIGNS OF LOSS OF CONSCIOUSNESS

When a hypnotic drug is administered to induce general anesthesia—usually as an intravenous bolus over a 5- to 10-second period—several physiologic signs are observed. If asked to count backwards from 100, the patient typically does not get beyond 85 to 90. This transition into unconsciousness can be followed easily by asking the patient to perform smooth pursuit of the anesthesiologist's finger.¹ In smooth pursuit, the patient is instructed to move his or her eyes to track the position of the anesthesiologist's finger. As loss of consciousness ensues, the lateral excursions of the eyes during smooth pursuit decrease, nystagmus may appear, blinking increases, and the eyes fix abruptly in the midline. The oculocephalic reflex and the corneal reflex are lost, but the pupillary response to light can remain intact. The patient typically becomes apneic, atonic, and unresponsive at the point when the oculocephalic reflex is lost.

The oculocephalic reflex is assessed by turning the patient's head from side to side, while lifting the eyelids. Before administration of the induction anesthetic, when the reflex is intact in a patient with no neurologic deficits, the eyes move in the direction opposite the motion of the head. When the reflex is lost, the eyes stay fixed in the midline.⁴ The oculocephalic reflex requires the circuits of cranial nerves III, IV, VI, and VIII to be intact. The motor nuclei associated with cranial nerves III and IV are located in the midbrain, whereas the nucleus of cranial nerve VI is located in the pons. The corneal reflex has traditionally been assessed using a wisp of cotton at the corner of the eye to stroke the cornea. An easier way to assess the reflex is to allow a drop of sterile water to fall on the cornea. Using a drop of sterile water may be safer than using the wisp of cotton, because the former is less likely to cause a corneal abrasion. With either approach, the reflex is intact if the eyes blink consensually, is impaired if there is a blink in one eye and not the other, and is absent if there is no blink. The afferent component of the corneal reflex travels to the sensory nucleus of the cranial nerve V through the ophthalmic branch, whereas the efferent component arises from the motor nucleus of the cranial nerve VII. The nuclei for these nerves associated with the oculocephalic reflex and the corneal reflex lie in close proximity to the arousal centers in the midbrain, pons, hypothalamus, and basal forebrain.⁴

Loss of the oculocephalic reflex suggests that the motor nuclei required for eye movements have been affected by the anesthetic. Similarly, loss of the corneal reflex suggests that the nuclei that control sensation and motor responses to sensation on the eyes and the face have also been affected. Because the loss of the oculocephalic and corneal reflexes

occur concomitantly with the loss of responsiveness, the anesthesiologists can also infer that the loss of consciousness is due at least in part to the effects of the anesthetics on the nearby arousal centers.^{1,4,5} Apnea, which commonly occurs on induction of general anesthesia with bolus administration of a hypnotic agent, is most likely due to the inhibitory effects of the anesthetic on the dorsal and ventral respiratory groups in the medulla and pons, respectively.⁶ Atonia can be due to anesthetic action at any one of multiple sites in the motor pathways between the primary motor areas and the spinal cord. The most likely brainstem sites are the pontine and medullary reticular nuclei.²

Loss of the oculocephalic reflex, the corneal reflex, apnea, and atonia occur concomitantly with loss of consciousness on induction of general anesthesia because of the actions of the hypnotic drug in the brainstem after an intravenous bolus. Blood containing the anesthetic reaches the brainstem through the basilar artery, which supplies the posterior cerebral arteries that provide the posterior input to the circle of Willis.⁵ Before terminating in the posterior cerebral arteries, the basilar artery runs on the dorsal surface of the brainstem and gives off multiple penetrating arteries that perfuse the brainstem nuclei with the anesthetic leading to the observed physiological effects.

ELECTROENCEPHALogram-MARKERS OF LOSS OF CONSCIOUSNESS

EEG-based indices are among the most commonly used methods for tracking loss of consciousness induced by general anesthesia.⁷ With induction of general anesthesia, these indices usually change from high values that indicate the awake state to lower values that indicate states of sedation and unconsciousness.

Maintenance of General Anesthesia: Physiologic Signs and the Nociceptive-Medullary-Autonomic Pathway

Despite the many advances in anesthesia care, the physiologic signs of changes in heart rate, arterial blood pressure, and movement are the measurements most commonly used to track the anesthetic state during maintenance of general anesthesia.⁸ When the state of general anesthesia is not adequate for the level of surgical (nociceptive) stimulation, heart rate and arterial blood pressure can increase dramatically. The changes in heart rate and arterial blood pressure that anesthetized patients show in response to a nociceptive stimulus can be explained in terms of the nociceptive-medullary-autonomic (NMA) circuit composed of the spinoreticular tract, the brainstem arousal circuits, and the sympathetic and parasympathetic efferent pathways (Fig. 40.1).^{1,9} It is important to understand how the NMA circuit works because it is the pathway most used by anesthesiologists for monitoring the patient's level of unconsciousness and antinociception. One example is a description of the NMA pathway in a clinical context that is commonly observed in the operating room.

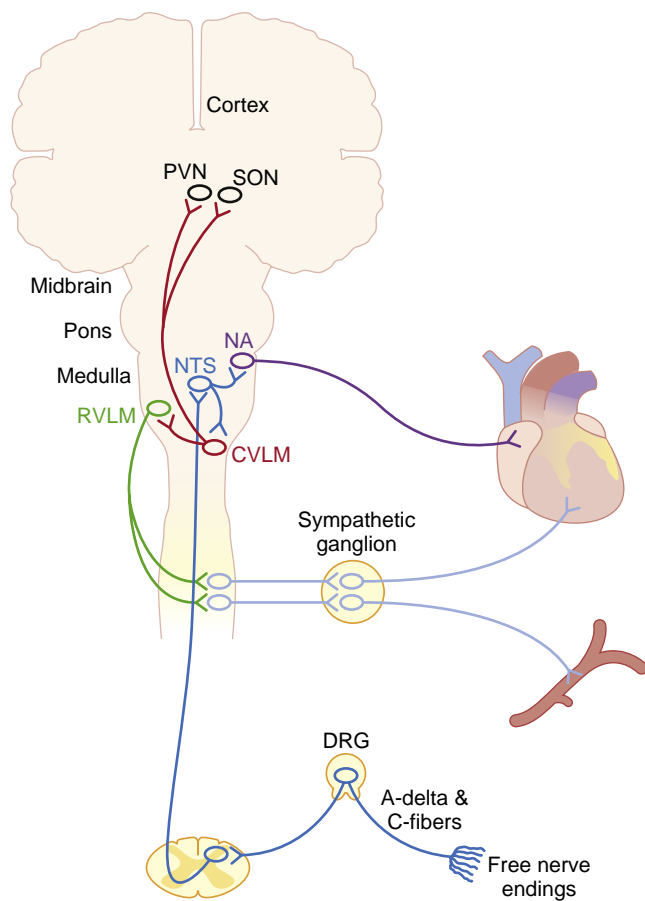


Fig. 40.1 Nociceptive medullary autonomic circuit. The ascending nociceptive (pain) pathway starts with C fibers and A-delta peripheral afferent fibers that synapse on projection neurons (PNs) in the dorsal horn. The PNs cross the midline, course to the brain where they synapse at several targets, including the nucleus of the tractus solitarius (NTS) in the medulla. The NTS mediates the autonomic response to a nociceptive stimulus by increasing sympathetic output through the rostral ventral lateral medulla (RVLM) and the caudal ventral lateral medulla (CVLM), which projects to the thoracolumbar sympathetic ganglia. The ganglia project to peripheral blood vessels and the heart. The nucleus ambiguus (NA) mediates the parasympathetic output to the sinoatrial node of the heart through the vagus nerve. The NTS projects also to the supraoptic nucleus (SON) and periventricular nucleus (PVN) in the hypothalamus. The NMA circuit is the reason why anesthesiologists use increases in blood pressure and heart rate as markers of increases in nociceptive stimulation and, possibly, a level of general anesthesia that is inadequate. DRG, Dorsal root ganglion. (Redrawn from Brown EN, Lydic R, Schiff ND. General anesthesia, sleep, and coma. *N Engl J Med*. 2010;363:2638–2650.)

Suppose that a patient is in a stable state of general anesthesia when, to gain better exposure, the surgeon moves the retractor. Suppose also that this maneuver induces an immediate increase in heart rate and arterial blood pressure. Assuming, that there are no occult hemodynamic or respiratory problems or other common issues that increase heart rate and arterial blood pressure, then these increases likely occurred because the level of general anesthesia did not maintain an adequate level of antinociception. By simultaneously monitoring, in addition, the level of muscle relaxation and oxygen saturation, and oxygen delivery, along with EEG-based indices to track level of unconsciousness, the anesthesia provider can determine that these increases are due to inadequate antinociception and decide to administer more analgesic.

The ascending nociceptive (pain) pathway begins with A-delta and C-fibers whose free nerve endings bring nociceptive information from the periphery to the spinal cord (see Fig. 40.1).¹⁰ In the spinal cord, these fibers synapse in the dorsal horn on projection neurons that travel through the anterolateral fasciculus and synapse at multiple sites in the brainstem, including the nucleus of the tractus solitarius in the medulla.^{1,9} The autonomic response to a nociceptive stimulus is initiated from the nucleus of the tractus solitarius, which mediates sympathetic output through the rostral ventral lateral medulla and the caudal ventral lateral medulla to the heart and peripheral blood vessels through projections to the thoracolumbar sympathetic ganglia.¹ The parasympathetic output from the nucleus of the tractus solitarius is mediated through the nucleus ambiguus, which projects through the vagus nerve to the sinoatrial node of the heart.¹ The nucleus of the tractus solitarius also projects to the periventricular nucleus and supraoptic nucleus in the hypothalamus. Thus the nociceptive stimulus of moving the retractor initiates an increase in sympathetic output and a decrease in parasympathetic output through the NMA circuit that rapidly results in the observed increases in heart rate and arterial blood pressure.

The NMA circuit explains why increases in heart rate and arterial blood pressure are used as a rapid indicator of an inadequate level of antinociception. If unconsciousness is sufficiently well maintained, then no EEG changes will likely be observed. If no acute changes in physiology occur for other reasons, such as bleeding, hypoxemia, disconnection of the breathing circuit, or inadequate dosing of the muscle relaxant, the appropriate treatment is administration of more analgesic medication.

Activity in the NMA circuit can be observed rapidly when a patient is under general anesthesia,¹¹ because this pathway is a fundamental component of the fight-or-flight response.¹² This circuit is used as a sentinel for detecting nociceptive stimuli that can lead to autonomic, stress, and arousal responses. Heart rate and arterial blood pressure changes are the principal markers of activity under general anesthesia because motor responses are often blocked by muscle relaxation. Neurologists frequently test the NMA circuit with nociceptive stimuli, such as total body pinches, nail bed pinches, and sternal rubs, to evaluate the level of arousal of patients with brain injuries that affect the level of consciousness.^{4,13,14}

Other signs of inadequate antinociception are perspiration, tearing, pupil dilation, and return of muscle tone and movement.⁸ Changes in muscle tone and movement are not observed if the patient is receiving a muscle relaxant. The galvanic skin response has also been studied as a potentially more objective measure of antinociception. However, it is not used in clinical practice.¹⁵

Maintenance of General Anesthesia: Electroencephalogram-Based Indices of Level of Consciousness

It is widely recognized that the EEG changes systematically in relation to the dose of anesthetic drug administered (Fig. 40.2).^{1,7,16-18} As a consequence, the unprocessed EEG and

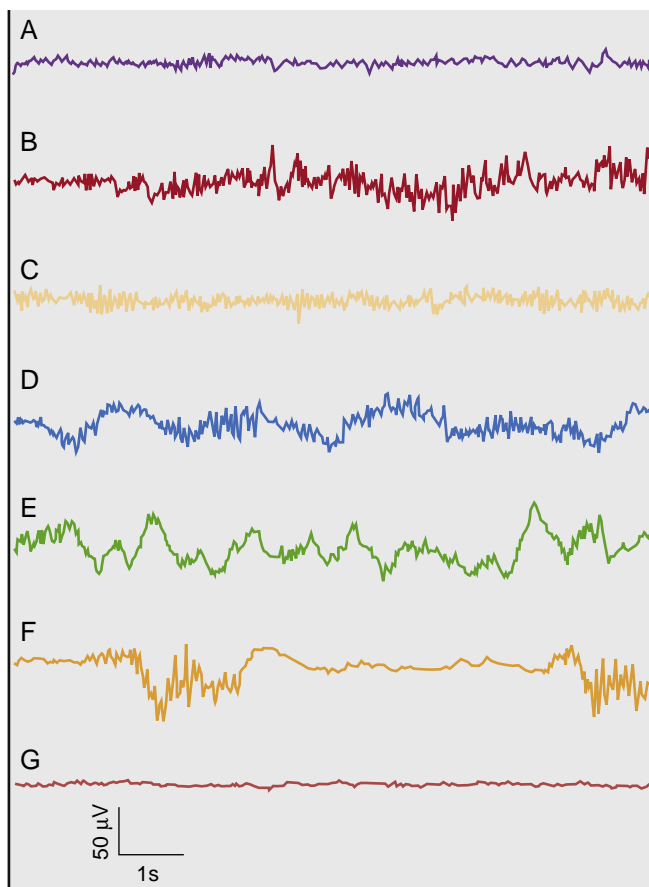


Fig. 40.2 Anesthetic states and electroencephalogram signatures of propofol. (A) Awake electroencephalogram pattern with eyes open. (B) State of paradoxical excitation. (C) Beta (13-25 Hz) oscillations frequently associated with an arousable state of sedation. (D) Slow (0.1-1 Hz), delta (1-4 Hz), and alpha (8-12 Hz) oscillations commonly seen during unconsciousness at surgical planes. (E) Slow oscillations typically recorded during propofol induction and during deep dexmedetomidine sedation (see Fig. 40.8, D). (F) Burst suppression, a state of profound anesthetic-induced brain inactivation, seen commonly in the elderly during normal maintenance, anesthetic-induced coma, and hypothermia. (G) Isoelectric electroencephalogram pattern commonly observed in brief periods during normal maintenance, in anesthetic-induced coma, and profound hypothermia.

various forms of processed EEG have been used to track the level of unconsciousness of patients receiving general anesthesia and sedation. Several EEG-based index systems have been studied and used in clinical practice. These systems process the EEG and provide an index value or set of values in real time or near real time that can be used to track the level consciousness. In general, the indices are designed to decrease with decreasing level of consciousness and increase as consciousness returns. In this way, the anesthesia provider can use these indices along with the physiological signs to track the patient's state of unconsciousness and, to some degree, antinociception. A summary of the EEG-based indices that have received the most use in clinical practice and clinical studies follows.

BISPECTRAL INDEX

The bispectral index (BIS) is an empirically derived scale that was proposed in 1994 by Aspect Medical Systems

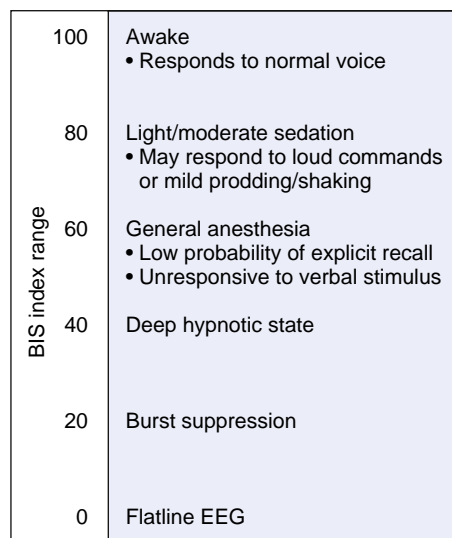


Fig. 40.3 Anesthetic states and the bispectral index (BIS). The chart provides a behavioral interpretation of the values of the BIS. EEG, Electroencephalogram. (Redrawn from Kelley SD. *Monitoring Consciousness: Using the Bispectral Index*. 2nd ed. Boulder, CO: Covidien; 2010.)

(later acquired by Covidien [Boulder, Colorado] and lastly by Medtronic [Minneapolis, Minnesota]) as a novel way to monitor anesthetic state in patients receiving general anesthesia and sedation.^{19,20} The algorithm processes the EEG in near real time and computes an index value between 0 and 100 that indicates the patient's anesthetic state (Fig. 40.3).^{21,22} A value of 100 corresponds to being completely awake, whereas 0 corresponds to a profound state of coma or unconsciousness that is reflected by an isoelectric or flat EEG. The BIS algorithm is proprietary, and the actual computation through which the index is derived is not public knowledge. However, it is known that BIS combines information from three EEG analyses: the spectrogram, the bispectrum, and a time domain assessment of burst suppression.²¹⁻²³ The spectrogram is a decomposition of the EEG into its power content by frequency as a function of time.²¹ The bispectrum measures the degree of nonlinear coupling between pairs of frequencies in the spectrogram.²¹ The BIS algorithm works by measuring specific features of the spectrogram, the bispectrum, and the level of burst suppression, and uses a predetermined weighting scheme to convert these features into the index value. The EEG also undergoes various artifact corrections. Along with the index value, the unprocessed EEG, the spectrogram, and the level of electromyographic activity are displayed on the monitor. Production of the index is computationally intensive, so that there is a 20- to 30-second lag between the time the EEG is observed and the computation of the corresponding BIS value.²⁴ A patient is considered to be appropriately anesthetized (i.e., unconscious) when the value of the BIS is between 40 and 60 (see Fig. 40.3).^{22,25} The EEG is recorded from a four-lead frontal montage.

Since its approval by the US Food and Drug Administration (FDA) in 1996, the BIS monitor has been studied extensively in clinical trials and used widely in anesthesiology practice. The changes in the index are correlated with the level of sedation and unconsciousness (see Fig. 40.3), primarily because for many anesthetics,

the EEG shows lower-frequency, higher-amplitude oscillations as patients achieve deeper states of unconsciousness (see Fig. 40.2). Three exceptions are the anesthetics ketamine, nitrous oxide, and dexmedetomidine. The dissociative anesthetic state produced by ketamine is associated with prominent high-frequency oscillations rather than slow wave oscillations.²⁶ As a consequence, patients can be unconscious with ketamine but have high index values.²⁷

The effect of nitrous oxide on the BIS index is ambiguous. Most recent studies state that nitrous oxide increases the amplitude of high-frequency EEG activity²⁸ and decreases the amplitude of low-frequency EEG activity,²⁹ yet it has little to no effect on the BIS index.^{22,30} However, these studies have not taken into account the state of profound transient large-amplitude slow oscillations, followed by lower amplitude gamma oscillations that have now been documented to be common features observed when nitrous oxide is administered in high-dose (>50%).³¹ In the case of dexmedetomidine, slow oscillations and an appreciable decrease in beta oscillation power^{32,33} are prominent during sedation.³⁴⁻³⁶ These dynamics most likely lead to BIS values that are typically in the unconscious range, even though the patient can be aroused by verbal commands or light shaking.

As we discuss in the “Changes in EEG Signatures with Aging” section, anesthetic-induced EEG oscillations change systematically with age.^{26,37} BIS appears to work poorly in older adults (>60), as patients in this age cohort tend to have lower amplitude oscillations, which the BIS algorithm can interpret as an awake state or state of unconsciousness. Similarly, the BIS algorithm is known to inaccurately reflect the anesthetic state of children because they generally have much more power across a broader range of frequency bands when appropriately anesthetized compared with adults in the 18 to 59 year age range.^{37,38} Hence, even though the children may be well anesthetized, the BIS algorithm provides numbers suggesting a state of sedation rather than unconsciousness.

Use of the BIS monitor has been proposed as a way to prevent intraoperative awareness, which is defined as the patient having explicit recall of events that transpired during the time that he or she was under general anesthesia. Use of the BIS monitor as a way to prevent intraoperative awareness was studied in the B-Aware Trial.³⁹ This study compared patients at high risk for awareness who were randomly assigned to monitoring with BIS using a target range of 40 to 60 and patients monitored with the standard of care at that particular institution. The patients in the BIS group had a significantly lower incidence of awareness.

The findings from this study were called into question because of several design concerns, and for this reason the B-Unaware Trial was conducted.⁴⁰ The B-Unaware Trial was a multicenter investigation that randomly assigned patients to either BIS monitoring or monitoring of the end-tidal anesthetic gas concentration to compare the two approaches for preventing awareness. The end-tidal gas concentration was maintained between 0.7 and 1.3 of the age-adjusted minimum alveolar concentration (MAC) of the anesthetic administered to the patient (discussed under End-Tidal Anesthetic Concentration). As in the

B-Aware Trial, the objective in the BIS-monitored group was maintenance of the BIS value between 40 and 60. This study found no significant difference in the incidence of awareness among the patients monitored with BIS compared with those monitored with the end-tidal gas concentration. The authors interpreted these findings to mean that BIS monitoring was not more effective than the end-tidal anesthetic criterion in preventing awareness in patients receiving general anesthesia using volatile anesthetics. Several concerns were expressed about the findings of this study as well. The most notable were subject selection and whether the study had sufficient power to detect actual differences, had they been present.^{41,42}

As a follow-up to this study, the investigators in the B-Unaware Trail conducted the BIS or Anesthetic Gas to Reduce Explicit Recall (BAG-RECALL) trial, a second trial investigating whether BIS was superior to the end-tidal anesthetic gas concentration in preventing intraoperative awareness in a larger group of patients at high risk for awareness.⁴¹ In this trial, the investigators found that the BIS-guided protocol was not superior to the end-tidal anesthetic concentration-guided protocol in preventing awareness. Because the B-Unaware trial and the BAG-RECALL trial used inhaled anesthetics as the primary agents, their conclusions do not apply to patients receiving total intravenous anesthesia.

Preventing awareness under general anesthesia is a solvable problem if strategies used to monitor the brain states of patients use markers that relate directly rather than indirectly to the mechanisms through which the anesthetics act at specific receptors and neural circuits to alter level of arousal.^{1,43,44} Unlike the current EEG-based indices, these markers will differ with patient age and different anesthetics, (See the Unprocessed EEG and the Spectrogram section).

PATIENT SAFETY INDEX

The Patient Safety Index (PSI) is like the BIS index—a proprietary algorithm that assesses anesthetic state based on the EEG for patients receiving general anesthesia or sedation. The PSI was approved by the FDA in 2000 and was originally developed by Physiometrix (North Billerica, Massachusetts), and was ultimately acquired by Masimo (Irvine, California). The development of the PSI was the outgrowth of several years of research conducted by E. Roy John at the Brain Research Laboratory at the New York University School of Medicine.⁴⁵ Like the BIS index, the PSI is also scaled between 0 and 100 (Fig. 40.4). However, the PSI range to ensure that the patient is unconscious is between 25 and 50.⁴⁶

The original formulation of the PSI used an electrode montage that included occipital and frontal EEG leads to monitor the phenomenon of anteriorization as a marker of change in anesthetic state. Anteriorization is the forward shift of spectral power from the occipital area to the frontal area during loss of consciousness and the posterior shift of this power from the frontal areas to the occipital areas during the return of consciousness.^{44,47-49} The current formulation of the PSI uses a four-lead frontal EEG montage. In addition to displaying the PSI, this monitor also shows

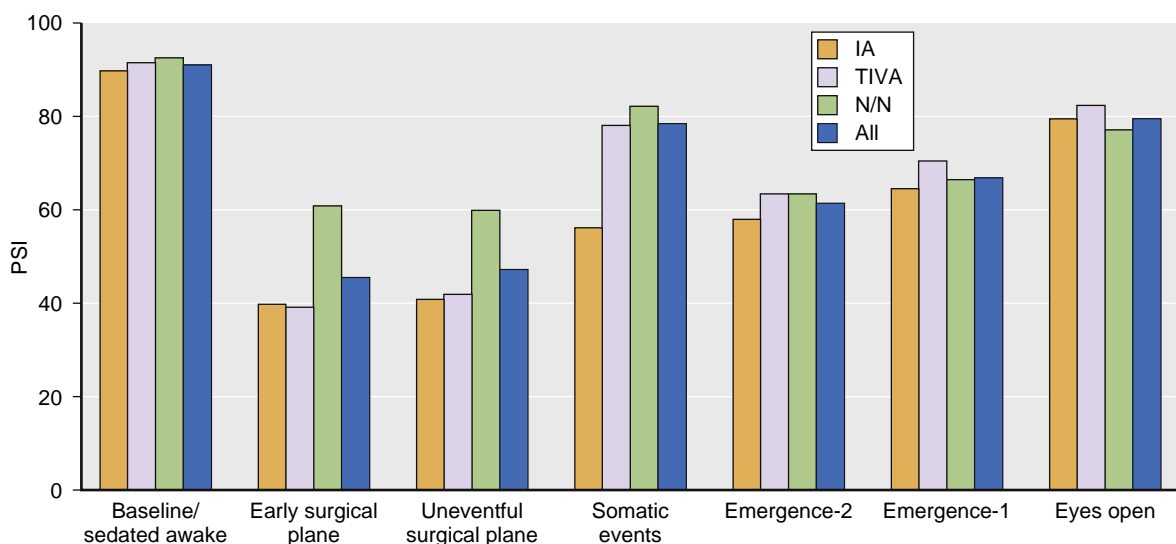


Fig. 40.4 Anesthetic states and the patient safety index (PSI). The histogram provides the anesthetic state interpretation of the values of the PSI. IA, Inhaled anesthetics; N/N, nitrous narcotic; TIVA, total intravenous anesthesia. (Redrawn from Drover D, Ortega HR. Patient state index. *Best Pract Res Clin Anaesthesiol*. 2006;20:121–128.)

in real time the unprocessed EEG and its spectrogram from both the left and right sides of the head, the level of electromyographic activity, an artifact index, and the suppression ratio. The suppression ratio is a number between 0 and 100 that measures the fraction of time the EEG is in burst suppression. The monitor also allows the user to change the viewing screen among various combinations of the unprocessed EEG traces, the spectrogram, and the time series of the PSI values.

In head-to-head comparisons, the PSI correlates strongly with the BIS readings in terms of tracking a patient's anesthetic state.^{50–52} This monitor has been less frequently studied in clinical investigations and has not received the same level of clinical use as the BIS monitor. In our experience, the PSI can also give ambiguous information for ketamine, nitrous oxide, dexmedetomidine, and pediatric patients.

NARCOTREND

The Narcotrend, produced by MonitorTechnik (Bad Bramstedt, Germany), is an EEG-based device designed to monitor the anesthetic state in patients receiving general anesthesia or sedation.⁵³ This monitor was developed at the University Medical School of Hanover, Germany, and has been approved by the FDA for use in the United States for patient care. Like the BIS and PSI, the Narcotrend uses a proprietary algorithm that converts the EEG into different states, denoted as *A* to *F* (Table 40.1).⁵⁴ Stage *A* corresponds to the patient being wide-awake, whereas stage *F* corresponds to increasing burst suppression down to an isoelectric state. The newer version of the Narcotrend monitor includes a Narcotrend Index, which is scaled between 0 and 100.⁵¹ In addition, the Narcotrend monitor displays the unprocessed EEG signal and its spectrogram. This monitor has also been validated with respect to the BIS index and separately. Its performance has been variable.^{24,55,56} Narcotrend has received less clinical use than BIS and PSI.

TABLE 40.1 Anesthetic States, the Narcotrend Stages, and Narcotrend Index Ranges

	Narcotrend Stage	Narcotrend Index
Awake	A	95-100
	B ₀	90-94
Sedated	B ₁	85-89
	B ₂	80-84
Light anesthesia	C ₀	75-79
	C ₁	70-74
	C ₂	65-69
General anesthesia	D ₀	57-64
	D ₁	47-56
	D ₂	37-46
General anesthesia with deep hypnosis	E ₀	27-36
	E ₁	20-26
	E ₂	13-19
General anesthesia with increasing burst suppression	F ₀	5-12
	F ₁	1-4

The table provides the anesthetic state interpretation of the Narcotrend Stages and the Narcotrend Index values.

From Kreuer S, Wilhelm W. The Narcotrend monitor. *Best Pract Res Clin Anaesthesiol*. 2006;20:111–119.

ENTROPY

The use of entropy to track the anesthetic state of patients is a relatively new monitoring approach. Entropy is a well-known concept in the physical sciences, mathematics, and information theory. Entropy measures the degree of disorder or the lack of synchrony or consistency in a system.⁵⁷ Entropy-based analyses have been applied to the EEG and have been used to construct EEG-based indices meant to indicate the depth of anesthesia. The Entropy monitor was developed by Datex-Ohmeda, which is now part of GE Healthcare (Little Chalfont, United Kingdom). The algorithm in the GE device uses frequency domain analysis,

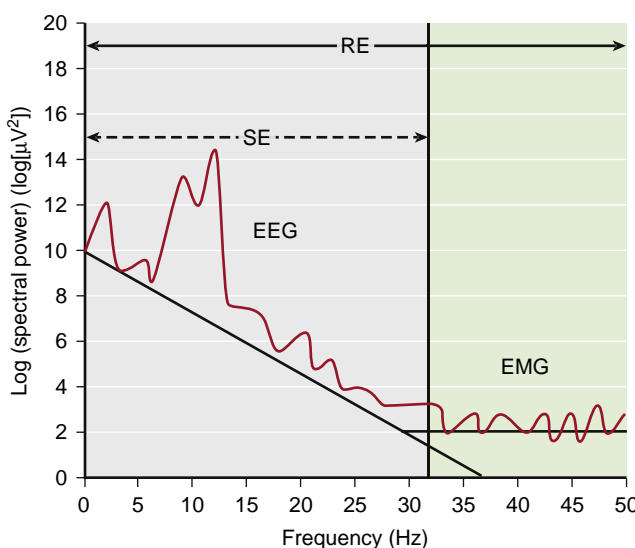


Fig. 40.5 Schematic representation of the spectral entropy. The response entropy (RE) is computed from the power in the frequencies between 0 and 47 Hz. The state entropy (SE) is computed from the power in the frequencies between 0 and 32 Hz. The power between 32 and 47 Hz is assumed to represent artifacts coming from the electromyogram (EMG). The difference between the RE and SE allows the anesthesiologist to distinguish between electroencephalogram (EEG) changes related to changes in the anesthetic state and changes that are due to artifact or movement. (Redrawn from Bein B. Entropy. Best Pract Res Clin Anaesthesiol. 2006;20:101–109.)

combined with burst suppression to measure the entropy of the EEG in patients receiving anesthetic drugs. Unlike several of the other algorithms we have discussed, the entropy algorithm used in the GE entropy device is publicly available.^{58,59}

A readily apparent feature of the EEG, as patients proceed through deeper anesthetic states, is that the patterns become more regular and ordered (see Fig. 40.2). That is, we observe an apparent decrease in the entropy of the EEG signal. The Entropy monitor reports two entropy numbers to aid in interpreting this monitor's EEG analysis (Fig. 40.5).⁶⁰ The first is the response entropy (RE) and the second is the state entropy (SE). The RE tracks the changes in the EEG power in the higher frequency range 0.8 to 47 Hz, whereas the SE tracks the changes in the EEG power in the lower frequency range of 0.8 to 32 Hz.⁵⁸ The relative changes in the RE and the SE have been proposed as a way to distinguish between real brain state changes versus those that are due to muscle activity on the electromyogram.⁵⁸ In general, electromyographic activity shows up in the higher frequency range tracked by the RE. As a patient becomes more profoundly unconscious, the RE declines faster than the SE, thereby making it possible to distinguish unconsciousness from movement artifacts. Monitoring entropy is consistent with changes with the BIS.⁶¹

Like the BIS, PSI, and Narcotrend, the Entropy scores correlate with anesthetic state. The Entropy monitor, like BIS and the PSI, can show paradoxically high readings for ketamine and nitrous oxide. The Entropy scores can be misleading when the patient is receiving dexmedetomidine, because the highly ordered slow waves that are present commonly during deep sedation with

dexmedetomidine do not necessarily indicate a profound state of unconsciousness.

END-TIDAL ANESTHETIC CONCENTRATION

In 1965, Eger and colleagues first introduced the concept of the MAC of an inhaled anesthetic required for immobility (defined as lack of movement in response to noxious stimulation).⁶² Five years later, Eger's group also introduced the concept of MAC-awake, or the MAC of inhaled anesthetic necessary to ablate response to a verbal command.⁶³ The median MAC value (i.e., the MAC of inhaled anesthetic required for immobility in 50% of patients) remains the gold standard for dosing inhaled anesthetics, and some modern anesthesia machines calculate age-adjusted MAC values based on the patient's end-tidal anesthetic gas concentration. However, the ratio of MAC to MAC-awake varies widely among general anesthetics,⁶⁴ suggesting that MAC cannot be used to define or predict brain states in anesthetized patients. This has been confirmed by animal experiments demonstrating that there is no clear association between anesthetic-induced EEG patterns and immobility,⁶⁵ and that inhaled anesthetics produce immobility primarily through their actions in the spinal cord, rather than the brain.^{66,67} Nevertheless, the widely accepted concept of MAC has led to the use of end-tidal anesthetic concentration as a way to monitor anesthetic state induced by inhaled anesthetics.

As mentioned previously, this use of MAC has been supported by the B-Unaware Trial, which reported no difference in the incidence of intraoperative awareness with an anesthetic protocol that maintained the BIS value between 40 and 60, and a protocol that maintained an end-tidal anesthetic concentration between 0.7 and 1.3 MAC.⁴⁰ Similarly, the BAG-RECALL Trial limited enrollment to patients at high risk for intraoperative awareness. Patients with BIS-guided general anesthesia experienced a small but statistically significant higher incidence of intraoperative awareness than patients receiving general anesthesia guided by an end-tidal anesthetic criterion.⁴¹

Unlike the BIS, PI, Entropy, and Narcotrend, which provide EEG-based measures of brain activity, the end-tidal anesthetic concentration is related to brain activity through the concentration of inhaled anesthetic expired in the lungs. This assumes that the lung anesthetic concentration is in equilibrium with the brain concentration. Moreover, this assumes that, except for age adjustment, the same brain concentration in every patient, regardless of brain health or physiological state, defines the same anesthetic state. The end-tidal anesthetic concentration is thus an indirect and less nuanced measure of anesthetic state, given that the relevant effects of the anesthetics for inducing unconsciousness are in the brain and not in the lungs. That an EEG-based criterion and a lung-gas criterion are comparable for monitoring the level of consciousness under general anesthesia suggests more of a flaw in the design of the EEG-based marker, rather than the accuracy of the end-tidal anesthetic concentration. Because it is a more indirect measure of anesthetic state, the success of the end-tidal anesthetic concentration in preventing awareness comes likely at the expense of overdosing some patients. A key drawback of the end-tidal anesthetic concentration is that it cannot be used with total intravenous anesthesia.

OTHER STRATEGIES FOR MONITORING LEVEL OF CONSCIOUSNESS

Other strategies for monitoring level of consciousness during general anesthesia and sedation have been studied. For example, the Cerebral State Monitor,⁶⁸ the SNAP Index,⁶⁹ and the AEP Index⁷⁰ are other EEG-based approaches that have been studied and applied in clinical practice.

Emergence From General Anesthesia

ELECTROENCEPHALOGRAPH-BASED INDICES AND RETURN OF CONSCIOUSNESS

As stated earlier, the EEG-based indices typically specify a range for maintenance of anesthetic state (see Figs. 40.3 to 40.5, and Table 40.1). When delivery of the anesthetic drugs is decreased or terminated, the indices increase toward values that are consistent with the awake state. As the values of the indices increase, the patient is more likely to become conscious. In this way, the EEG-based indices can be used to monitor changes in anesthetic state during emergence from general anesthesia. Although the values of the indices increase during emergence, none of the indices has a value at which the patient is certain to regain consciousness. The lack of any mechanistic relationship between the values of the EEG-based index and level of consciousness is due to imprecision in the definition of the indices, in that many different anesthetic states are presumed to map to the same index value. Friedman and colleagues and Joiner and colleagues found that neural inertia can play a role with inhaled anesthetics.^{71,72} Neural inertia is the extent to which equal brain concentrations of anesthetic on induction and emergence often yield different behavioral states. In other words, the history of the brain states helps determine arousability.

PHYSIOLOGIC SIGNS AND RETURN OF CONSCIOUSNESS

The state of the patient during emergence from general anesthesia can be tracked reliably by monitoring the patient's physiologic signs and performing neurologic examinations.¹ Many of these physiologic changes relate to the return of brainstem function (Box 40.1). Therefore, by relating the physiologic signs and the findings from the neurologic examinations to the brainstem centers responsible for them, anesthesia providers can track the return of function to specific brainstem sites during emergence from general anesthesia. Once neuromuscular blockade has been reversed, the patient may breathe unassisted. As the level of carbon dioxide in the cerebral circulation increases, most patients begin to breathe spontaneously. As the patient emerges from general anesthesia, the respiratory pattern can transition from one that is irregular with small tidal volumes to one that is regular with full normal tidal volumes.¹ Return of spontaneous breathing is a distinct indicator of return of function in the medulla and lower pons, as these are the locations of the dorsal and ventral respiratory groups, respectively.⁶

Over the ensuing several minutes and often concomitant with the return of spontaneous respiration, a series of other clinical signs begin to appear (see Box 40.1). These signs include swallowing, gagging, salivation, tearing, and grimacing.¹ The signs each represent return of a specific center in the brainstem and the associated sensory and motor pathways. Swallowing, gagging, and coughing represent return of the motor nuclei of the cranial nerves IX and X located in the medulla and the sensory afferent of these nerves arising from the trachea, larynx, and pharynx.¹⁰ These physiologic signs appear because with the progressive decrease in the hypnotic and antinociceptive effects of the anesthetics, the endotracheal tube becomes a progressively more noxious stimulus. Salivation reflects the return of the inferior salivatory nucleus in the medulla and superior salivatory nucleus in the pons. Both are part of the parasympathetic nervous system. The efferent pathways from these nuclei travel in cranial nerves VII and IX, respectively.⁹ Tearing also reflects the return of function in the superior salivatory nucleus. Grimacing, the use of muscles of facial expression, represents the return of function to the motor nucleus of cranial nerve VII, located in the pons.¹⁰ Return of muscle tone to the upper and lower extremities is another important clinical sign that clearly reflects return of function in a number of circuits including the spinal cord, the reticulospinal tract, the basal ganglia, and the primary motor tracts.¹ In addition, as the endotracheal tube is perceived as more noxious and motor tone has returned, the patient may commonly exhibit defensive posturing indicated by reaching for the endotracheal tube.

These physiologic signs are often present in advance of the patient responding to any verbal commands. The patient need not respond to commands to be extubated. Tracheal extubation only requires that the patient have sufficient return of airway reflexes and motor function to ventilate and oxygenate adequately with spontaneous breathing. To meet the criteria for extubation of the trachea, a patient can be in a vegetative state as defined by the criteria used by neurologists and rehabilitation specialists to assess the brain states of patients recovering from coma (see Box 40.1).^{13,14,73}

The corneal reflex typically returns before the oculocephalic reflex.¹ Return of the corneal reflex indicates return of function in the sensory nucleus of cranial nerve V and the motor nucleus of cranial nerve VII.⁴ The afferent pathway in the corneal reflex is the ophthalmic branch of cranial nerve V that projects to the trigeminal (cranial nerve V) nucleus, whereas the efferent pathway arises from the facial nerve (cranial nerve VII) nucleus. The consensual response in the corneal reflex indicates bilateral return of the sensory and motor components of this pathway. The trigeminal nucleus and the motor nucleus of cranial nerve VII lie in the pons. Return of the oculocephalic reflex indicates return of activity in the oculomotor (III), trochlear (IV), and abducens (VI) cranial nerves, which control movement of the eyes.⁴ The cranial nerves III and IV nerve nuclei are located in the midbrain, whereas the cranial nerve VI nerve nucleus is in the pons. Return of the oculocephalic and corneal reflexes provides indirect evidence that the nearby arousal centers in the pons, midbrain, hypothalamus, and basal forebrain, may have also recovered function.¹ The oculocephalic reflex may not return even though the patient is extubated.

BOX 40.1 Phases of Emergence From General Anesthesia and States of Coma Recovery

General Anesthesia

Stable administration of anesthetic drugs
Arousal not possible, unresponsive; eyes closed, with reactive pupils
Analgesia, akinesia
Drug-controlled blood pressure and heart rate
Mechanically controlled ventilation
EEG patterns ranging from delta and alpha activity to burst suppression

Brain-Stem Death

No respiratory response to apneic oxygenation test
Total loss of brain-stem reflexes
Isoelectric EEG pattern

Coma

Structural brain damage to both cerebral hemispheres, with or without injuries to tegmental midbrain, rostral pons, or both
Isolated bilateral injuries to midline tegmental midbrain, rostral pons, or both
Arousal not possible, unresponsive
Functionally intact brain stem, normal arterial blood gases
EEG pattern of low-amplitude delta activity and intermittent bursts of theta and alpha activity or possibly burst suppression

Vegetative State

Spontaneous cycling of eye opening and closing
Grimacing and nonpurposeful movements
EEG pattern of high-amplitude delta and theta activity
Absence of EEG features of sleep
Usually able to ventilate without mechanical support

Emergence, Phase 1

Cessation of anesthetic drugs
Reversal of peripheral-muscle relaxation (akinesia)
Transition from apnea to irregular breathing to regular breathing
Increased alpha and beta activity on EEG

Emergence, Phase 2

Increased heart rate and blood pressure
Return of autonomic responsiveness
Responsiveness to painful stimulation
Salivation (CN VII and IX nuclei)
Tearing (CN VII nuclei)
Grimacing (CN V and VII nuclei)
Swallowing, gagging, coughing (CN IX and X nuclei)
Return of muscle tone (spinal cord, reticulospinal tract, basal ganglia, and primary motor tracts)
Defensive posturing
Further increase in alpha and beta activity on EEG
Extubation possible

Emergence, Phase 3

Eye opening
Responses to some oral commands
Awake patterns on EEG
Extubation possible

Minimally Conscious State

Purposeful guarding movements, eye tracking
Inconsistent communication, verbalizations
Following oral commands
Return of sleep-wake cycles
Recovery of some EEG features of normal sleep-wake architecture

General anesthesia is a drug-induced, reversible coma. The physiological signs observed in the phases of emergence from general anesthesia can be related to changes in activity in specific brainstem nuclei. Emergence from general anesthesia has similarities and differences with recovery from coma due to a brain injury.

CN, Cranial nerve; **EEG**, electroencephalogram.

From Brown EN, Lydic R, Schiff ND. General anesthesia, sleep, and coma. *N Engl J Med*. 2010;363:2638–2650.

Patients commonly leave the operating room without return of this reflex, suggesting persistent sedation of the brainstem arousal centers. The pupils can remain pinpoint if the patient has received a substantial dose of an opioid. The pupillary light reflex can remain intact even when the patient is profoundly unconscious under general anesthesia⁴; therefore, the presence of the pupillary light reflex might not indicate a change in the level of consciousness while under general anesthesia.

Responding correctly to verbal commands, a criterion that is commonly used to assess the extent to which a patient has recovered from general anesthesia, and hence the patient's readiness for extubation, suggests a return of integrated function between the brainstem, the thalamus and cortex, and among cortical regions.^{1,74,75} Responding correctly to verbal commands means that the patient is correctly interpreting auditory information and that the cranial nerve VIII nuclei located in the pons and the auditory

pathways from the pons to the cortex and the relevant effector pathways have regained substantial function. If the patient inconsistently follows motor commands, then he or she is classified as being in a minimally conscious state by the criteria neurologists use in examining patients recovering from coma (see Box 40.1).^{13,14,73} With emergence, the physiologic signs and neurologic findings can be related to changes in activity in specific brainstem centers. Although the EEG shows the resumption of high-frequency activity consistent with the return of cognitive processing, normal brainstem-cortical, brainstem-thalamic, thalamocortical, and intracortical communication must clearly return for full return of consciousness.^{44,75-78} Current clinical monitoring approaches do not allow us to monitor these changes adequately.

Opening of the eyes is typically one of the last physiologic signs observed in patients emerging from general anesthesia. In particular, patients may respond reliably to verbal

commands, have substantial return of motor functions, yet not necessarily open their eyes.¹ In general, patients tend to keep their eyes closed even when consciousness has returned. In contrast, during coma recovery, patients can have their eyes open in a vegetative state (see **Box 40.1**).

Emerging Strategies for Monitoring the Brain States of General Anesthesia and Sedation

In the last several years, there has been strong growth in research on the neuroscience of general anesthesia. As a result, there are several reports of new approaches to monitoring the brain states under general anesthesia.

UNPROCESSED ELECTROENCEPHALogram AND THE SPECTROGRAM

Different anesthetics have different receptor targets⁷⁹ and neural circuit mechanisms of action.^{1,43} These differences in targets and neural circuits translate into different patterns of activity in the brain that are readily visible in the unprocessed EEG or its spectrogram.²⁶ The spectrum of a segment of EEG is the decomposition of the EEG signal into its power content by frequency.²⁶ Power is typically expressed in decibels which is 10 times the base 10 logarithm of the square of the amplitude of a given frequency component.²⁶ When the spectrum is computed on successive nonoverlapping or overlapping segments of EEG data, it is termed the *spectrogram*²⁶; it is called the *compressed spectral array* when the spectrogram is plotted in three dimensions⁸⁰ and the *density spectral array* when it is plotted in two dimensions.⁸¹

The EEG patterns of propofol have been related to its neural circuit mechanisms. The brain states under propofol are readily visible in the unprocessed EEG and the spectrogram (see **Figs. 40.2, 40.6 and 40.7, A**). Propofol acts primarily at GABA_A receptors throughout the brain and spinal cord to enhance inhibition in neural circuits.^{79,82} When patients are unconscious from propofol, the EEG shows a characteristic alpha (8-12 Hz) oscillation pattern along with slow (0.1-1 Hz) and delta (1-4 Hz) oscillation patterns (see **Fig. 40.7 A**).^{44,49,83,84} Another phenomenon that is observed in patients who are unconscious from propofol and several other anesthetics is anteriorization—the increase in power in the alpha and beta frequency ranges during unconsciousness across the front of the scalp relative to other areas of the scalp (see **Fig. 40.6, C and D**).^{44,47,49}

During unconsciousness, the alpha oscillations are highly coherent across the front of the scalp, whereas the slow and gamma oscillations are not coherent.^{44,49,84} Highly coherent alpha oscillations have also been identified in animal studies of inhaled anesthetics during unconsciousness.⁸⁵ The coherent structure in the alpha oscillations is most likely due to strong alpha oscillations between the thalamus and frontal cortex.⁸⁶ The slow oscillations are a marker of fragmented intracortical communication because in the presence of the slow oscillations, cortical neurons spike only in a limited phase dictated by their local slow oscillations.⁸⁴ As the slow oscillations are spatially incoherent and spiking is phase limited, neuronal communication among brain

regions that are separated by more than 1 cm is greatly impeded. There is a strong modulation of the alpha oscillation amplitude by the phase of the slow-delta oscillation⁴⁴. Patients are profoundly unconscious when the maximum amplitude of the alpha oscillations occurs at the peak of the slow oscillation waveform.⁴⁴ In contrast, patients are likely to be arousable when the maximum amplitude of the alpha oscillations occurs at the trough of the slow oscillation waveform.⁴⁴ With return of consciousness, the alpha and slow oscillations dissipate (see **Fig. 40.6, B**). A mechanism by which propofol produces unconsciousness is through hypersynchronous alpha oscillations impeding communication between the thalamus and prefrontal cortex and through highly desynchronous slow oscillations impeding intracortical communication.^{44,84,86,87}

Similarly, the EEG patterns of ketamine (see **Fig. 40.7, B**)²⁷ and dexmedetomidine (**Fig. 40.8, A and B**)³⁴ are distinctive and can be related to the mechanisms of actions of these drugs in the brain and central nervous system.^{1,3,43} Ketamine acts principally by binding to N-methyl-D-aspartate (NMDA) receptors.^{43,88} Thus, with small to moderate doses, ketamine has its primary effect by blocking excitatory glutamatergic inputs to inhibitory interneurons.^{89,90} Impaired control over pyramidal neurons is why increases in cerebral metabolism, and the appearance of altered behavioral states including hallucinations, dissociative states, euphoria, and dysphoria, are common with low-dose ketamine. Brain regions, such as the limbic system, cortex, and thalamus, continue to communicate but with much less regulatory control from the inhibitory interneurons—that is, information processing proceeds in the absence of proper coordination in time and space.^{1,43} Increasing the dose of ketamine blocks the NMDA receptors on the excitatory glutamatergic neurons, and eventual loss of consciousness, as when ketamine is used to induce anesthesia.⁹¹ The increased activity of pyramidal neurons throughout the brain is consistent with the high frequency (20-30 Hz) oscillations that are commonly observed in the EEG of patients receiving ketamine (see **Fig. 40.7 B**).^{27,92} This high-frequency EEG activity helps explain why EEG-based indices often give high values in patients receiving ketamine.

Dexmedetomidine induces its sedative effects primarily by actions on presynaptic α_2 -adrenergic receptors on neurons that project from the locus ceruleus.⁹³⁻⁹⁵ Binding of dexmedetomidine results in a decrease in the release of norepinephrine from these neurons.⁹⁶⁻⁹⁸ Loss of the norepinephrine-mediated inhibition to the preoptic area of the hypothalamus leads to activation of the preoptic area's GABAergic and galanergic inhibitory inputs to most of the principal arousal centers in the midbrain, pons, basal forebrain, and hypothalamus.⁹⁹ Activation of inhibitory inputs from the preoptic area is postulated to be a component of how nonrapid eye movement (NREM) sleep is initiated.^{100,101} This suggests why light sedation with dexmedetomidine shows spindles, intermittent bursts of 9 to 15 Hz oscillations, and slow-wave patterns in the EEG that closely resemble NREM sleep stage 2 (see **Fig. 40.8, A**). Recent studies have demonstrated that deep sedation with dexmedetomidine also shows the combined spindle and slow-delta oscillation patterns seen with light dexmedetomidine sedation (see **Fig. 40.8, A**), along with an appreciable decrease in beta oscillation power.^{32,33,102} Deep

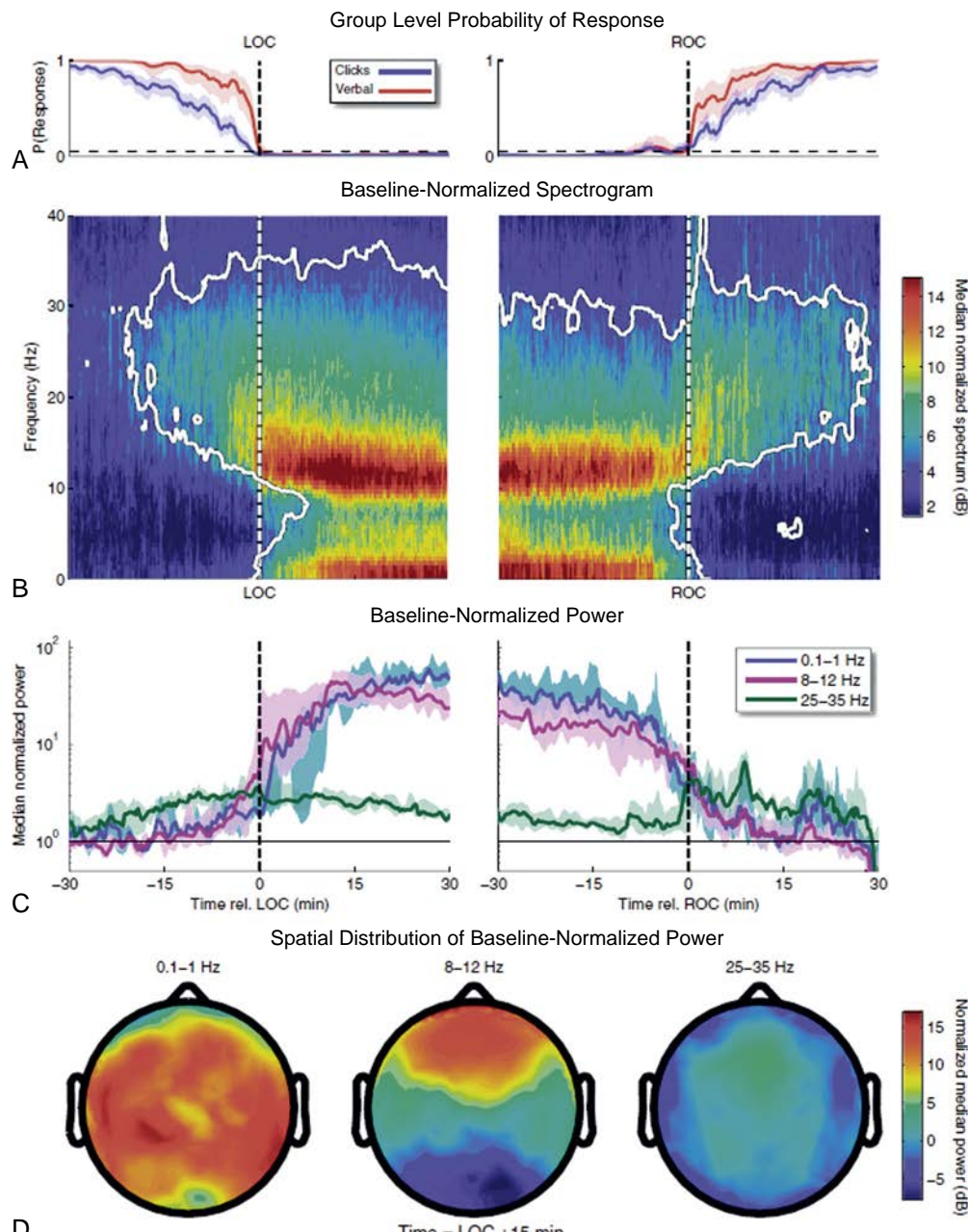


Fig. 40.6 Behavioral and electroencephalogram dynamics of loss and recovery of consciousness from propofol. (A) Group-level (10 subjects) click or nonsalient stimulus (blue, P_{clicks}) and verbal or salient stimulus (red, P_{verbal}) response-probability curves. (B) Group-level spectrograms computed by baseline-normalization from a frontal channel (approximately F_2 , using nearest-neighbor Laplacian reference) aligned across subject with respect to loss of consciousness (LOC). Area enclosed within the white borders show where power is significantly different from baseline ($P < .05$, sign test) and shows significant power increases spanning slow (0.1–1 Hz) through gamma (25–35 Hz) bands. (C) Time course of group-level power in slow, alpha (8–12 Hz), and gamma bands aligned with respect to LOC and recovery of consciousness (ROC). (D) Group-level spatial distribution of slow, alpha, and gamma power during unconsciousness (LOC + 15 min). The frontal increase in alpha power is termed *anteriorization*. These analyses illustrate that changes in broad-band gamma/beta power occur with the behavioral changes before LOC and after ROC, whereas changes in slow and alpha power occur with LOC and ROC. (From Purdon PL, Pierce ET, Mukamel EA, et al. Electroencephalogram signatures of loss and recovery of consciousness from propofol. *Proc Natl Acad Sci U S A*. 2013;110:E1142–E1151.)

sedation with dexmedetomidine can also show a slow-delta oscillation EEG pattern that closely resembles the patterns observed in NREM sleep stage 3 or slow-wave sleep (see Fig. 40.8 B).²⁶

Sevoflurane, like the other inhaled ether anesthetics, produces its physiologic and behavioral effects by binding at multiple targets in the brain and spinal cord. These include

binding to GABA_A receptors and enhancing GABAergic inhibition, and blocking glutamate release by binding to NMDA receptors, along with activating two-pore potassium channels and hyperpolarization-activated cyclic nucleotide-gated channels.⁷⁹ Although debates still exist over the relative importance of these targets, sevoflurane and the other ether anesthetics have distinct EEG signatures.

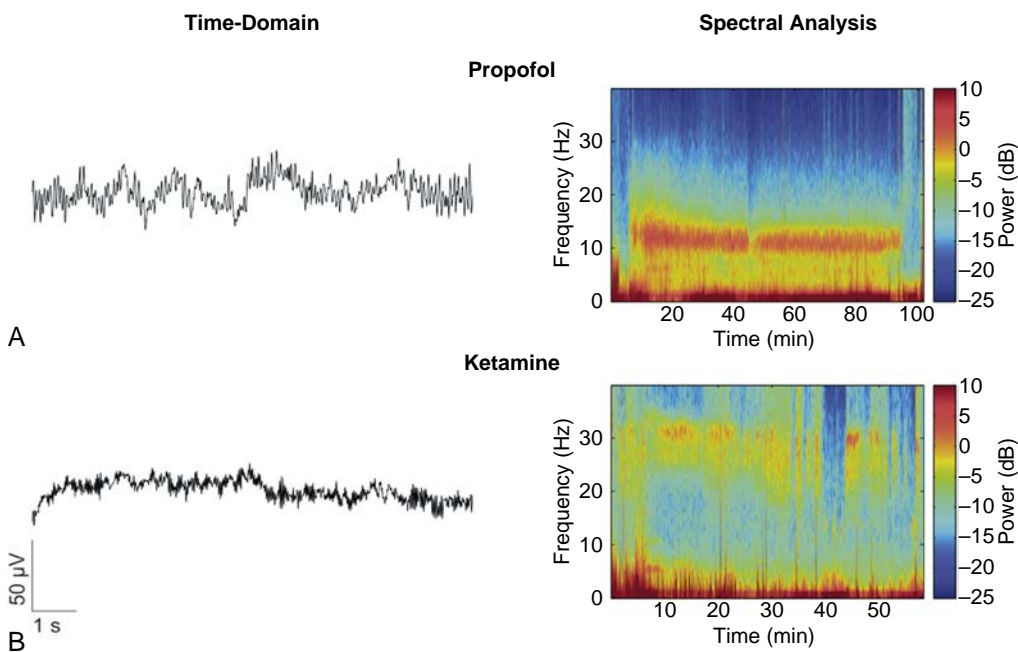


Fig. 40.7 Time-domain and spectral electroencephalogram (EEG) signatures of common anesthetics. The left column shows a 10-s time-domain (unprocessed) segment of the EEG for each anesthetic. The right column shows several minutes of the spectrogram (density spectral array) computed from the EEG for each anesthetic. (A) The EEG and spectrogram of propofol show its characteristic alpha (8-12 Hz) and slow-delta (0.1-4 Hz) oscillation pattern. (B) The ketamine EEG and spectrogram show high frequency oscillations in the high beta (20-24 Hz) and low gamma (25-35 Hz) range.

At doses of sevoflurane appropriate for general anesthesia, the EEG shows strong alpha and slow oscillations like propofol, in addition to a strong theta (4-8 Hz) oscillation (see Fig. 40.8 C). The presence of the theta oscillations creates a distinctive pattern of evenly distributed EEG power from the slow oscillation through the alpha oscillation range. The predominance of the alpha and slow oscillations in the sevoflurane spectrogram and those of the other inhaled ethers suggest that GABA_A-mediated inhibition is a primary mechanism of action of these anesthetics. This spectrogram pattern further suggests that a primary mechanism through which the inhaled ethers produce unconsciousness is largely similar to that of propofol.^{44,84,86,87}

Nitrous oxide has a highly distinctive EEG dynamic. A common practice in our institution, at the end of surgery, is to switch from the inhaled ether, isoflurane, to nitrous oxide to facilitate emergence from general anesthesia (Fig. 40.9 A). When nitrous oxide is administered at high doses (greater than 50%), it produces large slow-delta oscillations that last from 3 to 12 minutes before converting to high-frequency gamma oscillations (see Fig. 40.9 B).^{26,31,103,104} Why the slow-delta oscillations are transient is unknown. Nitrous oxide is known to act by blocking NMDA glutamate receptors.^{31,79,105,106} It is likely that the slow-delta oscillations reflect a transient profound state of unconsciousness most likely mediated through inactivation of key NMDA glutamate projections from the parabrachial nucleus and from the median pontine reticular formation into the central thalamus and basal forebrain.^{31,107}

Although the unprocessed EEG recordings of the anesthetics can look similar, the spectrograms make clear that each anesthetic has a distinct EEG signature. These signatures can be related to the mechanisms through which the drugs act at specific receptors in specific neural circuits

to alter arousal. Using the spectrogram to monitor brain function under general anesthesia and sedation is fundamentally different from using EEG-based indices that are predicated on the assumption that different anesthetics can create the same anesthetic state irrespective of mechanism. The differences in the spectral signatures between propofol (see Fig. 40.7 A) and ketamine (see Fig. 40.7 B) illustrate why the latter often gives a high index reading when clinically the patient is clearly sedated. Similarly, the predominance of the slow-wave oscillations observed during deep dexmedetomidine (see Fig. 40.8, B) sedation helps explain why this drug gives low index values consistent with profound unconsciousness yet the patient remains arousable.

CHANGES IN ELECTROENCEPHALogram SIGNATURES WITH AGING

In addition to changing systematically with anesthetic class, the EEG signatures of patients under general anesthesia change systematically with age. Fig. 40.10 shows the spectrogram of patients of different ages anesthetized with propofol. There are three principal changes in the EEG signatures of propofol with age. First, the EEG of children between 0 to 3 months of age, anesthetized with propofol or another GABAergic drug such as sevoflurane as the primary hypnotic, show only slow-delta oscillations (see Fig. 40.10, A and B).¹⁰⁸ Slow-delta and alpha oscillations do not appear together until children are at least 4 months of age or older (see Fig. 40.10 C).¹⁰⁸ The alpha oscillations become coherent and show anteriorization specifically at the alpha frequency, at approximately 1 year of age.^{37,38,108,109} Coherence means the oscillations are highly synchronized, whereas anteriorization means that the oscillations are predominant in the

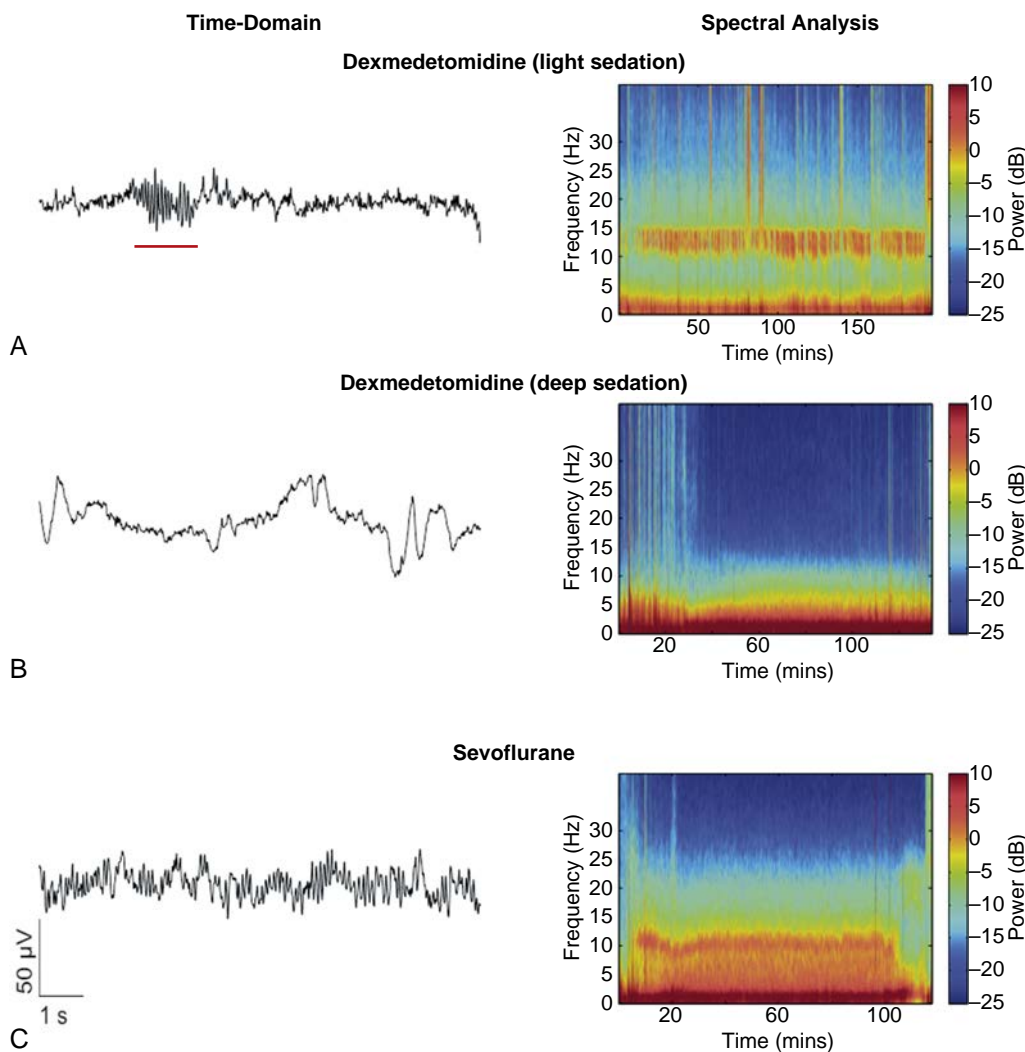


Fig. 40.8 Time-domain and spectral electroencephalogram (EEG) signatures of common anesthetics. The left column shows a 10-second time domain (unprocessed) segment of the EEG for each anesthetic. The right column shows several minutes of the spectrogram (density spectral array) computed from the EEG for each anesthetic. (A) The dexmedetomidine EEG and spectrogram for light sedation shows spindle (9-15 Hz) oscillations, and the slow (0.1-1 Hz) oscillations, and delta (1-4 Hz) oscillations similar to the EEG patterns observed in nonrapid eye movement (NREM) sleep stage 2. The spindle is apparent in the unprocessed EEG trace (red underscore). The spindles are intermittent and have less intensity than the alpha oscillations observed with propofol. (B) The EEG and spectrogram for deep dexmedetomidine sedation can be associated with an absence of spindles and a predominance of slow and delta waves similar to the slow waves seen in NREM sleep stage 3, termed *slow-wave sleep*. (C) The sevoflurane spectrogram is similar to propofol with the addition of oscillatory activity in the theta band from 4 to 8 Hz.

frontal EEG leads and completely absent in the occipital leads. The mechanisms underlying these age-dependent changes are unclear, but they almost certainly reflect development of underlying brain circuits in children.^{37,38,110} According to computational modeling studies propofol can generate alpha oscillations as a result of increasing inhibition in cortical networks.¹¹¹ When thalamocortical components are added to this model, the alpha oscillations become highly coherent.⁸⁶ Hence, the development of propofol- and sevoflurane-induced alpha oscillations in the first 6 months of life could reflect developing inhibition, particularly within cortical circuits.¹¹⁰ The later development of coherent alpha oscillations could reflect developing thalamocortical connections that facilitate coherent alpha oscillations.^{86,112} Although not shown in the figures presented here, the total power in the spectrogram increases with age from 0 months to a maximum at

approximately 6 to 8 years and then declines from there with each year of age.^{37,38}

Second, the alpha band is characteristic of young adults (approximately 18-35 years of age) and ranges from 8 to 15 Hz for this group (see Fig. 40.10 F). The corresponding band for ages below 18 years falls generally over a broader frequency range, 10 to 20 Hz (see Fig. 40.10, D and E), and has higher power relative to the alpha band of the young adults (see Fig. 40.10 F). The corresponding band for ages greater than 35 years falls generally over a narrower frequency range, 6 to 10 Hz (see Fig. 40.10 G), and has less power relative to the alpha band of the young adults (see Fig. 40.10 F). Third, the alpha oscillations in adults 55 years or older may be diminished and in the lower frequency range from 6 to 10 Hz or nearly absent (see Fig. 40.10, G-I).

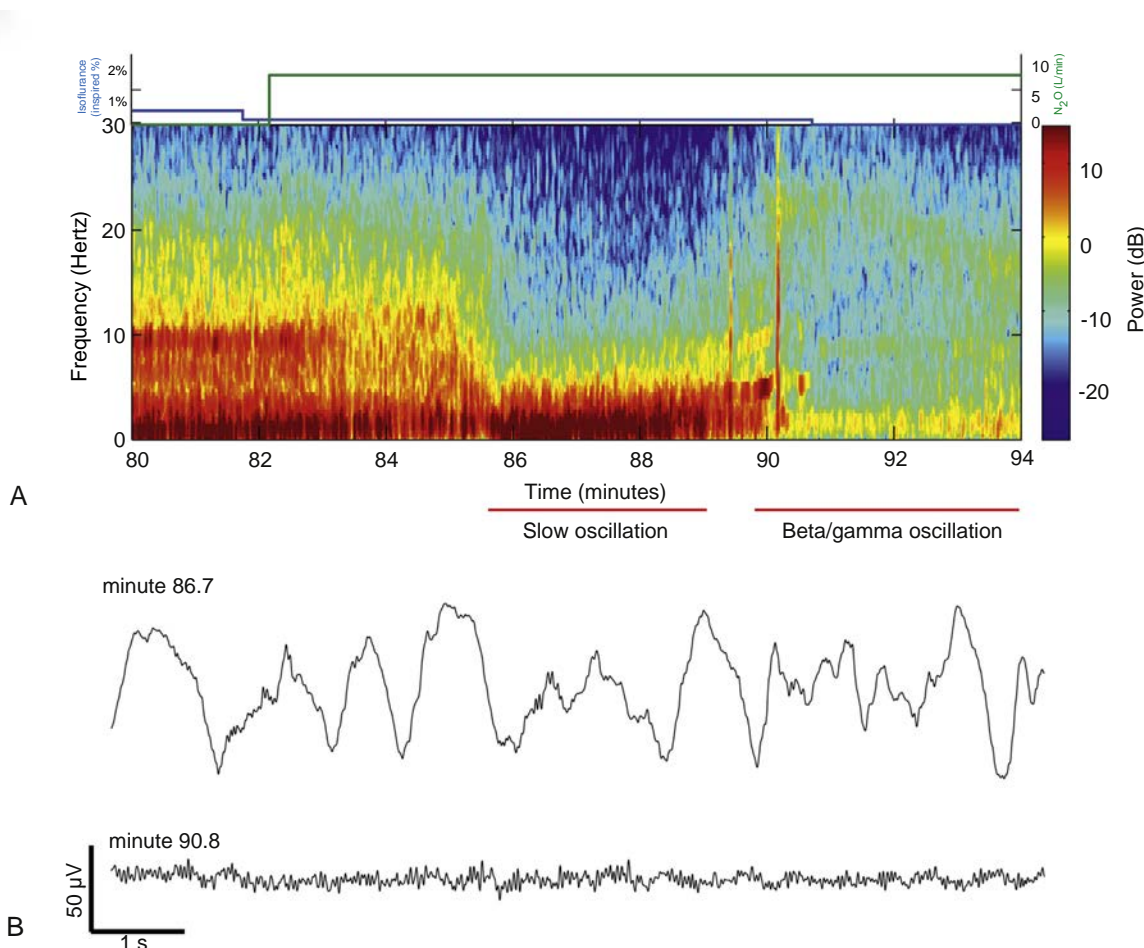


Fig. 40.9 Spectrogram displays of nitrous oxide-induced slow-delta and beta-gamma oscillations. (A) To facilitate emergence, a patient maintained on a mixture of 0.5% isoflurane and 58% oxygen at 3 L/min was changed to 75% nitrous oxide and 24% oxygen at 7 L/min. Between minutes 83 and 85 the slow-delta, theta, and alpha oscillation power decreased. The beta and theta band power appreciably decreased whereas the slow-delta oscillation power substantially increased beginning at minute 86. By minute 90 the slow-delta oscillation power has noticeably decreased, and beta-gamma oscillations begin to appear. (B) Electroencephalogram traces of the slow-delta oscillations recorded at minute 86.7 and the beta-gamma oscillations recorded at minute 90.8. Each trace is 10 s.

The changes in the slow-delta oscillations follow similar changes to the alpha oscillations band in that the band is broad with high power at younger ages (see Fig. 40.10, C-E) and becomes narrower with lower power with aging (see Fig. 40.10, F-I). Indeed, the alpha and slow-delta oscillations of the 56-year old patient and of the 81-year old patient are barely perceptible (see Fig. 40.10).

Fig. 40.10, F-G show that there can be significant between-person variation in power for patients of approximately the same age. The 57-year-old patient (see Fig. 40.10 G) has alpha and slow-delta oscillations that resemble the pattern seen in the 30-year-old patient (see Fig. 40.10 F), whereas the alpha and slow-delta oscillations of the 56-year-old patient (see Fig. 40.10 H) resemble those of the 81-year-old patient (see Fig. 40.10 I). We conjecture that these differences in oscillatory dynamics induced by propofol reflect between - individual variation in normal brain aging.¹¹³ The age-related EEG changes of sevoflurane, and presumably those associated with isoflurane and desflurane, are similar to those of propofol, given that all of these agents have primary GABAergic mechanisms of action.

IMPLICATIONS FOR MONITORING ANESTHETIC STATE

These observations suggest that the unprocessed EEG and the spectrogram can be used to monitor the brain states of patients receiving anesthesia care (see Figs. 40.6 to 40.10). The unprocessed EEG waveform has been advocated as a tool for monitoring “depth of anesthesia” since 1937.^{16,17,26,114,115} Although the spectrogram is easy to compute in real time and has been reported in studies of anesthetics,^{80,81,116} a strategy to use it in conjunction with the unprocessed EEG and the EEG-based indices for management of patients receiving anesthesia care is now being developed. Many of the current EEG brain function monitors display both the unprocessed EEG and the spectrogram.^{22,54,117} Training anesthesia providers to track brain states under general anesthesia and sedation by reading the unprocessed EEG and the spectrogram is a program being pursued currently in the Department of Anesthesia, Critical Care and Pain Medicine, of Massachusetts General Hospital in collaboration with the International Anesthesia Research Society (www.eegforanesthesia.iars.org).

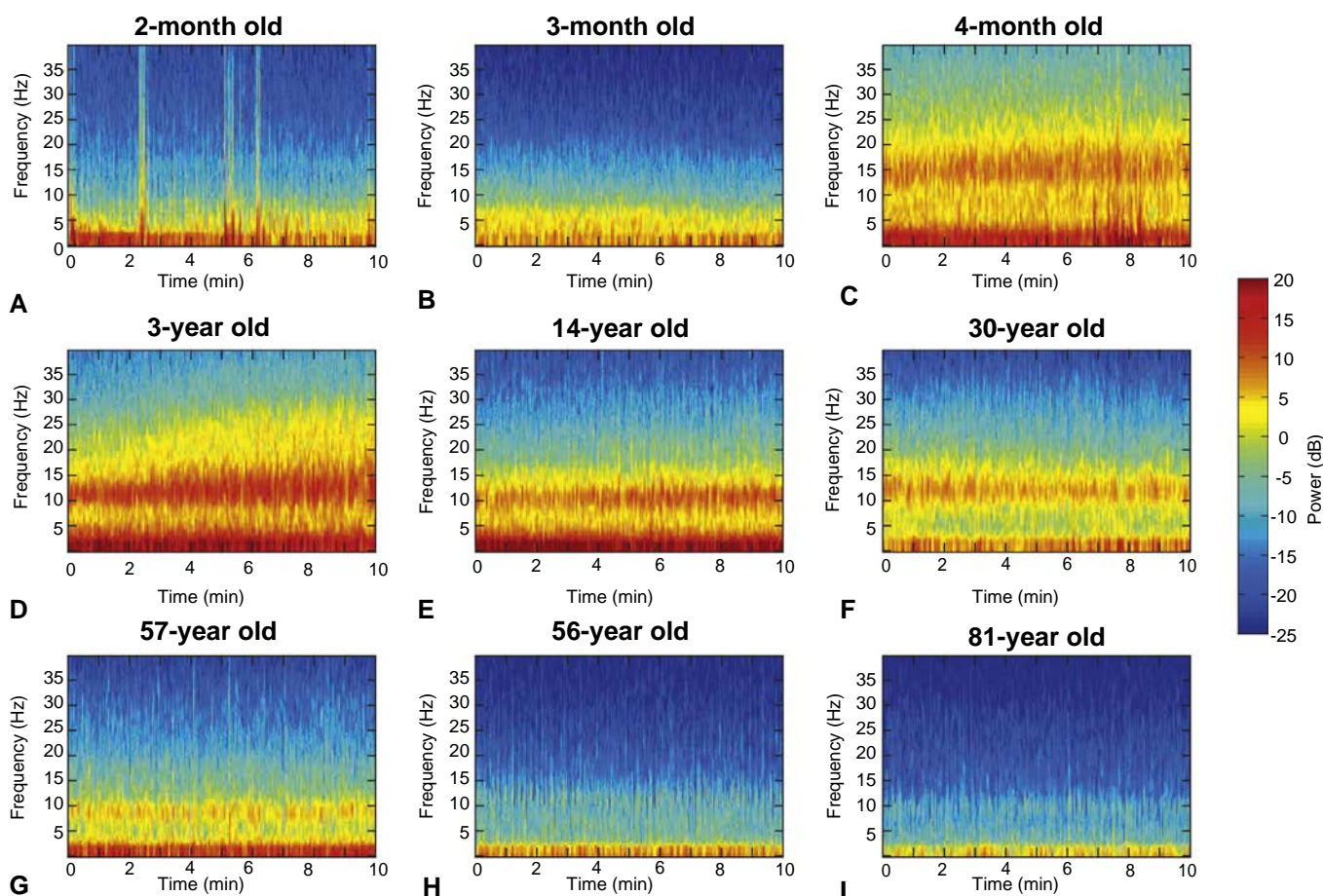


Fig. 40.10 Spectral electroencephalogram signatures of propofol as a function of age. Each panel is a 10-minute segment recorded from a patient receiving a propofol infusion as the primary anesthetic to maintain unconsciousness. The spectral power in all of the panels are plotted on the same decibel scale. (A) A 2-month-old patient. (B) A 3-month-old patient. (C) A 4-month-old patient. (D) A 3-year-old patient. (E) A 14-year-old patient. (F) A 30-year-old patient. (G) A 57-year-old patient. (H) A 56-year-old patient. (I) An 81-year-old patient. Children less than 4 months of age show only slow-delta oscillations. Alpha oscillations appear at 4 months of age. Although children greater than 4 months of age and adults from 18 to 55 years of age show both slow-delta and alpha oscillation patterns under propofol, the frequency range of the alpha oscillations and the power content changes with age. Elderly patients often have a noticeable decrease in or absence of alpha oscillations.

Another EEG education resource has been developed at Washington University (icetap.org). Highly structured oscillations are the sine qua non of anesthetic states. Therefore, use of the spectrogram to track level of consciousness under general anesthesia and sedation facilitates direct integration of clinical and research observations from EEG recordings with experimental studies and biophysically-based modeling studies that help define the neural circuit mechanisms of anesthetic actions.^{86,111,118,119}

NORMALIZED SYMBOLIC TRANSFER ENTROPY

A growing body of information suggests that a key marker or mechanism of unconsciousness under general anesthesia is loss of intracortical connectivity.^{74,75,84,91,120,121} The loss of functional connectivity between the frontal and parietal areas is associated with unconsciousness.^{91,120} By using the EEG recorded from a montage that includes both frontal and parietal electrodes, a mutual information technique termed normalized symbolic transfer entropy (NSTE) can be used to measure this loss of functional connectivity (Fig. 40.11). When NSTE is used to assess functional

connectivity from the parietal area to the frontal cortical area, it is termed *feedforward functional connectivity*, whereas when it is used to assess functional connectivity from the frontal area to the parietal area, it is termed *feedback functional connectivity*.

Unconsciousness induced by propofol, sevoflurane, or ketamine has been associated with loss of feedback functional connectivity (see Fig. 40.11).^{91,120} As a consequence, measuring NSTE to assess functional connectivity could provide a means of monitoring the level of consciousness in patients receiving general anesthesia. The loss of feedback functional connectivity is present for unconsciousness induced by all three anesthetics, suggesting that NSTE does not distinguish among the mechanisms of actions of these anesthetics.¹²⁰ Nevertheless, NSTE could still offer a way to track levels of unconsciousness.

A partial answer regarding the mechanism of loss of the feedback functional connectivity for unconsciousness induced by propofol and the inhaled ether anesthetics may be related to anteriorization (see Fig. 40.6, D). The model by Vijayan and colleagues¹¹⁹ shows that anteriorization can be explained by the differences in the electrophysiologic

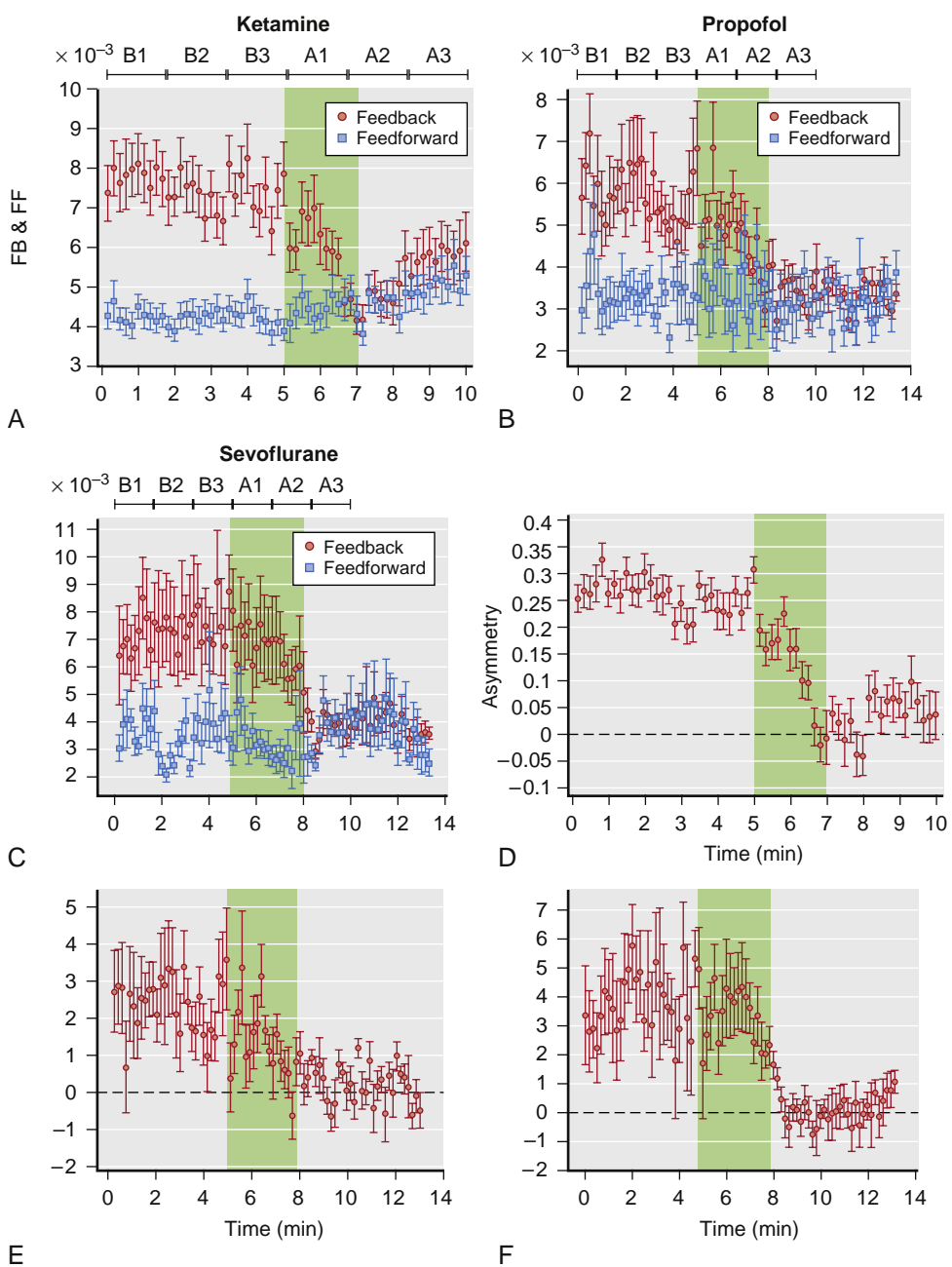


Fig. 40.11 Normalized symbolic transfer entropy. An analysis of loss of consciousness induced by ketamine, propofol, and sevoflurane using normalized symbolic transfer entropy. Asymmetry in the change of feedforward (FF) and feedback (FB) connectivity is common to all three anesthetics. The FF (blue)/FB (red) connections (A-C) and their associated asymmetry (D-F) in the frontal-parietal network displayed for (A and D) ketamine, (B and E) propofol, and (C and F) sevoflurane. Green shading highlights induction of general anesthesia. B1 to B3 define baseline substates. A1 to A3 define anesthetized substates. There were 30, 9, and 9 subjects in the ketamine, propofol, and sevoflurane groups, respectively. All three anesthetics show a greater loss in FB frontal-parietal connectivity than FF connectivity at loss of consciousness. (Redrawn from Lee U, Ku S, Noh G, et al. Disruption of frontal-parietal communication by ketamine, propofol, and sevoflurane. *Anesthesiology* 2013;118:1264–1275.)

properties, such as the resting membrane potentials and ionic currents, in the frontal thalamocortical connections compared with the posterior thalamocortical connections. If the parietal circuits resemble their nearby occipital counterparts neurophysiologically, then the neurophysiologic dynamics that lead to anteriorization could also contribute to loss of feedback functional connectivity. Studies of functional connectivity changes during loss of consciousness due to general anesthesia using the Vijayan model may

shed mechanistic light on the differences between changes in feedback connectivity and feedforward connectivity.

At present, the use of NSTE in the operating room is not tractable because it is not possible to compute these mutual information measures in real time.⁹¹ Moreover, the use of NSTE in its current form requires an EEG montage with both frontal and parietal electrodes, unlike the montages used with most current brain function monitors, which require only frontal electrodes.

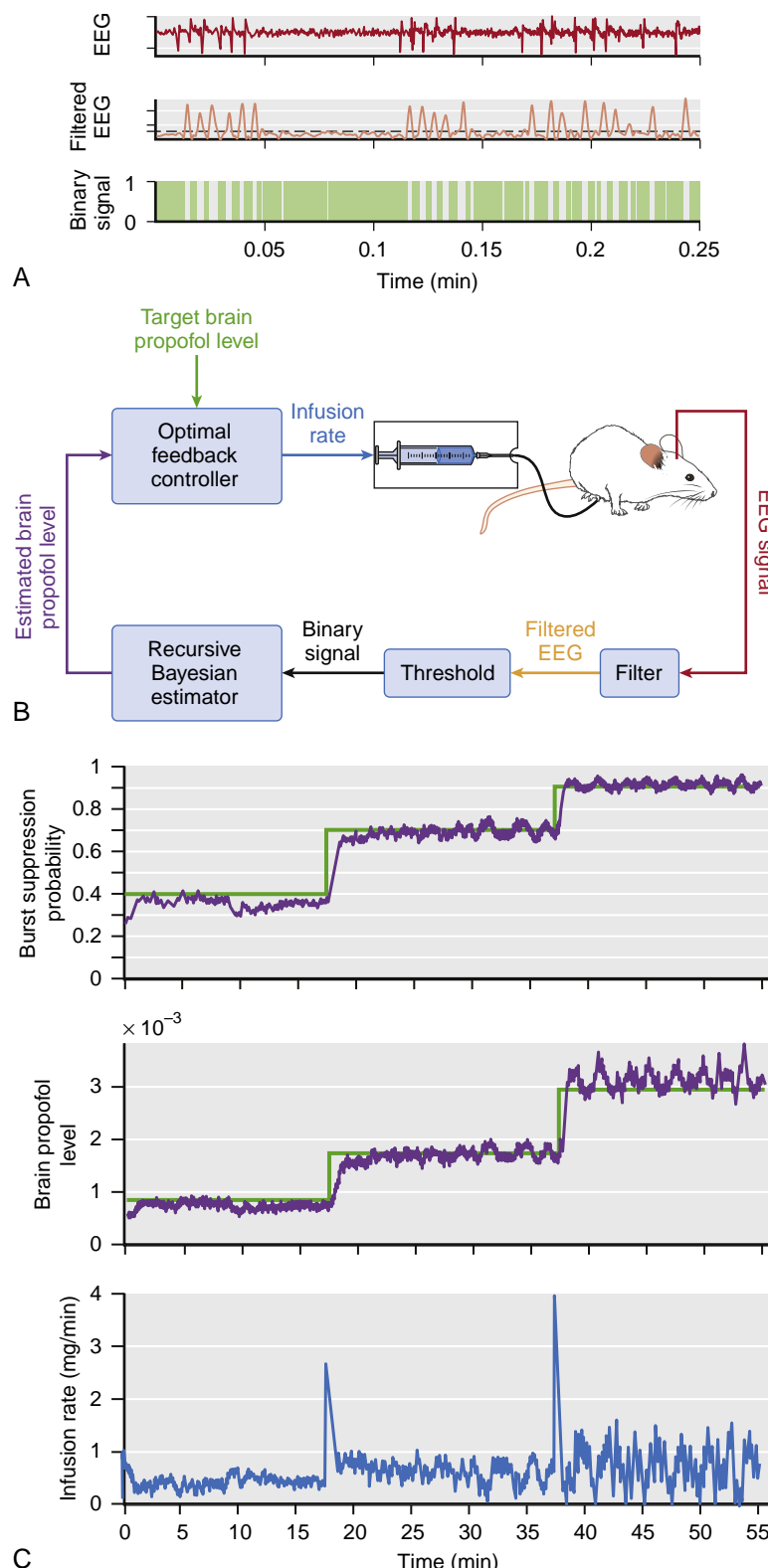


Fig. 40.12 An experimental closed loop anesthetic delivery system for control of medical coma by controlling burst suppression. (A) The electroencephalogram (EEG) of the rat in burst suppression is filtered, thresholded, and converted into binary observations (i.e., 0 for a burst and 1 for a suppression). (B) A target brain level of propofol is set by specifying a burst suppression probability. The Bayesian algorithm estimates the brain level of propofol from the EEG. The controller compares the estimated propofol level with the target level and adjusts the infusion rate every second to maintain the specified target burst suppression probability or, equivalently, the target brain propofol level. (C) The top panel shows that the target burst suppression probability (green line) was maintained at 0.4 for 20 minutes, changed to 0.7 for 20 minutes, and then changed to 0.9 for 15 minutes. The estimated burst suppression probability (purple curve) tracks exactly the targeted level. The middle panel shows the equivalent close tracking of the target brain propofol level (green line) by the estimated propofol level (purple curve). The bottom panel shows how the controller instantaneously changed the infusion rate to maintain the targeted level of burst suppression. This experimental study establishes the feasibility of real-time control of burst suppression and most likely other states of general anesthesia. (Redrawn from Shafechi M, Chemali JJ, Liberman M, et al. A brain-machine interface for control of medically-induced coma. *PLoS Comput Biol*. 2013;9:e1003284.)

CLOSED-LOOP ANESTHETIC DELIVERY SYSTEMS

Closed-loop anesthetic delivery (CLAD) systems for maintenance of general anesthesia and sedation have been proposed since the early 1950s. These studies have been summarized.^{122,123} The CLAD systems work by using an EEG marker of anesthetic state to define a desired state for maintenance during surgery. The EEG is monitored, the marker is computed from the EEG, and a computer-controlled infusion delivering the anesthetic drug is automatically changed based on the difference between the targeted level of the EEG marker and the actual level of the marker computed from the EEG analysis. Although numerous EEG markers have been used to guide delivery of anesthetics in CLAD systems, the most widely used marker is the BIS index.^{25,124} Use of the BIS requires a 20- to 30-second delay in computing updates.²⁴ Use of a CLAD system leads to maintenance of the desired anesthetic state while delivering significantly less anesthetic drug.^{25,125-127} Although most CLAD systems have focused on maintenance of unconsciousness, a recently developed control system has studied maintenance of unconsciousness and antinociception.^{128,129}

Recent simulation studies using rodent and human models, as well as recent experimental studies in rodents, have shown that highly reliable and accurate CLAD systems can be devised to maintain medical coma by using burst suppression (see Fig. 40.2 F) as the control variable.^{122,123} A CLAD system developed by Shanechi and colleagues¹³⁰ uses a stochastic control framework and, as the control variable, the burst suppression probability, which is the instantaneous probability that the brain is suppressed (Fig. 40.12).¹¹⁰ The burst suppression probability is a more reliable way to track burst suppression than the suppression ratio. The CLAD system precisely tracked the target level of burst suppression. If these results are successfully reproduced in human studies, the CLAD system could offer an automatic and highly efficient way to maintain medical coma in the many patients who require this therapy for multiple days to treat intractable status epilepticus or intracranial hypertension.

Several clinical studies have recently demonstrated the feasibility of CLAD systems as a means of controlling level of unconsciousness alone, level of unconsciousness and antinociception, and level of unconsciousness and volume status.¹³¹⁻¹³³ All of these studies have been conducted outside of the United States, as the FDA has not approved any CLAD system for administering general anesthesia. Many new findings and approaches will probably be reported in the near future because the study of CLAD systems is an active area of research by many investigators.

MONITORING ANTINOCICEPTION

The discussion of monitoring brain states under general anesthesia and sedation has focused largely on monitoring level of unconsciousness. Monitoring antinociception is an important, growing area of investigation. In the introduction, we modified the definition of general anesthesia given previously by Brown and colleagues¹ by substituting antinociception for analgesia.³ We did so to make a precise distinction between the concept of nociception, which is transmission of potentially harmful and noxious stimuli through the sensory system, and pain, which is conscious processing of nociceptive information. When a patient

is unconscious under general anesthesia, the anesthesia care provider is managing nociception, whereas when the patient is awake at the end of surgery, the care provider is managing pain. Antinociception is therefore the extent to which anesthetic and analgesic agents impede the flow of information regarding harmful and noxious stimuli through the nervous system.

At present, movement and the physiological responses of changes in heart rate, blood pressure, and perhaps respiratory rate, are the most commonly used markers of nociception. The changes in these physiological markers are a consequence of the NMA circuit responses to nociceptive information transmission in the central nervous system (see Fig. 40.1). Investigations are using multiple physiologic parameters including heart rate, heart rate variability (0.15-0.4 Hz band power), plethysmograph wave amplitude, skin conductance, skin conductance fluctuations, and the derivatives of these signals to track antinociception.^{134,135} In addition, nociception can be tracked by using infrared pupillometry to record pupillary activity.¹³⁶ Commercial monitors that track level of antinociception by monitoring physiologic variables are now commercially available.¹³⁷⁻¹⁴⁰ A recent report suggests that monitoring simultaneously unconsciousness and antinociception together allows the implementation of more principled multimodal strategies for choosing and administering anesthetic combinations.³ This new strategy offers the potential to achieve better nociceptive control intraoperatively and pain control postoperatively, and to reduce the likelihood of postoperative cognitive dysfunction and opioid overuse.

 Complete references available online at expertconsult.com.

References

1. Brown EN, et al. *N Engl J Med*. 2010;363:2638-2650.
2. Cellular and molecular mechanisms of anesthesia. In: Evers AS, PG Barash, BF Cullen, RK Stoelting ed. *Clinical Anesthesia*. 3rd ed. Philadelphia: Lippincott-Raven; 1997.
3. Brown EN, et al. *Anesth Analg*. 2018; 127: 1246-1258.
4. Posner J, et al. Oxford University Press; 2007.
5. Cote CJ, et al. *Anesthesiology*. 1981;55:703-705.
6. Feldman JL, Del Negro CA. *Nat Rev Neurosci*. 2006;7:232-242.
7. Palanca BJ, et al. *Curr Opin Anaesthesiol*. 2009;22:553-559.
8. Prys-Roberts C. *Br J Anaesth*. 1987;59:1341-1345.
9. Price DD. *Science*. 2000;288:1769-1772.
10. Purves D, et al. *Neuroscience*. 4th ed. Sunderland, MA: Sinauer Associates, Inc.; 2008.
11. Kertai MD, et al. *Anesth Analg*. 2012;114:533-546.
12. Pfaff D. Cambridge: Harvard University Press; 2005.
13. Giacino JT, et al. *Neurology*. 2002;58:349-353.
14. Giacino JT, et al. *Arch Phys Med Rehabil*. 2004;85:2020-2029.
15. Storm H. *Curr Opin Anaesthesiol*. 2008;21:796-804.
16. Bennett C, et al. *Anesth Analg*. 2009;109:539-550.
17. Gibbs FA, et al. *Arch Intern Med*. 1937;60:154-166.
18. Kiersey DK, et al. *Br J Anaesth*. 1951;23:141-152.
19. Kearse Jr LA, et al. *Anesthesiology*. 1994;81:1365-1370.
20. Glass PS, et al. *Anesthesiology*. 1997;86:836-847.
21. Rampil IJ. *Anesthesiology*. 1998;89:980-1002.
22. Kelley SD. *Monitoring Consciousness: Using the Bispectral Index*. 2nd ed. Boulder, CO: Covidien; 2010.
23. Bruhn J, et al. *J Clin Mon Comp*. 2000;16:593-596.
24. Pilge S, et al. *Anesthesiology*. 2006;104:488-494.
25. Struys MM, et al. *Anesthesiology*. 2001;95:6-17.
26. Purdon PL, et al. *Anesthesiology*. 2015;123:937-960.
27. Hayashi K, et al. *Br J Anaesth*. 2007;99:389-395.
28. Yamamura T, et al. *Anesth Analg*. 1981;60:283-288.
29. Foster BL, Liley DT. *Anesth Analg*. 2011;113:758-765.
30. Ozcan MS, et al. *J Neurosurg Anesthesiol*. 2010;22:309-315.

31. Pavone KJ, et al. *Clin Neurophysiol*. 2016;127:556–564.
32. Sleigh JW, et al. *Anesth Analg*. 2018;127:951–959.
33. Xi C, et al. *PLoS One*. 2018;13:e0199120.
34. Huupponen E, et al. *Acta Anaesthesiol Scand*. 2008;52:289–294.
35. Aksu R, et al. *Paediatr Anaesth*. 2011;21:373–378.
36. Mason KP, et al. *Paediatr Anaesth*. 2009;19:1175–1183.
37. Akeju O, et al. *Br J Anaesth*. 2015;115(suppl 1):i66–i76.
38. Lee JM, et al. *Anesthesiology*. 2017;127:293–306.
39. Myles PS, et al. *Lancet*. 2004;363:1757–1763.
40. Avidan MS, et al. *N Engl J Med*. 2008;358:1097–1108.
41. Avidan MS, et al. *N Engl J Med*. 2011;365:591–600.
42. Myles PS, et al. *N Engl J Med*. 2008;359:428–429; author reply 30–1.
43. Brown EN, et al. *Annu Rev Neurosci*. 2011;34:601–628.
44. Purdon PL, et al. *Proc Natl Acad Sci U S A*. 2013;110:E1142–E1151.
45. Prichep LS, et al. *Br J Anaesth*. 2004;92:393–399.
46. Drover D, Ortega HR. *Best Pract Res Clin Anaesthesiol*. 2006;20:121–128.
47. Tinker JH, et al. *Anesthesiology*. 1977;46:252–259.
48. Kochs E, et al. *Anesthesiology*. 1994;80:1026–1034.
49. Cimenser A, et al. *Proc Natl Acad Sci U S A*. 2011;108:8832–8837.
50. Chen X, et al. *Anesth Analg*. 2002;95:1669–1674, table of contents.
51. Soehle M, et al. *Br J Anaesth*. 2010;105:172–178.
52. Adesanya AO, et al. *J Crit Care*. 2009;24:322–328.
53. Schultz B, et al. *Anaesthetist*. 2003;52:1143–1148.
54. Kreuer S, Wilhelm W. *Best Pract Res Clin Anaesthesiol*. 2006;20:111–119.
55. Schneider G, et al. *Br J Anaesth*. 2003;91:329–335.
56. Schneider G, et al. *Anesthesiology*. 2004;101:1105–1111.
57. Bruhn J, et al. *Anesthesiology*. 2001;95:30–35.
58. Viertio-Oja H, et al. *Acta Anaesthesiol Scand*. 2004;48:154–161.
59. Jantti V, Alahuhta S. *Br J Anaesth*. 2004;93:150–151; author reply 1–2.
60. Bein B. *Best Pract Res Clin Anaesthesiol*. 2006;20:101–109.
61. Gruenewald M, et al. *Anesthesia*. 2007;62:1224–1229.
62. Eger 2nd EI, et al. *Anesthesiology*. 1965;26:756–763.
63. Stoelting RK, et al. *Anesthesiology*. 1970;33:5–9.
64. Solt K, Forman SA. *Curr Opin Anaesthesiol*. 2007;20:300–306.
65. Rampil IJ, Laster MJ. *Anesthesiology*. 1992;77:920–925.
66. Antognini JF, Schwartz K. *Anesthesiology*. 1993;79:1244–1249.
67. Rampil IJ. *Anesthesiology*. 1994;80:606–610.
68. Anderson RE, Jakobsson JG. *Eur J Anaesthesiol*. 2006;23:208–212.
69. Schmidt GN, et al. *Anesthesia*. 2005;60:228–234.
70. Kreuer S, et al. *Br J Anaesth*. 2003;91:336–340.
71. Friedman EB, et al. *PLoS One*. 2010;5:e11903.
72. Joiner WJ, et al. *PLoS Genet*. 2013;9:e1003605.
73. Hirschberg R, Giacino JT. *Neurol Clin*. 2011;29:773–786.
74. Alkire MT, et al. *Science*. 2008;322:876–880.
75. Hudetz AG. *Brain Connect*. 2012;2:291–302.
76. Langsjo JW, et al. *J Neurosci*. 2012;32:4935–4943.
77. Mhuircheartaigh RN, et al. *J Neurosci*. 2010;30:9095–9102.
78. Breshears JD, et al. *Proc Natl Acad Sci U S A*. 2010;107:21170–21175.
79. Hemmings Jr HC, et al. *Trends Pharmacol Sci*. 2005;26:503–510.
80. Bickford RG, et al. *Trans Am Neurol Assoc*. 1971;96:118–122.
81. Fleming RA, Smith NT. *Anesthesiology*. 1979;50:456–460.
82. Bai D, et al. *J Neurosci*. 1999;19:10635–10646.
83. Feshchenko VA, et al. *Neuropsychobiology*. 2004;50:257–266.
84. Lewis LD, et al. *Proc Natl Acad Sci U S A*. 2012;109:E3377–E3386.
85. Li D, et al. *Anesthesiology*. 2013;119:81–88.
86. Ching S, et al. *Proc Natl Acad Sci U S A*. 2010;107:22665–22670.
87. Sopelta AE, et al. *PLoS Comput Biol*. 2017;13:e1005879.
88. Sinner B, Graf BM. *Handb Exp Pharmacol*. 2008;31:3–33.
89. Olney JW, Farber NB. *Arch Gen Psychiatry*. 1995;52:998–1007.
90. Seamans J. *Nat Chem Biol*. 2008;4:91–93.
91. Lee U, et al. *Anesthesiology*. 2013;118:1264–1275.
92. Tsuda N, et al. *Acta Anaesthesiol Scand*. 2007;51:472–481.
93. Correa-Sales C, et al. *Anesthesiology*. 1992;76:948–952.
94. Chiu TH, et al. *Eur J Pharmacol*. 1995;285:261–268.
95. Mizobe T, et al. *J Clin Invest*. 1996;98:1076–1080.
96. Jorm CM, Stamford JA. *Br J Anaesth*. 1993;71:447–449.
97. Nacif-Coelho C, et al. *Anesthesiology*. 1994;81:1527–1534.
98. Nelson LE, et al. *Anesthesiology*. 2003;98:428–436.
99. Saper CB, et al. *Nature*. 2005;437:1257–1263.
100. Sherin JE, et al. *J Neurosci*. 1998;18:4705–4721.
101. Moraarty S, et al. *Neuroscience*. 2004;123:451–457.
102. Scheinin A, et al. *Anesthesiology*. 2018;129:22–36.
103. Avramov MN, et al. *Anesth Analg*. 1990;70:369–374.
104. HagiHIRA S, et al. *Anesth Analg*. 2012;115:572–577.
105. Mennerick S, et al. *J Neurosci*. 1998;18:9716–9726.
106. Jevtic-Todorovic V, et al. *Nat Med*. 1998;4:460–463.
107. Boon JA, Milsom WK. *Resp Phys Neurobiol*. 2008;162:63–72.
108. Cornelissen L, et al. *Elife*. 2015;4:e06513.
109. Cornelissen L, et al. *Br J Anaesth*. 2018;120:1274–1286.
110. Purdon PL. In: Benasich AA, Ribary U, eds. *Emergent Brain Dynamics: Prebirth to Adolescence*. Cambridge, MA: MIT Press; 2018.
111. McCarthy MM, et al. *J Neurosci*. 2008;28:13488–13504.
112. Flores FJ, et al. *Proc Natl Acad Sci U S A*. 2017;114:E6660–E6668.
113. Brown EN, Purdon PL. *Curr Opin Anaesthesiol*. 2013;26:414–419.
114. Martin JT, et al. *Anesthesiology*. 1959;20:359–376.
115. Wildes TS, et al. *BMJ Open*. 2016;6:e011505.
116. Levy WJ. *Anesthesiology*. 1984;60:430–434.
117. Drover DR, et al. *J Clin Mon Comp*. 2011;25:175–181.
118. Ching S, et al. *Proc Natl Acad Sci U S A*. 2012;109:3095–3100.
119. Vijayan S, et al. *J Neurosci*. 2013;33:11070–11075.
120. Ku SW, et al. *PLoS One*. 2011;6:e25155.
121. Casali AG, et al. *Sci Transl Med*. 2013;5:198ra05.
122. Ching S, et al. *Anesthesiology*. 2013.
123. Liberman MY, et al. *J Neural Eng*. 2013;10:046004.
124. Mortier E, et al. *Anesthesia*. 1998;53:749–754.
125. Agarwal J, et al. *Acta Anaesthesiol Scand*. 2009;53:390–397.
126. Puri GD, et al. *Anaesth Intensive Care*. 2007;35:357–362.
127. Hemmerling TM, et al. *Can J Anaesth*. 2010;57:725–735.
128. Liu N, et al. *Anesth Analg*. 2011;112:546–557.
129. Liu N, et al. *Anesthesiology*. 2012;116:286–295.
130. Shanchei M, et al. *PLoS Comp Bio*. 2013.
131. Dutta A, et al. *Anesth Analg*. 2018.
132. Joosten A, et al. *Anesth Analg*. 2018.
133. West N, et al. *Anesth Analg*. 2018;127:883–894.
134. Ben-Israel N, et al. *J Clin Mon Comp*. 2013.
135. Ledowski T, et al. *Anesthesia*. 2010;65:1001–1006.
136. Neice AE, et al. *Anesth Analg*. 2017;124:915–921.
137. The Dolosys Paintracker. (Accessed June 29, 2017, at <http://www.dolosys.de/Products-EN.htm>.)
138. ANI (Analgesia Nociception Index). (Accessed June 29, 2017, at <https://www.mdoloris.com/en/technologies/ani-analgesia-nociception-index/>.)
139. Storm H. Med-Storm, PainMonitorTM. 2016.
140. Huiku M, et al. *Surgical Plethysmographic Index (SPI) in Anesthesia Practice*; 2014.

References

1. Brown EN, Lydic R, Schiff ND. General anesthesia, sleep, and coma. *N Engl J Med*. 2010;363:2638–2650.
2. Cellular and molecular mechanisms of anesthesia. In: Evers AS, PG Barash, BF Cullen, RK Stoelting ed. *Clinical Anesthesia*. 3rd ed. Philadelphia: Lippincott-Raven; 1997.
3. Brown EN, Pavone KJ, Naranjo M. Multimodal general anesthesia: theory and practice. *Anesth Analg*. 2018;127: 1246–1258.
4. Posner J, Saper C, Schiff N, Plum F. *Plum and Posner's Diagnosis of Stupor and Coma*. Oxford University Press; 2007.
5. Cote CJ, Goudsouzian NG, Liu LM, Dedrick DF, Rosow CE. The dose response of intravenous thiopental for the induction of general anesthesia in unpremedicated children. *Anesthesiology*. 1981;55: 703–705.
6. Feldman JL, Del Negro CA. Looking for inspiration: new perspectives on respiratory rhythm. *Nat Rev Neurosci*. 2006;7:232–242.
7. Palanca BJ, Mashour GA, Avidan MS. Processed electroencephalogram in depth of anesthesia monitoring. *Curr Opin Anesthesiol*. 2009;22:553–559.
8. Prys-Roberts C. Anaesthesia: a practical or impractical construct? *Br J Anaesth*. 1987;59:1341–1345.
9. Price DD. Psychological and neural mechanisms of the affective dimension of pain. *Science*. 2000;288:1769–1772.
10. Purves D, Augustine GJ, Hall WC, Lamantia A, McNamara JO, White LE. *Neuroscience*. 4th ed. Sunderland, MA: Sinauer Associates, Inc.; 2008.
11. Kertai MD, Whitlock EL, Avidan MS. Brain monitoring with electroencephalography and the electroencephalogram-derived bispectral index during cardiac surgery. *Anesth Analg*. 2012;114:533–546.
12. Pfaff D. *Brain Arousal and Information Theory: Neural and Genetic Mechanisms*. Cambridge: Harvard University Press; 2005.
13. Giacino JT, Ashwal S, Childs N, et al. The minimally conscious state: definition and diagnostic criteria. *Neurology*. 2002;58:349–353.
14. Giacino JT, Kalmar K, Whyte J. The JFK Coma Recovery Scale-Revised: measurement characteristics and diagnostic utility. *Arch Phys Med Rehabil*. 2004;85:2020–2029.
15. Storm H. Changes in skin conductance as a tool to monitor nociceptive stimulation and pain. *Curr Opin Anesthesiol*. 2008;21: 796–804.
16. Bennett C, Voss LJ, Barnard JP, Sleigh JW. Practical use of the raw electroencephalogram waveform during general anesthesia: the art and science. *Anesth Analg*. 2009;109:539–550.
17. Gibbs FA, Gibbs LE, Lennox WG. Effects on the electroencephalogram of certain drugs which influence nervous activity. *Arch Intern Med*. 1937;60:154–166.
18. Kiersey DK, Bickford RG, Faulconer Jr A. Electro-encephalographic patterns produced by thiopental sodium during surgical operations: description and classification. *Br J Anaesth*. 1951;23:141–152.
19. Kearse Jr LA, Manberg P, Chamoun N, deBros F, Zaslavsky A. Bispectral analysis of the electroencephalogram correlates with patient movement to skin incision during propofol/nitrous oxide anesthesia. *Anesthesiology*. 1994;81:1365–1370.
20. Glass PS, Bloom M, Kearse L, Rosow C, Sebel P, Manberg P. Bispectral analysis measures sedation and memory effects of propofol, midazolam, isoflurane, and alfentanil in healthy volunteers. *Anesthesiology*. 1997;86:836–847.
21. Rampil IJ. A primer for EEG signal processing in anesthesia. *Anesthesiology*. 1998;89:980–1002.
22. Kelley SD. *Monitoring Consciousness: Using the Bispectral Index*. 2nd ed. Boulder, CO: Covidien; 2010.
23. Bruhn J, Bouillon TW, Shafer SL. Bispectral index (BIS) and burst suppression: revealing a part of the BIS algorithm. *J Clin Mon Comp*. 2000;16:593–596.
24. Pilge S, Zanner R, Schneider G, Blum J, Kreuzer M, Kochs EF. Time delay of index calculation: analysis of cerebral state, bispectral, and narcotrend indices. *Anesthesiology*. 2006;104:488–494.
25. Struys MM, De Smet T, Versichelen LF, Van De Velde S, Van den Broecke R, Mortier EP. Comparison of closed-loop controlled administration of propofol using bispectral index as the controlled variable versus “standard practice” controlled administration. *Anesthesiology*. 2001;95:6–17.
26. Purdon PL, Sampson A, Pavone KJ, Brown EN. Clinical electroencephalography for anesthesiologists: part I: background and basic signatures. *Anesthesiology*. 2015;123:937–960.
27. Hayashi K, Tsuda N, Sawa T, Hagihira S. Ketamine increases the frequency of electroencephalographic bicoherence peak on the alpha spindle area induced with propofol. *Br J Anaesth*. 2007;99:389–395.
28. Yamamura T, Fukuda M, Takeya H, Goto Y, Furukawa K. Fast oscillatory EEG activity induced by analgesic concentrations of nitrous oxide in man. *Anesth Analg*. 1981;60:283–288.
29. Foster BL, Liley DT. Nitrous oxide paradoxically modulates slow electroencephalogram oscillations: implications for anesthesia monitoring. *Anesth Analg*. 2011;113:758–765.
30. Ozcan MS, Ozcan MD, Khan QS, Thompson DM, Chetty PK. Does nitrous oxide affect bispectral index and state entropy when added to a propofol versus sevoflurane anesthetic? *J Neurosurg Anesthesiol*. 2010;22:309–315.
31. Pavone KJ, Akeju O, Sampson AL, Ling K, Purdon PL, Brown EN. Nitrous oxide-induced slow and delta oscillations. *Clin Neurophysiol*. 2016;127:556–564.
32. Sleigh JW, Vacas S, Flexman AM, Talke PO. Electroencephalographic arousal patterns under dexmedetomidine sedation. *Anesth Analg*. 2018;127:951–959.
33. Xi C, Sun S, Pan C, Ji F, Cui X, Li T. Different effects of propofol and dexmedetomidine sedation on electroencephalogram patterns: Wakefulness, moderate sedation, deep sedation and recovery. *PLoS One*. 2018;13:e0199120.
34. Huupponen E, Maksimow A, Lapinlampi P, et al. Electroencephalogram spindle activity during dexmedetomidine sedation and physiological sleep. *Acta Anaesthesiol Scand*. 2008;52:289–294.
35. Aksu R, Kumandas S, Akin A, et al. The comparison of the effects of dexmedetomidine and midazolam sedation on electroencephalography in pediatric patients with febrile convulsion. *Paediatr Anaesth*. 2011;21:373–378.
36. Mason KP, O'Mahony E, Zurakowski D, Libenson MH. Effects of dexmedetomidine sedation on the EEG in children. *Paediatr Anaesth*. 2009;19:1175–1183.
37. Akeju O, Pavone KJ, Thum JA, et al. Age-dependency of sevoflurane-induced electroencephalogram dynamics in children. *Br J Anaesth*. 2015;115(suppl 1):i66–i76.
38. Lee JM, Akeju O, Terzakis K, et al. A prospective study of age-dependent changes in propofol-induced electroencephalogram oscillations in children. *Anesthesiology*. 2017;127:293–306.
39. Myles PS, Leslie K, McNeil J, Forbes A, Chan MT. Bispectral index monitoring to prevent awareness during anaesthesia: the B-Aware randomised controlled trial. *Lancet*. 2004;363:1757–1763.
40. Avidan MS, Zhang L, Burnside BA, et al. Anesthesia awareness and the bispectral index. *N Engl J Med*. 2008;358:1097–1108.
41. Avidan MS, Jacobsohn E, Glick D, et al. Prevention of intraoperative awareness in a high-risk surgical population. *N Engl J Med*. 2011;365:591–600.
42. Myles PS, Leslie K, Forbes A. Anesthesia awareness and the bispectral index. *N Engl J Med*. 2008;359:428–429; author reply 30–31.
43. Brown EN, Purdon PL, Van Dort CJ. General anesthesia and altered states of arousal: a systems neuroscience analysis. *Annu Rev Neurosci*. 2011;34:601–628.
44. Purdon PL, Pierce ET, Mukamel EA, et al. Electroencephalogram signatures of loss and recovery of consciousness from propofol. *Proc Natl Acad Sci U S A*. 2013;110:E1142–E1151.
45. Prichard LS, Gugino LD, John ER, et al. The Patient State Index as an indicator of the level of hypnosis under general anaesthesia. *Br J Anaesth*. 2004;92:393–399.
46. Drover D, Ortega HR. Patient state index. *Best Pract Res Clin Anesthesiol*. 2006;20:121–128.
47. Tinker JH, Sharbrough FW, Michenfelder JD. Anterior shift of the dominant EEG rhythm during anesthesia in the Java monkey: correlation with anesthetic potency. *Anesthesiology*. 1977;46: 252–259.
48. Kochs E, Bischoff P, Pichlmeier U, Schulte am Esch J. Surgical stimulation induces changes in brain electrical activity during isoflurane/nitrous oxide anesthesia. A topographic electroencephalographic analysis. *Anesthesiology*. 1994;80:1026–1034.
49. Cimencer A, Purdon PL, Pierce ET, et al. Tracking brain states under general anesthesia by using global coherence analysis. *Proc Natl Acad Sci U S A*. 2011;108:8832–8837.
50. Chen X, Tang J, White PF, et al. A comparison of patient state index and bispectral index values during the perioperative period. *Anesth Analg*. 2002;95:1669–1674, table of contents.

51. Soehle M, Kuech M, Grube M, et al. Patient state index vs bispectral index as measures of the electroencephalographic effects of propofol. *Br J Anaesth.* 2010;105:172–178.
52. Adesanya AO, Rosero E, Wyrick C, Wall MH, Joshi GP. Assessing the predictive value of the bispectral index vs patient state index on clinical assessment of sedation in postoperative cardiac surgery patients. *J Crit Care.* 2009;24:322–328.
53. Schultz B, Kreuer S, Wilhelm W, Grouven U, Schultz A. [The Narcotrend monitor. Development and interpretation algorithms]. *Anaesthesia.* 2003;52:1143–1148.
54. Kreuer S, Wilhelm W. The Narcotrend monitor. *Best Pract Res Clin Anaesthesiol.* 2006;20:111–119.
55. Schneider G, Gelb AW, Schmeller B, Tschakert R, Kochs E. Detection of awareness in surgical patients with EEG-based indices--bispectral index and patient state index. *Br J Anaesth.* 2003;91:329–335.
56. Schneider G, Kochs EF, Horn B, Kreuzer M, Ningler M. Narcotrend does not adequately detect the transition between awareness and unconsciousness in surgical patients. *Anesthesiology.* 2004;101:1105–1111.
57. Bruhn J, Lehmann LE, Ropcke H, Bouillon TW, Hoeft A. Shannon entropy applied to the measurement of the electroencephalographic effects of desflurane. *Anesthesiology.* 2001;95:30–35.
58. Viertho-Oja H, Maja V, Sarkela M, et al. Description of the entropy algorithm as applied in the Datex-Ohmeda S/5 Entropy Module. *Acta Anaesthesiol Scand.* 2004;48:154–161.
59. Jantti V, Alahuhta S. Spectral entropy--what has it to do with anaesthesia, and the EEG? *Br J Anaesth.* 2004;93:150–151; author reply 1–2.
60. Bein B. Entropy. *Best Pract Res Clin Anaesthesiol.* 2006;20:101–109.
61. Gruenewald M, Zhou J, Schloemerkemper N, et al. M-Entropy guidance vs standard practice during propofol-remifentanil anaesthesia: a randomised controlled trial. *Anaesthesia.* 2007;62:1224–1229.
62. Eger 2nd EI, Saidman LJ, Brandstater B. Minimum alveolar anesthetic concentration: a standard of anesthetic potency. *Anesthesiology.* 1965;26:756–763.
63. Stoelting RK, Longnecker DE, Eger 2nd EI. Minimum alveolar concentrations in man on awakening from methoxyflurane, halothane, ether and fluroxene anesthesia: MAC awake. *Anesthesiology.* 1970;33:5–9.
64. Solt K, Forman SA. Correlating the clinical actions and molecular mechanisms of general anesthetics. *Curr Opin Anaesthesiol.* 2007;20:300–306.
65. Rampil IJ, Lester MJ. No correlation between quantitative electroencephalographic measurements and movement response to noxious stimuli during isoflurane anesthesia in rats. *Anesthesiology.* 1992;77:920–925.
66. Antognini JF, Schwartz K. Exaggerated anesthetic requirements in the preferentially anesthetized brain. *Anesthesiology.* 1993;79:1244–1249.
67. Rampil IJ. Anesthetic potency is not altered after hypothermic spinal cord transection in rats. *Anesthesiology.* 1994;80:606–610.
68. Anderson RE, Jakobsson JG. Cerebral State Monitor, a new small handheld EEG monitor for determining depth of anaesthesia: a clinical comparison with the bispectral index during day-surgery. *Eur J Anaesthesiol.* 2006;23:208–212.
69. Schmidt GN, Bischoff P, Standl T, et al. SNAP index and bispectral index during different states of propofol/remifentanil anaesthesia. *Anaesthesia.* 2005;60:228–234.
70. Kreuer S, Bruhn J, Larsen R, Hoepstein M, Wilhelm W. Comparison of Alaris AEP index and bispectral index during propofol-remifentanil anaesthesia. *Br J Anaesth.* 2003;91:336–340.
71. Friedman EB, Sun Y, Moore JT, et al. A conserved behavioral state barrier impedes transitions between anesthetic-induced unconsciousness and wakefulness: evidence for neural inertia. *PLoS One.* 2010;5:e11903.
72. Joiner WJ, Friedman EB, Hung HT, et al. Genetic and anatomical basis of the barrier separating wakefulness and anesthetic-induced unresponsiveness. *PLoS Genet.* 2013;9:e1003605.
73. Hirschberg R, Giacino JT. The vegetative and minimally conscious states: diagnosis, prognosis and treatment. *Neurol Clin.* 2011;29:773–786.
74. Alkire MT, Hudetz AG, Tononi G. Consciousness and anesthesia. *Science.* 2008;322:876–880.
75. Hudetz AG. General anesthesia and human brain connectivity. *Brain Connect.* 2012;2:291–302.
76. Langsjo JW, Alkire MT, Kaskinoro K, et al. Returning from oblivion: imaging the neural core of consciousness. *J Neurosci.* 2012;32:4935–4943.
77. Mhuircheartaigh RN, Rosenorn-Lanng D, Wise R, Jbabdi S, Rogers R, Tracey I. Cortical and subcortical connectivity changes during decreasing levels of consciousness in humans: a functional magnetic resonance imaging study using propofol. *J Neurosci.* 2010;30:9095–9102.
78. Breshears JD, Roland JL, Sharma M, et al. Stable and dynamic cortical electrophysiology of induction and emergence with propofol anesthesia. *Proc Natl Acad Sci U S A.* 2010;107:21170–21175.
79. Hemmings Jr HC, Akabas MH, Goldstein PA, Trudell JR, Orser BA, Harrison NL. Emerging molecular mechanisms of general anesthetic action. *Trends Pharmacol Sci.* 2005;26:503–510.
80. Bickford RG, Fleming N, Billinger T. Compression of EEG data. *Trans Am Neurol Assoc.* 1971;96:118–122.
81. Fleming RA, Smith NT. An inexpensive device for analyzing and monitoring the electroencephalogram. *Anesthesiology.* 1979;50:456–460.
82. Bai D, Pennefather PS, MacDonald JF, Orser BA. The general anesthetic propofol slows deactivation and desensitization of GABA(A) receptors. *J Neurosci.* 1999;19:10635–10646.
83. Feshchenko VA, Veselis RA, Reinsel RA. Propofol-induced alpha rhythm. *Neuropsychobiology.* 2004;50:257–266.
84. Lewis LD, Weiner VS, Mukamel EA, et al. Rapid fragmentation of neuronal networks at the onset of propofol-induced unconsciousness. *Proc Natl Acad Sci U S A.* 2012;109:E3377–E3386.
85. Li D, Voss LJ, Sleigh JW, Li X. Effects of volatile anesthetic agents on cerebral cortical synchronization in sheep. *Anesthesiology.* 2013;119:81–88.
86. Ching S, Cimenser A, Purdon PL, Brown EN, Kopell NJ. Thalamocortical model for a propofol-induced alpha-rhythm associated with loss of consciousness. *Proc Natl Acad Sci U S A.* 2010;107:22665–22670.
87. Sopelta AE, McCarthy MM, Sherfey J, et al. Thalamocortical control of propofol phase-amplitude coupling. *PLoS Comput Biol.* 2017;13:e1005879.
88. Sinner B, Graf BM. Ketamine. *Handb Exp Pharmacol.* 2008;313–333.
89. Olney JW, Farber NB. Glutamate receptor dysfunction and schizophrenia. *Arch Gen Psychiatry.* 1995;52:998–1007.
90. Seamans J. Losing inhibition with ketamine. *Nat Chem Biol.* 2008;4:91–93.
91. Lee U, Ku S, Noh G, Baek S, Choi B, Mashour GA. Disruption of frontal-parietal communication by ketamine, propofol, and sevoflurane. *Anesthesiology.* 2013;118:1264–1275.
92. Tsuda N, Hayashi K, Hagiwara S, Sawa T. Ketamine, an NMDA-antagonist, increases the oscillatory frequencies of alpha-peaks on the electroencephalographic power spectrum. *Acta Anaesthesiol Scand.* 2007;51:472–481.
93. Correa-Sales C, Rabin BC, Maze M. A hypnotic response to dexmedetomidine, an alpha 2 agonist, is mediated in the locus coeruleus in rats. *Anesthesiology.* 1992;76:948–952.
94. Chiu TH, Chen MJ, Yang YR, Yang JJ, Tang FI. Action of dexmedetomidine on rat locus coeruleus neurones: intracellular recording in vitro. *Eur J Pharmacol.* 1995;285:261–268.
95. Mizobe T, Maghsoudi K, Sitwala K, Tianzhi G, Ou J, Maze M. Antisense technology reveals the alpha2A adrenoceptor to be the subtype mediating the hypnotic response to the highly selective agonist, dexmedetomidine, in the locus coeruleus of the rat. *J Clin Invest.* 1996;98:1076–1080.
96. Jorm CM, Stamford JA. Actions of the hypnotic anaesthetic, dexmedetomidine, on noradrenaline release and cell firing in rat locus coeruleus slices. *Br J Anaesth.* 1993;71:447–449.
97. Nacif-Coelho C, Correa-Sales C, Chang LL, Maze M. Perturbation of ion channel conductance alters the hypnotic response to the alpha 2-adrenergic agonist dexmedetomidine in the locus coeruleus of the rat. *Anesthesiology.* 1994;81:1527–1534.
98. Nelson LE, Lu J, Guo T, Saper CB, Franks NP, Maze M. The alpha2-adrenoceptor agonist dexmedetomidine converges on an endogenous sleep-promoting pathway to exert its sedative effects. *Anesthesiology.* 2003;98:428–436.
99. Saper CB, Scammell TE, Lu J. Hypothalamic regulation of sleep and circadian rhythms. *Nature.* 2005;437:1257–1263.
100. Sherin JE, Elmquist JK, Torrealba F, Saper CB. Innervation of histaminergic tuberomammillary neurons by GABAergic and galaninergic neurons in the ventrolateral preoptic nucleus of the rat. *J Neurosci.* 1998;18:4705–4721.

101. Moraarty S, Rainnie D, McCarley R, Greene R. Disinhibition of ventrolateral preoptic area sleep-active neurons by adenosine: a new mechanism for sleep promotion. *Neuroscience*. 2004;123:451–457.
102. Scheinin A, Kallionpää RE, Li D, et al. Differentiating drug-related and state-related effects of dexmedetomidine and propofol on the electroencephalogram. *Anesthesiology*. 2018;129:22–36.
103. Avramov MN, Shingu K, Mori K. Progressive changes in electroencephalographic responses to nitrous oxide in humans: a possible acute drug tolerance. *Anesth Analg*. 1990;70:369–374.
104. Hagiwira S, Takashina M, Mori T, Mashimo T. The impact of nitrous oxide on electroencephalographic bicoherence during isoflurane anesthesia. *Anesth Analg*. 2012;115:572–577.
105. Mennerick S, Jevtovic-Todorovic V, Todorovic SM, Shen W, Olney JW, Zorumski CF. Effect of nitrous oxide on excitatory and inhibitory synaptic transmission in hippocampal cultures. *J Neurosci*. 1998;18:9716–9726.
106. Jevtovic-Todorovic V, Todorovic SM, Mennerick S, et al. Nitrous oxide (laughing gas) is an NMDA antagonist, neuroprotectant and neurotoxin. *Nat Med*. 1998;4:460–463.
107. Boon JA, Milsom WK. NMDA receptor-mediated processes in the parabrachial/kolliker fuse complex influence respiratory responses directly and indirectly via changes in cortical activation state. *Respir Phys Neurobiol*. 2008;162:63–72.
108. Cornelissen L, Kim SE, Purdon PL, Brown EN, Berde CB. Age-dependent electroencephalogram (EEG) patterns during sevoflurane general anesthesia in infants. *Elife*. 2015;4:e06513.
109. Cornelissen L, Kim SE, Lee JM, Brown EN, Purdon PL, Berde CB. Electroencephalographic markers of brain development during sevoflurane anaesthesia in children up to 3 years old. *Br J Anaesth*. 2018;120:1274–1286.
110. Purdon PL. Anesthesia-induced brain oscillations: a natural experiment in human neurodevelopment. In: Benasich AA, Ribary U, eds. *Emergent Brain Dynamics: Prebirth to Adolescence*. Cambridge, MA: MIT Press; 2018.
111. McCarthy MM, Brown EN, Kopell N. Potential network mechanisms mediating electroencephalographic beta rhythm changes during propofol-induced paradoxical excitation. *J Neurosci*. 2008;28:13488–13504.
112. Flores FJ, Hartnack KE, Fath AB, et al. Thalamocortical synchronization during induction and emergence from propofol-induced unconsciousness. *Proc Natl Acad Sci U S A*. 2017;114:E6660–E6668.
113. Brown EN, Purdon PL. The aging brain and anesthesia. *Curr Opin Anaesthesiol*. 2013;26:414–419.
114. Martin JT, Faulconer Jr A, Bickford RG. Electroencephalography in anesthesiology. *Anesthesiology*. 1959;20:359–376.
115. Wildes TS, Winter AC, Maybrier HR, et al. Protocol for the Electroencephalography Guidance of Anesthesia to Alleviate Geriatric Syndromes (ENGAGES) study: a pragmatic, randomised clinical trial. *BMJ Open*. 2016;6:e011505.
116. Levy WJ. Intraoperative EEG patterns: implications for EEG monitoring. *Anesthesiology*. 1984;60:430–434.
117. Droyer DR, Schmiesing C, Buchin AF, et al. Titration of sevoflurane in elderly patients: blinded, randomized clinical trial, in non-cardiac surgery after beta-adrenergic blockade. *J Clin Mon Comp*. 2011;25:175–181.
118. Ching S, Purdon PL, Vijayan S, Kopell NJ, Brown EN. A neurophysiological-metabolic model for burst suppression. *Proc Natl Acad Sci U S A*. 2012;109:3095–3100.
119. Vijayan S, Ching S, Purdon PL, Brown EN, Kopell NJ. Thalamocortical mechanisms for the anteriorization of alpha rhythms during propofol-induced unconsciousness. *J Neurosci*. 2013;33:11070–11075.
120. Ku SW, Lee U, Noh GJ, Jun IG, Mashour GA. Preferential inhibition of frontal-to-parietal feedback connectivity is a neurophysiologic correlate of general anesthesia in surgical patients. *PLoS One*. 2011;6:e25155.
121. Casali AG, Gosseries O, Rosanova M, et al. A theoretically based index of consciousness independent of sensory processing and behavior. *Sci Transl Med*. 2013;5:198ra05.
122. Ching S, Liberman MY, Chemali JJ, et al. Real-time closed-loop control in a rodent model of medically induced coma using burst suppression. *Anesthesiology*. 2013.
123. Liberman MY, Ching S, Chemali J, Brown EN. A closed-loop anesthetic delivery system for real-time control of burst suppression. *J Neural Eng*. 2013;10:046004.
124. Mortier E, Strauys M, De Smet T, Versichelen L, Rolly G. Closed-loop controlled administration of propofol using bispectral analysis. *Anaesthesia*. 1998;53:749–754.
125. Agarwal J, Puri GD, Mathew PJ. Comparison of closed loop vs. manual administration of propofol using the bispectral index in cardiac surgery. *Acta Anaesthesiol Scand*. 2009;53:390–397.
126. Puri GD, Kumar B, Aveek J. Closed-loop anaesthesia delivery system (CLADS) using bispectral index: a performance assessment study. *Anaesth Intensive Care*. 2007;35:357–362.
127. Hemmerling TM, Charabati S, Zaouter C, Minardi C, Mathieu PA. A randomized controlled trial demonstrates that a novel closed-loop propofol system performs better hypnosis control than manual administration. *Can J Anaesth*. 2010;57:725–735.
128. Liu N, Chazot T, Hamada S, et al. Closed-loop coadministration of propofol and remifentanil guided by bispectral index: a randomized multicenter study. *Anesth Analg*. 2011;112:546–557.
129. Liu N, Le Guen M, Benabbes-Lambert F, et al. Feasibility of closed-loop titration of propofol and remifentanil guided by the spectral M-Entropy monitor. *Anesthesiology*. 2012;116:286–295.
130. Shanechi M, Chemali JJ, Liberman M, Solt K, Brown EN. A brain-machine interface for control of medically-induced coma. *PLoS Comp Bio*. 2013.
131. Dutta A, Sethi N, Sood J, et al. The effect of dexmedetomidine on propofol requirements during anesthesia administered by bispectral index-guided closed-loop anesthesia delivery system: a randomized controlled study. *Anesth Analg*. 2018.
132. Joosten A, Jame V, Alexander B, et al. Feasibility of fully automated hypnosis, analgesia, and fluid management using 2 independent closed-loop systems during major vascular surgery: a pilot study. *Anesth Analg*. 2018.
133. West N, van Heusden K, Gorges M, et al. Design and evaluation of a closed-loop anesthesia system with robust control and safety system. *Anesth Analg*. 2018;127:883–894.
134. Ben-Israel N, Kliger M, Zuckerman G, Katz Y, Edry R. Monitoring the nociception level: a multi-parameter approach. *J Clin Monit Comput*. 2013.
135. Ledowski T, Pascoe E, Ang B, et al. Monitoring of intra-operative nociception: skin conductance and surgical stress index versus stress hormone plasma levels. *Anaesthesia*. 2010;65:1001–1006.
136. Neice AE, Behrends M, Bokoch MP, Seligman KM, Conrad NM, Larson MD. Prediction of opioid analgesic efficacy by measurement of pupillary unrest. *Anesth Analg*. 2017;124:915–921.
137. The Dolosys Paintracker. (Accessed June, 29, 2017, at <http://www.dolosys.de/Products-EN.htm>.)
138. ANI (Analgesia Nociception Index). (Accessed June 29, 2017, at <http://www.mdoloris.com/en/technologies/ani-analgesia-nociception-index/>.)
139. Storm H. Med-Storm, PainMonitorTM. 2016.
140. Huiku M, Kamppari L, Vierito-Oja H. *Surgical Plethysmographic Index (SPI) in Anesthesia Practice*; 2014.

DAVID W. KACZKA, HOVIG V. CHITILIAN, and MARCOS F. VIDAL MELO

KEY POINTS

- Intraoperative respiratory monitoring is a fundamental component of the American Society of Anesthesiologists' standards for basic anesthetic monitoring. Monitoring of oxygenation and ventilation is essential for the safe conduct of an anesthetic.
- A thorough understanding of the physiological and technological principles underlying respiratory monitoring is essential for its appropriate clinical application.
- The majority of respiratory monitors in clinical use provide information at the systemic and whole-lung level from which inferences are made regarding the regional lung and tissue-level conditions.
- The degree of invasiveness of utilized monitors should be determined by clinical requirements.
- Pulse oximetry is a noninvasive, reliable, and simple method for continuously monitoring the fractional arterial oxygen saturation.
- Ventilation-perfusion mismatch, shunt, and hypoventilation are the most common causes of hypoxemia in the perioperative period. Monitoring of gas exchange, and its response to various interventions, may differentiate etiologies for hypoxemia.
- Mixed venous oxygen saturation ($S\bar{v}O_2$) allows for monitoring of the global balance between oxygen delivery and consumption. Its measurement provides information on gas exchange, cardiac output, and global oxygen consumption.
- Systems utilizing near infrared spectroscopy are used clinically to monitor regional tissue oxygenation, particularly in the brain. The value of regional tissue oxygenation monitoring for clinical management is currently being established.
- Capnography is the primary quantitative method to assess ventilation in the perioperative period. Besides providing physiologic information on ventilation, pulmonary blood flow, and aerobic metabolism, capnography is important for verifying the endotracheal tube positioning, and determining the integrity of the breathing circuit.
- End-tidal carbon dioxide (CO_2) is not always a reliable approximation of arterial CO_2 tension, especially in the presence of significant heterogeneity in the distribution of ventilation and perfusion.
- Measurement of the pressures, flows, and volumes associated with ventilation is necessary to optimize mechanical ventilation, as well as to detect pathophysiologic mechanical derangements of the respiratory system (i.e., increased airway resistance or reduced lung compliance).
- Imaging techniques have emerged as important tools for respiratory monitoring. Lung ultrasonography is increasingly utilized in emergency and perioperative settings, allowing for prompt bedside assessments of pulmonary abnormalities such as pneumothorax, lung edema, consolidation, and pleural effusions. Electrical impedance tomography is another noninvasive imaging technique that provides information on lung aeration and recruitment.
- Current approaches to respiratory monitoring primarily assess pulmonary mechanical and global gas exchange processes. The monitoring of tissue and subcellular respiration remains a desirable goal for future innovation.

Overview of Respiratory Monitoring

Respiratory monitoring is essential to every anesthetic. Its major relevance for maintenance of homeostasis and patient safety is acknowledged by its mandatory position in national and international standards for anesthetic monitoring.^{1,2} Through the decades, advances in respiratory monitoring have resulted in substantial reduction in anesthetic morbidity and mortality, and opened a new era of safe anesthetic practice.³

Respiration is the transport of oxygen (O_2) from the environment to the body cells and the transport of carbon dioxide (CO_2) from those cells to the environment. The concept includes a component of cellular respiration, the process by which cells obtain energy in the form of adenosine triphosphate from the controlled reaction of hydrogen with O_2 to form water.⁴ Thus, in its broadest sense, respiratory monitoring refers to the continuous or periodic assessment of processes involved with the exchange of respiratory gases between the environment and the subcellular pathways where those gases are utilized and produced (Fig. 41.1).⁴

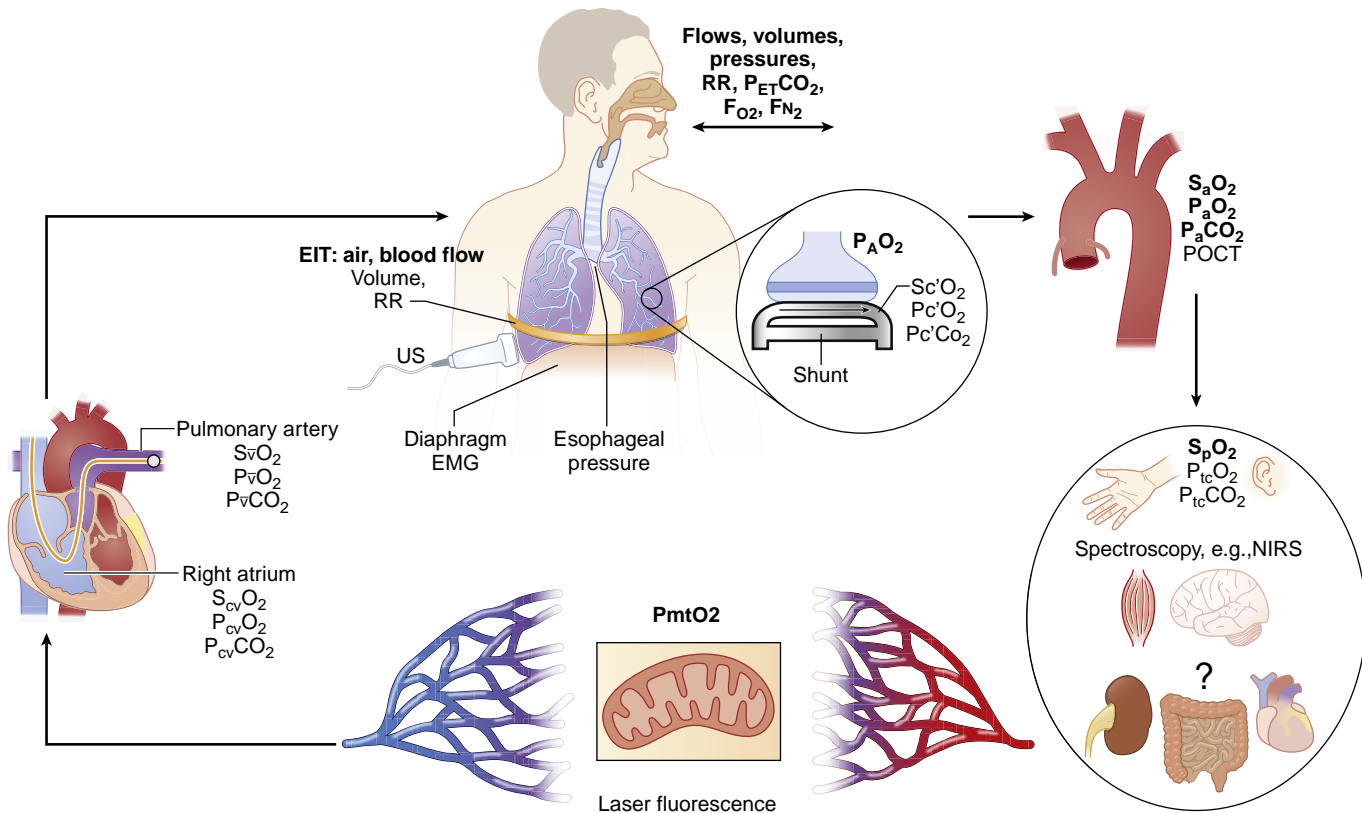


Fig. 41.1 Respiratory Processes and Measurement Sites for Current Respiratory Monitoring Techniques. Most monitored variables are derived from sites at the entrance of the airway and systemic blood (bold) and assess the elements of respiration related to global pulmonary mechanics and gas exchange. Pulse oximetry represents a transition between systemic and local tissue oxygenation assessment. Methods for routine and reliable clinical monitoring of respiratory processes at the tissue, cellular, and subcellular levels are limited. *EMG*, Electromyography; *EIT*, electrical impedance tomography; F_N , nitrogen fraction; F_O , oxygen fraction; *NIRS*, near-infrared spectroscopy; P_aCO_2 , arterial partial pressure of carbon dioxide; P_aO_2 , arterial partial pressure of oxygen; P_AO_2 , alveolar partial pressure of oxygen; P_cCO_2 , end-capillary partial pressure of carbon dioxide; P_cO_2 , end-capillary partial pressure of oxygen; $P_{cv}CO_2$, central venous partial pressure of carbon dioxide; $P_{cv}O_2$, central venous partial pressure of oxygen; $P_{ET}CO_2$, end-tidal partial pressure of carbon dioxide; $P_{cv}CO_2$, mixed venous partial pressure of carbon dioxide; $P_{cv}O_2$, mixed venous partial pressure of oxygen; *POCT*, point of care testing; $P_{tc}CO_2$, transcutaneous partial pressure of carbon dioxide; $P_{tc}O_2$, transcutaneous partial pressure of oxygen; *RR*, respiratory rate; S_aO_2 , arterial oxygen saturation; S_cO_2 , end-capillary oxygen saturation; $S_{cv}O_2$, central venous oxygen saturation; SvO_2 , mixed venous oxygen saturation; S_pO_2 , peripheral oxygen saturation; *US*, ultrasound.

Respiratory monitoring includes assessment of (1) convective and diffusive gas transport through the branching airway tree and alveoli, (2) equilibration of gases between alveoli and pulmonary capillary blood, (3) mass balance of the distinct regional ventilation and perfusion contributions to produce expired gases and arterial and mixed venous blood, (4) gas transport between the blood and body tissues through the microcirculation, (5) gas diffusion between tissues and mitochondria, and (6) cellular respiration with O_2 use and CO_2 production.

Advances in physiologic measurements have enhanced our understanding of these stages of respiratory function during anesthesia. This chapter provides an overview of current and emerging techniques of respiratory monitoring. Despite these technical advancements, current instrumentation is limited in providing accurate and comprehensive information on respiratory function in anesthetized and critically ill patients. The area is therefore rich for research to advance the monitoring of all components of respiration.^{5,6}

AMERICAN SOCIETY OF ANESTHESIOLOGISTS STANDARDS

The word *monitoring* is often associated with electronic instrumentation, and it is noteworthy that the current American Society of Anesthesiologists' (ASA) Standards for Basic Anesthetic Monitoring states in Standard I that "Qualified anesthesia personnel shall be present in the room throughout the conduct of all general anesthetics, regional anesthetics, and monitored anesthesia care" (Box 41.1). This precedes reliance on any instrumentation (as implied in Standard II), and clearly indicates that the anesthesia provider brings essential expertise and interpretation to monitoring beyond information provided by equipment. Increased safety in our specialty lies primarily in high-quality training and environments that encourage continuing education, and not exclusively on new technology.⁷ The ASA Standards for Basic Anesthetic Monitoring reflect monitoring principles during anesthesia established in the 1980s³ and should be systematically followed. The

BOX 41.1 American Society of Anesthesiologists Standards for Basic Anesthetic Monitoring Related to Respiratory Monitoring

Standard I

Qualified anesthesia personnel shall be present in the room throughout the conduct of all general anesthetics, regional anesthetics, and monitored anesthesia care.

Standard II

During all anesthetics, the patient's oxygenation, ventilation, circulation, and temperature shall be continually[†] evaluated.

Oxygenation

Objective: To ensure adequate oxygen concentration in the inspired gas and the blood during all anesthetics.

Methods

Inspired gas: During every administration of general anesthesia using an anesthesia machine, the concentration of oxygen in the patient breathing system shall be measured by an oxygen analyzer with a low oxygen concentration limit alarm in use.*

Blood oxygenation: During all anesthetics, a quantitative method of assessing oxygenation such as pulse oximetry will be employed.* When the pulse oximeter is utilized, the variable pitch pulse tone and the low threshold alarm will be audible to the anesthesiologist or the anesthesia care team personnel.* Adequate illumination and exposure of the patient are necessary to assess color.*

Ventilation

Objective: To ensure adequate ventilation of the patient during all anesthetics.

Methods

Every patient receiving general anesthesia will have the adequacy of ventilation continually evaluated. Qualitative clinical signs such

as chest excursion, observation of the reservoir breathing bag and auscultation of breath sounds are useful. Continual monitoring for the presence of expired carbon dioxide will be performed unless invalidated by the nature of the patient, procedure, or equipment. Quantitative monitoring of the volume of expired gas is strongly encouraged.*

When an endotracheal tube or laryngeal mask is inserted, its correct positioning must be verified by clinical assessment and by identification of carbon dioxide in the expired gas. Continual end-tidal carbon dioxide analysis, in use from the time of endotracheal tube/laryngeal mask placement, until extubation/removal or initiating transfer to a postoperative care location, will be performed using a quantitative method such as capnography, capnometry, or mass spectroscopy.* When capnography or capnometry is utilized, the end tidal CO₂ alarm will be audible to the anesthesiologist or the anesthesia care team personnel.†

When ventilation is controlled by a mechanical ventilator, there will be in continuous use a device that is capable of detecting disconnection of components of the breathing system. The device must give an audible signal when its alarm threshold is exceeded.

During regional anesthesia (with no sedation) or local anesthesia (with no sedation), the adequacy of ventilation will be evaluated by continual observation of qualitative clinical signs. During moderate or deep sedation the adequacy of ventilation will be evaluated by continual observation of qualitative clinical signs and monitoring for the presence of exhaled carbon dioxide unless precluded or invalidated by the nature of the patient, procedure, or equipment.

[†] Note that "continual" is defined as "repeated regularly and frequently in steady rapid succession" whereas "continuous" means "prolonged without any interruption at any time."

Under extenuating circumstances, the responsible anesthesiologist may waive the requirements marked with an asterisk (); it is recommended that when this is done, it should be so stated (including the reasons) in a note in the patient's medical record.

standards represent a foundation to additional monitoring according to clinical requirements.

The Physical Examination

Physical examination remains an essential component of perioperative respiratory monitoring. It provides essential information for diagnosis and treatment, and may be the first indication of changes in patient status requiring intervention. Physical examination has limitations, but it routinely allows for detection of information relevant for the management of the patient.

Respiratory monitoring starts with inspection of the patient, either awake or during anesthesia. In elective cases, the anesthesiologist will have time to investigate causes for abnormal presentations. In emergent situations, careful inspection may be the only source of information for timely and accurate anesthetic management. The observation of respiratory distress should prompt immediate search for specific causes. Assessment of the respiratory rate provides a measure of the breathing pattern. For example, during sepsis, respiratory rate is significantly correlated with disease severity.⁸ Anatomic signs relevant to respiration include (but are not limited to) deformities of the chest

wall and spine, goiter, tracheostomy scar, and tracheal deviation. Functional elements to be noticed include the components of inspiration and expiration (diaphragmatic versus thoracic), duration and difficulty of inspiration and expiration, paradoxical chest wall motion, use of accessory muscles, central and peripheral cyanosis, pallor, wheezing, stridor, cough and sputum, aphonia, splinting, and clubbed fingers. Neck vein distension should be examined for a potential cardiovascular contribution to respiratory distress, noting that it is a less reliable indicator of central venous pressure during significant dyspnea. Attention should be paid to painful respiration in trauma patients, as well as the possibility of flail chest, pericardial tamponade, hemothorax, pneumothorax, pulmonary contusion, and tension pneumothorax.

Auscultation of the lung during anesthesia is another essential skill in physical diagnosis. Ambient noise, individual hearing limitations, and the acoustic properties of the stethoscope all influence the anesthesiologist's clinical judgment. A stethoscope of sufficient quality will allow for identification of distinctive normal and abnormal breath sounds: vesicular sounds, ronchi, wheezes, fine and coarse crackles, inspiratory stridor, and pleural friction. A clear understanding of the acoustic mechanisms for each of these sounds is essential for adequate clinical assessment.^{9,10}

Pulse Oximetry

PHYSIOLOGIC FUNDAMENTALS

The primary role of the cardiorespiratory system is the transport of O_2 and CO_2 throughout the body. O_2 delivery is quantified as the product of arterial O_2 content and cardiac output (see Chapter 13, “Respiratory Physiology and Pathophysiology”). Arterial O_2 content (C_aO_2 , in mL of O_2 per 100 mL of blood [hemoglobin—Hb], mL/100 mL) is calculated as

$$C_aO_2 = (1.34 \times S_aO_2 \times Hb) + 0.0031 \times P_aO_2 \quad (41.1)$$

where 1.34 mL/g is the O_2 binding capacity of Hb (i.e., Hüfner constant, theoretically equal to 1.39 mL/g but experimental range between 1.31 and 1.37 mL/g because of the presence of small amounts of other Hb species¹¹); S_aO_2 is the O_2 saturation of Hb in the arterial blood (percent saturation/100); Hb is the concentration of Hb in the arterial blood (g/dL); 0.0031 is the solubility of O_2 in blood (mL/100 mL/mm Hg); and P_aO_2 is the arterial partial pressure of O_2 (mm Hg). As can be inferred from Eq. (41.1), S_aO_2 and Hb are the major determinants of O_2 content in the blood and consequently O_2 delivery to the tissues.

Five species of Hb are found in adult blood: oxygenated Hb (O_2Hb), deoxygenated Hb (de O_2 Hb); carboxyhemoglobin (COHb); methemoglobin (MetHb); and sulfhemoglobin (SHb). Under normal circumstances, the concentrations of COHb, MetHb, and SHb are small (1%–3% for COHb and less than 1% for MetHb and SHb). *Functional* O_2 saturation (S_aO_2) refers to the amount of O_2Hb as a fraction of the total amount of O_2Hb and de O_2 Hb and is expressed as

$$\text{Functional } S_aO_2 = \frac{[O_2Hb]}{[O_2Hb] + [\text{de}O_2Hb]} \times 100\% \quad (41.2)$$

The O_2Hb fraction or *fractional* saturation is defined as the amount of O_2Hb as a fraction of the total amount of Hb¹²:

$$\text{Fractional } S_aO_2 = \frac{[O_2Hb]}{[O_2Hb] + [\text{de}O_2Hb] + [\text{COHb}] + [\text{MetHb}] + [\text{SHb}]} \times 100\% \quad (41.3)$$

S_aO_2 is a function of the P_aO_2 . The relationship between the two is described by the O_2Hb dissociation curve (Fig. 41.2). As can be appreciated by inspection of the curve, the relationship is not linear. This has important consequences. First, a high S_aO_2 cannot discriminate between normoxic and hyperoxic conditions; this can be relevant when attempting to limit O_2 exposure in neonates or patients at risk for O_2 toxicity. Second, a large numeric change in P_aO_2 at the flat portion of the curve (P_aO_2 approximately above 70 mm Hg) has relatively small consequences in terms of blood O_2 content. Furthermore, changes in temperature, pH, P_aCO_2 , and erythrocyte 2,3-diphosphoglycerate concentration can shift the curve such that the same S_aO_2 can be present under a range of different oxygen partial pressures (PO_2). This may be relevant, given that diffusion from the microcirculation to tissue depends on PO_2 gradients.

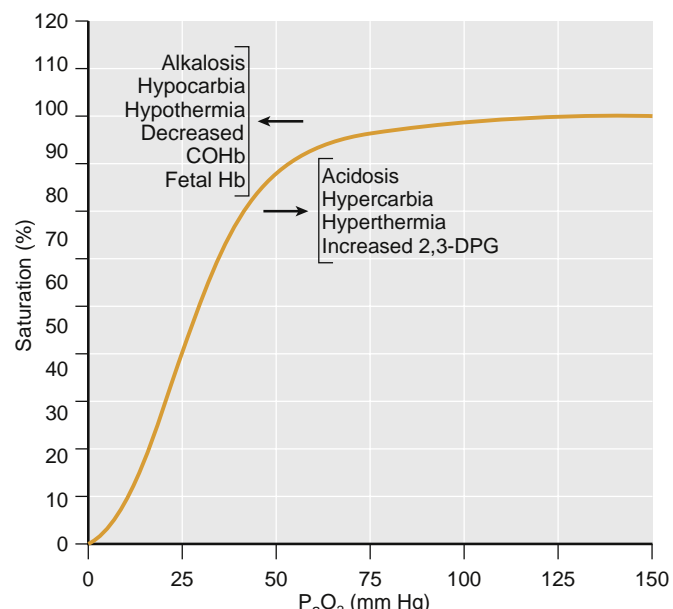


Fig. 41.2 Oxyhemoglobin Dissociation Curve. The relationship between oxyhemoglobin saturation and arterial partial pressure of oxygen is nonlinear and affected by a number of different factors such as pH, PCO_2 , and temperature. Given the nonlinear nature of the curve, it is difficult to determine the partial pressure of oxygen at the higher range of oxygen saturations. 2,3-DPG, 2,3-diphosphoglycerate; COHb, carboxyhemoglobin. (Redrawn from Longnecker DE, Brown DL, Newman MF, Zapol WM, eds. *Anesthesiology*. 2nd ed. New York, NY: McGraw-Hill; 2012.)

MEASUREMENT PRINCIPLES

Oximetry

Oximetry is the measurement of the O_2 saturation of Hb. It is an application of the Beer-Lambert law (Eq. 41.4), which relates the transmission of light through a solution to the concentration of the solute in the solution.¹³ For each solute in a solution,

$$I_{\text{trans}} = I_{\text{in}} e^{-DC\epsilon} \quad (41.4)$$

where I_{trans} is the intensity of transmitted light, I_{in} is the intensity of the incident light, e is the base of the natural logarithm, D is the distance the light is transmitted through the solution, C is the concentration of the solute, and ϵ is the extinction coefficient of the solute.

The concentration of a single solute in solution can be calculated by measuring the amount of light transmitted through the solution as long as the other variables are known. For a solution containing multiple solutes, the calculation of the concentrations of the different solutes requires that light absorption be measured at a number of different wavelengths at least equal to the number of solutes. In a sample of blood in a cuvette, the absorption of a given wavelength of light passing through the blood will depend on the concentrations of the different species of Hb. Fig. 41.3A illustrates the absorption spectra of the five species of Hb for wavelengths of light along the visible spectrum. To measure the concentrations of all five species of Hb in a sample of blood, light absorption of at least five different wavelengths must be measured. This measurement is typically conducted using a co-oximeter. A co-oximeter uses the principle of oximetry to measure the S_aO_2 as well as the concentrations of other Hb species in a blood sample.

Co-oximetry is considered the gold standard for S_aO_2 measurements and is relied on in circumstances when pulse oximetry readings are inaccurate or unobtainable.

Pulse Oximetry

Standard pulse oximetry aims to provide a noninvasive, *in vivo*, and continuous assessment of functional S_aO_2 . Estimates of S_aO_2 based on pulse oximetry are denoted as S_pO_2 . The history of the development of the pulse oximetry has been reviewed in detail elsewhere.¹⁴

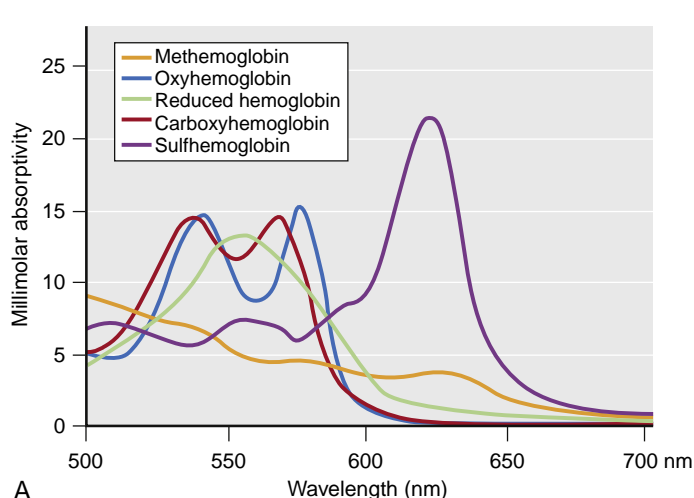
Pulse oximetry takes advantage of the pulsatility of arterial blood flow to provide an estimate of S_aO_2 by differentiating light absorption by arterial blood from light absorption by other components. When compared with *in vitro* oximetry of an arterial blood sample, the challenge of obtaining arterial O_2 saturation *in vivo* is to ensure that the light is sampling arterial blood and to account for its absorption by other tissues. As illustrated in Fig. 41.4, light absorption by tissue can be divided into a time-varying (pulsatile) component, historically referred to as "AC" (from "alternating current"), and a

steady (nonpulsatile) component, referred to as "DC" ("direct current"). In conventional pulse oximetry, the ratio (R) of AC and DC light absorption at two different wavelengths is calculated. The wavelengths of light are selected to maximize the difference between the ratios of the absorbances of O_2Hb and deO_2Hb (see Fig. 41.3B). The most commonly used wavelengths of light are 660 nm and 940 nm. At 660 nm, there is greater light absorption by deO_2Hb than by O_2Hb . At 940 nm, there is greater light absorption by O_2Hb than by deO_2Hb .

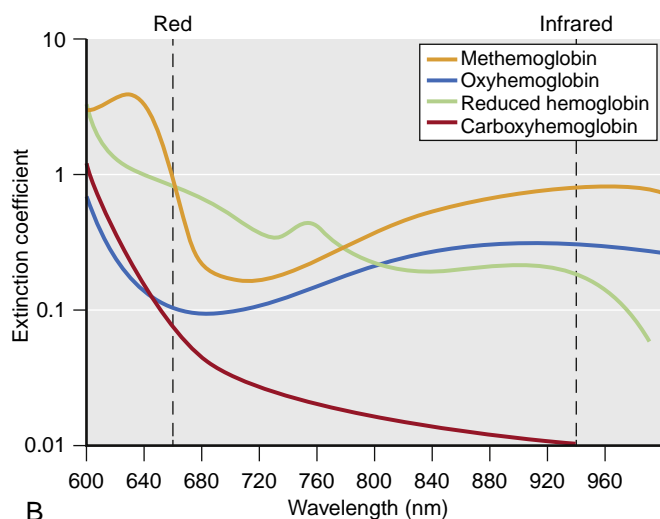
$$R = \frac{AC_{660}/DC_{660}}{AC_{940}/DC_{940}} \quad (41.5)$$

where AC_{660} , AC_{940} , DC_{660} , and DC_{940} denote the corresponding AC and DC components of the 660-nm and 940-nm wavelengths.

The ratio R is then empirically related to O_2 saturation based on a calibration curve internal to each pulse oximeter (Fig. 41.5).¹⁵ Each manufacturer develops its own calibration curve by having volunteers breathe hypoxic gas mixtures to create a range of S_aO_2 values between 70% and 100%. The FDA



A



B

Fig. 41.3 (A) Absorption spectra of five species of hemoglobin for wavelengths of light across the visible spectrum. (B) Extinction coefficients of the most frequently measured hemoglobin species extending to infrared wavelengths used for pulse oximetry. The vertical lines indicate specific wavelengths for red and infrared light applied in pulse oximeters. The differences in the extinction coefficients of oxyhemoglobin and reduced hemoglobin (deoxygenated hemoglobin) are pronounced at these wavelengths. Note that the extinction coefficients of carboxyhemoglobin and methemoglobin are similar to those of oxyhemoglobin and reduced hemoglobin, respectively, at 660 nm. ([A] Redrawn from Zwart A, van Kampen EJ, Zijlstra WG. Results of routine determination of clinically significant hemoglobin derivatives by multicompartiment analysis. *Clin Chem*. 1986;32:972–978. [B] Modified from Tremper KK, Barker SJ. Pulse oximetry. *Anesthesiology*. 1989;70:98–108.)

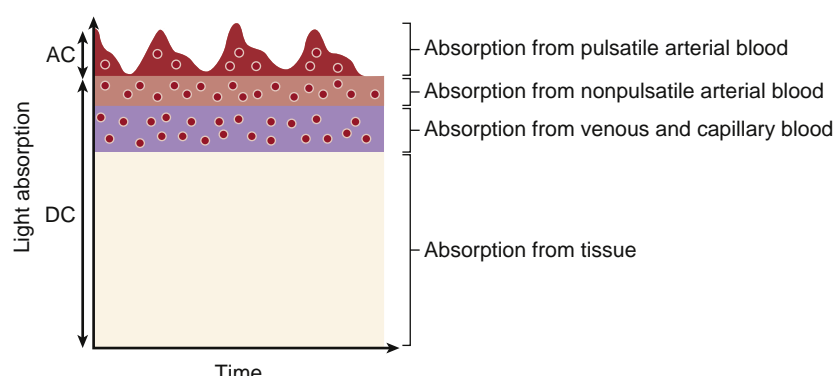


Fig. 41.4 Schematic of the Pulse Principle. Absorption of light passing through tissue is characterized by a pulsatile component (AC) and a nonpulsatile component (DC). The pulsatile component of absorption is due to arterial blood. The nonpulsatile component is due to venous blood and the remainder of the tissues. (Redrawn from Severinghaus JW. Nomenclature of oxygen saturation. *Adv Exp Med Biol*. 1994;345:921–923)

recommends root mean square differences between measured values (S_pO_2) and reference values (S_aO_2) under normal conditions ranging from 70% to 100% S_pO_2 of $\leq 3.0\%$ for transmittance, wrap and clip pulse oximeter sensors and of $\leq 3.5\%$ for ear clip and reflectance sensors.^{14a} Most manufacturing literature reports an accuracy of $\pm 2\%$ to 3% S_pO_2 over this range.¹⁵ The dependence of S_pO_2 on pulsatility may result in inaccurate estimates of S_aO_2 when pulsatility is reduced or absent.

A pulse oximeter probe is composed of a light emitter and a photodetector. Transmission pulse oximetry involves the placement of the emitter and detector on opposite sides of the tissue being measured, usually of a finger. Reflectance pulse oximetry probes have the emitters and detector arranged on the same side. They are typically placed on the forehead. In a typical pulse oximeter, two light-emitting diodes (LEDs) are used to emit light at the two wavelengths. During operation, each LED is turned on and off in sequence. The photodetector measures transmission of light from each LED. When both LEDs are turned off, the photodetector measures ambient light and subtracts it from the signals obtained throughout the remainder of the cycle.¹⁶

Pulse oximetry has been an integral component of intraoperative anesthetic management since the first anesthetic monitoring standards were introduced in 1986.³ It was adopted as a minimum monitoring standard by the ASA the same year and has subsequently been defined as a minimum standard for intraoperative monitoring by the World Federation of Societies of Anaesthesiologists and the World Health Organization (WHO).¹⁷ The use of pulse oximetry is a part of the WHO safe surgery checklist.¹⁸

Multiwavelength pulse oximeters—that is, pulse oximeters with additional wavelengths of light to allow for the continuous noninvasive measurement of total hemoglobin concentration (S_pHb)¹⁹—as well as concentrations of MetHb and COHb utilizing up to 12 wavelengths have been developed.^{20,21} S_pHb in the surgical and intensive care unit (ICU) settings has shown reasonable bias and precision when compared with laboratory measurements.²²⁻²⁴ However, few of the measurements were obtained in patients

with Hb concentrations within the clinically relevant range of 6 to 10 mg/dL.²⁵ Another limitation of S_pHb may be its absent or unreliable signal under conditions of low peripheral perfusion.²⁶ To date, noninvasive COHb measurements have not shown enough precision to replace laboratory measurements.^{26,27} Accuracy has improved at hypoxic O₂ levels, but detecting COHb for S_aO_2 less than 87% is still unreliable.^{28,29} Pulse oximetry-based MethHb measurements with a newer device are accurate, even under conditions of hypoxia.³⁰

Universal pulse oximetry has been recommended by the US Secretary of Health and Human Services to screen newborns for critical congenital heart disease.^{31,32} Use of a clinical algorithm based on detection of S_pO_2 lower than 95% in either right upper or lower limbs, or more than a 2% difference led to a sensitivity of 75% in suspected cases and 58% in cases that were not suspected. When this modality is combined with a routine anomaly scan and newborn physical examination screening, 92% of critical congenital heart disease lesions can be identified.^{33,34}

Photoplethysmography. Along with measuring O₂ saturation, the pulse oximeter can also be used as a photoplethysmograph. Because the absorption of light is proportional to the amount of blood between the transmitter and photodetector, changes in the blood volume are reflected in the pulse oximeter trace (Fig. 41.6).³⁵ During anesthesia, the plethysmographic trace is affected by changes in blood volume pulsations, which depends on the distensibility of the vessel wall, as well as on the intravascular pulse pressure.³⁵ Variations in the amplitude of the pulse oximeter plethysmographic waveform (ΔPOP) have been shown to predict fluid responsiveness in mechanically ventilated patients.³⁶ An index derived from the percent difference between the maximum and minimum amplitudes of the plethysmographic waveform during a respiratory cycle (PVI, Pleth Variability Index) has been incorporated into a commercially available pulse oximeter and used to quantify ΔPOP and predict fluid responsiveness.^{37,38} A number of studies have shown it to be a reasonably reliable indicator of fluid responsiveness perioperatively and in critically ill patients.^{39,40} The technique does have greater reliability in mechanically ventilated patients compared with spontaneously breathing patients, but its accuracy may be compromised by the presence of cardiac arrhythmias.³⁹ Its accuracy has also been shown to be better for 500 mL fluid challenges compared with 250 mL.⁴¹ Goal-directed fluid management based on PVI has been shown to improve outcomes in major abdominal surgery.⁴²

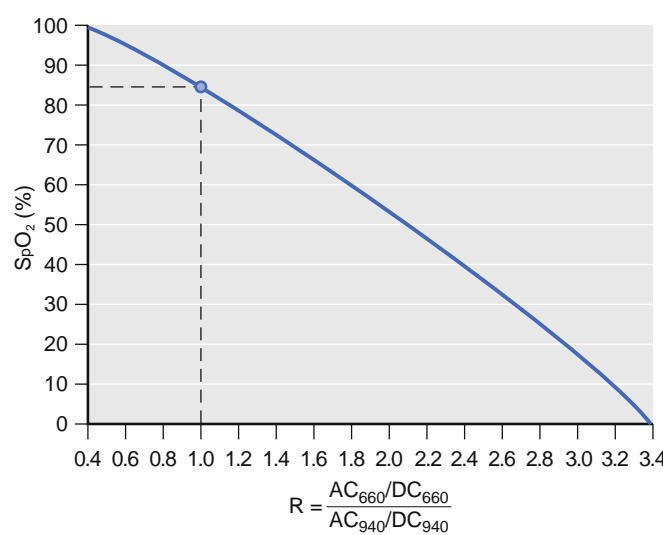


Fig. 41.5 Typical Pulse Oximeter Calibration Curve Relating Oxygen Saturation to the R Value. These curves are developed using healthy volunteers and incorporated into the pulse oximeter. R , Ratio of AC and DC light absorption; S_pO_2 , peripheral oxygen saturation. [Tremper KK and Barker SJ. Pulse Oximetry. *Anesthesiology*. 1989;70:90-108.]

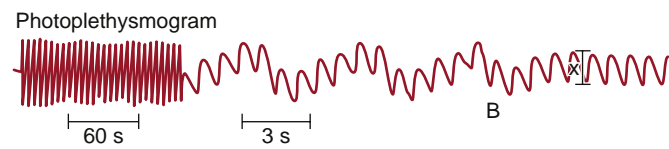


Fig. 41.6 Photoplethysmogram Recorded at Two Speeds Demonstrating Respiratory Variation. At time point (B) ventilation has been stopped, and no variation is observed. The plot illustrates the effect of intrathoracic blood volume on the pulse oximeter trace. The variation in the trace with respiration is associated with the fluid responsiveness of the patient. (Redrawn from Dorlas JC, Nijboer JA. Photo-electric plethysmography as a monitoring device in anaesthesia. Application and interpretation. *Br J Anaesth*. 1985;57:524-530.)

LIMITATIONS AND SOURCES OF ERROR

S_pO_2 is an estimate of S_aO_2 of circulating hemoglobin. As a consequence, it does not provide information about *tissue* oxygenation. Because S_pO_2 is a measurement of functional and not fractional S_aO_2 , the presence of other Hb variants can significantly affect its accuracy. The nonlinearity of the Hb dissociation curve prevents the detection of hyperoxia with S_pO_2 for high S_aO_2 , whereas for low saturations such as at altitude, small changes in P_aO_2 can produce large changes in S_pO_2 . There is significant variability in the actual in vivo Hb dissociation curve.⁴³ Thus changes in S_pO_2 are not necessarily well correlated with changes in S_aO_2 .^{44,45} These measurements illustrate that knowledge of the individual Hb dissociation curve is important for correct interpretation of S_aO_2 and P_aO_2 . More importantly, pulse oximetry does not provide information about ventilation or acid-base status.

A number of conditions can lead to inaccuracies in pulse oximeter readings (Table 41.1). These conditions include decreased perfusion, motion artifact, venous pulsation, low S_aO_2 , variant Hb species, the presence of intravascular dyes, and the presence of nail polish.

Despite the recommendations of numerous boards and guidelines, there is no evidence that the use of pulse oximetry improves patient outcomes, not during transfers to ICUs nor in terms of improving patient mortality.^{45a,b} There is evidence that pulse oximetry reduces the incidence of hypoxemia,^{45a} and the duration and cost of ICU stay, suggesting it allows for early intervention.^{45c}

The calibration of pulse oximeters is based on curves obtained in normal individuals under experimental conditions with S_aO_2 as low as 70%. As such, pulse oximeters have limited accuracy for S_aO_2 values less than 70%. Moreover, systematic errors in S_pO_2 tend to increase as S_aO_2 falls below 90%.⁴⁶ At S_aO_2 levels under 70%, a positive or negative bias of the S_pO_2 value can be observed, depending on the manufacturer of the pulse oximeter.⁴⁷ Manufacturers have developed pulse oximeters with increased accuracy at saturations as low as 60%. Preliminary data suggest that these probes may be useful in neonates with cyanotic congenital heart disease.⁴⁸

Hypoperfusion leads to a reduction in the amplitude of the pulsatile component of the light absorbance waveform, the essential signal for pulse oximetry, consequently giving rise to absent or inaccurate readings. Significantly erroneous reductions in S_pO_2 may be observed for systolic blood pressures lower than 80 mm Hg.⁴⁹ Motion artifact can produce considerable error in the pulse oximeter reading. Manufacturers have developed advanced proprietary signal processing algorithms that effectively filter out noise caused by motion.^{50,51}

With continued clinical use, the performance of the LEDs in the probe may be degraded, leading to inaccuracy in the S_pO_2 value outside of the range specified by the manufacturer. These inaccuracies are expected to be more pronounced at lower saturations (i.e., <90%).¹⁵

Venous pulsations may result in the detection of venous O_2Hb saturation by the pulse oximeter, resulting in artifactual reduction of the presumed arterial S_pO_2 being measured. Venous pulsations can be due to excessively tight placement of adhesive finger probes, severe tricuspid regurgitation, probe placement in dependent positions (e.g., forehead during Trendelenburg position), and possibly in distributive shock when vasodilation may result in physiologic arteriovenous shunting.^{18,19,52}

TABLE 41.1 Potential Sources of Artifacts in Pulse Oximetry and Their Effects on Measurements

Source of Error	Effect on S_pO_2 Relative to S_aO_2
Hypotension	↓
Anemia	↓
Polycythemia	No significant effect
Motion	↓
Low S_aO_2	variable
Methemoglobinemia	↓/↑ (S_pO_2 approaches 85%)
Carboxyhemoglobinemia	↑
Cyanmethemoglobin	No significant effect
Sulfhemoglobin	No significant effect
Hemoglobin F	No significant effect
Hemoglobin H	No significant effect
Hemoglobin K	↓
Hemoglobin S	No significant effect
Methylene blue	↓
Indigo carmine	↓
Indocyanine green	↓
Isosulfan blue	No significant effect/↓
Fluorescein	No significant effect
Nail polish	Black, dark blue, purple ↓
Acrylic fingernails	No significant effect
Henna	Red—No significant effect ↓
Skin pigmentation	At S_aO_2 >80%, no significant effect At S_aO_2 <80%, ↑
Jaundice	No significant effect
Ambient light	No significant effect
Sensor contact	↓
IABP	↑

IABP, Intraaortic balloon pump; S_aO_2 , arterial oxygen saturation; S_pO_2 , peripheral oxygen saturation.

The presence of additional species of Hb can also generate erroneous pulse oximeter readings. As outlined earlier, the function of the pulse oximeter is predicated on the assumption that the only components present in the blood capable of absorbing light at the two wavelengths used are O_2Hb and deO_2Hb . Under normal circumstances, this assumption is valid, and the S_pO_2 readings accurately reflect the S_aO_2 . However, the presence of significant concentrations of other Hb species or substances absorbing light at the used wavelengths will lead to erroneous S_pO_2 readings. As illustrated in Fig. 41.3, both COHb and MetHb absorb light at one or both of the wavelengths used by the pulse oximeter. Accordingly, the presence of these Hb species will produce errors in S_pO_2 . The absorption of light at 660 nm by COHb is similar to that of O_2Hb . At 940 nm, COHb absorbs virtually no light. Thus, in a patient with carbon monoxide poisoning, the S_pO_2 will be falsely elevated.⁵³ MetHb absorbs a significant amount of

light at both 660 nm and 940 nm. As a result, in its presence, the ratio of light absorption R (Eq. 41.5) approaches unity. An R -value of 1 represents the presence of equal concentrations of O_2 Hb and de O_2 Hb and corresponds to an S_pO_2 of 85%. Thus, in a patient with methemoglobinemia, the S_pO_2 will be 80% to 85%, irrespective of the S_aO_2 .⁵⁴ SHb absorbs red light (660 nm) more than deoxyhemoglobin (HHb) or MetHb, and likely as much near the infrared spectrum.⁵² This results in S_pO_2 values close to 85% in severe cases of sulfhemoglobinemia. Although newer generations of co-oximeters can detect SHb, most existing co-oximeters cannot; consequently, additional clinical laboratory testing may be required if sulfhemoglobinemia is suspected.⁵²

With normal S_aO_2 , anemia has little effect on S_pO_2 .⁵⁵ However, in the presence of hypoxia, S_pO_2 readings underestimate S_aO_2 in anemic patients with true hypoxemia.⁵⁶ Pulse oximeters are sufficiently accurate in adult patients with sickle cell disease,⁵⁷ as well as in the presence of fetal Hb.⁵⁸ However caution is warranted when using pulse oximetry in patients with sickle cell disease, because heme metabolism may result in elevated COHb.⁵² Some studies also suggest that S_pO_2 may overestimate S_aO_2 during vaso-occlusive crises.^{59,60} Another relevant point is that in patients with sickle cell disease, the affinity of O_2 for Hb is normal under normoxic conditions but becomes low during hypoxia.

A relatively uncommon cause for reduced S_pO_2 readings is the presence of congenital variants of Hb. Some variants, such as Hb Bassett, Hb Rothschild, and Hb Canabiere, have a reduced affinity for O_2 , and changes in S_pO_2 appropriately reflect changes in S_aO_2 .⁶¹ Other variants, such as Hb Lansing, Hb Bonn, Hb Koln, Hb Cheverly, and Hb Hammersmith, have altered absorption spectra (closer to HHb) that result in low S_pO_2 readings in the setting of normal S_aO_2 .⁶¹

The administration of intravenous dyes can result in inaccurate S_pO_2 readings. Methylene blue leads to a transient, marked decrease in S_pO_2 down to 65% due to its peak light absorption at 668 nm, which is very close to that of HHb. Indigo carmine and indocyanine green also artificially decrease S_pO_2 measurements, although to a lesser extent than methylene blue, because they do not substantially absorb red light.⁶² Isosulfan blue can produce a prolonged reduction at higher doses.⁶²

Although all colors of nail polish can reduce the calculated value of S_pO_2 , black, purple, and dark blue colors have the greatest effect. Nonetheless, the error generally remains within 2%.⁶³ Depending on the brand of pulse oximeter, artificial acrylic nails may impair S_pO_2 readings, although generally not to a clinically significant extent.⁶⁴ Under conditions of normal S_aO_2 , skin pigmentation has no effect on S_pO_2 estimates.⁶⁵ However, increased skin pigmentation is associated with S_pO_2 values that overestimate S_aO_2 by as much as 8% for S_aO_2 less than 80%.^{47,66}

In the presence of severe hyperbilirubinemia (30 mg/dL or greater) caused by increased hemolysis or liver disease, the fraction of oxygenated hemoglobin (FO_2 Hb) may be falsely low by artifactual increase in MetHb and COHb, resulting in more accurate S_pO_2 than FO_2 Hb measurements.⁵² Although earlier case reports and small studies have suggested that ambient light may interfere with the accuracy of S_pO_2 readings,^{67,68} a large prospective study found no significant effect on S_pO_2 accuracy with exposure to five types of light sources: quartz-halogen, incandescent, fluorescent, infant bilirubin lamp, and infrared.⁶⁹ Infrared light pulses from image guidance systems used for navigational neurosurgery can interfere with pulse

oximetry readings by causing decreased readings or disruptions in S_pO_2 waveform detection.⁷⁰ Different pulse oximeters show variable susceptibility to such interference.⁷¹ Shielding the probe with a single layer of aluminum foil can protect from this effect.^{70,71} Misplacement of the probe can allow for direct detection of LED light by the photodetector. This optical shunt gives rise to an S_pO_2 reading of 85%.⁷²

In patients with intraaortic balloon pump support, S_pO_2 accuracy depends on the brand of pulse oximeter used as well as the support ratio. Accuracy is generally reduced in the setting of higher support ratios.⁷³ In patients with continuous flow ventricular assist devices, pulse oximetry may not be possible because of the absence of pulsatile flow. In these cases, the use of cerebral oximetry as an adjunct is advocated.⁷⁴

Pulse Oximeter Probes

Probes are usually applied to accessible body areas with high vascularity, such as the finger, nose, ear lobe, or forehead. The probes may be reusable or disposable. The advantages of reusable clip probes are that they are more cost-effective compared with disposable adhesive probes, can be rapidly applied, and are amenable to multiple applications in cases of low signal-to-noise ratio at the specified wavelengths. However, disposable probes allow for more secure placement (in case of patient movement) and provide the capability of monitor sites other than acral areas. Although reduced infectious transmission is a purported benefit of disposable probes, evidence is limited, and one must consider that pulse oximetry probes represent a small fraction of anesthetic equipment requiring decontamination.⁷⁵ Accordingly, different probe models may be advantageous in specific conditions. For instance, ear and forehead probes may be more reliable during vasoconstriction compared with finger probes, given that the arterial vessels of such regions are less responsive to circulating catecholamines. As an example, in hypotensive patients that require vasopressors, ear and forehead probes may provide more accurate value of S_pO_2 , because these areas are less likely to vasoconstrict with endogenous and exogenous catecholamines compared to fingers or toes.^{76,77} During hypothermia with secondary vasoconstriction, the forehead probe is more reliable compared with the finger probe.^{78,79}

Emerging Techniques: Pulse spectroscopy is a new technique that utilizes hundreds of wavelengths to assess normal and dysfunctional hemoglobins. Initial results are promising with accurate S_pO_2 determinations, as well as COHb and MetHb assessment during normoxia and hypoxia.⁸⁰

Mixed Venous Oxygen Saturation

PHYSIOLOGIC FUNDAMENTALS

Mixed venous oxygen saturation ($S\bar{v}O_2$) is the O_2 saturation of blood at the proximal pulmonary artery. It has been a frequently monitored variable in critically ill patients, since it reflects the average O_2 saturation of the blood returning from the body to the right heart, weighted by the respective regional blood flows. As such, it is a measure of the balance between global oxygen delivery (DO_2) and global oxygen uptake (V_{O_2}), and a useful resuscitation target.⁸¹ Factors that influence the $S\bar{v}O_2$ can be illustrated through a derivation of the mixed venous O_2 content equation.

\dot{V}_{O_2} (mL/min) is defined as

$$\dot{V}_{O_2} = 10 \times \dot{Q}_T \times (C_a O_2 - \bar{C}V O_2) \quad (41.6)$$

where \dot{Q}_T is the cardiac output (L/min), and $\bar{C}V O_2$ is the O_2 content of the mixed venous blood (mL/100 mL).

Rearranging Eq. (41.6) to solve for $\bar{C}V O_2$ yields

$$\bar{C}V O_2 = C_a O_2 - \dot{V}_{O_2} / \dot{Q}_T \quad (41.7)$$

The contribution of dissolved O_2 to the blood O_2 content is small. By expanding the definition of O_2 content (Eq. 41.1) and ignoring the term for dissolved O_2 , Eq. (41.7) can be rewritten as

$$\bar{S}V O_2 = S_a O_2 - \dot{V}_{O_2} / (1.34 \cdot Hb \cdot \dot{Q}_T) \quad (41.8)$$

Normal values of $\bar{S}V O_2$ range between 65% and 80%.^{82,83} Values close to 40% are associated with tissue hypoxia, anaerobic metabolism, and lactate production. $PV O_2$ can be derived from $\bar{S}V O_2$ values by utilizing the O_2 Hb dissociation curve adjusted to mixed-venous pH, PCO_2 , and temperature (see Fig. 41.2). The normal value of $PV O_2$ is 40 mm Hg.

DO_2 is defined as

$$DO_2 = \dot{Q}_T \times C_a O_2 \quad (41.9)$$

As is evident from Eq. (41.8), a low $\bar{S}V O_2$ indicates either a reduction in DO_2 secondary to low $S_a O_2$, low Hb, or low \dot{Q}_T , or an increase in \dot{V}_{O_2} . The association among $\bar{S}V O_2$, DO_2 , and \dot{V}_{O_2} can be illustrated by expressing $\bar{S}V O_2$ as a function of the O_2 extraction ratio, ERO_2 .

$$ERO_2 = \dot{V}_{O_2} / DO_2 \quad (41.10)$$

Expanding the terms yields

$$ERO_2 = 1 - \bar{C}V O_2 / C_a O_2 \quad (41.11)$$

Assuming that the O_2 dissolved in plasma is a negligible component to total O_2 content dissolved in the arterial or mixed venous blood, Eq. (41.11) can be rewritten as

$$ERO_2 = 1 - \bar{S}V O_2 / S_a O_2 \quad (41.12)$$

For conditions in which the arterial blood is fully saturated, Eq. (41.12) may be further simplified:

$$ERO_2 = 1 - \bar{S}V O_2 \quad (41.13)$$

Solving for $\bar{S}V O_2$ yields

$$\bar{S}V O_2 = 1 - ERO_2 \quad (41.14)$$

Thus a reduction in $\bar{S}V O_2$ results from an increase in ERO_2 , from either an increased \dot{V}_{O_2} or a decreased DO_2 (Fig. 41.7). A decrease in DO_2 occurs in conditions such as hemorrhagic or hypovolemic shock. An increase in \dot{V}_{O_2} may occur in conditions such as stress, pain, shivering, sepsis, and thyrotoxicosis. Conversely, an increase in $\bar{S}V O_2$ indicates either an increase in O_2 supply (elevated $S_a O_2$, Hb, or \dot{Q}_T) or a reduction in \dot{V}_{O_2} , as occurs during hypothermia.

There are some subtle considerations in the interpretation of changes in $\bar{S}V O_2$. At PO_2 values typical of venous

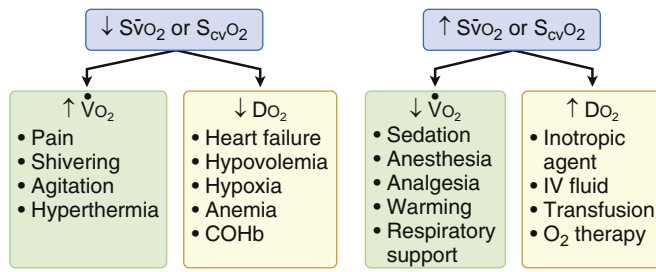


Fig. 41.7 Mixed venous saturation is a measure of the balance between global oxygen delivery and uptake. Conditions which increase \dot{V}_{O_2} or decrease DO_2 will lead to a reduction in $\bar{S}V O_2$. Conversely, conditions which decrease \dot{V}_{O_2} or improve DO_2 will lead to an increase in the $\bar{S}V O_2$. (Modified from Shepherd SJ, Pearse RM. Role of central and mixed venous oxygen saturation measurement in perioperative care. *Anesthesiology*. 2009;111:649–656.)

blood, small increases in the fraction of inspired oxygen ($F_I O_2$) can cause significant increases in $\bar{S}V O_2$ because of the shape of the O_2 Hb dissociation curve (Fig. 41.2). Therefore, when $\bar{S}V O_2$ is tracked as a measure of cardiac function, changes in $F_I O_2$ must be taken into account during its interpretation.⁸⁴ In the setting of septic shock, impairment in O_2 extraction may yield normal $\bar{S}V O_2$ values, despite the presence of tissue hypoxia.

Direct measurement of $\bar{S}V O_2$ requires the insertion of a pulmonary artery catheter, a procedure associated with some morbidity. However, in most clinical situations, the O_2 saturation of a blood sample drawn from a central venous catheter will suffice. Thus the use of central venous saturation can be a surrogate for $\bar{S}V O_2$. The saturation of blood at the level of a central venous catheter placed in the superior vena cava ($S_{cv} O_2$) reflects the balance between O_2 supply and demand in the brain and upper extremities. Under normal physiologic conditions, $S_{cv} O_2$ is typically 2% to 5% less than $\bar{S}V O_2$, primarily because of the higher O_2 content of splanchnic and renal venous blood.⁸⁵ However, during hemodynamic instability, as circulation is redistributed to the upper body, the relationship between $\bar{S}V O_2$ and $S_{cv} O_2$ may reverse, and the difference between the two may increase significantly.^{86–88} Although trends in $S_{cv} O_2$ may reflect those in $\bar{S}V O_2$, the two measures cannot be used interchangeably.^{88–96}

Mixed venous CO_2 has been used to compute the arteriovenous CO_2 difference ($\Delta PCO_2 = PV CO_2 - P_a CO_2$). In conditions of steady-state CO_2 production, ΔPCO_2 changes inversely and nonlinearly with cardiac output as a result of the Fick equation.⁹⁷ Accordingly, ΔPCO_2 is an indicator of the adequacy of cardiac output to provide adequate clearance of tissue CO_2 . However, because of several limitations, the parameter has not yet found widespread clinical use.⁹⁷

MEASUREMENT PRINCIPLES

The measurement of venous O_2 saturation can be performed intermittently by co-oximetry of blood sampled from the distal tip of a pulmonary artery catheter ($\bar{S}V O_2$) or a central venous catheter ($S_{cv} O_2$). Falsely increased values can occur in the presence of a wedged pulmonary artery tip, mitral regurgitation, or left-to-right shunts.⁹⁸ Venous saturations can also be measured continuously by spectrophotometry using specialized fiberoptic catheters,

which transmit infrared light and detect the amount of light reflected from red blood cells.^{99,100} Specialized venous oximetry catheters are available for both pulmonary artery and central venous monitoring and have the advantage of providing continuous measurements of O₂ saturation. Their disadvantage is the cost. Although continuous venous oximetry catheters trend changes, their reported absolute values are not equivalent to concurrently obtained co-oximetry measurements.¹⁰¹⁻¹⁰³

APPLICATIONS AND INTERPRETATION

In patients undergoing major abdominal or cardiac surgery, intraoperative reductions in S_vO₂ and S_{cv}O₂ have been associated with postoperative complications.¹⁰⁴⁻¹⁰⁸ Protocol-based interventions that target specific values of S_vO₂ or S_{cv}O₂ have been shown to reduce the length of stay, organ dysfunction, and mortality in patients undergoing major surgery and patients presenting with sepsis.¹⁰⁹⁻¹¹¹ Goal-directed therapy based on S_{cv}O₂ has been advocated for the management of sepsis, and the implementation of such protocols is associated with improvements in mortality.^{112,113} The use of S_{cv}O₂ as a therapeutic endpoint remains controversial for several reasons: S_{cv}O₂ may be increased in sepsis because of impaired tissue O₂ extraction¹¹⁴; the increased cost associated with the use of S_{cv}O₂-measuring catheters¹¹⁵; and other measures, such as lactate clearance, are less costly while leading to similar outcomes.¹¹⁶ Furthermore, the management of sepsis without an S_{cv}O₂ endpoint can yield equally favorable results.¹¹⁵ The difference between S_vO₂ and S_{cv}O₂ has been proposed as a marker of complications after cardiac surgery.¹¹⁷

Tissue Oxygenation

Arterial and venous O₂ saturations are measures of DO₂ and uptake by the whole body. Although useful, these global measures do not provide information regarding organ or tissue oxygenation, which reflects the important local balance between O₂ supply and demand. Regional O₂ balance can differ both among organs as well as within regions of the same organ.¹¹⁸ Current noninvasive methods for the assessment of microcirculatory oxygenation make use of reflectance spectroscopy using light either in the visible spectrum (VLS) or in the near-infrared spectrum (NIRS). A recent technique based on the protoporphyrin IX triplet state lifetime aims at the assessment of mitochondrial O₂ tension in vivo, and opens the prospect of future clinical monitoring (see Fig. 41.1).¹¹⁹

Reflectance spectroscopy probes have light emitters and receivers positioned in line (Fig. 41.8). When they are placed on a tissue surface, light transmission through the tissue is affected by reflection, absorption, and scatter. Reflection depends on the angle of incidence of the light beam and the wavelength of light, whereas scatter depends on the number and type of tissue interfaces. As previously outlined, the Beer-Lambert law relates the absorption of light by the tissue to the concentration of tissue chromophores, the extinction coefficient of each, and the pathlength of the light through the tissue.¹²⁰ The predominant tissue chromophore is hemoglobin. The pathlength of the

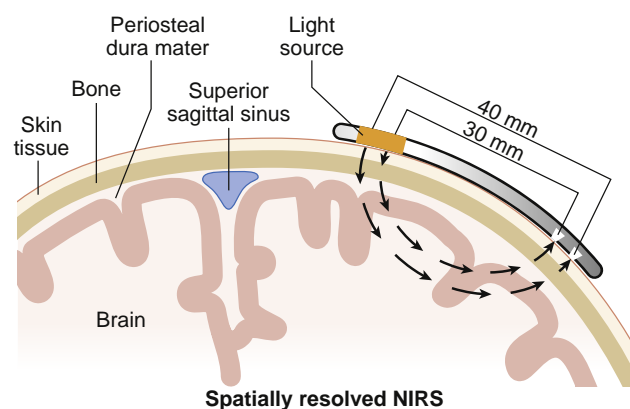


Fig. 41.8 Near Infrared Spectroscopy Applied to Cerebral Oximetry. In this case, a reflectance oximeter is placed on the forehead. Near infrared wavelength light is emitted from the light source and enters the underlying tissue. Light is scattered, reflected, and absorbed. Light that reaches the photodetector travels an arc-shaped path. The depth of the path is a function of the distance between the emitter and the detector. The measured value is the oxygen saturation of the tissue through which the light travels on its way to the detector. It is a primarily venous-weighted value. **NIRS**, Near infrared spectroscopy. (Redrawn from Casati A, Spreafico E, Putzu M, et al. New technology for noninvasive brain monitoring: continuous cerebral oximetry. *Minerva Anestesiol*. 2006;72:605-625.)

light is affected by both reflection and scatter, so it cannot be measured directly, but rather must be estimated. Most of the detected photons travel in an arc between the two detectors (see Fig. 41.8). The depth of penetration of the arc into the tissue is proportional to the wavelength of light and the distance between the transmitter and detector.^{120,121}

VLS makes use of white light with wavelengths of 500 to 800 nm, whereas NIRS employs light in the 700 to 1100 nm range.¹²² In general, the depth of penetration of VLS is less than that of NIRS, thus allowing superficial measurements of up to 16 mm and making it suitable for measurements of small subsurface volumes. NIRS can penetrate tissue to a depth of several centimeters and allows sampling of a larger volume of tissue.¹²³ The O₂ saturation displayed is that of a volume of tissue. This volume includes arteries, capillaries, and veins, and has a predominantly venous weighting.¹²⁴

CLINICAL APPLICATIONS

A number of applications have been described for VLS. Buccal microvascular Hb saturation has been associated with survival in patients with sepsis.¹²⁵ VLS has also been used for monitoring flap viability following reconstructive surgery.¹²⁶ During gastrointestinal and esophageal surgery, reductions in gastrointestinal tissue saturation, measured by VLS, have been associated with postoperative anastomotic complications.^{127,128} Endoscopic VLS differentiates between normal and ischemic areas of colon,¹²⁹ and it may be useful for the diagnosis of mesenteric ischemia.¹³⁰ In addition, mucosal O₂ saturation of the gastric conduit following esophagectomy is useful and explores the benefits of ischemic preconditioning.¹³¹

The most widespread application of NIRS has been in cerebral oximetry,¹¹⁸ with probes placed on the forehead to measure frontal cortical oxygenation (rSO₂). Several NIRS systems are commercially available, with each

manufacturer offering a different specific technology. As there is no gold standard for cerebral oximetry, it is difficult to compare the accuracy of the devices. Furthermore, each device has its own set of “normal” values. For this reason, acquisition of baseline values for each patient at the start of the procedure has been recommended.¹³² Typical values of rSO_2 range from 51% to 82% with a mean baseline of 66%.¹³³ A reduction of rSO_2 below 20% to 25% of the baseline, or lower than an absolute value of 50%, is a suggested threshold for intervention.^{134,135}

The utility of cerebral oximetry has been explored in cardiovascular, abdominal, thoracic, and orthopedic surgery. In the cardiac surgical setting, intraoperative reductions in rSO_2 have been associated with early postoperative cognitive dysfunction and prolonged ICU and hospital lengths of stay.¹³⁵⁻¹³⁸ Baseline rSO_2 measurements have been associated with 30-day mortality after left ventricular assist device surgery.¹³⁹ As a guide to therapy, interventions for rSO_2 reductions less than 75% of baseline in patients undergoing coronary artery bypass graft surgery have been shown to significantly reduce the incidence of major organ morbidity and mortality, as well as ICU length of stay.¹³⁴

During carotid endarterectomy, intraoperative reductions in rSO_2 correlate well with changes in transcranial Doppler measurements,¹⁴⁰⁻¹⁴⁴ electroencephalographic waveforms,¹⁴⁵⁻¹⁴⁷ and stump pressure^{144,148,149}, which are consistent with ischemia. Although some studies indicate that reductions in rSO_2 that are less than 20% of baseline are well tolerated, data are lacking for a clear rSO_2 threshold for carotid shunt placement.^{150,151} NIRS has also been preliminarily used during and following ICU open thoracoabdominal aortic aneurysm repair for continuous monitoring of spinal cord oxygenation.¹⁵²

In elderly patients undergoing major abdominal surgery, protocol-based intraoperative treatment of reductions in rSO_2 results in decreases in postoperative cognitive decline and hospital length of stay.¹⁵³ In patients undergoing thoracic surgical procedures with single-lung ventilation, early postoperative cognitive dysfunction is directly related to intraoperative exposure time to rSO_2 less than 65%.¹⁵⁴ Patients undergoing shoulder surgery in the beach chair position have a lower baseline rSO_2 and a larger number of episodes of cerebral desaturation, although the clinical implications of these findings are unclear.¹⁵⁵⁻¹⁵⁷

Shock is a condition in which patients may have inadequate *regional* perfusion in the setting of normal *global* perfusion parameters. In such circumstances, the use of NIRS to monitor tissue perfusion holds some promise. Values obtained by the application of an NIRS probe to the thenar eminence (S_tO_2) discriminate between healthy volunteers and patients with shock.¹⁵⁸ Furthermore, in patients with major trauma who present with shock, S_tO_2 values can identify patients who proceed to develop multiorgan dysfunction or actually die.^{159,160}

Overall, available information is still limited to warrant clinical decision making exclusively based on NIRS measurements. Currently there is insufficient evidence to support the use of perioperative NIRS monitoring in adults to reduce short-term or mild postoperative cognitive dysfunction, postoperative stroke, delirium, or death.¹⁶¹ Of note, in a 2015 retrospective study, patients who self-identified as African American had lower rSO_2 compared with those

who self-identified as Caucasian, a finding attributed to light attenuation by skin pigmentation.¹⁶² Further investigations are necessary to improve our understanding of NIRS and its relevance for clinical management.

Capnometry and Capnography

GENERAL CONCEPTS

The presence CO_2 in exhaled breath reflects the fundamental physiologic processes of ventilation, pulmonary blood flow, and aerobic metabolism. Its continued monitoring ensures the anesthesiologist of correct placement of an endotracheal tube (ETT) or laryngeal mask airway (LMA), as well as the integrity of a breathing circuit. Exhaled CO_2 provides information primarily on ventilation. It is also used to estimate the adequacy of cardiac output. In combination with P_aCO_2 , exhaled CO_2 can be used to estimate the ratio of physiologic dead space (V_D) to tidal volume (V_T) by using the Bohr equation¹⁶³:

$$\frac{V_D}{V_T} = \left(\frac{P_aCO_2 - P_{\bar{E}}CO_2}{P_aCO_2} \right) \quad (41.15)$$

where $P_{\bar{E}}CO_2$ is the mixed expired CO_2 partial pressure, such as measured in exhaled air collected in a mixing bag chamber, or computed from a volumetric capnogram. The ability to detect and quantify CO_2 is a crucial component of respiratory monitoring in anesthesia and critical care medicine.

Considerable confusion arises from inconsistent and interchangeable terminology as applied to medical CO_2 gas analysis.¹⁶³⁻¹⁶⁵ In a very general sense, *capnometry* refers to the measurement and quantification of inhaled or exhaled CO_2 concentrations at the airway opening. *Capnography*, however, refers not only to the method of CO_2 measurement, but also to its graphic display as a function of time or volume. A *capnometer* is simply a device that measures CO_2 concentrations. A capnometer may display a numeric value for inspired or exhaled CO_2 . A *capnograph*, however, is a device that records and displays CO_2 concentrations, usually as a function of time. A *capnogram* refers to the graphic display that the capnograph generates. Fig. 41.9 illustrates a typical CO_2 concentration profile for three breaths as a function of time.

MEASUREMENT PRINCIPLES

Various methods exist for detecting and quantifying CO_2 concentrations in respiratory gases, such as mass spectrometry, Raman spectrometry, or gas chromatography.^{166,167} The most commonly used method in clinical environments relies on nondispersive infrared absorption.¹⁶⁸ With this technique, a beam of infrared light is passed through a gas sample, and the resulting intensity of the transmitted light is measured by a photodetector.¹⁶⁴ Gaseous CO_2 absorbs light over a very narrow bandwidth centered around 4.26 μm . Its presence in the sample cell decreases the amount of infrared light at this wavelength that reaches the detector in proportion to its concentration. Because the absorption spectrum for CO_2 partially overlaps with the spectra of other gaseous species commonly encountered in anesthesia (i.e., water and nitrous oxide¹⁶⁹), infrared filters and

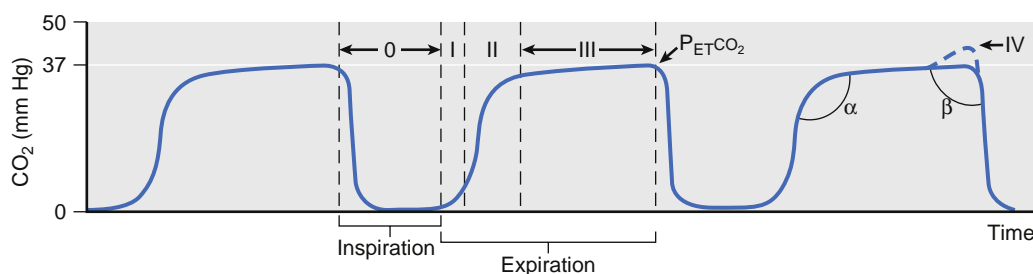


Fig. 41.9 Representative Time Capnogram for Three Breaths. The expiratory segment is divided into phases I, II, III, and IV. The inspiratory segment is referred to as phase 0 in this figure. α denotes the angle between phases II and III, whereas β denotes the angle between phase III and the descending limb of phase 0. Phase IV (dashed line in third breath) denotes the upstroke observed at the end of phase III in some patients. PETCO₂, Partial pressure of end-tidal carbon dioxide. (Courtesy Respirationics, Inc., Murrysville, PA, with permission.)

compensation algorithms are used to minimize this interference and improve accuracy.¹⁷⁰

Most capnometers rely on infrared-light source that is focused on a chopper disk that rotates at approximately 60 revolutions per second. The chopper allows the beam to be alternately directed through (1) the sample cell with the gas to be analyzed and (2) a reference cell with no detectable CO₂. In addition, the light source is completely blocked at various points during the revolution of the chopper disk. The photodetector and associated circuitry process these three signals to estimate the changes in CO₂ concentration continuously in the sample cell. Alternatively, CO₂ concentration may be estimated with solid-state technology, using a beam splitter instead of a chopper wheel. The splitter allows for the measurement of infrared energy at wavelengths within and outside the absorption spectrum of CO₂.

Capnometers fall into two general categories: sidestream (diverting) and mainstream (nondiverting). Sidestream analyzers are more frequently used in clinical environments. Their CO₂ sensors are physically located away from the airway gases to be measured. Sidestream analyzers incorporate a pump or compressor that aspirates gases into a sample cell located at the unit's console (Fig. 41.10A). Typical tubing length for this aspiration may be 6 feet, and gas withdrawal rates may vary from 30 to 500 mL/min. This lost gas volume may need to be considered during closed-circuit anesthesia or during ventilation of neonates and infants. The volume can be returned to the circuit, or it can be routed to a scavenger to prevent contamination of the environment with anesthetic or waste gases. Gases must also pass through various filters and water traps before they are presented to the sample cell.¹⁶⁴ Sidestream capnometers have a transport delay time corresponding to the rate at which gas is sampled and the washout of the analyzing chamber (see Fig. 41.10B). The capnograms generated by sidestream analyzers also have an associated rise time, defined as the time required for the analyzer to respond to a sudden change in CO₂ concentration.¹⁷¹ By convention, this is usually the time interval required for the analyzer output to change from 10% to 70% of its final value.*¹⁷¹ Typical rise times for commercially available capnometers range from 10 to 400 ms, and they can depend on the rotation of the chopper wheel, the rate of gas aspiration, the volume of aspiration tubing and water traps,

and the dynamic response of the infrared filters and other electronics.

With mainstream analyzers, the sample cell is placed directly into the patient's breathing circuit. Thus the inspiratory or expiratory gases pass directly through the infrared light path (see Fig. 41.10C). An advantage of mainstream analyzers is that they have no delay time (see Fig. 41.10D). Moreover, their rise time is generally faster than that of sidestream analyzers.¹⁷¹ A disadvantage is the potential increase in dead space, although recent developments in solid-state electronics have made this much less of an issue.¹⁷² In addition, the sample cell is usually heated to 40°C to minimize the condensation of water vapor, which can bias the measurement. This increase in temperature, combined with the proximity of the sensor to the patient's airway, can potentially increase the risk of facial burns.

TIME CAPNOGRAM

The simplest and most widely used form of display for exhaled CO₂ is the *time capnogram*. The time capnogram displays both inspiratory and expiratory phases. Fig. 41.9 shows a typical time capnogram for three breaths. The expiratory phase is divided into three distinct components. Phase I corresponds to the exhalation of dead space gas from the central conducting airways or any equipment distal to the sampling site, which ideally should have no detectable CO₂ (i.e., partial pressure of CO₂, PCO₂ ~ 0). During phase II, a sharp rise in PCO₂ to a plateau indicates the sampling of transitional gas between the airways and alveoli. The plateau region of the capnogram, phase III, corresponds to the PCO₂ in the alveolar compartment. For a lung with relatively homogeneous ventilation, phase III is approximately flat throughout expiration. In fact, various mechanisms contribute to the slight upsloping of CO₂ concentration versus time during phase III. Most of these mechanisms reflect a heterogeneous distribution of ventilation-perfusion (V/Q) or alveolar CO₂ partial pressure (P_ACO₂) throughout the lung. Well-ventilated and well-matched V/Q regions tend to have lower PCO₂ and shorter time constants, and they empty earlier during the expiratory phase. Less well-ventilated and poorly matched V/Q regions have higher CO₂ levels, and they empty later in the expiratory cycle. Respiratory pathologies associated with an increase in ventilation heterogeneity, such as asthma, chronic obstructive pulmonary disease (COPD), or acute lung injury,¹⁷³ yield a steeper upslope of phase III. Interventions that improve ventilation

*Rise time may also be defined as the time required for the analyzer output to change from 10% to 90% of its final value.

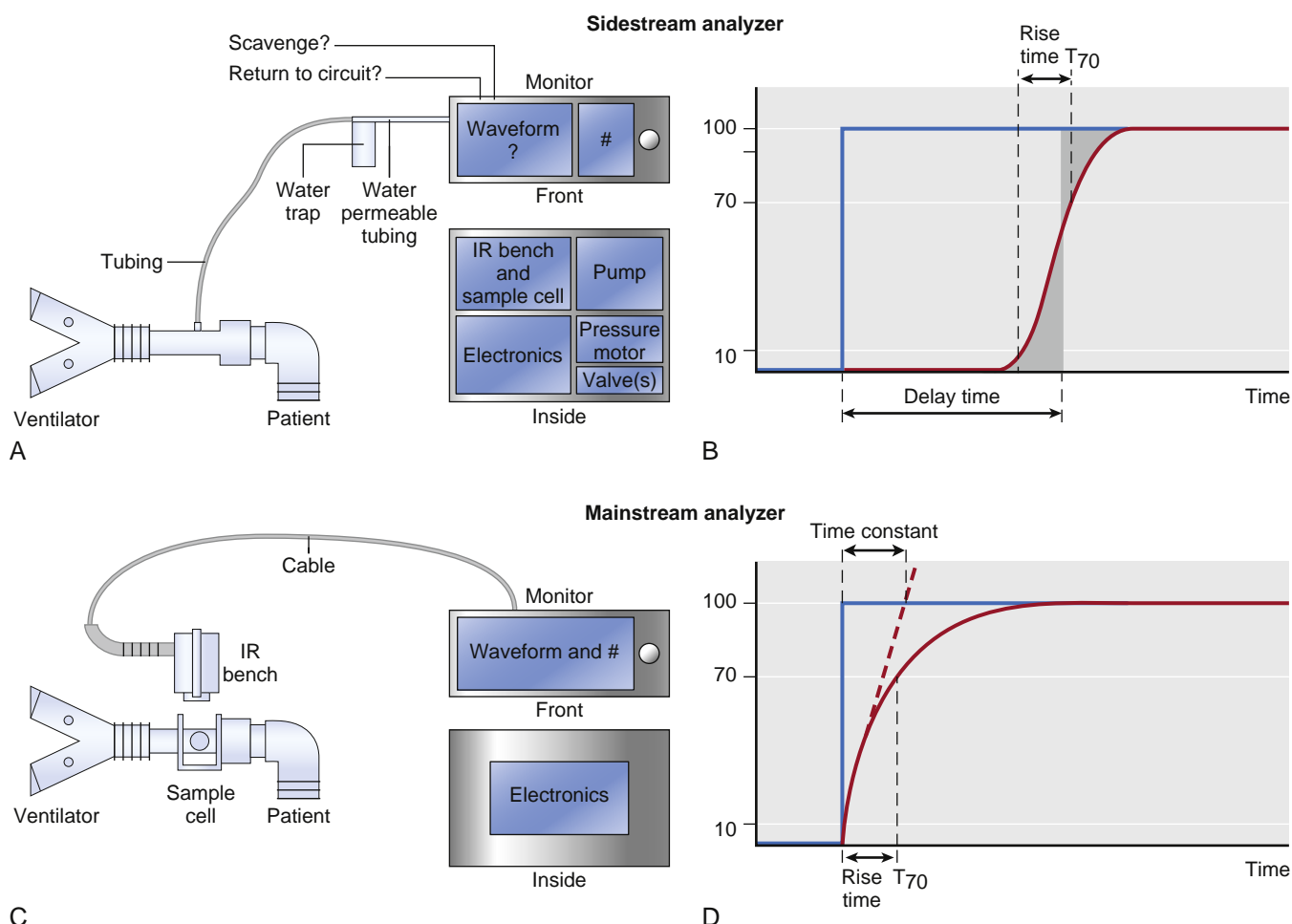


Fig. 41.10 Schematics of sidestream (A) and mainstream (C) capnometry sampling methods, along with corresponding representative time capnograms (curves in B and D) following a step increase in CO₂ concentration (blue lines). Rise time (T_{70}) corresponds to the time required for either sensor to change from 10% to 70% of its final value. A delay time is observed for the sidestream analyzer, corresponding to the aspiration rate of the sampled gas and the washout of the analyzing chamber. IR, Infrared. (Modified from Jaffe MB. Mainstream or sidestream capnography? Technical considerations. Wallingford, CT: Respiration Novametric, Inc, 2002; and Brunner JX, Westenskow DR. How the rise time of carbon dioxide analysers influences the accuracy of carbon dioxide measurements. *Br J Anaesth.* 1988;61:628–638.)

homogeneity, such as positive end-expiratory pressure (PEEP) or bronchodilators, flatten phase III. Mechanical disturbances may also be present during phase III, reflecting processes such as spontaneous breathing efforts, cardiogenic oscillations, or surgical manipulation (Fig. 41.11). Following phase III, a sharp downstroke of PCO₂ occurs as fresh inspired gas moves past the sampling site and washes out the remaining CO₂. This is referred to as the beginning of phase 0 by some authors,^{165,174} or phase IV by others.¹⁶⁶ Occasionally, a sharp upstroke in PCO₂ is observed at the very end of phase III, which is termed phase IV or IV', depending on the author.¹⁷⁵ This upstroke probably results from the closure of lung units with relatively low PCO₂ and allows for regions of higher CO₂ to contribute a greater proportion of the exhaled gas to be sampled.¹⁶⁵ Additional insights into various abnormalities in ventilation or perfusion are also obtained by trending time capnograms over many breaths for long periods (Fig. 41.12).

The term “end-tidal” CO₂ (P_{ET}CO₂) generally refers to the final value of the exhaled PCO₂ curve, at the very end of the expiratory phase. The method used to determine this number is not universal, and varies according to the manufacturer of

the particular capnograph in use. For example, P_{ET}CO₂ may simply be (1) the PCO₂ value just before inspiration, (2) the largest PCO₂ value during a single exhalation cycle, or (3) the PCO₂ value at a specified time in the capnogram averaged across several breaths. If P_{ET}CO₂ is measured during a reasonably flat and undistorted phase III, it may be well correlated with P_aCO₂.¹⁷⁰ This may not be the case if the duration of phase III is truncated, or if CO₂ is measured from gas that is contaminated with room or O₂-enriched air (i.e., during spontaneous breathing with a nasal cannula or facemask). Potential causes of increased or decreased P_{ET}CO₂ are listed in Table 41.2. In healthy individuals with homogeneous ventilation, the difference between P_aCO₂ and P_{ET}CO₂ is usually less than 5 mm Hg, thereby expressing the equilibration between alveolar and pulmonary capillary blood. Several disease states compromise this equilibration and produce increased P_aCO₂ – P_{ET}CO₂ difference (Box 41.2). There are situations in which P_{ET}CO₂ can be greater than P_aCO₂, especially in the presence of severe ventilation heterogeneity and lung units with very low V/Q. For steady-state conditions, the P_{ET}CO₂ usually reflects the relative balance between CO₂ production and alveolar ventilation.

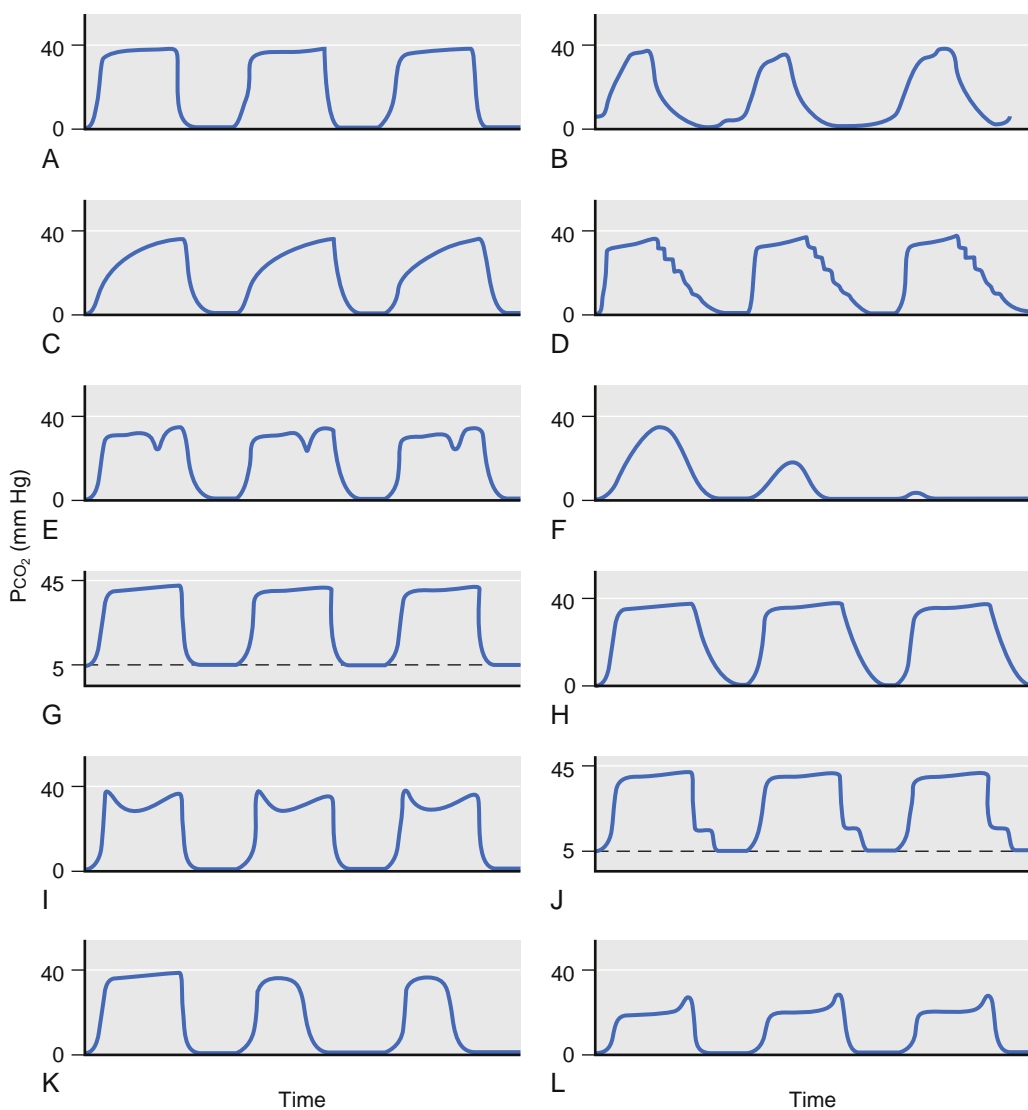


Fig. 41.11 Representative Time Capnograms under Normal and Abnormal Conditions. (A) Normal capnogram during controlled mechanical ventilation; (B) normal capnogram during spontaneous breathing; (C) increased upslope of phase III, as may occur during bronchospasm (asthma, chronic obstructive pulmonary disease), or partially obstructed endotracheal tube/breathing circuit; (D) cardiogenic oscillations at the end of exhalation as flow decreases to zero and the beating heart causes emptying of different lung regions and back-and-forth motion between exhaled and fresh gas; (E) clefts during phase III indicating spontaneous breathing efforts during controlled mechanical ventilation; (F) esophageal intubation; (G) rebreathing of CO_2 , as may occur with faulty expiratory valve or exhausted absorber system. Inspiratory CO_2 is consistently above 0; (H) faulty inspiratory valve, resulting in a slower downslope, which extends into the inhalation phase (phase 0) as CO_2 in the inspiratory limb is rebreathed; (I) two peaks in phase III suggestive of sequential emptying of two heterogeneous compartments, as may be seen in a patient with a single lung transplant; (J) faulty inspiratory valve; (K) sudden shortening of the duration of phase III during controlled mechanical ventilation, suggesting the abrupt onset of a ruptured or leaking endotracheal tube cuff; (L) dual plateau in phase III, suggesting the presence of a leak in a sidestream sample line. Early portion of phase III abnormally low due to dilution of exhaled gas with ambient air. The sharp increase in CO_2 at the end of phase III reflects a diminished leak resulting from the increased circuit pressure at the onset of inspiration. PCO_2 , Partial pressure of carbon dioxide. (Modified from Hess D. Capnometry and capnography: technical aspects, physiologic aspects, and clinical applications. *Respir Care*. 1990;35:557-576; Roberts WA, Maniscalco WM, Cohen AR, et al. The use of capnography for recognition of esophageal intubation in the neonatal intensive care unit. *Pediatr Pulmonol*. 1995;19:262-268; and Eskaros SM, Papadakos PJ, Lachmann B. Respiratory monitoring. In: Miller RD, Eriksson LI, Fleisher LA, eds. *Miller's Anesthesia*. 7th ed. New York, NY: Churchill Livingstone; 2010:1427.)

VOLUME CAPNOGRAM

Although time capnography is relatively straightforward to monitor in clinical environments, a major limitation of the technique is its lack of information regarding respiratory flows or volumes.¹⁷⁴ The *volume capnogram* is a graphic display of CO_2 concentration or partial pressure versus exhaled volume.¹⁶⁶ The inspiratory phase is not defined in a volume capnogram. Similar to its temporal counterpart, it is also partitioned into three distinct phases (I, II, and III)

corresponding to anatomic dead space, transitional, and alveolar gas samples (Fig. 41.13). However, it possesses several advantages over the time capnogram. First, it allows for estimation of the relative contributions of anatomic and alveolar components of physiologic dead space.^{175a,176} Second, it is more sensitive than the time capnogram in detecting subtle changes in dead space that are caused by alterations in PEEP, pulmonary blood flow, or ventilation heterogeneity (Fig. 41.14). Finally, the numeric integral of PCO_2 as a function of volume allows for determination of

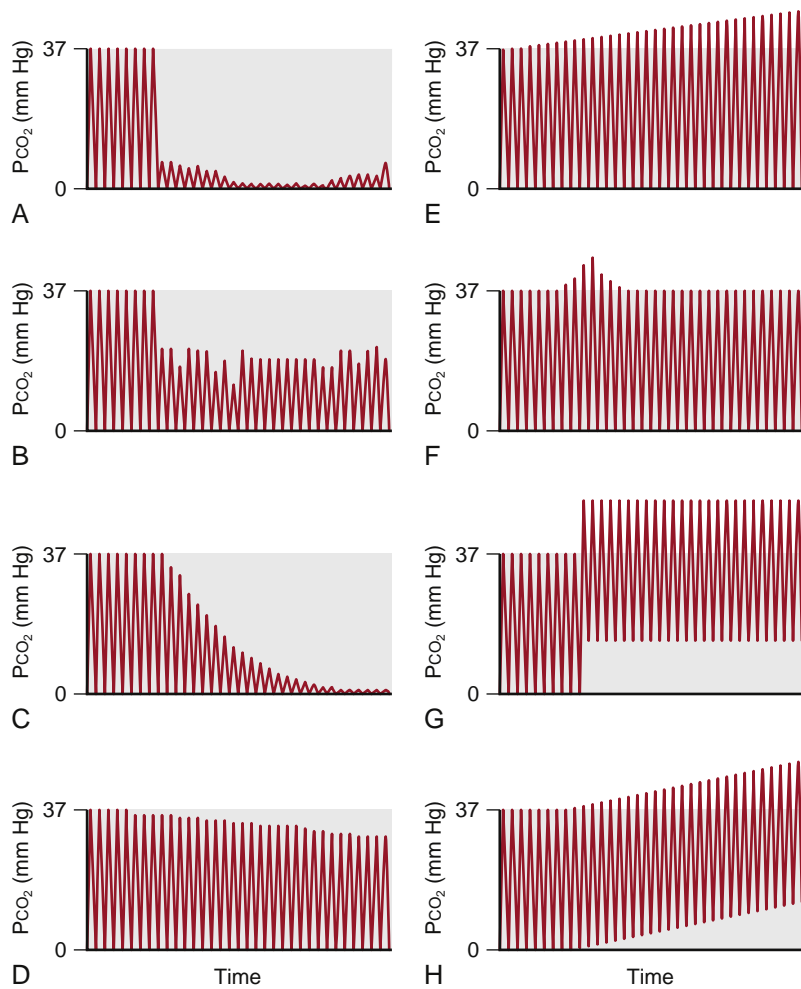


Fig. 41.12 Representative time capnograms trended over many breaths, illustrating various abnormalities in ventilation and/or perfusion. (A) sudden drop in CO_2 due to catastrophic loss of ventilation; (B) leak or partial obstruction in breathing circuit; (C) sudden interruption in pulmonary perfusion, as may occur during cardiac arrest; (D) gradual decrease in CO_2 due to hyperventilation, decreased metabolism, or decreased pulmonary perfusion; (E) gradual increase in CO_2 as may occur during hypoventilation, laparoscopic insufflation, increased metabolism, or increased pulmonary perfusion; (F) transient rise in CO_2 indicated acute increase in CO_2 delivery to the lungs, as may occur during release of a tourniquet or administration of a bicarbonate bolus; (G) rise in both the baseline and end-tidal CO_2 , consistent with a contaminated sample cell; (H) gradual rise in baseline and end-tidal CO_2 , consistent with rebreathing. PCO_2 , Partial pressure of CO_2 . (Modified from Swedlow DB. Capnometry and capnography: the anesthesia disaster early warning system. *Semin Anesth*. 1986;5:194–205.)

the total mass of CO_2 exhaled during a breath and provides for the estimation of \dot{V}_{CO_2} .

Blood Gas Analysis

PHYSIOLOGIC FUNDAMENTALS

Arterial blood gas analysis is used to assess oxygenation, ventilation, and acid-base status. This section focuses on the use of arterial blood gases to assess oxygenation and ventilation. For a discussion of acid-base status, see [Chapter 48](#), “Perioperative Acid-Base Balance.”

Oxygenation is reflected in the P_{aO_2} , which is a function of the alveolar partial pressure of O_2 (P_{AO_2}) and the efficiency of O_2 transfer from alveoli to the pulmonary capillary blood. In healthy adults breathing room air at sea level, P_{aO_2} ranges between 80 and 100 mm Hg. The normal value of P_{aO_2} decreases with increasing age and increasing altitude. Hypoxemia is defined as a P_{aO_2}

less than 80 mm Hg. There are five physiologic causes of hypoxemia: (1) hypoventilation, (2) \dot{V}/\dot{Q} mismatching, (3) right-to-left shunt, (4) diffusion limitation, and (5) diffusion-perfusion mismatch. The first three causes explain the majority of hypoxemia in the perioperative setting. Reduced inspired PO_2 (e.g., in faulty closed or partially closed anesthesia breathing circuits or at high altitude) is an additional cause of hypoxemia.

These factors produce hypoxemia by affecting different steps of O_2 transport from the environment to the arterial blood. A low inspired PO_2 , as well as hypoventilation, reduces the P_{AO_2} . \dot{V}/\dot{Q} mismatch, right-to-left shunt, and alveolar diffusion limitation affect the efficiency of O_2 exchange. Diffusion limitation plays a role in conditions that thicken the alveolar-capillary barrier, such as interstitial lung diseases, and in hypoxemia induced by exercise or altitude.^{177,178} In the clinical setting, impairment of diffusion of O_2 or CO_2 rarely occurs to a significant extent. The remainder of this section focuses on \dot{V}/\dot{Q} mismatch and right-to-left shunt.

TABLE 41.2 Causes of Changes in Partial Pressure of End-Tidal Carbon Dioxide

$\uparrow P_{ET}CO_2$	$\downarrow P_{ET}CO_2$
$\uparrow CO_2$ Production and Delivery to the Lungs	$\downarrow CO_2$ Production and Delivery to the Lungs
Increased metabolic rate	Hypothermia
Fever	Pulmonary hypoperfusion
Sepsis	Cardiac arrest
Seizures	Pulmonary embolism
Malignant hyperthermia	Hemorrhage
Thyrotoxicosis	Hypotension
Increased cardiac output (e.g., during CPR)	
Bicarbonate administration	
\downarrow Alveolar Ventilation	\uparrow Alveolar Ventilation
Hypoventilation	Hyperventilation
Respiratory center depression	
Partial muscular paralysis	
Neuromuscular disease	
High spinal anesthesia	
COPD	
Equipment Malfunction	Equipment Malfunction
Rebreathing	Ventilator disconnect
Exhausted CO_2 absorber	Esophageal intubation
Leak in ventilator circuit	Complete airway obstruction
Faulty inspiratory/expiratory valve	Poor sampling
	Leak around endotracheal tube cuff

CO_2 , Carbon dioxide; COPD, chronic obstructive pulmonary disease; CPR, cardiopulmonary resuscitation; $P_{ET}CO_2$, partial pressure of end-tidal carbon dioxide. Modified from Hess D. Capnometry and capnography: technical aspects, physiologic aspects, and clinical applications. *Respir Care*. 1990;35:557–576.

BOX 41.2 Causes of Increased Arterial-to-End-Tidal Carbon Dioxide Pressure Difference $P_{(a-ET)CO_2}$

Increased ventilation-perfusion heterogeneity, particularly with high V/Q regions
Pulmonary hypoperfusion
Pulmonary embolism
Cardiac arrest
Positive pressure ventilation (especially with PEEP)
High-rate low-tidal-volume ventilation

PEEP, Positive end-expiratory pressure. Modified from Hess D. Capnometry and capnography: technical aspects, physiologic aspects, and clinical applications. *Respir Care*. 1990;35:557–576.

\dot{V}/\dot{Q} mismatch is the most common cause of hypoxemia in the clinical setting. Ventilation and perfusion are non-uniformly distributed throughout the normal lung, with worsening mismatch in the setting of lung disease, general anesthesia, and mechanical ventilation. Areas with low or zero \dot{V}/\dot{Q} yield low end-capillary PO_2 , whereas areas with normal or high \dot{V}/\dot{Q} produce higher end-capillary PO_2 . However, because of the plateau of the O_2 -Hb dissociation curve (see Fig. 41.2), the normal and high \dot{V}/\dot{Q} regions are limited in the extent to which they increase the O_2 content and compensate for the low \dot{V}/\dot{Q} regions (Fig. 41.15). Consequently, \dot{V}/\dot{Q} mismatch results in hypoxemia.

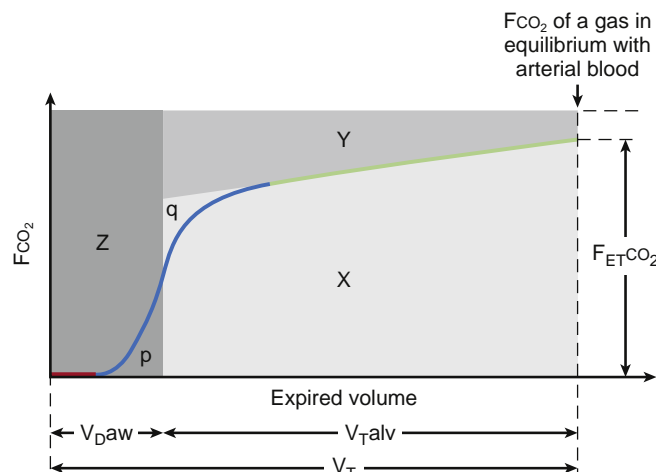


Fig. 41.13 The volume capnogram is a plot of the fraction of CO_2 (FCO_2) in exhaled gas versus exhaled volume. It is divided into three phases, which reflect the same sources of expired gas as present in the time capnograph: anatomic dead space (Phase I, red), transitional (Phase II, blue), and alveolar gas (Phase III, green). The volume capnogram allows for the partition of total tidal volume (V_T) into airway dead space volume (V_{Daw}) and an effective alveolar tidal volume (V_{Talv}) by a vertical line through Phase II, positioned such that the approximately triangular areas p and q are equal. It also provides the slope of Phase III as a quantitative measure of the heterogeneity of alveolar ventilation. The total area below the horizontal line (denoting the FCO_2 of a gas in equilibrium with arterial blood) can be divided into three distinct areas: X , Y , and Z . Area X corresponds to the total volume of CO_2 exhaled over a tidal breath. This value can be used to compute the CO_2 production (\dot{V}_{CO_2}), and the mixed expired CO_2 fraction or partial pressure to be used in the Bohr equation (Eq. [41.15]) based on the division of the exhaled CO_2 volume by the exhaled tidal volume. Area Y represents wasted ventilation due to alveolar dead space, while area Z corresponds to wasted ventilation due to anatomic deadspace (V_{Daw}). Thus areas $Y + Z$ represent the total physiologic dead space. The volume capnogram can also be plotted as a PCO_2 versus exhaled volume curve. $F_{ET}CO_2$, Fraction of end-tidal carbon dioxide. (Modified from Fletcher R, Jonson B, Cumming G, et al. The concept of deadspace with special reference to the single breath test for carbon dioxide. *Br J Anaesth*. 1981;53:77–88.)

Right-to-left shunt is the amount of blood that flows from the pulmonary artery to the systemic arterial circulation without undergoing pulmonary gas exchange. It represents an extreme case of \dot{V}/\dot{Q} mismatch in which the ratio equals zero and the end-capillary gas partial pressures are equal to the values found in mixed venous blood. In healthy awake spontaneously breathing subjects, intrapulmonary shunt is negligible,¹⁷⁹ and a small (<1% of cardiac output) extrapulmonary shunt results from drainage of the bronchial and Thebesian veins into the arterial side of the circulation.¹⁸⁰ During general anesthesia, a right-to-left shunt can develop as a result of atelectasis.^{181,182} Right-to-left shunt can also be seen in pathologic conditions such as pneumonia and acute lung injury. The effect of the shunt on P_aO_2 is a function of the magnitude of the shunt, F_iO_2 , and the cardiac output (Fig. 41.16). Importantly, increases in F_iO_2 have a small effect on P_aO_2 in the presence of large true right-to-left shunt (see Fig. 41.16).

The traditional method to estimate flow through shunting regions (\dot{Q}_s) as a fraction of the total cardiac output (\dot{Q}_T) is based on the modeling of the lung as a three-compartment system (Fig. 41.17).¹⁸³ The three compartments represent (1) lung regions receiving both ventilation and perfusion,

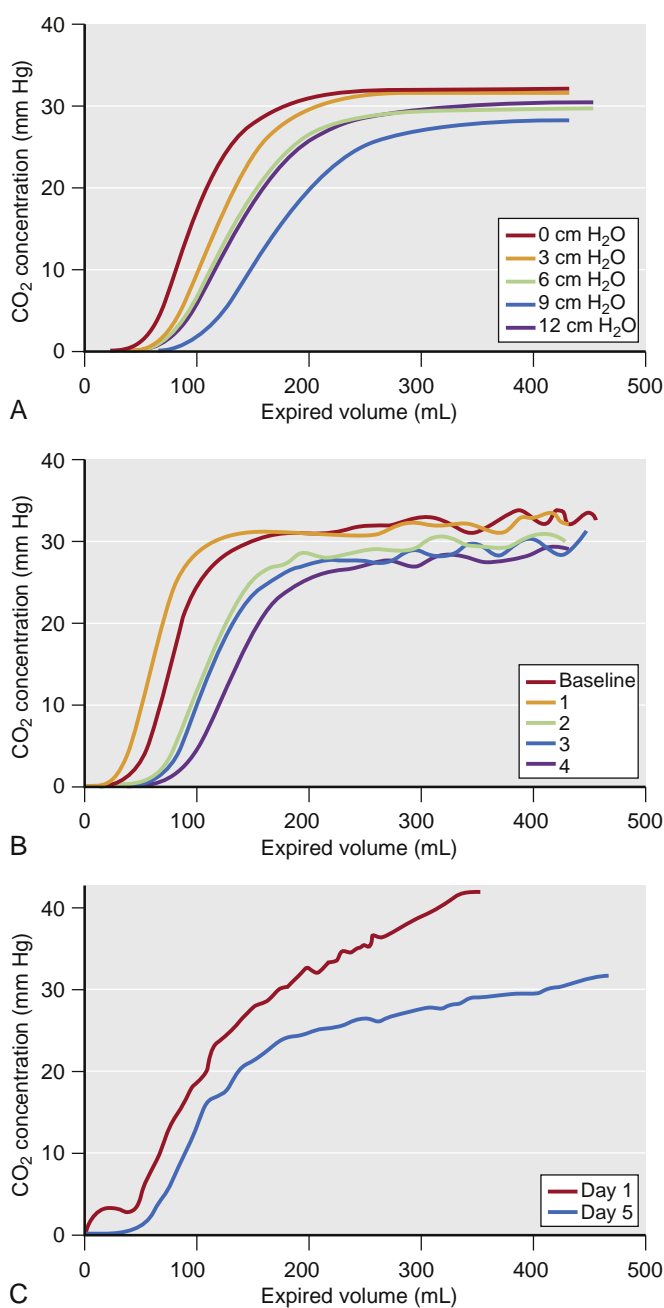


Fig. 41.14 Representative Single-breath Volume Capnograms, Illustrating Various Abnormalities in Ventilation or Perfusion. (A) alterations in phases II and III with corresponding changes in positive end-expiratory pressure (0, 3, 6, 9, and 12 cm H₂O) during positive pressure ventilation; (B) alterations in phases II and III with corresponding changes in pulmonary perfusion (increasing numbers correspond to decreasing pulmonary blood flow); (C) pronounced positive slope of phase III during acute bronchospasm (Day 1). Following resolution (Day 5), there is a noticeable reduction in the slope phase III. CO₂, Carbon dioxide. (Modified from Thompson JE, Jaffe MB. Capnographic waveforms in the mechanically ventilated patient. *Respir Care*. 2005;50:100–108.)

(2) a shunt compartment ($\dot{V}/\dot{Q} = 0$), and (3) a dead space compartment with ventilation but no perfusion ($\dot{V}/\dot{Q} = \infty$). The application of the concept of mass balance to this model yields the shunt fraction (\dot{Q}_s/\dot{Q}_T) expression

$$\dot{Q}_s/\dot{Q}_T = \frac{(Cc' O_2 - C_a O_2)}{(Cc' O_2 - C_{\bar{v}} O_2)} \quad (41.16)$$

where \dot{Q}_s is the shunted blood flow, and $Cc' O_2$ is the end-capillary O₂ content. $Cc' O_2$ is calculated using Eq. (41.1), assuming equilibration between the end-capillary blood and alveolar gas. The P_{aO_2} is calculated using the ideal alveolar gas equation:

$$P_{aO_2} = F_i O_2 \cdot (P_{atm} - P_{H_2O}) - P_a CO_2/R \quad (41.17)$$

where $F_i O_2$ is the inspired O₂ fraction, P_{atm} is barometric pressure (typically assumed to be the pressure of one standard atmosphere at sea level, 760 mm Hg), and P_{H_2O} is partial pressure of water vapor (47 mm Hg at 37°C). R, the respiratory quotient, is the ratio of pulmonary CO₂ elimination to O₂ uptake ($R = \dot{V}_{CO_2}/\dot{V}_{O_2}$), which equals the value of 0.8 under normal diet and metabolic conditions.

The three-compartment model is a simplification of the real lung. As a result, under conditions of $F_i O_2$ less than 100%, \dot{Q}_s/\dot{Q}_T computed with Eq. (41.16) represents a combination of all factors producing hypoxemia, predominantly true right-to-left shunt and \dot{V}/\dot{Q} mismatch. Under such conditions, \dot{Q}_s/\dot{Q}_T is referred to as venous admixture. When $F_i O_2$ is 100%, the effects of \dot{V}/\dot{Q} heterogeneity on O₂ exchange are eliminated and the equation exclusively yields the right-to-left shunt fraction.¹⁸⁴ The administration of 100% O₂ (i.e., $F_i O_2$ of 1.0) can lead to the development of absorption atelectasis in compartments with very low \dot{V}/\dot{Q} , thus leading to an increase in true right-to-left shunt.¹⁸⁴

If the assumptions are made that end-capillary blood has an O₂ saturation of 100% and the O₂ content of blood is predominantly determined by Hb saturation, the shunt fraction equation can be simplified to

$$\dot{Q}_s/\dot{Q}_T = \frac{(1 - S_a O_2)}{(1 - S_{\bar{v}} O_2)} \quad (41.18)$$

where $S_a O_2$ is arterial saturation, and $S_{\bar{v}} O_2$ is mixed venous saturation.

Other indices of oxygenation: The calculation of the shunt fraction is a fundamental measure of O₂ exchange impairment. However, a pulmonary artery catheter is required for the measurement of $S_{\bar{v}} O_2$. For this reason, indices of oxygenation that rely on less invasive measures have been developed. An ideal index should reflect the efficiency of oxygenation, change with changes in lung function, remain constant with changes in extrapulmonary conditions (such as $F_i O_2$), and provide clinically useful diagnostic and prognostic information.¹⁸⁵ Although P_{aO_2} certainly reflects arterial blood oxygenation, it is limited in providing a measure of the magnitude of the O₂ exchange deficiency because of its dependence on the $F_i O_2$ and to the non-linear relationship between P_{aO_2} and blood O₂ content.¹⁸⁵ As a consequence, several indices based on the P_{aO_2} that account for the $F_i O_2$ or the P_{aO_2} have been developed: the alveolar-arterial partial pressure gradient of O₂ ($[A-a]PO_2$), the respiratory index ($[A-a]PO_2/P_{aO_2}$), the arterial-alveolar ratio of O₂ partial pressures (P_{aO_2}/P_{AO_2}), and the ratio between P_{aO_2} and $F_i O_2$ ($P_{aO_2}/F_i O_2$).¹⁸⁵

The advantages of indices based on P_{aO_2} are that their calculations are fairly simple and require only arterial blood sampling. However, an important limitation is that these indices vary with the $F_i O_2$, P_{aCO_2} , Hb, and O₂ consumption (\dot{V}_{O_2}).^{186,187} Consequently, changes in those variables can lead to changes in the values of the indices in the absence of

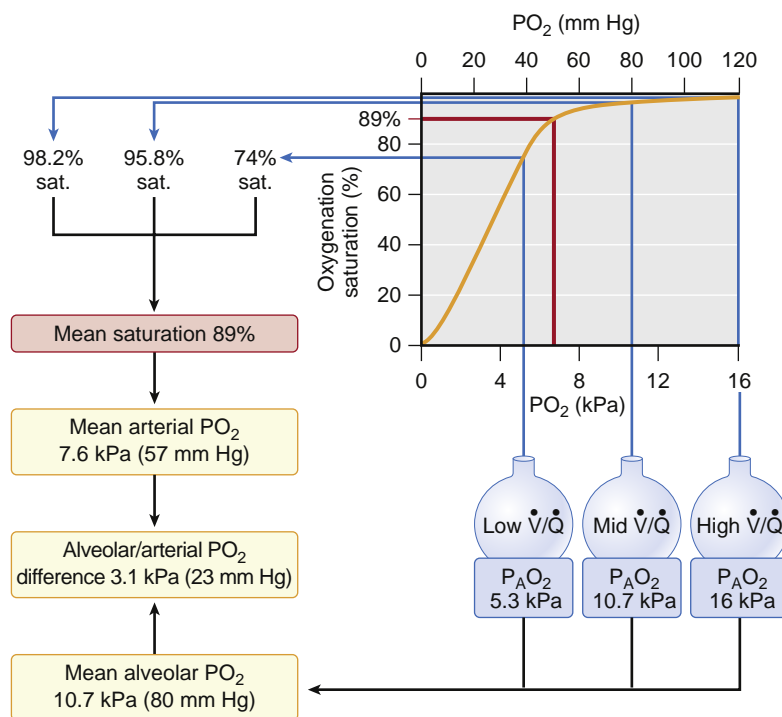


Fig. 41.15 Effect of Different Ventilation-Perfusion (V/Q) Regions on Partial Pressure of Arterial Oxygen (PaO₂). Because of the shape of the oxyhemoglobin dissociation curve, regions of lung with low V/Q have a disproportionately greater effect on lowering the arterial saturation than do regions of lung with normal or higher V/Q to increase PaO₂. Assuming equal blood flow, the average partial pressure of alveolar oxygen (P_AO₂) of the V/Q regions represented in the illustration is 10.7 kPa (80 mm Hg). Based on the oxyhemoglobin dissociation curve, however, the average saturation of the arterial blood is 89%, producing an average PaO₂ equal to 7.6 kPa (57 mm Hg). PO₂, Partial pressure of oxygen. (Modified from Lumb AB. *Nunn's Applied Respiratory Physiology*, 6th ed. Philadelphia: Elsevier/Butterworth Heinemann; 2005.)

any change in lung gas exchange function. Another limitation is the failure of these indices to account for changes in V/Q matching resulting from changes in the F_iO₂. In addition, indices that use P_AO₂ rely on the assumptions of the alveolar gas equation, including P_ACO₂ = P_aCO₂, which may not hold true in pathologic conditions.

An early index developed to assess oxygenation that used only peripheral blood sampling was the (A-a)PO₂.¹⁸⁸ The (A-a)PO₂ can help to differentiate V/Q mismatch, shunt, and diffusion limitation from hypoventilation and low F_iO₂ as causes of hypoxemia. This is because the (A-a)PO₂ is unchanged under conditions of decreased F_iO₂ and hypoventilation but increased with V/Q mismatch, shunt, and diffusion limitation.

The A-a gradient of O₂ is calculated as

$$(A-a) \text{ PO}_2 = P_{A\text{O}_2} - P_{a\text{O}_2} \quad (41.19)$$

The normal value of the (A-a)PO₂ is less than 10 mm Hg in young adults breathing room air, and it increases with age and the administration of supplemental O₂. The change in (A-a)PO₂ with age can be estimated by¹⁸⁹

$$(A-a) \text{ PO}_2 = 0.21 \cdot (\text{age} + 2.5) \quad (41.20)$$

The (A-a)PO₂ varies significantly with the F_iO₂ such that the application of supplemental O₂ can lead to an increase in the (A-a)PO₂ independent of pulmonary disease.¹⁸⁶ Like the (A-a)PO₂, the respiratory index (A-a)PO₂/P_AO₂ and the P_AO₂/P_AO₂ are sensitive to F_iO₂, especially in the presence of a high degree of V/Q mismatch, such as during acute respiratory distress syndrome (ARDS), and less so in the absence

of true shunt or when low V/Q regions are minimal (e.g., in healthy lung or pulmonary embolus).¹⁹⁰

Unlike the other indices based on partial pressures, the P_AO₂/F_iO₂ ratio does not use the P_AO₂ and its associated assumptions. This index is more stable, particularly under conditions relevant to ARDS such as P_AO₂ lower than 100 mm Hg in the setting of an F_iO₂ greater than 0.5.^{186,187} P_AO₂/F_iO₂ values are part of the diagnostic criteria for ARDS and have been correlated with outcomes in these patients.¹⁹¹ When repeated arterial blood sampling is not possible, the S_pO₂/F_iO₂ (also referred to as SF) ratio may be useful. SF ratio values have shown good correlation with P_AO₂/F_iO₂ values in both adults and children with respiratory failure who have S_pO₂ values in the range of 80% to 97%.^{192,193}

The P_AO₂/F_iO₂ ratio does not characterize factors associated with the severity of respiratory failure such as ventilator settings or respiratory system mechanics.¹⁹⁴⁻¹⁹⁶ Another drawback of the P_AO₂/F_iO₂ ratio is its dependence on PEEP or mean airway pressure, because increases in these variables result in lung recruitment and improved oxygenation. As a consequence, the oxygenation index (OI) was proposed as a more robust alternative to the P_AO₂/F_iO₂ ratio¹⁹⁷:

$$OI = 100\% \times \frac{F_{i\text{O}_2} \bar{P}_{ao}}{P_{a\text{O}_2}} \quad (41.21)$$

where \bar{P}_{ao} denotes the mean airway pressure. The OI has been used as a prognostic indicator in pediatric patients

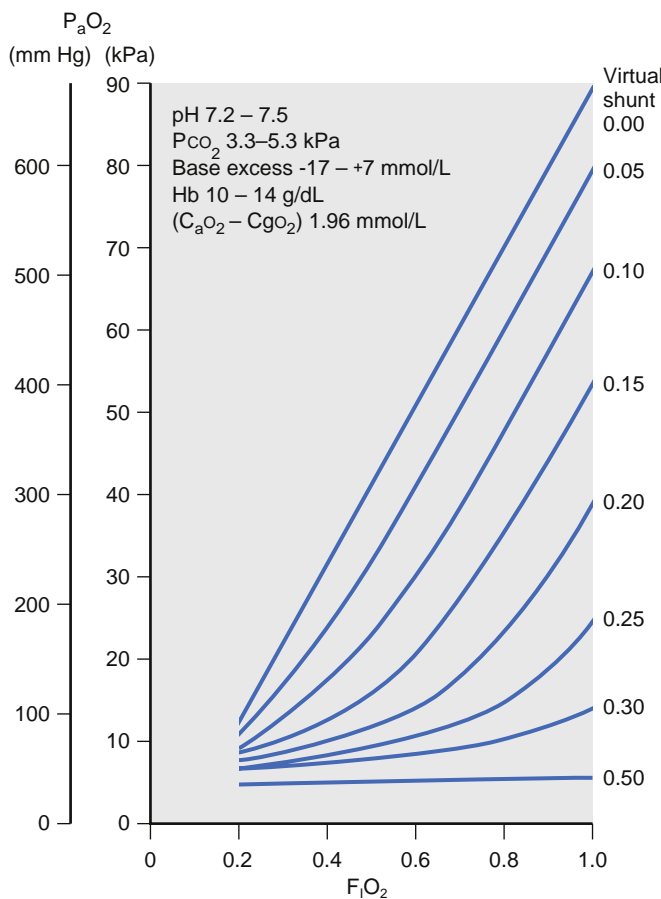


Fig. 41.16 Relationship between partial pressure of arterial oxygen (P_aO_2) and fraction of inspired oxygen (F_1O_2) for different values of shunt fraction computed for normal values of barometric pressure, pH, partial pressure of carbon dioxide (PCO_2), base excess, hemoglobin (Hb) concentration, and arterial-mixed venous oxygen content difference ($C_aO_2 - CgO_2$). Note the small increase in P_aO_2 with F_1O_2 in the presence of large shunt. This graph corresponds to the so-called isoshunt diagram presented by Lawler and Nunn. (From Welsby PD, Earis JE. Some high pitched thoughts on chest examination. *Postgrad Med J*. 2001;77:617–620.)

with acute hypoxic respiratory failure,¹⁹⁸ as a predictor of mortality in adult ARDS,^{196,199} and as an index of enhanced lung recruitment during oscillatory ventilation.²⁰⁰ An alternative “oxygenation saturation index” (OSI) has also been recently proposed:

$$OSI = 100\% \times \frac{F_1O_2 \bar{P}_{ao}}{S_pO_2} \quad (41.22)$$

Similar to the pulse oximetric saturation S_pO_2/F_1O_2 (SF) ratio, the OSI eliminates the need for invasive arterial blood gas sampling by using pulse oximetry. When computed on the day of ARDS diagnosis, it correlates well with the OI and is associated with increased mortality and fewer ventilator free days.¹⁹⁴

Unlike P_aO_2 , P_aCO_2 can be maintained in the normal range in the presence of significant \dot{V}/\dot{Q} mismatching. The reason is that the CO_2 content curve has no plateau. In this way, compensatory hyperventilation can be used to reduce elevations in P_aCO_2 .²⁰¹ The dependence of P_aCO_2 on CO_2 elimination (\dot{V}_{CO_2}) and alveolar ventilation (\dot{V}_A), with

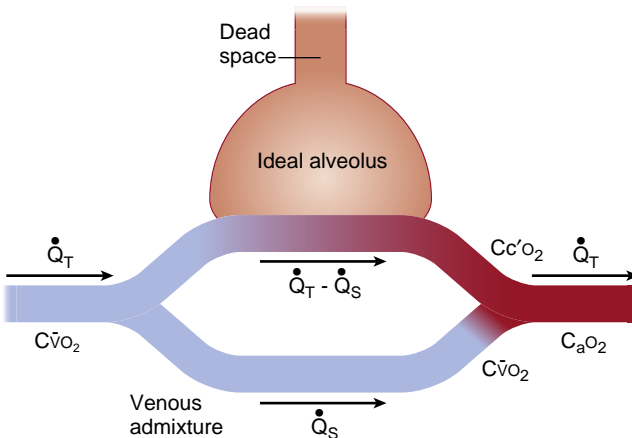


Fig. 41.17 Three-Compartment Model of Gas Exchange. The lung is represented as three functional units: alveolar dead space, “ideal” alveoli, and venous admixture (shunt). Note that the model doesn’t differentiate between true shunt or true dead space and components of shunt and dead space that are caused by ventilation-perfusion (\dot{V}/\dot{Q}) mismatch. CaO_2 , Arterial oxygen content; CvO_2 , oxygen content of end pulmonary capillary blood; \dot{V}_{CO_2} , mixed venous oxygen content; Q_s , shunted blood flow; Qt , total blood flow. (From Lumb AB. *Nunn’s Applied Respiratory Physiology*. 6th ed. Philadelphia: Elsevier/Butterworth Heinemann; 2005.)

k in the equation as a conversion factor equal to 0.863, is expressed by

$$P_aCO_2 = k \times (\dot{V}_{CO_2}/\dot{V}_A) \quad (41.23)$$

In steady-state conditions (constant \dot{V}_{CO_2}), P_aCO_2 changes inversely with the alveolar ventilation. The traditional measure of ventilation inefficiency has been the fraction of dead space to tidal volume (V_D/V_T) as calculated using the Bohr equation (Eq. 41.15) and the assumption that the arterial and alveolar partial pressures of CO_2 are equivalent (i.e., $P_aCO_2 = P_aCO_2$). The dead space fraction determined in this manner includes alveolar (i.e., nonperfused alveoli) and anatomic dead space, as well as regions of high \dot{V}/\dot{Q} ratio. As with the discussion on shunt, the dead space fraction characterizes not only real anatomic dead space, but also areas of inefficient ventilation (see Fig. 41.17).

MEASUREMENT PRINCIPLES

P_aO_2 is measured using a Clark electrode. The electrode consists of a cathode (either platinum or gold) and an anode in an electrolytic bath, surrounded by a thin O_2 permeable membrane. The electrode is inserted into the sample, and O_2 diffuses through the membrane and is reduced by the cathode, generating a current. The current is proportional to the PO_2 in the sample.²⁰² The PCO_2 electrode measures the change in pH brought about by the equilibration of blood with a bicarbonate solution.²⁰³

Effect of Temperature

The solubility of CO_2 and O_2 in blood is affected by temperature. At lower temperatures, solubility is increased, leading to a reduction in partial pressure. Blood gas analyzers measure gas partial pressures at 37°C. As blood from a hypothermic patient is warmed to 37°C by the analyzer, CO_2 and O_2 will come out of solution, leading to P_aCO_2 and P_aO_2

higher than those present in the patient. Blood gas analyzers make use of algorithms to correct the reported values to the patient's actual temperature.²⁰⁴ The temperature effects on blood gas analysis are most relevant during management of hypothermic patients, such as during hypothermic cardiopulmonary bypass (HCPB) or deep hypothermic circulatory arrest (DHCA).

Two strategies have been developed for the management of arterial gas partial pressures under these conditions: alpha-stat and pH-stat. During alpha-stat management, blood gas measurements obtained after the analyzer warms the sample to 37°C are used for acid-base and gas exchange management. Potential benefits of alpha-stat management include the preservation of cerebral autoregulation and the maintenance of protein function.²⁰⁵ During pH-stat management, measurements are corrected to the patient's temperature before they are used for acid-base and gas exchange management. Because patients are hypothermic, the P_aO_2 and P_aCO_2 at the patient's temperature are lower and the pH higher than those measured in the analyzer at 37°C. CO_2 is usually added to the oxygenator to maintain the temperature-corrected P_aCO_2 and pH at normothermic values. The theoretical benefits of pH-stat management are increased cerebral vasodilation leading to more homogeneous cerebral cooling.²⁰⁶

Studies have compared the two strategies with respect to outcomes with varying results.²⁰⁷⁻²¹⁴ In general, clinical studies support the use of pH-stat management in pediatric cardiac surgical procedures during HCPB or DHCA.^{209,213,215} In adult patients, the use of alpha-stat management is supported for HCPB.²¹⁶ For procedures involving DHCA in adults, the use of pH-stat management has been suggested to increase the rate and uniformity of cooling and alpha-stat management during rewarming.²¹⁷

LIMITATIONS AND SOURCES OF ERRORS

Proper handling of arterial blood gas samples is important to prevent errors. Two common sources of error are delays in sample analysis and the presence of air in the sampling syringe.²¹⁸ A delay in sample analysis by 20 minutes at room temperature or at 4°C can lead to a decline in P_aO_2 .²¹⁸ The decline is attributed to the metabolic activity of leukocytes and is not observed in samples placed on ice. The presence of an air bubble in the syringe can lead to a change in the measured P_aO_2 toward the PO_2 of the bubble and decline in P_aCO_2 .²¹⁸

Monitoring Lung Flows, Volumes, and Pressures:

As an organ of gas exchange, the human respiratory system relies on convective and diffusive gas transport processes for VO_2 and elimination of CO_2 . The transport of air to the alveoli and alveolar gas to the environment requires the creation of a pressure gradient, which results in volume changes in the elastic components of the respiratory system, flow in the airways, velocity of moving tissues, and acceleration of air and tissues. The lung consists of a complex branching network of airway segments and viscoelastic tissues that, during the processes of spontaneous breathing or

mechanical ventilation, gives rise to tremendous variations in gas velocities and flow regimens. The movement of gas flow (\dot{V}) into and out of the lungs requires pressure (P) to overcome the resistive (P_R), elastic (P_E), and at times inertial (P_I) forces offered by the airway tree, parenchymal tissues, and chest wall:

$$P = P_R + P_E + P_I \quad (41.24)$$

Eq. (41.24) can be used to describe the mechanical behavior of the total respiratory system, the lungs alone, or the chest wall, depending on whether P refers to airway pressure relative to atmosphere (transrespiratory pressure), airway pressure relative to pleural pressure (transpulmonary pressure), or pleural pressure alone.²¹⁹⁻²²¹

DYNAMIC RESPIRATORY MECHANICS

As a first approximation to Eq. (41.24), the mechanical behavior of the respiratory system during breathing or ventilation can be described according to the simple equation of motion that encompasses its resistive (R), elastic (E), and inertial (I) properties^{219,222}:

$$P = R\dot{V} + EV + I\ddot{V} + P_o \quad (41.25)$$

where V is volume, \ddot{V} denotes volume acceleration (i.e., the first time-derivative of flow or the second time-derivative of volume), and P_o is the distending pressure at end expiration. The coefficients R, E, and I in Eq. (41.25) may refer to the mechanical properties of the total respiratory system (rs), the lungs alone (L), or the chest wall (cw), depending on whether P refers to transrespiratory pressure, transpulmonary pressure, or intrapleural pressure, respectively.²²¹ The resistive properties of the respiratory system (R_{rs}) are generally assumed to arise from viscous and turbulent losses associated with gas flowing through the airway tree and the deformation of parenchymal and chest wall tissues. Hence, airway resistance may reflect airway caliber.²²³ Provided that variations in flow are small, resistive pressure losses are assumed to be linearly related to flow according to the first term of Eq. (41.25). With more rapid flow rates, as may be seen during exercise or forced vital capacity maneuvers, resistive losses vary nonlinearly with flow, which may more accurately be described according to²²⁴

$$P_R = K_1 \dot{V} + K_2 \dot{V}^2 \quad (41.26)$$

where K_1 and K_2 are empirically determined constants. Additional energy losses arise from the tension within the alveolar surface film,²²⁵ friction within the pleural space, and various tissue components of the parenchyma and chest wall,²²⁰ as well as cross-bridge cycling of contractile elements within the airway walls and lung tissues.^{226,227} Such losses are collectively termed "tissue resistance."^{228,229} If these tissue resistive losses are assumed to be proportional to flow according to Eq. (41.25), one will observe that they vary inversely with breathing frequency,^{226,230} a phenomenon commonly associated with viscoelastic materials.²²⁰ In adult patients, lung tissue resistance comprises about 60% of subglottal total lung resistance at typical breathing rates.²³¹ During volume-cycled ventilation with an end-inspiratory pause, resistance can quickly be estimated from the difference between the peak (P_{peak}) and plateau (P_{plat}) airway pressures (i.e., the resistive pressure loss P_R) divided

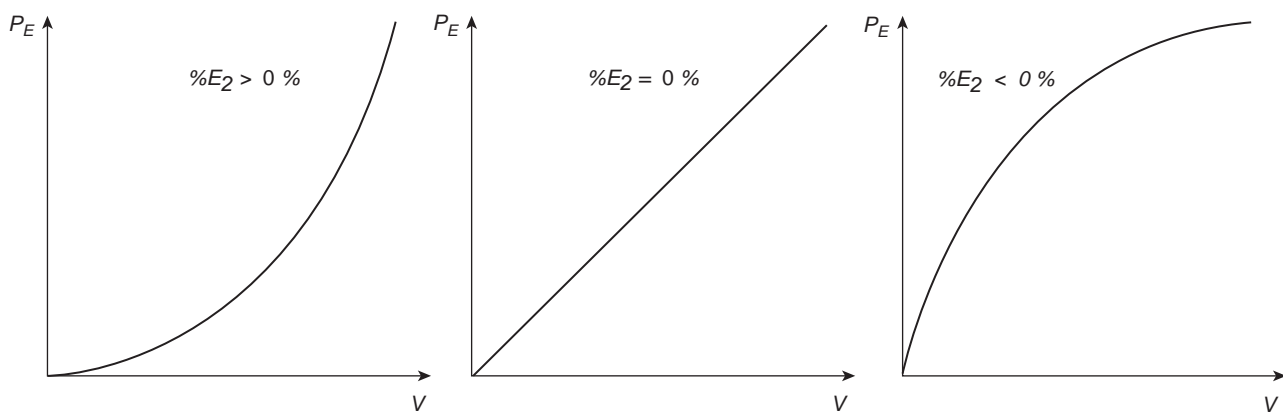


Fig. 41.18 Example elastic pressure (P_E) versus volume (V) curves and corresponding percentage of volume-dependent respiratory system elastance ($\%E_2$) values. (Modified from D'Antini D, Huhle R, Herrmann J, et al. Respiratory system mechanics during low versus high positive end-expiratory pressure in open abdominal surgery: a substudy of PROVHILO randomized controlled trial. *Anesth Analg*. 2018;126:143–149.)

by the inspiratory flow (\dot{V}_I) immediately before the end-inspiratory pause:

$$R = \frac{P_{\text{peak}} - P_{\text{plat}}}{\dot{V}_I} = \frac{P_R}{\dot{V}_I} \quad (41.27)$$

Thus, for a specified flow rate, alterations in P_R may reflect changes in airway caliber, as may occur during an intraoperative asthma exacerbation (Fig. 41.18, center panel), or obstruction within the ETT or breathing circuit.

Elastic pressures arise from the recoil of the lungs and chest wall when their normal anatomic configurations are deformed, either by contraction of the diaphragm and intercostal muscles, or by some external force such as a ventilator.²³² Elastance is defined as the change in distending pressure (transrespiratory, transpulmonary, or intrapleural) for a given change in volume. *Dynamic elastance* refers to the change in elastic (i.e., nonresistive) distending pressure per unit volume during the process of breathing or ventilation.[†] Elastance of the total respiratory system (E_{rs}) comprises both lung (E_L) and chest wall (E_{cw}) elastances:

$$E_{\text{rs}} = E_L + E_{\text{cw}} \quad (41.28)$$

In clinical settings, elastance is usually expressed as its reciprocal, compliance (i.e., change in volume per unit change in pressure). This leads to an alternate form of Eq. (41.28), expressing the relationships of the compliant components of the total respiratory system (C_{rs}), lungs (C_L), and chest wall (C_{cw}):

$$\frac{1}{C_{\text{rs}}} = \frac{1}{C_L} + \frac{1}{C_{\text{cw}}} \quad (41.29)$$

Factors that increase total respiratory or lung elastance (or likewise reduce the corresponding total respiratory or lung compliance) include consolidation, pulmonary edema, pneumothorax, atelectasis, interstitial disease, pneumonectomy or surgical resection, lung overdistension, and main-stem intubation. Lung compliance generally increases in emphysema. Factors that reduce chest wall compliance are abdominal distension, abdominal compartment syndrome,

chest wall edema, thoracic deformity, muscle tone, and extensive thoracic or abdominal scar (e.g., from burns); C_{cw} is reduced with muscle relaxation and flail chest.

In some situations, the magnitude of V_T , relative to the functional lung size, may be such that the linear dependence of P_E on V (Eq. [41.24] and [41.25]) is no longer an accurate description of the pressure-volume (PV) relationship of the lungs and/or chest wall. In these cases, elastic pressure may be more accurately described by a quadratic relationship with volume.^{232a,232b}:

$$P_E = E_1 V + E_2 V^2 \quad (41.30)$$

in which E_1 and E_2 denote the so-called volume-independent and volume-dependent components of elastance, respectively, since P_E will be reduced to $E_1 V$ when E_2 is negligible (Eq. [41.23]). An advantage of using Equation 41.30 is that it readily allows for the determination of the percentage of volume-dependent elastance contributing to P_E :^{232c}

$$\% E_2 = \frac{E_2 V_T}{E_1 + E_2 V_T} \times 100 \% \quad (41.31)$$

Since the $\%E_2$ index quantifies the deviation of linearity between P_E and V , it may provide quantitative information on the degree of intratidal recruitment or overdistention occurring during a mechanical breath.^{232d} For example, positive values of $\%E_2$ (see Fig. 41.18A) indicate a convex P_E - V relationship, with probable overdistention occurring for $\%E_2$ greater than 30%.^{232c} By contrast, negative values of $\%E_2$ (see Fig. 41.18C) indicate concave P_E - V relationship, with likely intratidal recruitment occurring during the breath.^{232e}

For the special case of constant inspiratory flow during volume-cycled ventilation, the curvature of the inspiratory pressure-time profile can also be used to infer the processes of intratidal recruitment and overdistention. Raneiri and associates^{232f} described this relationship using a simple power law expression:

$$P = at^b + c \quad (41.32)$$

where, similar to Eq. (41.24), P may refer to either transrespiratory or transpulmonary pressure, and t is time. The constants a , b , and c can be estimated from the inspiratory pressure profile using various nonlinear regression techniques.^{232g} The exponent b is referred to as the “stress

[†]Certain conventions of nomenclature incorrectly define dynamic elastance as the peak airway pressure divided by tidal volume. However, such a definition of dynamic elastance includes both resistive and elastic pressures, and thus is not an index of purely elastic processes.

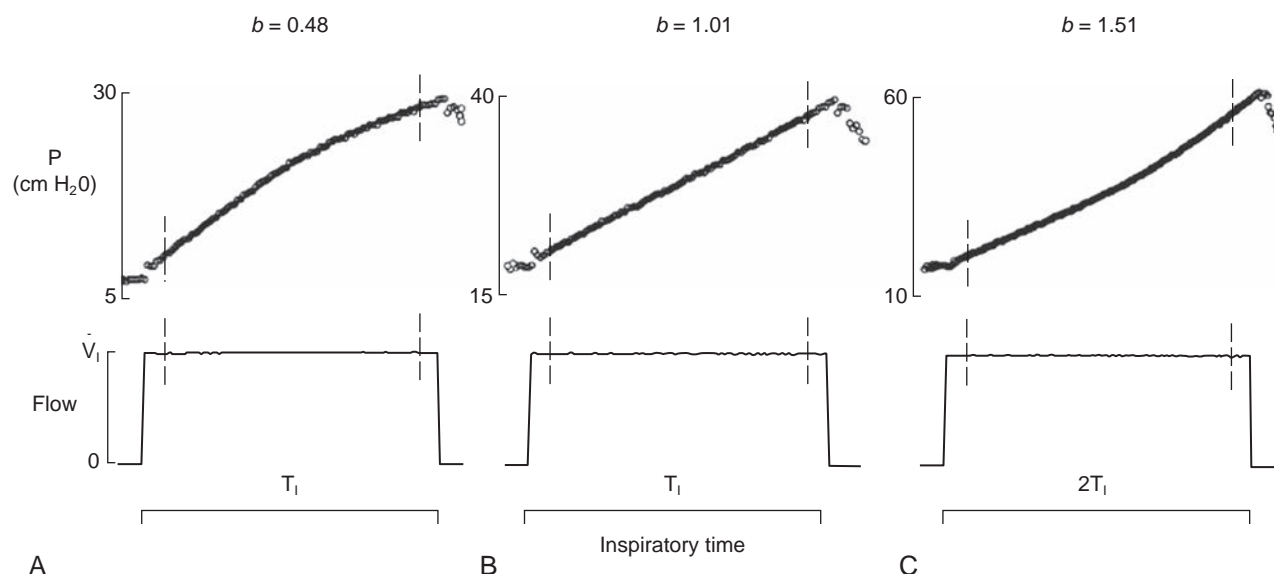


Fig. 41.19 Conceptual example of the stress index during constant inspiratory flow levels of \dot{V}_I over durations of T_I and $2T_I$, assuming that the power law $P = at^b + c$ can describe the pressure-time (P-t) curve. (A) $b < 1.0$, yielding a convex P-t curve, suggesting the dominance of intratidal recruitment; (B) $b \sim 1.0$, yielding a straight P-t line, suggesting minimal recruitment or overdistension; and (C) $b > 1.0$, yielding a concave P-t curve, suggesting the dominance of parenchymal overdistension. (Modified from Ranieri VM, Zhang H, Mascia L, et al. Pressure-time curve predicts minimally injurious ventilatory strategy in an isolated rat lung model. *Anesthesiology*. 2000;93:1320–1328.)

index,” and its estimated value characterizes the convexity ($b < 1.0$), concavity ($b > 1.0$), or linearity ($b = 1.0$) of the inspiratory pressure with time (Fig. 41.19). Similar to %E₂, b may also provide some insight into the relative contributions of intratidal recruitment ($b < 1.0$) and parenchymal overdistension ($b > 1.0$) to inspiratory pressure, or when these processes may be appropriately balanced ($b \sim 1$). However, as noted, the stress index is only interpretable during volume-cycled with constant inspiratory flows, in contrast to the %E₂ index, which can be used during other ventilatory modalities.^{232h} Moreover, the interpretation of the stress index may be obscured during certain clinical situations, such as abdominal insufflation, abdominal compartment syndrome, or pleural effusion.^{232i,j,k}

Similar to Eq. (41.27) to estimate R_{rs}, linear approximations to respiratory system elastance (E_{rs}) can be easily determined during volume-cycled ventilation for periods of zero-flow (i.e., during an end-inspiratory pause, when resistive pressures are zero) as the difference between P_{plat} and PEEP (i.e., the elastic pressure P_E) divided by the V_T:

$$E_{rs} = \frac{P_{plat} - PEEP}{V_T} = \frac{P_E}{V_T} \quad (41.33)$$

Since the value of E_{rs} in Eq. (41.33) is obtained during zero-flow, it is often referred to as “static elastance.” The corresponding static C_{rs} is usually between 50 and 100 mL/cm H₂O in normal mechanically ventilated lungs. Alterations in P_E for a specified V_T may be observed during processes that alter lung or chest wall elastance, such as a pneumothorax during thoracotomy or abdominal insufflation during laparoscopic surgical procedures (Fig. 41.20, right panel). In contrast to static E_{rs}, dynamic E_{rs} is estimated during periods of nonzero-flow by using multiple linear regression techniques (see later), and is higher than static elastance because of viscoelasticity²²² and gas redistribution.²³³ Both the apparent static or dynamic E_{rs} will decrease

following a recruitment maneuver because of an increase in aerated or functional lung volume. However, E_{rs} may also be increased due to *strain stiffening* of the lung tissues,^{233a} in which collagen fibers within the extracellular matrix of the parenchyma become progressively recruited with increasing strain. Recruitment of stiff collagen fibers results in their dominance of load-bearing within the lung, in contrast to the more stretchable elastin fibers that are the main load-bearing elements during low levels of tissue strain.^{233b} Such behavior may allow for titration of PEEP to achieve an optimal balance between intratidal recruitment and parenchymal overdistension—that is, the PEEP for which E_{rs} is minimized or, equivalently, C_{rs} is maximized.^{232b,c,233c-f} The clinical utility of such PEEP titration in patients with ARDS is still not entirely established.^{233e,233g}

Finally, inertial pressures are associated with the kinetic energy of accelerating the gas column in the central airways, as well as the motion of the respiratory tissues.²³⁴ Inertial pressures are typically expressed as the product of a lumped “inertia” parameter and volume acceleration (Eq. [41.25]). Inertia is usually not a significant contributor to the apparent airway pressure or the work of breathing, except during sudden changes in air flow, as may occur during inspiratory step profiles or various modalities of high-frequency ventilation (HFV).^{235,235a,b}

Eqs. (41.27) and (41.33) cannot be used to estimate R_{rs} and E_{rs} if an end-inspiratory pause is not present in the ventilator waveform. This is because one cannot easily separate the resistive and elastic pressures by visual inspection alone. For example, during pressure-controlled ventilation (PCV), the airway opening is exposed to a constant inflation pressure during inspiration (Fig. 41.21). Airway flow and V_T during PCV are determined not by the ventilator, but rather by the gradient between airway and alveolar pressures. Thus a more robust method of estimating respiratory

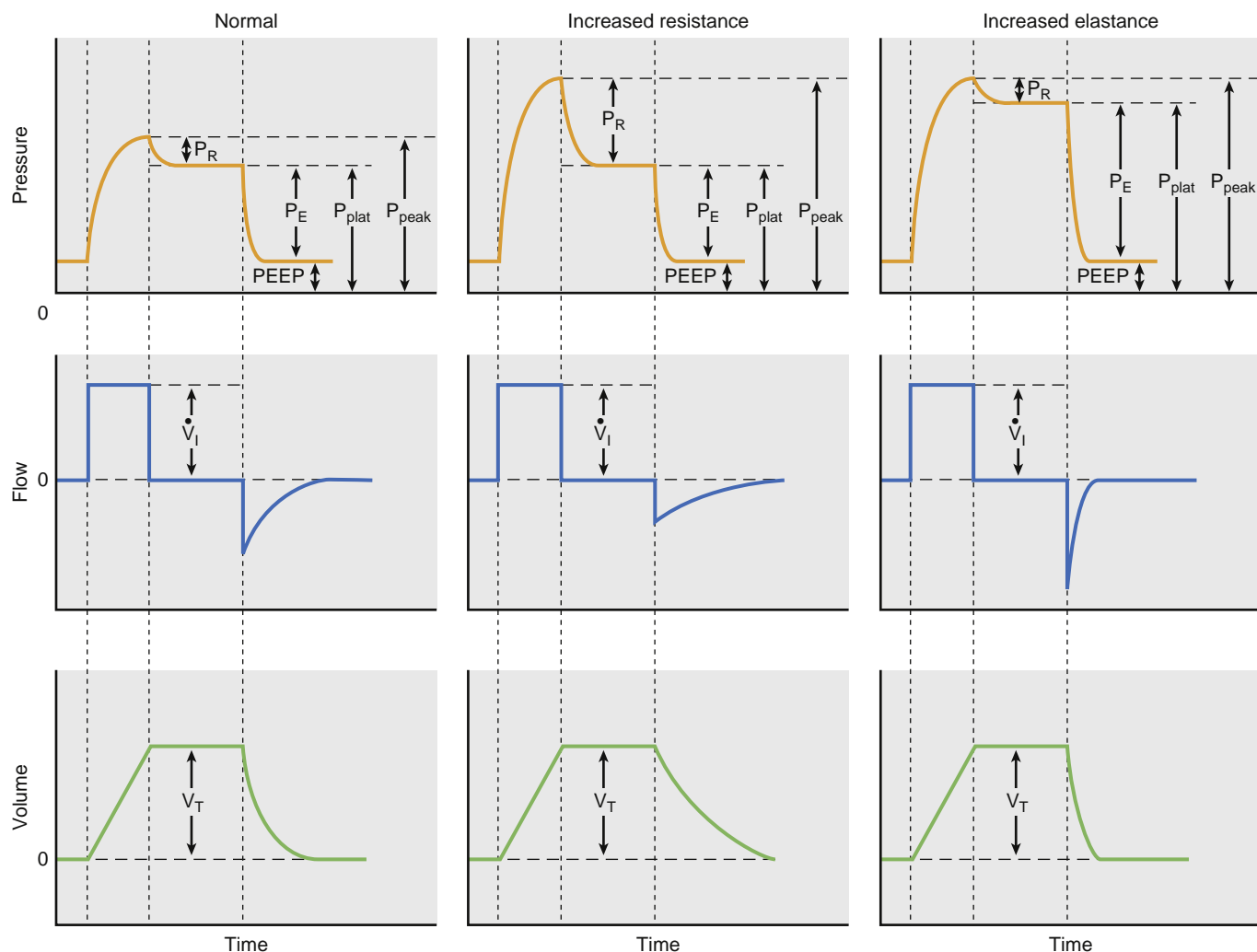


Fig. 41.20 Airway pressure, flow, and volume waveforms during constant-flow volume-cycled ventilation with an end-inspiratory pause. The components of the peak inspiratory pressure (P_{peak}) and the plateau pressure (P_{plat}) are presented: P_R , resistive pressure; P_E , elastic pressure; and PEEP, positive end-expiratory pressure. The same peak flow (\dot{V}_I) and tidal volume (V_T) are delivered by the mechanical ventilator in each case. Leftmost panels represent waveforms in a healthy patient. There is a small resistive pressure component, with most of the peak pressure comprised of elastic pressure. Expiratory flow decreases to zero before the start of the next inspiration, indicating appropriate I:E ratio and the absence of slowly emptying lung regions. Volume, as the integral of flow, also returns to zero before the initiation of the next breath. Middle panels represent waveforms in a patient with an increase in airways resistance. There is a significant increase in the resistive component P_R , and consequently P_{peak} . The elastic component is unchanged, as reflected in identical P_{plat} as compared with the healthy condition. Because increased resistance slows the process of lung emptying, the expiratory phase of the flow and volume curves now take longer to reach the zero. In several cases, the zero will not be reached, and a change in the I:E ratio will be necessary to avoid volume trapping and auto-PEEP. Rightmost panels represent a subject with increased P_E as may occur during laparoscopic insufflation or pneumothorax. There is an increase in P_{plat} consistent with the increased elastance of the respiratory system, and a fast emptying of the lungs during exhalation.

R_{rs} and E_{rs} involves multiple linear regression of the coefficients in Eq. (41.25) on sampled flow and pressure data.²³⁶⁻²³⁸ Such numerical approaches are present in commercially available respiratory mechanics monitors, and they can be used on almost all ventilator waveforms. Moreover, estimates of mechanical properties based on linear regression are not restricted to volume- or time-cycled waveforms with an end-inspiratory pause. One can separately estimate R_{rs} and E_{rs} during the inspiratory and expiratory phases, which may be different in some patients because of dynamic airway compression or derecruitment.^{239,240}

Dynamic estimates of total respiratory R_{rs} and E_{rs} based on positive airway opening pressures are valid only during controlled modes of ventilation when the chest wall is

relaxed. Although this is certainly the case during general anesthesia with neuromuscular blockade, the situation is more complicated during spontaneous breathing or assisted modes of ventilation. In such situations, the mechanics of the chest wall can be accounted for, if transpulmonary pressure is estimated using esophageal manometry, as described later.

STATIC RESPIRATORY MECHANICS

As previously illustrated, elastance (or compliance) is most easily measured during periods of zero flow because during these conditions the measured distending pressure is exclusively associated with elastic processes. However, a

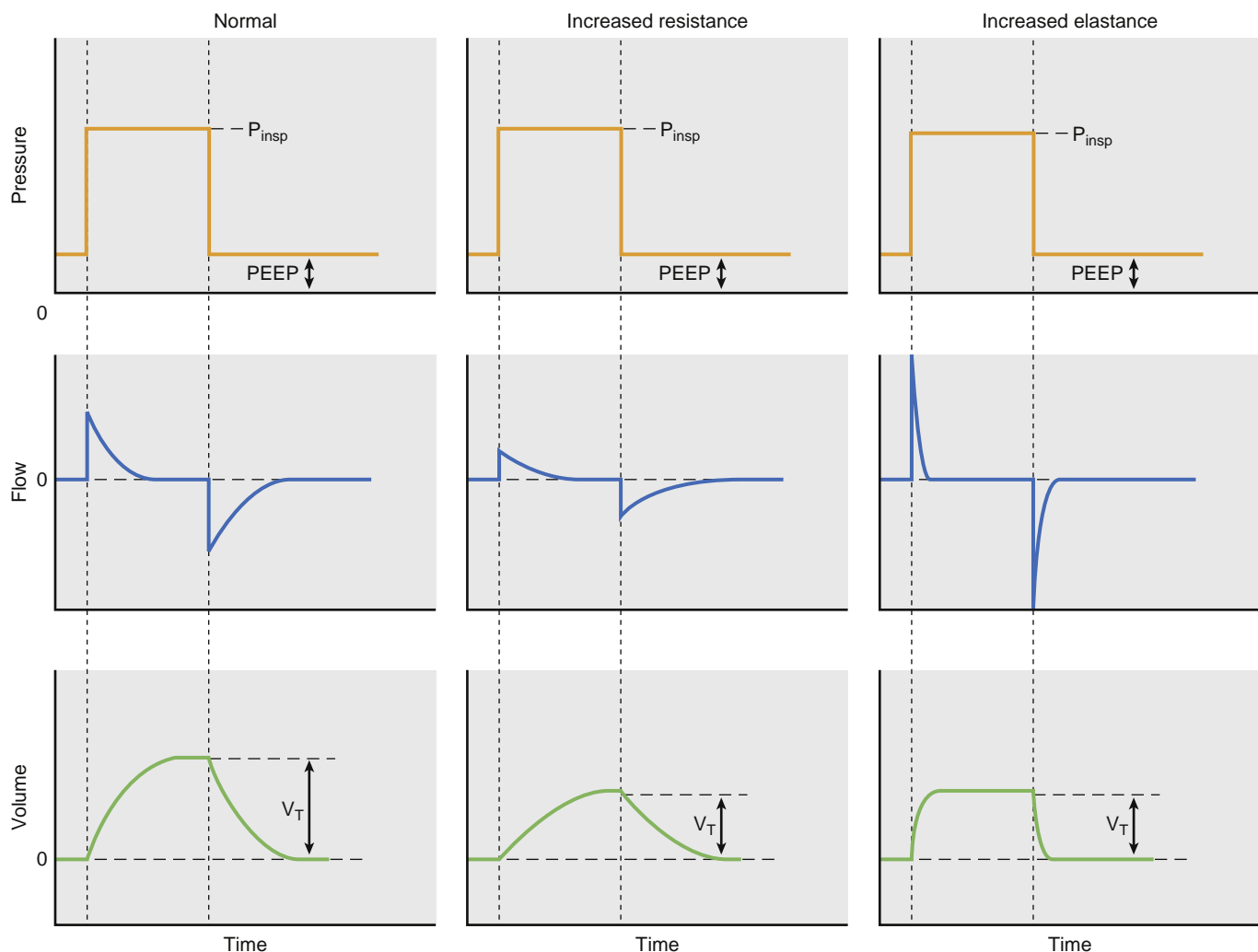


Fig. 41.21 Airway pressure, flow, and volume waveforms during pressure-controlled ventilation for the same patients depicted in [Fig. 41.18](#). In this ventilatory mode, the ventilator delivers a fixed pressure during the inspiratory phase, irrespective of the resistance and compliance. Airflow and tidal volume will consequently change with changes in those parameters. Leftmost panels represent waveforms in a patient with normal lungs. Middle panels represent waveforms in a patient with airway obstruction. Note the absence of a peak-plateau difference as compared with the volume-controlled mode, a lower V_T , and a prolonged time for airflow to reach zero during exhalation as compared to the normal patient. Rightmost panels represent a subject with increased elastance, as may occur during laparoscopic insufflation or pneumothorax. Note a reduction in V_T and a shorter time to reach zero flow consistent with a more rigid lung. *PEEP*, positive end-expiratory pressure; P_{insp} , inspiratory pressure; V_T , tidal volume.

more comprehensive characterization of elastance can be obtained by plotting cumulative inspired or expired lung volume against the distending pressure across the lungs or total respiratory system. This quasi-static PV curve can be constructed during very slow inflations or deflations²⁴¹ (when resistive pressures are negligible), or during periodic flow occlusions.²⁴² For example, the expiratory limb of the PV curve can be constructed by inflating the lungs to a specified volume (usually total lung capacity) and then allowing a passive deflation with flow interruptions of 1 to 2 seconds.

The quasi-static PV curves of the lungs or total respiratory system are inherently nonlinear ([Fig. 41.22](#)); that is, compliance, defined as the local slope (dP/dV) of the PV curve, varies with lung volume. Empirically, PV curves are described using single exponential²⁴³ or sigmoidal²⁴⁴ functions. When they are described using sigmoidal functions, two points are usually demarcated on such curves, which have traditionally been termed the upper inflection point

(UIP) and lower inflection point (LIP)[‡]. The UIP is thought to represent the point at which lung overdistention occurs, as during parenchymal strain-stiffening.²²⁰ The LIP is thought to reflect the process of maximum alveolar recruitment. During protective ventilation, one seeks to ventilate a patient in the most linear region of the PV curve.

Enough PEEP needs to be applied to avoid the LIP, where cyclic recruitment and derecruitment occur, along with lower V_{Ts} to avoid the UIP and overdistention.²⁴² Also, PV curves exhibit hysteresis, a phenomenon in which the lung volume at a specified pressure depends on the direction from which the distending pressure is approached (i.e., either inspiration or expiration). The reasons that the PV curve of the lungs or total respiratory system exhibits hysteresis are numerous and complex, and include the biophysical

[‡]The formal mathematical definition of an inflection point is a point on a curve at which its concavity (i.e., its second derivative) changes sign from positive to negative or vice versa.

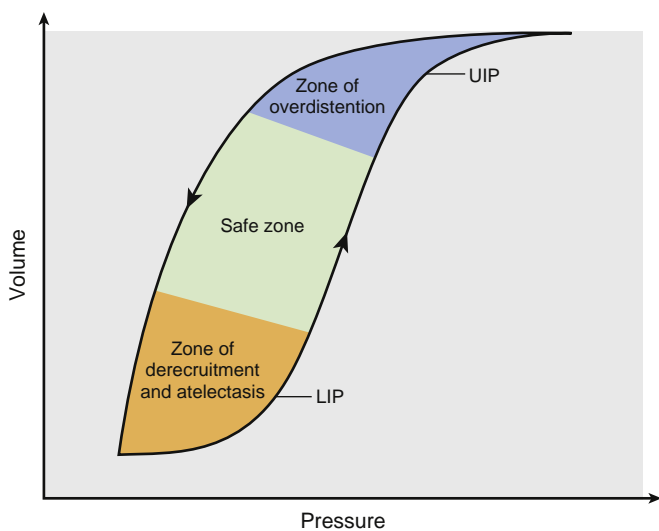


Fig. 41.22 Schematic of a pressure–volume curve for the lungs or total respiratory system, demonstrating hysteresis between inspiratory and expiratory limbs. Upper inflection point (UIP) and lower inflection point (LIP) are demarcated on the inspiratory limb. During mechanical ventilation, lung regions should be in the Safe Zone for optimal lung protection.

properties of surfactant,²⁴⁵ time-dependent recruitment or derecruitment,²⁴⁶ as well as contact friction among various connective tissue elements.²⁴⁷

There are a number of problems with managing ventilation based on quasi-static PV curves. First, PV curves are constructed only during periods of zero flow or near zero flow, and they do not reflect the mechanics of the lungs or total respiratory system during the dynamic processes of breathing or mechanical ventilation. In fact, the dynamic PV relationships for the same patient may be very different. Second, the UIP and LIP are not always visually apparent. Finally, a PV curve for the lungs or total respiratory system represents the averaged static behavior of a population of many lung units, with each operating on different portions of their own individual PV curves.

WORK OF BREATHING AND MECHANICAL POWER

The work of breathing (W) represents the energy required to inflate or deflate the lungs, or chest wall, or both, by a specified volume. In its simplest form, it can be represented as the product of the applied distending pressure and resulting volume change:

$$W = PV \quad (41.34)$$

However, when pressure and volume vary as functions of time (as during the course of a spontaneous or controlled breath), work may be expressed as the cumulative product²⁴⁸

$$W = \int PdV \quad (41.35)$$

or equivalently as the integral of the pressure-flow product with respect to time²⁴⁹

$$W = \int_{t=0}^T P(t) \dot{V}(t) dt \quad (41.36)$$

where T is the duration over which W is determined. For example, if T corresponds to the duration of inspiratory period and P the transpulmonary pressure, then W corresponds to the work required to overcome both the resistive and elastic forces opposing the entry of air into the lungs (Fig. 41.23). If T corresponds to the duration of an entire breath, the energy initially stored in the elastic recoil of the lung tissues will be recovered during a passive exhalation. In this case, the area of the resulting PV loop represents the work performed (i.e., energy lost) overcoming purely resistive losses in the airways and tissues. In general, W is assessed during inspiration only because the respiratory musculature (or a ventilator) must overcome both elastic and resistive pressures to bring air into the lungs. For a given V_T , W varies as a function of respiratory rate and, in most cases, achieves a minimum at a specified frequency. This frequency is termed the *energetically optimum breathing frequency*,²⁴⁹ as this is the rate at which energy expenditure is minimized. The derivative of W with respect to time is referred to as the *instantaneous mechanical power*, P,

$$P = \frac{dW}{dt} \quad (41.37)$$

which, based on Eq. (41.31), can simply be expressed as the pressure-flow product with respect to time:

$$P(t) = P(t) \dot{V}(t) \quad (41.38)$$

Mechanical power, as an index of the *rate* of energy dissipation, can be used to assess the risk of developing ventilator-induced lung injury,^{249a} particularly with changes in transpulmonary pressure during ventilation.^{249b} Moreover, if the relationship between pressure and flow during ventilation can be described by relatively simple mathematical expressions (e.g., Eqs. [41.25]–[41.27]), the mechanical power likewise can be embodied by simple analytic formulae.^{249c,d}

MONITORING OF RESPIRATORY PRESSURES

Fundamental to any quantitative assessment of respiratory mechanics is the measurement of pressure. Such pressures may include those measured in the inspiratory or expiratory limb of the anesthesia machine, at the proximal end of an ETT, or within the trachea or esophagus. Pressure allows for the inference of the forces associated with the movement of gases through the airway tree, as well as the distension of the parenchymal tissues and chest wall, according to the elements described in Eq. (41.24). The most accessible and familiar pressure to the anesthesiologist or intensivist is the airway pressure during controlled mechanical ventilation. Ideally, this should be the pressure measured in the trachea or at the airway opening, exclusive of any distortions from airway devices or breathing circuits. However, for practical reasons, this “airway” pressure is not the actual pressure at the airway opening or within the trachea, but is the pressure transduced at the anesthesia machine or ventilator and reflects the resistive and compliant properties of the breathing circuit and face mask or ETT, as well as the mechanical properties of the respiratory system. Although many ventilators now use computer algorithms to provide some compensation for flow and pressure losses in the breathing circuit,²⁵⁰ such approaches often rely on idealized, linear models that do not truly reflect the complex

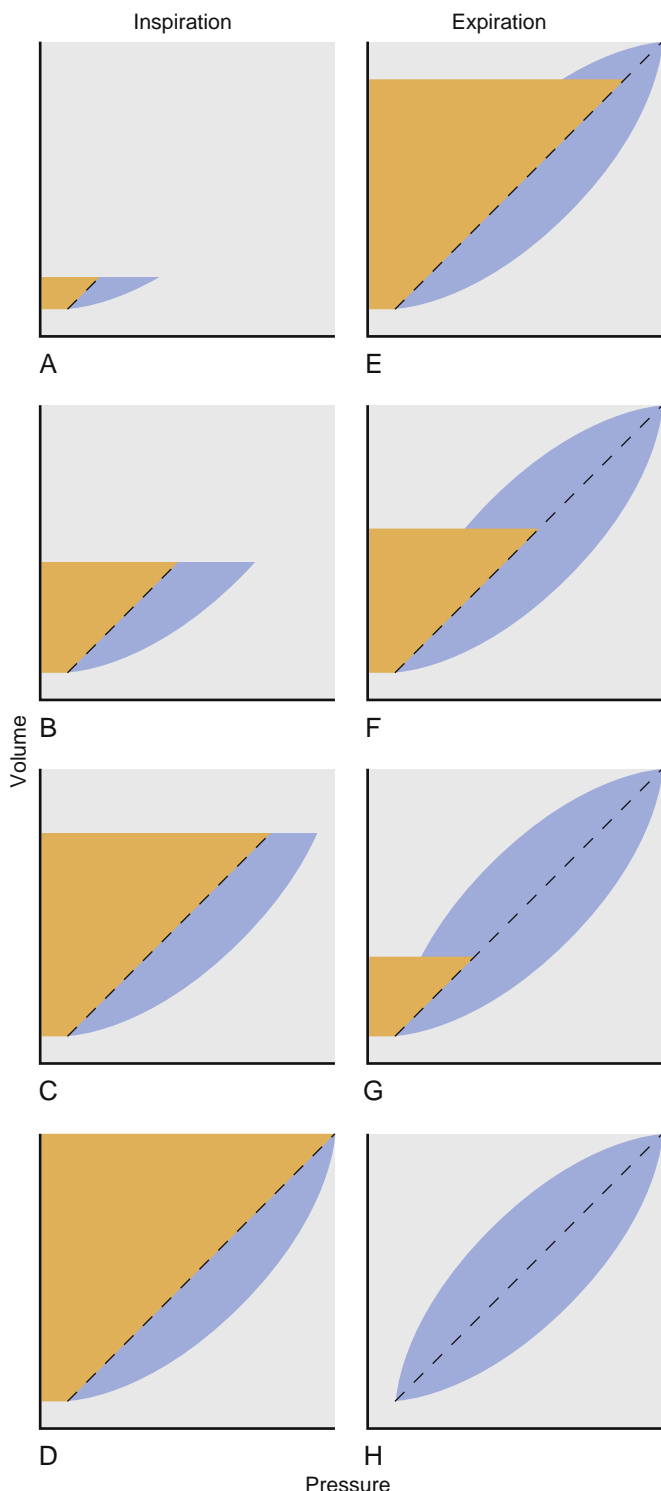


Fig. 41.23 Volume plotted against transpulmonary or (transrespiratory) pressure during the course of a single breath. Plots are shown during inspiration (panels A through D) and expiration (panels E through H). Gray area denotes the work of breathing due to tissue elasticity, while the hatched area denotes the work of breathing due to airways and tissue resistance. Energy stored in elastic recoil at the end of inspiration will be entirely recovered during expiration. However, resistive energy will always be lost during both inspiration and expiration.

processes of turbulent air flow, polytropic gas compression, or viscoelastic tubing walls.^{251,252} Therefore, one must use caution when making physiologic inferences based on airway pressures and volumes reported by a ventilator.

Often airway pressure is improperly used as a surrogate for lung distention. *Transrespiratory pressure* refers to the pressure drop across the lungs and chest wall, which during positive-pressure ventilation is usually determined by the difference between airway pressure and atmospheric pressure. Several processes that may contribute to increased transrespiratory pressure do not correspond to excessive lung inflation. For example, obesity, abdominal insufflation, or steep Trendelenburg position all may contribute to high airway opening pressures, but they do not necessarily indicate parenchymal overdistention.

By contrast, *transpulmonary pressure* refers to the distending pressure across the lungs alone. Its determination requires not only measurement of airway opening pressure, but also estimates of the pressure within the pleural space. This can be obtained relatively noninvasively using an esophageal balloon catheter, because the pressure measured within the esophagus is relatively close to intrapleural pressure.^{253,253a} Such catheters are typically 100 cm long, with side holes in the distal tip covered by a thin-walled balloon (Fig. 41.24). The catheter can be placed through the mouth or nares and positioned in the middle-to-distal third of the esophagus. The catheter is connected to a transducer by a three-way stopcock, and a small amount of air is injected into the balloon such that its walls remain flaccid and do not contribute an additional recoil pressure to the measurement. Because the local values of pleural pressure vary depending on gravity, the balloon should be several centimeters in length to provide an average estimate of the pressure field surrounding the lungs. Estimating pleural pressure based on esophageal manometry has several limitations, including mediastinal compression of the balloon in supine patients, catheter migration, and cardiac artifact on the tracing.^{254,255} Nonetheless, its use in critically ill patients and under certain special conditions such as obesity, abdominal hypertension (primary or during laparoscopic insufflation), and extreme Trendelenburg position may be valuable in the adjustment of appropriate levels of PEEP.^{256,256a} Peak and plateau pressures, which are typical in clinical practice, are obtained from the *transrespiratory pressure*. Accordingly, they do not characterize the pressures acting exclusively on the lungs, but on the whole respiratory system. Current recommendations suggest limiting transrespiratory plateau pressures to 26 to 30 cm H₂O, to minimize alveolar overdistension.²⁵⁷ However, such recommendations should be applied in appropriate clinical context, given that the same plateau pressure could correspond to very different transpulmonary pressures, and consequently to very different degrees of risk for lung injury, depending on the partitioning between lung and chest wall pressure components.^{257a,b}

More recent studies suggest that the “driving pressure”—that is, the V_T normalized by the respiratory system compliance ($\Delta P = V_T/C_{rs}$)—may be one of the most important ventilatory variables to consider when stratifying mortality risk during ARDS.^{257c,d} Its relationship to postoperative pulmonary complications in surgical patients has also been demonstrated.^{258,259} In practice, driving pressure may be computed as the difference between P_{plat} and PEEP.^{257c}

Auto-PEEP or *intrinsic-PEEP* is the positive pressure present within the alveoli at end-exhalation and is typically observed in ventilated patients with COPD, who demonstrate dynamic airway compression and expiratory flow limitation, as well as a significant portion of patients with ARDS, sepsis, and respiratory muscle weakness.²⁶⁰ Auto-PEEP can promote significant respiratory and hemodynamic compromise. It is usually caused by a combination of

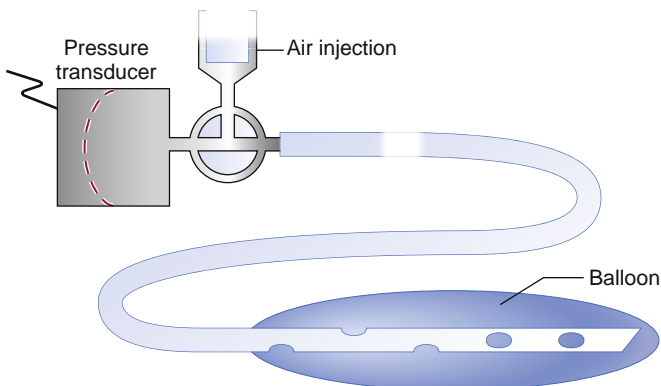


Fig. 41.24 Example of an Esophageal Balloon Catheter. The proximal end of the catheter is connected to a pressure transducer, and air is injected into the balloon via a three-way stopcock. (Modified from Bates JHT. *Lung Mechanics: an Inverse Modeling Approach*. Cambridge: Cambridge University Press; 2009:220.)

increased airway resistance and reduced lung elastic recoil (i.e., an increase in the expiratory time constant of the respiratory system). Other factors are a decrease in expiratory time, an increase in V_T , an increase in external expiratory resistance, and persistent inspiratory muscle activity during exhalation. The amount of auto-PEEP can be estimated in mechanically ventilated patients by occluding the airway at end exhalation, and observing a rise in airway pressure during the occlusion maneuver until a plateau is visible (<4 seconds) (Fig. 41.25). Auto-PEEP is then defined as the difference between end-occlusion to preocclusion airway pressures. Other methods can be used to assess auto-PEEP under dynamic conditions, as well as in spontaneously breathing patients with the use of an esophageal balloon.^{260,261}

Any measurement of pressure requires pressure transducers. Most pressure transducers are differential sensors with two input channels, and they produce an electrical output that is proportional to the pressure difference between these channels (Fig. 41.26A). Such transducers exhibit a high common-mode rejection ratio, defined as the tendency of the transducer to produce zero output if both of its inputs are exposed to identical pressures. Many pressure waveforms are transduced relative to atmosphere with one of the two inputs left opened to ambient air (see Fig. 41.26B), otherwise referred to as gauge configuration. In clinical settings, pressure is most commonly measured using relatively inexpensive, piezoresistive transducers.²²² These devices rely on a pressure-sensing diaphragm

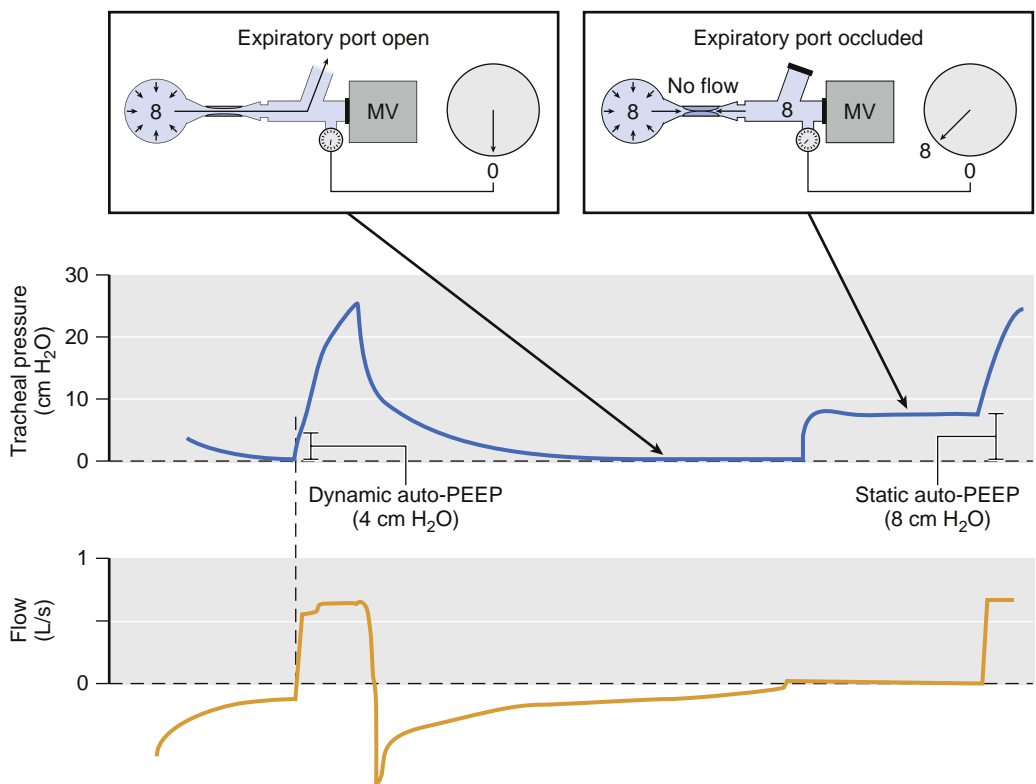


Fig. 41.25 Concept of Intrinsic Positive End-Expiratory Pressure (auto-PEEP). Shown are tracheal pressure and flow waveforms during controlled mechanical ventilation. Dynamic auto-PEEP can be estimated at the beginning of inspiration as the tracheal pressure when the flow trace equals zero. Static auto-PEEP can be estimated as the tracheal pressure following a prolonged expiratory occlusion. (Modified from Blanch L, Bernabé F, Lucangelo U. Measurement of air trapping, intrinsic positive end-expiratory pressure, and dynamic hyperinflation in mechanically ventilated patients. *Respir Care*. 2005;50:110–123; and Moon RE, Camporesi EM. Respiratory monitoring. In: Miller RD, Fleisher LA, Johns RA, eds. *Miller's Anesthesia*. 6th ed. New York, NY: Churchill Livingstone; 2005:1255, 1295.)

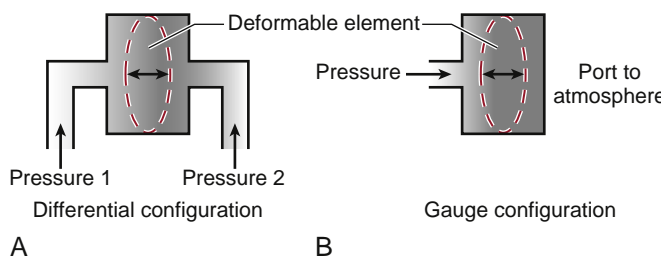


Fig. 41.26 Pressure transducers arranged in differential (A) or gauge (B) configurations. (Modified from Bates JHT. *Lung Mechanics: An Inverse Modeling Approach*. Cambridge: Cambridge University Press; 2009:220.)

whose electrical resistance changes when it is deformed in response to a differential pressure. This change in electrical resistance can be sensed with a standard Wheatstone bridge circuit, which produces an output-voltage signal appropriate for amplification and filtering. In general, piezoresistive transducers have adequate frequency responses sufficient for most respiratory applications.^{262,263} However, this frequency response can be easily degraded if the transducer is connected to the pressure-sensing location with long, compliant tubing.²⁶⁴

MONITORING OF RESPIRATORY FLOWS

Ideally, any measurement of flow should indicate the exact rate at which gas is entering and leaving the patient's lungs. This can be most easily accomplished by placing the flow-measuring device as close to the patient as possible, such as between the circuit Y-connector and the proximal end of the ETT or LMA. However, for practical reasons, most ventilators and anesthesia machines measure flow close to the machine console. This flow can be considerably different from that close to the patient because of the effects of gas compression, wall distention of the breathing circuit, and changes in gas humidity.

An important clinical use of flow monitoring is the detection of nonzero end-expiratory flows. This indicates that a gradient of pressure exists between alveolar regions and the upper airway with incomplete lung emptying at end-expiration, characteristic of auto-PEEP (PVolFl-7). As a consequence, end-expiratory lung volumes would be larger than those in the absence of auto-PEEP, with risk of dynamic lung hyperinflation and reduction of venous return. Increase in expiratory time and reduction of V_T or respiratory rate should be considered to eliminate the issue.

During ventilation, airway flow can often be inferred according to time-dependent changes in delivered or inspired V_T or from the displacement waveform of a piston or cylinder arrangement or bellows.²⁶⁵⁻²⁶⁷ Preferably, flow is measured using transducers designed specifically for this task. The most common method involves the measurement of a differential pressure decrease (ΔP) across a fluid resistive element. Ideally, this ΔP is linearly related to the corresponding flow through the device. Such a principle forms the basis for one of the oldest and most widely used flowmeters, the pneumotachograph. Although the instruments provide accurate measurement of flow, pneumotachographs are very sensitive to changes in temperature, humidity, and gas composition,²⁶⁸ and require frequent calibration using various electronic or software-based techniques to ensure

accurate measurements.^{269,270} This sensitivity, combined with difficulties in cleaning and sterilization, limits the routine use of these instruments in clinical environments. Orifice flowmeters also have the advantage of having relatively large internal diameters that limit the formation of condensation and minimize obstruction with secretions. Given that these devices can be manufactured using inexpensive plastic injection molding techniques, many orifice flowmeters are designed to be disposable, thus making their use increasingly popular for respiratory applications in clinical environments.²⁷¹

Most anesthesia machines use hot wire anemometers for flow measurement,²⁷² which rely on temperature-dependent changes in the electrical resistance of a current carrying wire. When gas flows past the wire, the corresponding temperature drop changes the conductivity of the filament, which can be sensed with appropriate electronic circuits.²⁷³ Because a single wire filament cannot sense the direction of flow, two different anemometers can be used in the ventilator circuit: one for the inspiratory limb, and the other for the expiratory limb. Alternatively, two wires in series must be used for sensing bidirectional flow through a single conduit,²⁷⁴ with the flow direction determined according to which wire is cooled first. In general, hot wire anemometers have a better dynamic response compared with pneumotachographs or orifice flowmeters,²⁷⁵ making them ideal for flow measurement during HFV.^{235a,276} However, these devices must also be calibrated to account for variations in gas density or humidity as well.^{276a}

MONITORING OF RESPIRATORY VOLUME

Similar to flow measurement, the ideal measurement of volume should be an accurate accounting of the gas quantity moving into and out of the patient. However, delivered or exhaled V_T measurement is subjected to the same limitations of flow measurement because most anesthesia machines and ventilators determine volume by electrically or numerically integrating the corresponding flow signal.²²² Care must be taken to ensure any drifts or offsets from the flow transducer are minimized, given that their integration will result in errors in estimated volume. This may be accomplished by appropriately zeroing the transducer periodically, such as at the end of a breath. Although electronic or digital high-pass filters may be used to remove drifts and offsets in real-time, these tend to have long transient responses.^{276b,c}

Finally, besides the pathophysiologic and monitoring applications described in this section, monitoring of pressures, volumes, and flows has been applied to monitoring, training, and education for neonatal resuscitation.²⁷⁷

Plethysmographic Monitoring

Respiratory inductance plethysmography (RIP) is a non-invasive respiratory monitoring technique that quantifies changes in the cross-sectional area of the chest wall and the abdominal compartments. The method is used to assess V_T , respiratory rate, adequacy of high-frequency oscillatory ventilation (HFOV), lung volume changes during tracheobronchial suctioning, and thoracoabdominal

synchrony.²⁷⁸ RIP relies on the principle that a current applied through a loop of wire generates a magnetic field normal to the orientation of the loop (Faraday's law) and that a change in the area enclosed by the loop creates an opposing current within the loop directly proportional to the change in the area (Lenz's law). Two elastic bands containing a conductor are used: one typically placed around the patient's chest, 3 cm above the xiphoid process; and the other around the abdomen. Each of these bands produces an independent signal representative of the thoracic and abdominal cross-sectional area, and the sum of these two signals calibrated against a known gas volume yields lung volume change.

There have been several pediatric applications of RIP to monitor V_T and respiratory rate, building on the advantage that a facemask, LMA, or ETT is not required for measurements.²⁷⁹⁻²⁸¹ The technique could also guide lung-protective ventilation strategies by facilitating the construction of PV curves for individual patients. These can be used to optimize lung recruitment, maintain an open lung, and limit overdistension (see the section on "Static Respiratory Mechanics"). RIP has found several applications in sleep studies.

Intraoperatively, RIP may be useful in areas for which accurate monitoring of V_T is required but not possible with the usual anesthesia machine monitors. This could occur with a shared airway (e.g., laryngotracheal surgery,²⁸² flexible and rigid bronchoscopy²⁸³), or a patient whose trachea is not intubated (e.g., monitored anesthesia care and noninvasive pressure support ventilation).

Limitations of intraoperative RIP include the fact that it cannot be used during thoracic and abdominal surgery, because of the need for the measurement bands. Also, the calibration characteristics of the device are affected by changes in the pattern of breathing.²⁸⁴

Respiratory Rate Monitoring: Apnea Monitoring

Apnea and bradypnea are life-threatening events frequently observed in the intraoperative and postoperative periods of anesthesia. Prematurity, morbid obesity, age, obstructive sleep apnea, and central nervous system depressant medications have been associated with risk of apnea or bradypnea.^{285,286} Accordingly, many different approaches have been developed for detecting those events.^{287,288} Two main types of apnea are observed: central and obstructive. Central apnea is defined as apnea resulting from a failure of the central nervous system to drive respiration. Obstructive apnea is that resulting from upper airway obstruction. Current monitors assess at least one of three processes occurring during breathing to detect apnea²⁸⁸: chest wall expansion, gas flow, and gas exchange.

Chest wall expansion is usually measured as follows:

1. Changes in thoracic electrical impedance (impedance pneumography) of the chest wall. The method is based on the changes in electrical conductivity of the chest to an electrical current as air moves in and out of the lungs during breathing and blood volume changes in the same period. This is because air is a poor electrical conductor

and blood is a good electrical conductor. A low electrical current at high frequency is applied in two chest electrodes, corresponding changes in voltage of the chest are measured, and the impedance is continuously calculated from these. The technique is implemented in several commercial systems using routine electrocardiographic leads and is also used in home monitoring of neonatal apnea.

2. Inductive plethysmography (as described earlier).
3. Abdominal and chest fiberoptic and resistive strain gauges (a pressure pad placed alongside the infant's rib cage, pneumatic abdominal sensors) are used.
4. Electromyographic signal of respiratory muscles is not frequently used because of the low signal-to-noise ratio.

An important drawback of techniques based on chest expansion is their inaccuracy in the presence of movement. Thus obstructive apnea may be falsely assessed as normal respirations.²⁸⁹

Gas flow methods are based on measurements of different variables directly related to the presence of air flow in the airway:

1. Pressure gradients along the breathing circuit. This approach uses the Poiseuille principle ($\Delta P = k \times V$) and differential pressure transducers to detect flow.
2. Temperature of the breathed air in the nose or mouth is used.
3. Rapid response hygrometer is based on assessment of humidity in the exhaled air.

Techniques based on gas exchange focus essentially on exhaled CO_2 , as routinely used in intubated patients in the operating room. In nonintubated patients, the use of specifically designed cannulae combining DO_2 and breathed gas sampling facilitates the monitoring of exhaled CO_2 . Capnography allows for early detection of respiratory depression before O_2 desaturation, particularly when supplemental O_2 is administered.^{290,290a} Off-line or in-line infrared sensors are the most common technique. Respiratory rate measurements using these techniques were more accurate than those obtained with thoracic impedance tomography in extubated patients in postanesthesia care units, even with supplemental O_2 at high flows.²⁹¹ Accurate end-tidal CO_2 measurements through a nasal cannula may be difficult in mouth breathers, including obese patients and those with obstructive sleep apnea. In such cases, a nasal cannula with an oral guide may improve measurement accuracy.²⁹² Simulation studies indicated that respiratory rate can be accurately monitored during esophagogastroduodenoscopies using a CO_2 sampling bite block or a nasal cannula with oral cup. The accuracy of $P_{ET}CO_2$ measurements depends on the device used, O_2 flow, the intensity of oral breathing, and minute ventilation.²⁹³

Pulse oximetry cannot be used as the primary monitor of apnea or bradypnea because O_2 desaturation occurs only late in a well-oxygenated apneic patient. However, pulse oximetry adds an additional level of safety combined with primary monitors of ventilation. For example, in a study using pulse oximetry and noninvasive capnography for continuous monitoring of 178 patients receiving patient-controlled analgesia, respiratory depression measured by O_2 desaturation occurred in 12% of the patients, in line

with previous studies.²⁸⁵ In contrast to previous estimates, episodes of bradypnea (respiratory rate < 10 breaths/min) were present in 41% of patients, far more frequently than the previously reported 1% to 2%.²⁹⁴⁻²⁹⁶

Respiratory rate monitoring is also critical to infant apnea monitoring. Combinations of transthoracic impedance and pulse oximetry may maximize the detection of true episodes of apnea in home monitors for neonatal apnea.²⁹⁷ This is because pulse oximetry provides an additional level of monitoring in cases of poor performance of transthoracic impedance secondary to motion artifacts. The value of combining monitors of ventilation such as capnography with pulse oximetry to maximize the detection of alveolar hypoventilation has been confirmed.²⁹⁸ Capnography allowed for early detection of arterial O₂ desaturation in cases of alveolar hypoventilation in the presence of supplemental O₂.

False-positive and false-negative alarms occur during apnea monitoring. The most dangerous conditions occur when artifacts are detected as breathing and alarms are not activated. Such artifacts include vibrations, cardiac motion, patient movement, and electromagnetic interference from other instrumentation. Impedance pneumographs are subject to cardiovascular artifacts, whereas pressure pads are subject to patient motion artifacts. A more common (yet less dangerous) problem is when an alarm sounds in a patient without apnea. Frequent causes include inadequate sensitivity settings, malfunctioning electrodes, and movement of the patient. Motion transducers based on sensing of acceleration were used in neonates undergoing HFOV, and results showed that monitoring of regional tidal displacement may enable the early recognition of deteriorating ventilation during HFOV that eventually leads to hypoxemia.²⁹⁹ This study found that in approximately half of the cases, hypoxemia had causes other than slowly deteriorating ventilation.²⁹⁹

Current recommendations of the Anesthesia Patient Safety Foundation for Essential Monitoring Strategies to Detect Clinically Significant Drug-Induced Respiratory Depression in the Postoperative Period (<http://www.apsf.org/initiatives.php>), including opioid-induced ventilatory impairment, state that continuous electronic monitoring of oxygenation and ventilation should be available and considered for all patients, not only those at risk for postoperative respiratory insufficiency. This is because selective monitoring is likely to miss respiratory depression in patients without risk factors. These recommendations stress that maintaining status quo while awaiting newer technology is not acceptable, and that intermittent "spot checks" of oxygenation (pulse oximetry) and ventilation (nursing assessment) are not adequate for reliably recognizing clinically significant evolving drug-induced respiratory depression. Continuous electronic monitoring should not replace traditional intermittent nursing assessment and vigilance. All patients should have oxygenation continuously monitored by pulse oximetry. Capnography or other monitoring modalities that measure ventilation and airflow are indicated when supplemental O₂ is needed to maintain acceptable O₂ saturations. The recommendations also call attention to threshold-based alarm limits on individual physiologic variables, which may result in failure to recognize early signs of progressive hypoventilation by either being insufficiently, or too, sensitive (excess false alarms).

Unexpected death has been associated with three patterns of respiratory depression.³⁰⁰⁻³⁰² (1) Hyperventilation compensated respiratory distress (e.g., from sepsis, pulmonary embolus, or congestive heart failure): patients present initially with stable S_pO₂ and decreasing P_aCO₂ as metabolic acidosis develops with associated compensatory hyperventilation. High respiratory rate is typical of this pattern. Ultimately, a slow desaturation is followed by an abrupt fall in oxygenation as the ventilatory response to worsening acidosis fails. (2) Progressive unidirectional hypoventilation or CO₂ narcosis: frequently due to opioid or other sedative overdose, it is characterized by a rise in P_aCO₂ (and P_{ET}CO₂) initially because of decreased minute ventilation, often while S_pO₂ remains above 90%. (3) Sentinel rapid airflow/O₂ saturation reduction with precipitous S_pO₂ fall: observed in patients with obstructive sleep apnea, who are dependent on the arousal state to maintain oxygenation. Sleep results in precipitous hypoxemia during apnea with potential sudden arrest.

Imaging for Respiratory Monitoring

Imaging as a monitoring technique provides tremendous insight into pulmonary structure, function, and inflammation in both health and disease.³⁰³⁻³⁰⁵ However, exposure to radiation and bulky devices has prevented its use at the bedside. Technologic advances have led to the introduction of new modalities with more compact equipment for clinical use. This may herald an important shift in respiratory monitoring toward the increased use of bedside imaging. Such improvements come with the advantages of less radiation exposure, noninvasiveness, and more detailed physiologic information.

CHEST RADIOGRAPHY

Chest radiography has been the traditional imaging method to assess intrathoracic conditions in the operating room, postoperative anesthesia care unit, and ICUs. Anesthesiologists should be familiar with basic radiologic findings representative of important pulmonary conditions such as interstitial infiltrates, hyperinflation, pneumothorax, pleural effusion, and consolidation. The image during chest radiography, as well as computed tomography, is based on the physical principle that x-rays reaching a detector (e.g., film) depend on tissue absorption, which varies linearly with tissue density. However, radiation exposure restricts frequency of use. Furthermore, technical difficulties limit image quality. These difficulties include reduced resolution caused by patient movement during acquisition, and image distortion related to proximity of the x-ray beam source to the film/detector and posterior position of the film cassette.

ULTRASONOGRAPHY

Lung ultrasonography is a technique increasingly used in the perioperative, critical care, and emergency settings in adults and children.³⁰⁶⁻³⁰⁹ Critical and systematic approaches have proven that important clinical information can be obtained with lung ultrasonography at levels

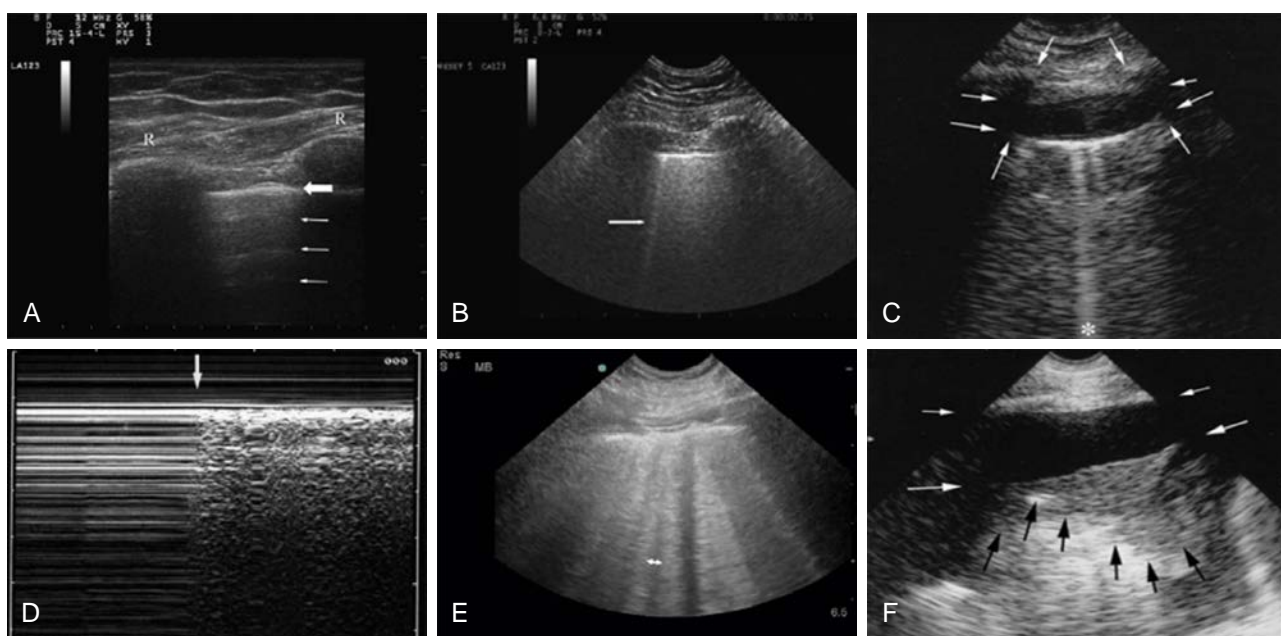


Fig. 41.27 (A) Typical thoracic view depicting adjacent ribs (R) producing acoustic shadowing. The white echogenic pleural line (block arrow), is approximately 0.5 cm below the ribs. A-line artifacts (line arrows) are seen at equidistant spaces below the pleural line; (B) B-line, or comet-tail artifact (line arrow), is the hyperechoic artifact extending from the pleural line to the edge of the screen, erasing the A-line. A solitary B-line is a usual finding in normal lungs; (C) pleural effusion: image obtained at the posterolateral region showing the parietal pleural (upper horizontal arrows), the rib shadows (vertical arrows), and the visceral pleura (line indicated by the lower horizontal arrows) with the underlying lung. The dark anechoic region between the parietal and visceral pleura represents the pleural effusion. A B-line artifact (asterisk) originates from the lung and not from the pleural line, implying the presence of aeration; (D) M-mode of lung of lung ultrasound illustrative of the “lung point” for diagnosis of pneumothorax. The sudden inspiratory transition from a parallel line pattern indicative of absence of lung motion (pneumothorax) to a granular pattern indicative of lung tissue can be observed (arrow); (E) Interstitial syndrome case showing B-lines 7 mm or less apart. Notice the increased number of B-lines as compared to panel (B). The pleural line (arrow) and ribs are also appreciated; (F) Lung consolidation with pleural effusion. As in (C), the image was obtained at the posterolateral region showing the parietal pleura (upper horizontal arrows) and the visceral pleura and lung (lower horizontal arrows) with an anechoic pleural effusion between them. Lung tissue denser than that presented in (C) with gas barriers (vertical arrows). This indicates pleural fluid with alveolar fluid often seen in critically ill patients. ([A, B, D, E] From Turner JP, Dankoff J. Thoracic ultrasound. *Emerg Med Clin North Am*. 2012;30:451–473, ix. [C, F] From Lichtenstein DA. BLUE-protocol and FALLS-protocol: two applications of lung ultrasound in the critically ill. *Chest*. 2015;147[6]:1659–1670. doi: 10.1378/chest.14-1313.)

comparable to computed tomography.³⁰⁹ Such features add to the advantages of practicality, low cost, and absence of radiation or other significant biologic side effects. Excellent reviews have been published, and the reader should refer to those for additional learning.^{308,309}

Lung ultrasonography has been applied successfully in the assessment of pneumothorax, interstitial syndrome (i.e., cardiogenic and permeability pulmonary edema), lung consolidation, and pleural effusion. Currently available multipurpose ultrasonography probes can be used for specific portions of the pulmonary exam according to their characteristics. For instance, the high-frequency (10-12 MHz) linear array probe allows for detailed examination of the pleura and superficial changes, such as pneumothorax. This probe's limitations include its size, which impedes access to larger areas of lung tissue because of the interference of the ribs, and high frequency, which limits assessment of deeper structures. A lower frequency (1-5 MHz) probe provides improved depth penetration and is used to assess supradiaphragmatic structures (pleural space, lung). To optimize lung visualization with a single probe, frequently probes with emission frequencies of 5 to 7 MHz are used and are usually small with a tip shaped so that an acoustic window on the lung parenchyma can be obtained on intercostal spaces. The 5 MHz microconvex probe is frequently favored,^{306,307} although curvilinear and phased-array probes are also appropriate.³⁰⁸

When examining the patient, a methodical approach should be used to ensure comprehensive assessment of lung structure and function. The I-AIM (Indication, Acquisition, Interpretation, Medical Decision-Making) framework has been recently proposed for point of care lung ultrasound.³⁰⁸ A complete exam involves the bilateral assessment of the anterior, lateral, and posterior lung. Although protocols vary, in the supine patient, each hemithorax should be assessed in at least six zones during emergencies: two anterior (separated by the third intercostal space), two lateral, and two posterior. In routine assessments, 8-zone and 12-zone protocols are most commonly used.^{308,310,311} Because of the significant acoustic impedance differences between air, tissue, and bone (ribs), thoracic ultrasound is based primarily on characteristic artifacts and not only on the visualization of anatomic structures.³¹² Videos of 1 to 2 breaths should be acquired to take advantage of the lung dynamics in the findings. Machine settings should be optimized at the start of the examination.³⁰⁸ Usually, studies are initiated with the identification of the ribs as hyper-echoic lines producing significant ultrasonography shadow (Fig. 41.27A), followed by visualization of the pleural line approximately 0.5 to 1.0 cm deeper and between the ribs. This is typically a bright, slightly curved line. These are major structures to be identified, because many pathologies of relevance to the anesthesiologist affect their observed pattern. In the normal lung, lung sliding represents the

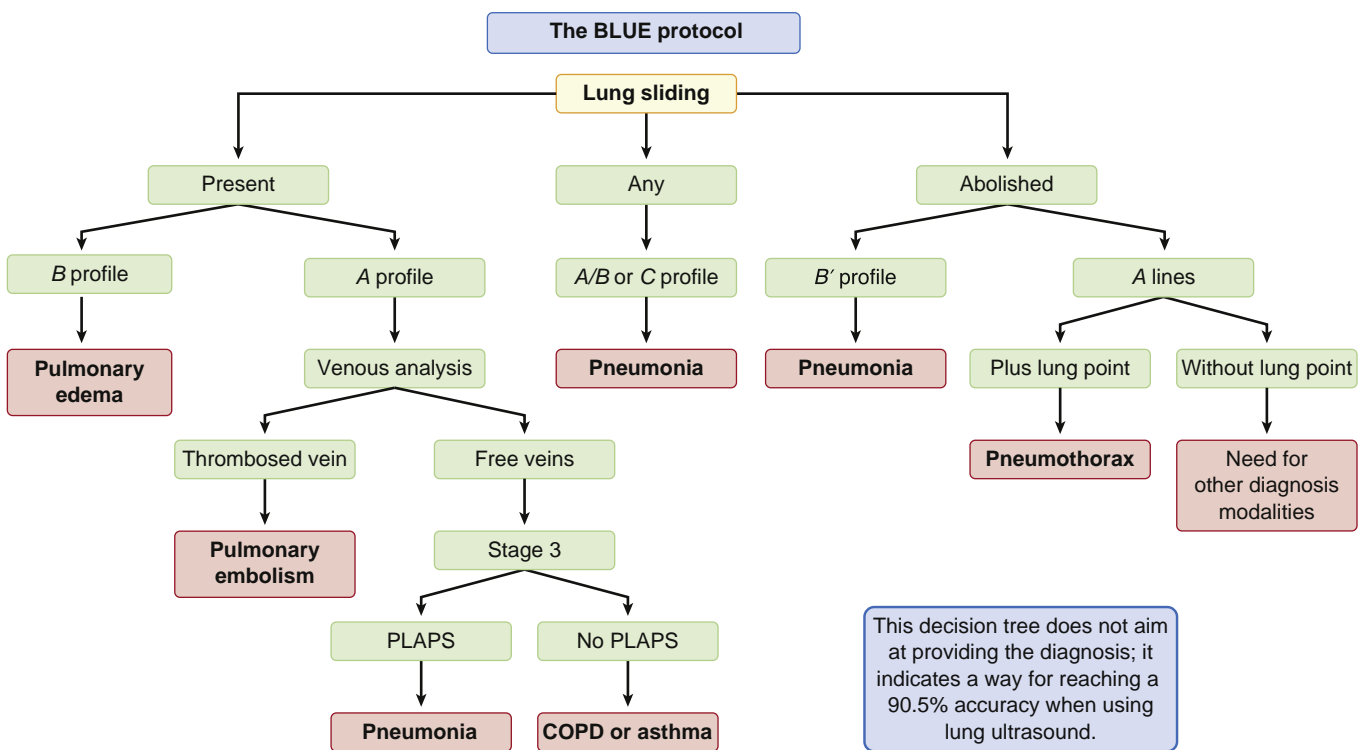


Fig. 41.28 The BLUE protocol algorithm based on the particular ultrasound profile of the different kinds of respiratory failure. It uses three lung ultrasound signs with binary answers: anterior lung sliding, multiple B-lines visible between two ribs in the anterior lung, and posterior and/or lateral alveolar and/or pleural syndrome. These are combined with venous analysis to yield 90.5% accuracy in the diagnosis of respiratory failure. COPD, Chronic obstructive pulmonary disease; PLAPS, posterolateral alveolar and/or pleural syndrome. (Redrawn from Lichtenstein DA, Meziere GA. Relevance of lung ultrasound in the diagnosis of acute respiratory failure: the BLUE protocol. *Chest*. 2008;134:117–125; Milner QJ, Mathews GR. An assessment of the accuracy of pulse oximeters. *Anesthesia*. 2012;67:396–401; and Pologe JA. Pulse oximetry: technical aspects of machine design. *Int Anesthesiol Clin*. 1987;25:137–153.)

movement of the visceral on the parietal pleura during respiration and is another key sonographic finding to be appreciated. The magnitude of the movement is larger in regions closer to the diaphragm than those near the lung apex.

Below the pleura, hyperechoic horizontal reverberation artifacts at regular distances are referred to as A lines (see Fig. 41.27A). Another artifact is the B line, a discrete laser-like vertical hyperechoic reverberation artifact that arises from the pleural line (previously described as “comet tails”), extends to the bottom of the screen without fading, moves synchronously with lung sliding, and erases A lines (see Fig. 41.27B and C). Solitary B lines are a normal finding in the normal lung, and increased numbers are observed in disease. Based on the recognition of such artifacts, pathologic conditions are identified.^{306–308,313} Most acute disorders involve the lung surface, and this explains the utility of thoracic ultrasound in visualizing them. Ultrasonography findings for pneumothorax are the absence of lung sliding, B lines, and lung pulse, and the presence of lung points.

Pleural effusions are characterized by a usually anechoic space between the parietal and visceral pleurae (see Fig. 41.27C and F) and by respiratory movement of the lung within the effusion (“sinusoid sign”). The presence of echo-geneic material within the effusion suggests an exudate or hemorrhage, although some exudates are anechoic. Most transudates are anechoic. The M-mode ultrasound scan shows parallel lines indicative of no moving structure underlying the probe. The ultrasonographic finding designated

as a lung point is found in the presence of pneumothorax and represents the imaging of the cyclic transition during breathing from the absence of any sliding or moving B lines at a physical location (i.e., air with no lung parenchyma) to the visualization of lung sliding, B lines, or altered A lines indicative of lung tissue (see Fig. 41.27D).^{307,314} Bedside ultrasound scans can detect pneumothorax with sensitivity similar to a CT scan.^{306,307}

An interstitial syndrome is characterized by the presence of multiple B lines. A positive region is defined by three or more B lines in a longitudinal plane between two ribs (see Fig. 41.27E).³⁰⁷ Lung consolidation is characterized sonographically by a subpleural echo-poor region or one with tissue-like echo-texture (see Fig. 41.27F). Lung consolidations may be caused by infection, pulmonary embolism, lung cancer and metastasis, compression atelectasis, obstructive atelectasis, and lung contusion. Additional sonographic signs that may help determine the cause of lung consolidation include the quality of the deep margins of the consolidation, the presence of comet-tail reverberation artifacts at the far-field margin, the presence of air or fluid bronchograms, and the vascular pattern within the consolidation. Advances in clinical research and experience in lung ultrasonography allowed for the proposal of an algorithm to assess severe dyspnea in the acute setting (Fig. 41.28). The denominated BLUE protocol is a stepwise ultrasonographic approach to the patient with acute respiratory failure that aims at expeditious diagnosis with 90.5% accuracy.^{309,313,315}

ELECTRICAL IMPEDANCE TOMOGRAPHY

Electrical impedance tomography (EIT) is a noninvasive and radiation-free imaging modality used to assess regional lung function at the bedside. The method is clinically available and has moderate to low spatial resolution but high temporal resolution, thus allowing for assessment of regional ventilation in real-time.^{235a,305,316} Its use in estimating regional lung volume and optimizing mechanical ventilation settings brought significant attention to applications in ICUs and operating rooms.³⁰⁵

EIT is based on electrical impedance, a physical variable that reflects the opposition to the passage of a current through an object when a voltage is applied across it.³¹⁷ The impedance of biological tissues depends on the tissue composition. High concentrations of electrolytes, extracellular water content, large cells, and number of cell connections by gap junctions as present in blood and muscles reduce impedance. Air, fat, and bone have high electrical impedance. Pathologic changes of tissue composition influence impedance. These include extravascular lung water (EVLW) (e.g., pulmonary edema), intrathoracic blood volume, fluid in cavities (pleural effusion, pericardial effusion, bronchial and alveolar fluid), foreign bodies (pleural drain), and lung fibrosis (e.g., after ARDs or as a primary disorder). During the breathing cycle, thoracic bioimpedance is influenced fundamentally by both ventilation and perfusion.

EIT relies on an array of electrodes (typically 16-32) around the chest region of interest. The location is chosen based on the clinical information desired, usually at the fifth intercostal space for standard lung assessment. The impedance information is provided in the form of a functional EIT image, or EIT waveforms that quantify changes in lung volume or perfusion in the studied thoracic cross section. Usually, images are presented with pixels representing relative impedance change, so-called functional EIT, because air corresponds to high impedances and fluid and tissue to low impedances, and the image represents regional lung ventilation. Absolute EIT (a-EIT) is the modality in which the image represents the actual impedance values. Direct

assessment of lung conditions can be accomplished by comparing low impedance (e.g., hemothorax, pleural effusion, atelectasis and lung edema) with high impedance (e.g., pneumothorax, emphysema).³¹⁸ EIT has compared successfully with standard methods, including computed tomography.³¹⁹

Because the technique provides direct real-time assessment of changes in regional aeration, several applications related to regional lung function have been identified.^{316,319} These include the effect of induction and tracheal intubation on the expiratory lung level and regional ventilation in children (Fig. 41.29)³²⁰; perioperative monitoring of the distribution of ventilation during spontaneous and controlled breathing,^{321,322} including HFOV^{235a,278,323}; effects of PEEP on regional ventilation during laparoscopic surgery³²⁴; the magnitude of bedside lung recruitment; and PEEP titration with assessment of alveolar collapse and hyperdistention in ARDS³²⁵ and obese patients.³²⁶ EIT may also allow for real-time detection of pneumothorax.³²⁷ Recent advances show the potential of EIT to provide measurements of regional perfusion,^{319,328} which could be valuable for bedside assessment of \dot{V}/\dot{Q} matching during spontaneous and mechanical ventilation.

Point of Care Tests

Point-of-care testing (POCT) is the performance of laboratory measurements near the site of patient care. POCT technology includes portable analyzers and use of small blood samples. For the anesthesiologist, it implies the availability of rapid, precise, and accurate measurements in operating rooms and ICUs. POCT yields improvements in patient outcome through expeditious detection of physiologic deterioration and prompt treatment. Respiratory monitoring is a major element of POCT and includes analysis of arterial blood gases (P_aO_2 , P_aCO_2 , pH), Hb, and lactate.

Blood gas measurements can be obtained with acceptable levels of accuracy and precision with POCT.³²⁹⁻³³¹ For instance, different platforms for arterial blood gases and Hb were found to show coefficients of variation of

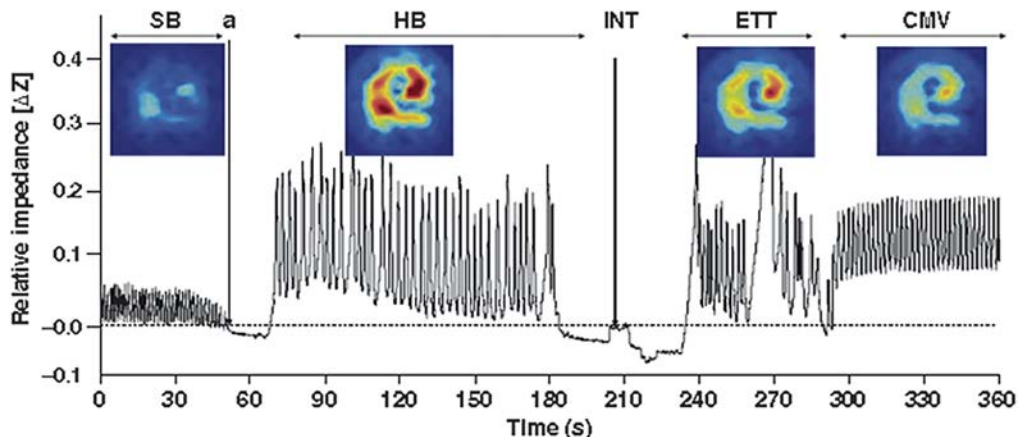


Fig. 41.29 Relative impedance signal at five key stages during induction of anesthesia in children. (a) There is a small impedance signal during spontaneous breathing (SB) as muscle paralysis develops. Effective hand bagging (HB) produces a high intensity signal, which is zeroed during tracheal intubation (INT). Distribution of regional impedances during hand bagging with the endotracheal tube (ETT) and conventional mechanical ventilation (CMV) are also visualized. (From Humphreys S, Pham TM, Stocker C, Schibler A. The effect of induction of anesthesia and intubation on end-expiratory lung level and regional ventilation distribution in cardiac children. *Paediatr Anaesth*. 2011;21:887-893.)

approximately 3% to 6%.^{330,331} Accuracy is present in wide ranges of P_aO_2 and pH³²⁹⁻³³¹, and shows bias of some devices for P_aCO_2 .³³¹

Hb is measured using either conductivity-based methods where hematocrit is assessed and the Hb concentration calculated (Hb [g/dL] = hematocrit \times 0.34) or with optical methods, such as using the azide-metHb reaction and photometry absorbance.³³² Conductivity-based Hb measurements can be less than those reported by standard systems, with a clinically significant bias of at least -1.2 g/dL in the Hb range of 8.5 to 14.2 g/dL and a trend to underestimate the Hb value at low ranges.^{330,331} Variable measurement agreement across devices, and bias resulting from inspired O₂ fraction are issues that still limit noninvasive Hb assessment.^{331,333,334}

The site of blood sampling can influence POCT results. For capillary blood samples obtained from finger and ear punctures, a significant correlation exists between optical-based and automated laboratory Hb analysis, with a nonsignificant bias. Fingerstick samples may approximate standard laboratory Hb measurements better than earlobe samples.²² Capillary blood samples (lancet puncture to middle or ring finger and fourth drop used) in patients with gastrointestinal bleeding resulted in high deviations (>1 g/dL) in 21% of cases and very high deviations (>2 g/dL) in 4% of cases.³³⁵ In critically ill patients, poor agreement with reference measurements is reported,³³⁶ especially with capillary blood samples and in patients with extremity pitting edema. POCT proved relevant in the assessment of arterial blood gases during pseudohypoxemia (also called “spurious hypoxemia” and “leukocyte larceny”). This is a known cause of inaccurate blood gas measurements and occurs when P_aO_2 is reduced by increased O₂ consumption as a result of markedly elevated white blood cell counts in the arterial blood sample. Measurement error is further aggravated by delayed laboratory analysis or incorrect sampling. Pseudohypoxemia occurs not only in hyperleukocytosis but also in thrombocytosis associated with polycythemia vera.

As POCT progresses, relevant limitations will need to be addressed, including cost, accuracy, data management, and evidence for improved outcomes. Contrary to some expectations, availability of POCT in academic centers does not increase the number of tests performed.³³⁷ Characteristics of individual institutions should be considered before POCT is implemented. For instance, POCT blood-gas analysis may offer minimal time savings and cost benefits compared with central laboratory analysis in an institution with short turnaround time.

Respiratory Monitoring in Special Conditions

As methods for life support are advanced, the physiologic patterns that serve as the basis for assessment of gas exchange and respiratory mechanics can be dramatically changed. This occurs, for instance, during HFV when significant reductions in V_T are combined with large increases in respiratory rate. During rigid bronchoscopy or laryngeal interventions, the anesthesiologist is required to share management of the airway with the surgeon. This may result in intermittent loss of information regarding airway flow,

volume, and pressure, as well as end-tidal gas concentration. In these situations, clinical assessment based on physical examination (i.e., inspection, auscultation) becomes paramount. Specific considerations for respiratory monitoring in special conditions are detailed in the next section.

HIGH-FREQUENCY VENTILATION

HFV is a ventilatory mode using V_T smaller than the anatomic dead space, 10-fold to 50-fold higher respiratory frequencies, and high instantaneous flow rates. The HFV is a broad term encompassing various modalities. These include high-frequency jet ventilation (HFJV) and high-frequency percussive ventilation (HFPV), both of which allow for passive exhalation, as well as HFOV, in which exhalation is actively driven by the device. The mechanisms for gas exchange during HFV are complex and include convective transport, turbulence, pendelluft, velocity profile distortion and asymmetry, Taylor dispersion, molecular diffusion, collateral ventilation, and cardiogenic mixing.³³⁸⁻³⁴⁰ This method results in a fundamentally different relationship for CO₂ elimination (\dot{V}_{CO_2}) compared with conventional ventilation.³⁴¹ For example, during conventional ventilation,

$$\dot{V}_{CO_2} \propto f(V_T - V_D) \quad (41.39)$$

where f is the breathing frequency and V_D is dead space volume. However, during HFOV^{342,342a},

$$\dot{V}_{CO_2} \propto f \frac{V_T^2}{V_D} \quad (41.40)$$

The use of HFOV for neonates in respiratory distress failing conventional ventilation is common.³⁴³⁻³⁴⁵ However, its use in adult patients with ARDS has been limited in light of recent clinical trials,^{345a,b} despite the sound physiologic rationale of using high mean airway pressures and low V_T to achieve alveolar recruitment without overdistention.³⁴⁶⁻³⁵⁰

Most high-frequency oscillators use pistons to actively drive flow into and out of the airway at respiratory rates between 3 to 20 Hz.^{351,352} However, some oscillators, and most jet ventilators, rely on solenoid valves.³⁵³⁻³⁵⁵ With HFOV, fresh gas and CO₂ may be removed by a continuous bias flow of warmed, humidified gas past the proximal end of the ETT, and mean airway pressure is regulated by an adjustable valve venting the bias flow and exhaled gas from the circuit. These devices may be either pressure or time cycled, and both the mean airway pressure and oscillatory pressure amplitude are displayed on the console to the clinician. However, for the frequencies used during HFV, a significant portion of the oscillatory pressure amplitude results from the inertia of the gas column contained in the breathing circuit and the patient's airways, and thus it should not be used as a surrogate for lung distention.

Clinically useful physiologic information inferred from airway flow and pressure measurements is somewhat limited during HFV. During conventional mechanical ventilation, airway pressure and flow are related according to basic mechanical properties of the respiratory system, such as airway resistance and tissue compliance. However, during HFV, airway pressure and flow reflect complex resistive and inertial gas properties in the central airways. Many investigators have assessed respiratory mechanics during HFV by transiently switching patients to conventional mechanical

ventilation to obtain basic estimates of resistance and compliance,³⁵⁶ or even making intermittent low-frequency oscillatory measurements to measure airway and tissue properties.³⁵⁷ The pressure transmission index, defined as the ratio of the pressure measured directly in the trachea to the pressure at the proximal end of the breathing circuit (i.e., the pressure amplitude measured at the oscillator), is strongly correlated with tissue elastance.^{357,358}

An important component of monitoring during any form of HFV is the assessment of mechanical function. Many important physiologic parameters, such as mean airway pressure and V_T , are not explicitly controlled by most high-frequency ventilators.^{358a,b} Thus the relationship between pressure transduced at the proximal end of the breathing circuit and the V_T delivered to the patient is difficult to assess. Indeed, this relationship is highly nonlinear,³⁴³ and it depends on frequency, gas composition and inertia, and the overall mechanics of the patient's respiratory system.^{235,276} Given the important role that V_T plays in CO_2 elimination during HFV (Eq. [41.40]), accurate measurement of airway flow is important for the development and standardization of clinical trials.³⁵⁹ Hot wire anemometry yields the most accurate estimates of airway flow and delivered V_T during HFOV compared with other measuring devices.^{235,276}

Adequacy of gas exchange is essential during HFV. Analysis of arterial blood gas measurements should be performed within 30 minutes of any change in ventilator settings, and at least twice per day on stable settings.³⁴⁶ Whereas oxygenation is usually assessed with continuous pulse oximetry, CO_2 elimination is more technically challenging to monitor. Attempts have been made to incorporate various forms of capnography into HFV circuits,³⁶⁰⁻³⁶³ with varying degrees of success. Depending on where exhaled gases are sampled, there may be adequate correlation between $P_{ET}CO_2$ and P_aCO_2 during HFV.^{362,363} This is often a reflection of the slower response time of many sidestream CO_2 analyzers.¹⁷¹ The PCO_2 sampled at the airway opening may thus underestimate the true alveolar CO_2 levels.³⁶¹ The most accurate measurement of alveolar PCO_2 is obtained when it is measured at the very distal tip of the ETT,³⁶⁴ although this is not always clinically feasible. Transcutaneous measurements of PCO_2 may hold considerable promise for assessment of CO_2 clearance during HFV.³⁶⁵

Although HFOV has not been shown to improve outcomes in adult patients with ARDS,^{345a,b} this finding may reflect the variable effects of frequency, amplitude, and mean airway pressure with oscillating of a heterogeneously injured lung,^{342a,348} as well as the poorly understood phenomena of gas distribution, volume recruitment, and \dot{V}/Q matching in individual patients. Recent studies suggest that oscillation using multiple simultaneous frequencies may improve the efficiency of gas exchange, reduce the heterogeneity of parenchymal strain, and maintain lung recruitment at lower mean airway pressures.^{235a,365a} Despite significant gaps in our understanding of the use of HFOV in acute respiratory failure, this modality may still have some clinical application as part of a lung-protective ventilatory strategy, particularly in patients with severe hypoxemia.^{290a} Future clinical trials will guide both therapy and technologic development of HFOV,³⁴⁷ thus providing a scientific basis for the rational use of this technology in critically ill patients.

JET VENTILATION

Jet ventilation is commonly used for procedures in which the surgeon requires unobstructed access to the airway.³⁶⁶ During inspiration, O_2 or an O_2 -air mixture is applied under high pressure to the airway through either a specialized catheter or a rigid bronchoscope. This jet of gas, along with entrained air from the surrounding environment, leads to insufflation of the lungs. Expiration takes place through passive recoil. The entire system is open to the environment, thus leading to significant escape of respiratory gases.³⁵⁴

Oxygenation during jet ventilation can be adequately monitored using pulse oximetry. Ascertaining the presence and adequacy of ventilation, especially during HFJV, is more challenging because the composition and volume of the exhaled gases cannot be directly measured. Arterial sampling of P_aCO_2 is accurate but intermittent and invasive. Gas can be sampled at the distal end of the catheter or rigid bronchoscope through a dedicated channel. Quantitative capnography during HFJV does not accurately reflect P_aCO_2 because V_T is smaller than dead space.³⁶⁷ This problem can be overcome by the intermittent suspension of HFJV or reduction in frequency to 10 breaths/min or less. $P_{ET}CO_2$ measurements obtained in this manner accurately reflect the P_aCO_2 and allow the intermittent monitoring of ventilation.^{363,368-370} The measurement of transcutaneous PCO_2 ($P_{tc}CO_2$) is noninvasive and continuous. Although $P_{tc}CO_2$ is not as accurate as capnometry and has a slower response time to changes in P_aCO_2 , its use may allow for tracking of changes in P_aCO_2 .³⁷⁰ The absence of V_T and continuous $P_{ET}CO_2$ monitoring precludes standard ventilator disconnect monitoring during intraoperative HFJV. RIP, which uses changes in the inductance of bands placed around the chest to monitor respirations, has been demonstrated to discriminate reliably between the presence and absence of HFJV and may be developed as a monitor to detect disconnect or the absence of adequate thoracic excursion during HFJV.²⁸²

PATIENT TRANSPORT

Intrahospital transport of critically ill patients is a frequent occurrence. Transport of adult and pediatric patients from locations with advanced monitoring to more remote locations is fraught with difficulty, ranging from simple equipment malfunction to major disasters.³⁷¹⁻³⁷³ Complex monitoring and numerous pieces of equipment are often required for safe transfer, especially when additional devices such as extracorporeal membrane oxygenators and ventricular assist devices are present. The lack of standardized monitoring techniques and terminology explains the widely reported discrepancies in the incidence of adverse events. Overall, a high incidence of respiratory complications following transport has been reported.³⁷²⁻³⁷⁴

Respiratory monitoring during transport should ideally be the same as that in the operating room or ICU before relocation. In practice, at least clinical signs (e.g., skin color, chest expansion, auscultation, endotracheal secretions), pulse oximetry, and respiratory rate, together with EKG and blood pressure, should be monitored throughout intra-hospital transport. If a transport ventilator is used, airway pressures should be readily available in numeric or graphic

formats. Human factors are essential during transport, and a specialized transport team using standardized management procedures with preparatory, transfer, and post-transport stabilization phases likely limits the frequency of adverse events.³⁷⁵⁻³⁷⁷ This is particularly important when high-risk patients are involved.³⁷⁶ Equipment and medications needed to establish and maintain a secure airway and hemodynamics should be available during any transfer. Adequate O₂ supply with functioning low-pressure alarms should be verified during pretransport preparation. A transport ventilator can provide better oxygenation and reduce variability in pH and PCO₂ compared with manual ventilation.^{374,378} The transfer phase may require several professionals under the coordination and supervision of an attending anesthesiologist.

Automated Data Systems

Electronic anesthesia records are part of routine clinical practice in many institutions. Such systems provide data from medical devices, clinical information management systems, and laboratory data. The availability of large amounts of real-time data in digital form allows for introduction of new approaches to monitoring that may have been conceptualized, but not yet clinically implemented. In fact, although decision-support research has been done for years, little progress has been made in clinical decision support for the acute management of unstable patients, a major challenge in the operating room and ICU.³⁷⁹⁻³⁸¹ Computerized monitoring has significant potential to improve clinical monitoring.^{379,382} However, it has limitations resulting from typical requirements not well-suited for human performance, such as monitoring graphic displays over extended periods, or the execution of overt responses to low-probability events. Humans are limited in their ability to analyze large quantities of data accurately and continuously. Accordingly, computer algorithms that identify subtle but meaningful trends in physiologic data are desirable. Such tools require relevant contextualization of measurement to improve accuracy, as well as minimization of false-negative and false-positive alarms. This automated monitoring should depend not only on timely measurements, but also on prior information. Alarms should not be fixed to specified thresholds, but rather dynamically adapted to information as it becomes available. Algorithms with established clinical rules provide the opportunity to detect subtle changes in time-series data,³⁸³ which exceed human discrimination.³⁸⁴ Such automated systems minimize monitoring failures and promote timely responses, thus enhancing the performance of anesthesia delivery during long periods. Some tools of respiratory monitoring have been assessed in adult and pediatric populations.^{379,385-387} Data banks have been developed for research.³⁸¹ Another potential interest in these systems is that of creating closed-loop systems, such as those currently implemented to adjust settings in commercial mechanical ventilators.^{386,388}

Although these methods are not currently established for clinical use, they are expected to find increasing application as reliable monitoring algorithms are implemented and validated. Such automated systems allow for the implementation of additional levels of safety. The detection of potentially

dangerous events, such as continuously low S_aO₂ or the absence of P_{ET}CO₂ measurements for several breaths, can generate an automated alarm, a screen alert, or an automated page to the supervising anesthesiologist.³⁸⁹ In a different condition, for example when changes in oxygenation occur over a period of minutes, improved processes should be directed to the anesthesia provider in direct contact with the patient, to initiate prompt treatment, assess artifacts, and/or call for assistance.³⁸⁹

Additional Monitored Variables

NITROGEN WASHOUT AND END-EXPIRATORY LUNG VOLUME

There has been a resurgence of interest in the use of nitrogen washout methods for adult^{390,391} and pediatric³⁹² patients. Nitrogen washout techniques are found in commercial mechanical ventilators for intensive care use. The main parameter of interest has been the end-expiratory lung volume, a potentially valuable measurement to optimize lung expansion during mechanical ventilation, and for the assessment of ventilatory interventions such as PEEP adjustment.³⁹¹ The measurements are performed by introducing a step change in the inspired air (traditionally from room air to 100% O₂, in current systems a nitrogen washout/wash-in method with 10% to 20% change in F_iO₂) and solving mass balance equations for the lung volume. In patients with ARDS, measurements of end-expiratory lung volume demonstrated good accuracy and reproducibility, with a coefficient of variation of less than 4%.³⁹¹ In 30 intensive care patients undergoing computed tomography for clinical reasons, the end-expiratory lung volume measured with the modified nitrogen washout/wash-in technique was well correlated ($r^2 = 0.89$) with computed tomography measurements with a bias of 94 ± 143 mL ($15 \pm 18\%$, $P = .001$), within the limits of accuracy provided by the manufacturer.³⁹⁰ Nitrogen washouts can also provide measures of ventilation heterogeneity.³⁹²

TRANSCUTANEOUS MEASUREMENTS OF PARTIAL PRESSURES OF OXYGEN AND CARBON DIOXIDE

Gas exchange is a dynamic and at times rapidly changing process. Conventional direct measurements of arterial blood gases, although still the gold standard for P_aO₂, P_aCO₂, and pH monitoring, provide only an isolated picture of that process. Expedited assessment of circulating blood gases could facilitate faster initiation of required therapy and adjustment of implemented ventilation. A method for noninvasive continuous monitoring of P_aO₂ and P_aCO₂ is a current clinical need.

Transcutaneous measurements of PCO₂ (P_{tc}CO₂), in addition to transcutaneous PO₂ (P_{tc}O₂), aim to provide noninvasive estimates of arterial CO₂ and O₂, or at least trends associated with them. These measurements have been useful in intensive care management of neonates and infants,³⁹³ and in the fields of wound healing and hyperbaric O₂ therapy. An advantage is that transcutaneous monitoring can be applied when expired gas sampling is limited

such as during HFOV, apnea testing, and noninvasive ventilation. The measurements are based on the diffusion of O₂ and CO₂ through the skin. Because the skin is not entirely permeable to gases, warming is used to facilitate gas diffusion. Such an increase in temperature (usually 42°C-45°C) promotes increased O₂ and CO₂ partial pressure at the skin surface resulting from changes in structure of the stratum corneum that increase diffusion and dermal hyperemia and shift the Hb dissociation curve. This process ultimately results in arterialization of the regional blood. P_{tc}O₂ and P_{tc}CO₂ are influenced not only by the arterial gas partial pressures but also by skin O₂ consumption, CO₂ production, and regional blood flow. Accordingly, P_{tc}O₂ is usually lower than P_aO₂, and P_{tc}CO₂ is usually higher than P_aCO₂.

O₂ transducers are electrochemical polarographic Clark-type electrodes in which the rate of chemical reaction is related to an electrical signal proportional to the O₂ concentration. For CO₂, a transducer using a pH electrode to measure PCO₂ (Stow-Severinghaus electrode) is used, where a change in pH is proportional to the logarithm of the PCO₂ change. For CO₂ monitors, a temperature correction factor is used to estimate P_aCO₂ from P_{tc}CO₂. In vivo correction is available in some devices based on arterial blood gases. The thin epidermal layer of infants facilitates the measurements, in contrast to the diffusion barrier introduced by the thicker adult skin. A lower electrode temperature in P_{tc}CO₂ monitoring produces systematic bias of the transcutaneous electrode. However, in very preterm babies, monitoring at 40°C or 41°C to reduce the risk of burns is possible, provided a bias correction of 12% to 15% is applied.³⁹⁴

The main application of P_{tc}CO₂ is in the neonatal ICU population.³⁹³ Even in very low-birth-weight infants, the mean difference between P_{tc}CO₂ and P_aCO₂ is 3.0 mm Hg (95% confidence interval, 0.2 to 6.0 mm Hg; $P < .05$).³⁹⁵ In addition, P_{tc}CO₂ may be used to assess the efficacy of mechanical ventilation continuously during respiratory failure. In this setting, in children 1 to 16 years, P_{tc}CO₂ was more accurate and precise than P_{ET}CO₂ in relation to P_aCO₂. P_{tc}CO₂-P_aCO₂ differences were 2.3 ± 1.3 mm Hg in children 1 to 3.4 years old and 2.6 ± 2.0 mm Hg in children 4 to 16 years old.³⁹³ P_{ET}CO₂-P_aCO₂ differences were larger (6.8 ± 5.1 and 6.4 ± 6.3 mm Hg) for the same age ranges. When compared with P_{ET}CO₂, P_{tc}CO₂ monitoring is equally accurate in patients with normal respiratory function. Accuracy and precision in the perioperative period of cardiac surgery for congenital heart disease in infants and children were better for P_{tc}CO₂ than P_{ET}CO₂ in relation to P_aCO₂, with the exception of patients receiving significant amounts of vasoactive medications and in low cardiac output states.

In adults, P_{tc}CO₂ has proven to be a less accurate and precise surrogate for P_aCO₂. Nonetheless, P_{tc}CO₂ could be suitable for specific conditions. Laparoscopic surgery with prolonged pneumoperitoneum is one condition in which P_{tc}CO₂ may be a more accurate estimate of P_aCO₂ compared with P_{ET}CO₂,³⁹⁶ even for trending P_aCO₂.³⁹⁷ During deep sedation for ambulatory hysteroscopy in healthy patients, earlobe P_{tc}CO₂ agreed better with P_aCO₂ than did nasal sidestream P_{ET}CO₂, with lower bias (1.7 vs. -7.0 mm Hg) and smaller mean differences to P_aCO₂ (3.2 ± 2.6 vs. 8.0 ± 6.0 mm Hg).³⁹⁸ The sensitivity of the P_{tc}CO₂ monitor for

detecting P_aCO₂ values higher than 50 mm Hg was also greater than for P_{ET}CO₂ (66.7% vs. 33.3%; $P < .01$).³⁹⁸ P_{tc}CO₂ is also helpful during weaning from mechanical ventilation after off-pump coronary artery bypass graft.³⁹⁹ In adults admitted to an emergency department for acute respiratory failure, agreement between P_aCO₂ and P_{tc}CO₂ was 0.1 mm Hg, and the limits of agreement were from -6.0 to 6.2 mm Hg). In patients undergoing noninvasive ventilation, unacceptably wide variability may be observed.⁴⁰⁰ In mechanically ventilated ICU patients, P_{tc}CO₂ correlated better and with less bias to P_aCO₂ than P_{ET}CO₂ even if still with sizeable variability (mean P_{tc}CO₂ - P_aCO₂ = 2.2 ± 5.7 mm Hg).⁴⁰¹ P_{tc}CO₂ does not replace P_{ET}CO₂ monitoring, which remains the standard of care to confirm intratracheal placement of the ETT following intubation, or to actuate a disconnect alarm in the operating room.

P_{tc}O₂ from normal to extremely low-birth-weight infants agreed well with P_aO₂ measurements, with mean P_{tc}O₂-P_aO₂ difference 2.3 (-1.5 to 6.8) mm Hg, clinically acceptable in current neonatal ICUs. P_{tc}O₂ in neonates is additionally important to detect hyperoxia, which is not feasible with pulse oximetry. The use of P_{tc}O₂ in adults has been focused on wound management, peripheral vascular disease, and hyperbaric medicine. Although attempts for applications in adults were promising, such as the use of P_{tc}O₂ to support resuscitative efforts,⁴⁰² measurements following off-pump coronary artery surgical procedures still present very high variability.⁴⁰³ The dependence of P_{tc}O₂ on low-flow states has been used in conjunction with analysis of arterial blood gases to estimate adequacy of cutaneous blood flow and, by inference hemodynamic, stability.^{404,405}

In summary, transcutaneous measurements are favorably positioned for continuous gas exchange monitoring in neonates and infants. In contrast, widespread applications of transcutaneous techniques in the perioperative settings are still hindered by limitations, such as poor cutaneous blood flow, need for frequent calibration, slow response time, and risk for skin burns with prolonged application.

LUNG WATER

Pulmonary edema is a hallmark of lung injury. It can result from increased hydrostatic pressure in the pulmonary capillaries (cardiogenic), increased permeability of the alveolar capillary membrane (noncardiogenic), and reduced lymphatic drainage from the lungs. Such mechanisms can be caused by pulmonary or extrapulmonary factors. For these reasons, interest in the development of methods to quantify EVLW has been considered, because this may assist in the diagnosis and management of those conditions, including early detection, differential diagnosis, fluid therapy, diuretics, and mechanical ventilation.⁴⁰⁶ In patients, assessment of pulmonary edema is made with imaging techniques (e.g., chest radiography, ultrasonography, and computed tomography), thermodilution, bioimpedance, bioreactance, and remote dielectric sensing.

Imaging Techniques

The method used primarily in clinical practice remains bedside chest radiograph. It allows for semiquantitative assessment of EVLW, its distribution, and its possible etiology. The chest radiograph has limited diagnostic accuracy. This

is because (1) edema may not be visible until the amount of lung water increases by 30%⁴⁰⁷; (2) any radiolucent material that fills the air spaces (e.g., alveolar hemorrhage, pus, and bronchoalveolar carcinoma) will produce a radiographic image similar to that of pulmonary edema; (3) technical issues including rotation, inspiration, positive-pressure ventilation, patient position, and underpenetration or overpenetration can reduce sensitivity and specificity; and (4) substantial interobserver variability exists in interpretation of chest radiographs.^{408,409} Computed tomography is another radiographic technique to quantify EVLW. In animal experiments, computed tomography densitometry could detect an increase in EVLW by as little as 50%.¹⁶² Computed tomography-based studies indicated that significant hypoxemia secondary to pulmonary edema may not develop until the increase in EVLW approaches 200% to 300%.¹⁶³ Lack of portability and high radiation exposure limit the use of computed tomography as a continuous intraoperative monitor. Positron emission tomography¹⁶⁵ and nuclear magnetic resonance¹⁶⁶ are imaging techniques that can assess lung water. However, they are not amenable for routine clinical use in the perioperative setting. Lung ultrasonography is garnering greater acceptance as another method for assessing lung edema.

Indicator Dilution Methods

Such measurements of EVLW have been expected to be superior to blood oxygenation and chest radiography. They are based on the kinetics of one or two tracers injected centrally and measured in an artery. Initial techniques were based on a double-indicator dilution method. These techniques gained renewed attention with the introduction of a clinical device to assess EVLW using the transpulmonary thermodilution technology, which facilitated bedside measurements.⁴¹⁰ The device uses cold saline as the single indicator injected in a central venous line. EVLW and additional hemodynamic parameters (i.e., cardiac output) are computed from the curve of temperature in the peripheral artery.⁴¹¹ Good reproducibility and correlation can occur with gravimetric methods and can be a useful clinical and research tool. EVLW may be a predictor of mortality in patients with severe sepsis⁴¹² and ARDS.^{413,414} It is a diagnostic tool in detecting early pulmonary edema,^{415,416} including reperfusion edema after pulmonary endarterectomy,⁴¹⁷ after lung transplantation,⁴¹⁸ and in evaluating the effect of ventilatory modes during esophagectomy.⁴¹⁹ The measurement has also been proposed to guide fluid therapy in ARDS⁴²⁰ and subarachnoid hemorrhage,⁴²¹ as well as assess the effect of steroids during cardiac surgery.⁴²² EVLW was the primary outcome variable in clinical trials to study the efficacy of salbutamol to resolve pulmonary edema in patients with ARDS (the Beta-Agonist Lung Injury Trial)⁴²³ and lung resection.⁴²⁴

The limitations on this technique derive from the considerable and at times conflicting assumptions.^{411,425} Measurement premises include that the thermal indicator reaches all lung regions and equilibrates in all of them and that the central circulation volumes between the injection and temperature measurement sites can be described as a small number of individual well-mixed compartments, each showing a monoexponential decay of temperature with time. Experimental evidence indicated that assumptions for

the method do not apply to all conditions; an important factor is the changes in the regional distribution of perfusion during lung injury.^{411,426,427} These changes may compromise the measurement.⁴²⁵ Indeed, redistribution of lung perfusion can produce measurement changes larger than those seen in the Beta-Agonist Lung Injury Trial between treatment and control groups.^{423,426} Such results are also consistent with the influence of the type of lung injury on the accuracy of EVLW measurements,⁴²⁸⁻⁴³⁰ as well as with the poor correlation between transpulmonary thermodilution EVLW and computed tomographic estimates of EVLW.^{431,432} Thus the expected reliability of transpulmonary thermodilution EVLW to follow trends⁴³³ cannot be taken for granted, and it requires interpretation in light of potential simultaneous changes in regional perfusion. Finally, the technique requires placement of arterial and central venous catheters, thereby increasing invasiveness.

 Complete references available online at expertconsult.com.

References

1. American Society of Anesthesiologists. *Standards for Basic Anesthetic Monitoring*; 2011.
2. International Task Force on Anaesthesia Safety. *World Federation of Societies of Anaesthesiologists: International Standards for a Safe Practice of Anaesthesia*; 2010.
3. Eichhorn JH, et al. *JAMA*. 1986;256:1017.
4. Botham KM, Mayes PA. Biologic oxidation. Harper's illustrated biochemistry. In: Murray RK, Rodwell VW, Bender D, Botham KM, Weil PA, Kennelly PJ, eds. *eBook Collection (EBSCOhost)*. 28th ed. McGraw-Hill Medical; 2009:98.
5. Severinghaus JW. *J Clin Monit Comput*. 2011;25:155.
6. Severinghaus JW. *Anesthesiology*. 2009;110:721.
7. Campbell S, et al. *Paediatr Anaesth*. 2011;21:815.
8. Kenzaka T, et al. *Intern Med*. 2012;51:871.
9. Welsby PD, Earis JE. *Postgrad Med J*. 2001;77:617.
10. Epstein O, et al. The respiratory system, Clinical examination. In: *Anonymous*. 4th ed. Elsevier Health Sciences; 2008.
11. Thomas C, Lumb AB. *Contin Educ Educ Anaesth Crit Care Pain*. 2012;12:251.
12. Severinghaus JW. *Adv Exp Med Biol*. 1994;345:921.
13. Tremper KK, Barker SJ. *Anesthesiology*. 1989;70:98.
14. Severinghaus JW, Honda Y. *Int Anesthesiol Clin*. 1987;25:205.
- 14a. Pulse Oximeters <https://www.fda.gov/RegulatoryInformation/Guidances/ucm341718.htm>.
15. Milner QJ, Mathews GR. *Anaesthesia*. 2012;67:396.
16. Pologe JA. *Int Anesthesiol Clin*. 1987;25:137.
17. Merry AF, et al. *Can J Anaesth*. 2010;57:1027.
18. Haynes AB, et al. *N Engl J Med*. 2009;360:491.
19. Macknet MR, et al. *Anesth Analg*. 2010;111:1424.
20. Barker SJ, et al. *Anesthesiology*. 2006;105:892.
21. Roth D, et al. *Ann Emerg Med*. 2011;58:74.
22. Lamhaut L, et al. *Anesthesiology*. 2011;115:548.
23. Frasca D, et al. *Crit Care Med*. 2011;39:2277.
24. Berkow L, et al. *Anesth Analg*. 2011;113:1396.
25. Morey TE, et al. *Anesth Analg*. 2011;113:1289.
26. Shamir MY, et al. *Anesth Analg*. 2012;114:972.
27. Maisel WH, Lewis RJ. *Ann Emerg Med*. 2010;56:389.
28. Caboot JB, et al. *Pediatr Pulmonol*. 2012;47:808.
29. Feiner JR, et al. *Anesth Analg*. 2013;117:847.
30. Feiner JR, Bickler PE. *Anesth Analg*. 2010;111:1160.
31. Mahle WT, et al. *Circulation*. 2009;120:447.
32. Mahle WT, et al. *Pediatrics*. 2012;129:190.
33. Ewer AK, et al. *Lancet*. 2011;378:785.
34. Thangaratinam S, et al. *Lancet*. 2012;379:2459.
35. Dorlas JC, Nijboer JA. *Br J Anaesth*. 1985;57:524.
36. Cannesson M, et al. *Anesthesiology*. 2007;106:1105.
37. Cannesson M, et al. *Anesth Analg*. 2008;106:1189.
38. Cannesson M, et al. *Anesth Analg*. 2008;106:1195.
39. Yin JY, Ho KM. *Anaesthesia*. 2012;67:777.

40. Wu CY, et al. *Eur J Anaesthesiol*. 2016;33:645.
41. Sandroni C, et al. *Intensive Care Med*. 2012;38:1429.
42. Forget P, et al. *Anesth Analg*. 2010;111:910.
43. Gothgen IH, et al. *Scand J Clin Lab Invest Suppl*. 1990;203:87.
44. Perkins GD, et al. *Crit Care*. 2003;7:R67.
45. Van de Louw A, et al. *Intensive Care Med*. 2001;27:1606.
- 45a. Pedersen T, et al. *Cochrane Database Syst Rev*. 2014;(3):CD002013.
- 45b. Moller JT, et al. *Anesthesiology*. 1993;78(3):445.
- 45c. Ochroch EA, et al. *Anesth Analg*. 2006;102(3):868.
46. Mannheimer PD. *Anesth Analg*. 2007;105:S10.
47. Feiner JR, et al. *Anesth Analg*. 2007;105:S18.
48. Cox P. *Anesthesiology*. 2007;107:A1540.
49. Hinkelbein J, et al. *Resuscitation*. 2005;64:315.
50. Barker SJ. *Anesth Analg*. 2002;95:967.
51. Shah N, et al. *J Clin Anesth*. 2012;24:385.
52. Chan ED, et al. *Respir Med*. 2013;107:789.
53. Hampson NB. *Chest*. 1998;114:1036.
54. Eisenkraft JB. *Anesthesiology*. 1988;68:279.
55. Jay GD, et al. *Ann Emerg Med*. 1994;24:32.
56. Severinghaus JW, Koh SO. *J Clin Monit*. 1990;6:85.
57. Ortiz FO, et al. *Am J Respir Crit Care Med*. 1999;159:447.
58. Rajadurai VS, et al. *J Paediatr Child Health*. 1992;28:43.
59. Ahmed S, et al. *Eur J Haematol*. 2005;30:974.
60. Comber JT, Lopez BL. *Am J Emerg Med*. 1996;14:16.
61. Verhovsek M, et al. *Am J Hematol*. 2010;85:882.
62. Scheller MS, et al. *Anesthesiology*. 1986;65:550.
63. Hinkelbein J, et al. *Resuscitation*. 2007;72:82.
64. Hinkelbein J, et al. *Resuscitation*. 2007;74:75.
65. Adler JN, et al. *Acad Emerg Med*. 1998;5:965.
66. Bickler PE, et al. *Anesthesiology*. 2005;102:715.
67. Amar D, et al. *J Clin Monit*. 1989;5:135.
68. Trivedi NS, et al. *J Clin Anesth*. 1997;9:179.
69. Fluck RR Jr, et al. *Respir Care*. 2003;48:677.
70. van Oostrom JH, et al. *Can J Anaesth*. 2005;52:379.
71. Mathes AM, et al. *Anesth Analg*. 2008;107:541.
72. Kelleher JF, Ruff RH. *Anesthesiology*. 1989;71:787.
73. Zoremba N, et al. *Acta Anaesthesiol Scand*. 2011;55:322.
74. Oleyar M, et al. *J Cardiothorac Vasc Anesth*. 2010;24:820.
75. Mabadeje O, et al. *J Hosp Infect*. 2010;76:93.
76. Evans ML, Geddes LA. *Med Instrum*. 1988;22:29.
77. Sinex JE. *Am J Emerg Med*. 1999;17:59.
78. Berkenbosch JW, Tobias JD. *Respir Care*. 2006;51:726.
79. MacLeod DB, et al. *Anesthesia*. 2005;60:65.
80. Kulcke A, et al. *Anesth Analg*. 2016;122:1856.
81. Smit M, et al. *J Cardiothorac Vasc Anesth*. 2016;30:379.
82. Jenstrup M, et al. *Acta Anaesthesiol Scand Suppl*. 1995;107:29.
83. Harms MP, et al. *Exp Physiol*. 2003;88:611.
84. Ho KM, et al. *Shock*. 2008;29:3.
85. Dahn MS, et al. *Intensive Care Med*. 1988;14:373.
86. Martin C, et al. *Intensive Care Med*. 1992;18:101.
87. Varpula M, et al. *Intensive Care Med*. 2006;32:1336.
88. Ho KM, et al. *J Cardiothorac Vasc Anesth*. 2010;24:434.
89. Reinhart K, et al. *Chest*. 1989;95:1216.
90. Chawla LS, et al. *Chest*. 2004;126:1891.
91. Dueck MH, et al. *Anesthesiology*. 2005;103:249.
92. Lorentzen AG, et al. *J Cardiothorac Vasc Anesth*. 2008;22:853.
93. Grissom CK, et al. *Crit Care Med*. 2009;37:2720.
94. Kopterides P, et al. *Shock*. 2009;31:561.
95. Dahmani S, et al. *Eur J Anaesthesiol*. 2010;27:714.
96. Lequeux PY, et al. *Eur J Anaesthesiol*. 2010;27:295.
97. Lamia B, et al. *Minerva Anestesiol*. 2006;72:597.
98. Suter PM, et al. *Crit Care Med*. 1975;3:175.
99. Pond CG, et al. *J Cardiothorac Vasc Anesth*. 1992;6:280.
100. Maddirala S, Khan A. *Crit Care Clin*. 2010;26:323.
101. Scuderi PE, et al. *Anesthesiology*. 1994;81:245.
102. Baulig W, et al. *J Clin Monit Comput*. 2008;22:183.
103. Baulig W, et al. *Eur J Anaesthesiol*. 2010;27:720.
104. Schmidt CR, et al. *Crit Care Med*. 1984;12:523.
105. Routsi C, et al. *Anesth Analg*. 1993;77:1104.
106. Polonen P, et al. *Acta Anaesthesiol Scand*. 1997;41:810.
107. Pearse R, et al. *Crit Care*. 2005;9:R694.
108. Collaborative Study Group on Perioperative Scvo2 Monitoring. *Crit Care*. 2006;10:R158.
109. Polonen P, et al. *Anesth Analg*. 2000;90:1052.
110. Rivers E, et al. *N Engl J Med*. 2001;345:1368.
111. Donati A, et al. *Chest*. 2007;132:1817.
112. Dellinger RP, et al. *Crit Care Med*. 2008;36:296.
113. Otero RM, et al. *Chest*. 2006;130:1579.
114. Bellomo R, et al. *Crit Care*. 2008;12:130.
115. Peake SL, et al. *Resuscitation*. 2009;80:811.
116. Jones AE, et al. *JAMA*. 2010;303:739.
117. Suehiro K, et al. *J Cardiothorac Vasc Anesth*. 2014;28:528.
118. Bickler P, et al. *Anesth Analg*. 2017;124:72.
119. Ubbink R, et al. *J Clin Monit Comput*. 2017;31:1143.
120. Wahr JA, et al. *J Cardiothorac Vasc Anesth*. 1996;10:406.
121. Cui W, et al. *Opt Lett*. 1991;16:1632.
122. Schober P, Schwarze LA. *J Clin Monit Comput*. 2012;26:255.
123. Jobsis FF. *Science*. 1977;198:1264.
124. Watzman HM, et al. *Anesthesiology*. 2000;93:947.
125. Sakr Y, et al. *Eur J Anaesthesiol*. 2010;27:388.
126. Holzle F, et al. *Int J Oral Maxillofac Surg*. 2010;39:21.
127. Karliczek A, et al. *Colorectal Dis*. 2010;12:1018.
128. Pham TH, et al. *Ann Thorac Surg*. 2011;91:380.
129. Friedland S, et al. *Gastrointest Endosc*. 2003;57:492.
130. Friedland S, et al. *Gastrointest Endosc*. 2007;65:294.
131. Bludau M, et al. *Ann Thorac Surg*. 2010;90:1121.
132. Highton D, et al. *Curr Opin Anaesthesiol*. 2010;23:576.
133. Chan MJ, et al. *J Cardiothorac Vasc Anesth*. 2017;31:1155.
134. Murkin JM, et al. *Anesth Analg*. 2007;104:51.
135. Slater JP, et al. *Ann Thorac Surg*. 2009;87:36. discussion 44.
136. Yao FS, et al. *J Cardiothorac Vasc Anesth*. 2004;18:552.
137. Fischer GW, et al. *J Thorac Cardiovasc Surg*. 2011;141:815.
138. de Tournay-Jette E, et al. *J Cardiothorac Vasc Anesth*. 2011;25:95.
139. Ghosal S, et al. *J Cardiothorac Vasc Anesth*. 2018;32:1185.
140. Kirkpatrick PJ, et al. *J Neurosurg*. 1998;89:389.
141. Grubhofer G, et al. *Anesth Analg*. 2000;91:1339.
142. Vets P, et al. *Acta Anaesthesiol Belg*. 2004;55:215.
143. Al-Rawi PG, Kirkpatrick PJ. *Stroke*. 2006;37:2720.
144. Moritz S, et al. *Anesthesiology*. 2007;107:563.
145. de Letter JA, et al. *Neurol Res*. 1998;20(suppl 1):S23.
146. Hirofumi O, et al. *J Clin Neurosci*. 2003;10:79.
147. Rigamonti A, et al. *J Clin Anesth*. 2005;17:426.
148. Yamamoto K, et al. *Int Angiol*. 2007;26:262.
149. Jonsson M, et al. *Eur J Vasc Endovasc Surg*. 2017;53:783.
150. Samra SK, et al. *Anesthesiology*. 2000;93:964.
151. Mille T, et al. *Eur J Vasc Endovasc Surg*. 2004;27:646.
152. Boezeman RP, et al. *Ann Thorac Surg*. 2015;99:1267.
153. Casati A, et al. *Anesth Analg*. 2005;101:740.
154. Tang L, et al. *Br J Anaesth*. 2012;108:623.
155. Murphy GS, et al. *Anesth Analg*. 2010;111:496.
156. Moerman AT, et al. *Eur J Anaesthesiol*. 2012;29:82.
157. Tange K, et al. *Minerva Anestesiol*. 2010;76:485.
158. Crookes BA, et al. *J Trauma*. 2005;58:806. discussion 813.
159. Cohn SM, et al. *J Trauma*. 2007;62:44. discussion 54.
160. Ikossi DG, et al. *J Trauma*. 2006;61:780. discussion 788.
161. Yu Y, et al. *Cochrane Database Syst Rev*. 2018;1:CD010947.
162. Sun X, et al. *Br J Anaesth*. 2015;114:276.
163. Bohr C. *Skandinavisches Archiv Für Physiologie*. 1891;2:236.
164. Mogue LR, Rantala B. *J Clin Monit*. 1988;4:115.
165. Bhavani-Shankar K, et al. *J Clin Monit*. 1995;11:175.
166. Gravenstein JS, et al. *Capnography in Clinical Practice*. Boston: Butterworth; 1989.
167. Gravenstein JS, et al. *Gas Monitoring in Clinical Practice*. Boston: Butterworth-Heinemann; 1995.
168. Jaffe MB. *Anesth Analg*. 2008;107:890.
169. Raemer DB, Calalang I. *J Clin Monit*. 1991;7:195.
170. Hess D. *Respir Care*. 1990;35:557.
171. Brunner JX, Westenskow DR. *Br J Anaesth*. 1988;61:628.
172. Jaffe MB. *Mainstream or Sidestream Capnography? Technical Considerations*. Wallingford, Conn: Respiromics Novametric; 2002.
173. Kaczka DW, et al. *J Appl Physiol*. 2011;110:1473.
174. Bhavani-Shankar K, Philip JH. *Anesth Analg*. 2000;91:973.
175. Moon RE, Camporesi EM. Respiratory monitoring. In: Miller RD, ed. *Miller's Anesthesia*. 6th ed. New York: Churchill Livingstone; 2005:1255–1295.
- 175a. Mondoñedo JR, et al. *ASME J of Medical Diagnostics*. 2018;1(031003):031003–031010.
176. Fletcher R, et al. *Br J Anaesth*. 1981;53:77.
177. McKenzie DC. *Br J Sports Med*. 2012;46:381.
178. Grocott MP, et al. *N Engl J Med*. 2009;360:140.

179. Wagner PD, et al. *J Clin Invest*. 1974;54:54.
180. Ravin MB, et al. *J Appl Physiol*. 1965;20:1148.
181. Brismar B, et al. *Anesthesiology*. 1985;62:422.
182. Rothen HU, et al. *Br J Anaesth*. 1998;81:681.
183. Riley RL, Cournand A. *J Appl Physiol*. 1949;1:825.
184. Whiteley JP, et al. *Br J Anaesth*. 2002;88:771.
185. Gould MK, et al. *Crit Care Med*. 1997;25:6.
186. McCahon RA, et al. *Br J Anaesth*. 2008;101:358.
187. Kathirgamanathan A, et al. *Br J Anaesth*. 2009;103:291.
188. Lilenthal JL Jr, Riley RL. *Am J Physiol*. 1946;147:199.
189. Mellegaard K. *Acta Physiol Scand*. 1966;67:10.
190. Gowda MS, Klocke RA. *Crit Care Med*. 1997;25:41.
191. Definition Task Force ARDS, Ranieri VM, et al. *JAMA*. 2012;307:2526.
192. Rice TW, et al. *Chest*. 2007;132:410.
193. Khemani RG, et al. *Crit Care Med*. 2012;40:1309.
194. DesPrez K, et al. *Chest*. 2017;152:1151–1158.
195. Villar J, et al. *BMJ Open*. 2015;5. e006812.2014-006812.
196. Balzer F, et al. *BMC Anesthesiol*. 2016;16:108. 016-0272-4.
197. Ortiz RM, et al. *Pediatr Clin North Am*. 1987;34:39–46.
198. Trachsel D, et al. *Am J Respir Crit Care Med*. 2005;172:206–211.
199. Gajic O, et al. *Crit Care*. 2007;11:R53.
200. Kaczka DW, et al. *Anesthesiology*. 2015;123:1394.
201. Christiansen J, et al. *J Physiol*. 1914;48:244.
202. Severinghaus JW, Astrup PB. *J Clin Monit*. 1986;2:125.
203. Severinghaus JW. *Anesthesiology*. 2002;97:253.
204. Andritsch RF, et al. *Anesthesiology*. 1981;55:311.
205. Kern FH, Greeley WJ. *J Cardiothorac Vasc Anesth*. 1995;9:215.
206. Burrows FA. *J Cardiothorac Vasc Anesth*. 1995;9:219.
207. Patel RL, et al. *J Thorac Cardiovasc Surg*. 1996;111:1267.
208. Engelhardt W, et al. *Acta Anaesthesiol Scand*. 1996;40:457.
209. du Plessis AJ, et al. *J Thorac Cardiovasc Surg*. 1997;114:991. discussion 1000.
210. Bellinger DC, et al. *J Thorac Cardiovasc Surg*. 2001;121:374.
211. Kiziltan HT, et al. *Anesth Analg*. 2003;96:644.
212. Piccioni MA, et al. *Artif Organs*. 2004;28:347.
213. Sakamoto T, et al. *J Thorac Cardiovasc Surg*. 2004;127:12.
214. Hoover LR, et al. *Anesth Analg*. 2009;108:1389.
215. Nagy ZL, et al. *Circulation*. 2003;108:577.
216. Murkin JM, et al. *J Thorac Cardiovasc Surg*. 1995;110:349.
217. Svyatets M, et al. *J Cardiothorac Vasc Anesth*. 2010;24:644.
218. Biswas CK, et al. *Br Med J (Clin Res Ed)*. 1982;284:923.
219. Kaczka DW, et al. Computational analyses of airway flow and lung tissue dynamics, image-based computational modeling of the human circulatory and pulmonary systems: methods and applications. In: Chandran KB, Udaykumar HS, Reinhardt JM, eds. *Image-based computational modeling of the human circulatory and pulmonary systems: Methods and applications*. 1st ed. New York: Springer; 2011;375,402; 10.
220. Kaczka DW, Smallwood JL. *Respir Physiol Neurobiol*. 2012;183:75.
221. Warner DO. *J Clin Monit Comput*. 2000;16:417.
222. Bates JHT. *Lung Mechanics: An Inverse Modeling Approach*. Cambridge: Cambridge University Press; 2009:220.
223. Pedley TJ, et al. *Respir Physiol*. 1970;9:387.
224. Rohrer F. *Pfluegers Arch Gesamte Physiol Menschen Tiere*. 1915;162:225.
225. Mora R, et al. *Am J Physiol Lung Cell Mol Physiol*. 2000;279:L342.
226. Fredberg JJ, Stamenovic D. *J Appl Physiol*. 1989;67:2408.
227. Fredberg JJ, et al. *Am J Respir Crit Care Med*. 1997;156:1752.
228. McIlroy MB, et al. *J Appl Physiol*. 1955;7:485.
229. Bachofen H. *J Appl Physiol*. 1968;24:296.
230. Hantos Z, et al. *J Appl Physiol*. 1992;72:168.
231. Kaczka DW, et al. *J Appl Physiol*. 1997;82:1531.
232. Hoppin FG Jr, Hildebrandt J. Mechanical properties of the lung. In: West JB, ed. *Bioengineering Aspects of the Lung*. New York: Marcel Dekker; 1977;83–162.
- 232a. Kano S, et al. *J Appl Physiol* (1985). 1994;77:1185.
- 232b. Amini R, et al. *IEEE Trans Biomed Eng*. 2017;64:681.
- 232c. Carvalho AR, et al. *Intensive Care Med*. 2008;34:2291.
- 232d. Carvalho AR, et al. *Anesth Analg*. 2013;116:677.
- 232e. D'Antini D, et al. *Anesth Analg*. 2018;126:143.
- 232f. Ranieri VM, et al. *Anesthesiology*. 2000;93:1320.
- 232g. Motulsky H, Christopoulos A. *Fitting Models to Biological Data using Linear and Nonlinear Regression. A Practical Guide to Curve Fitting*. New York: Oxford University Press; 2004:351.
- 232h. Huhle R, et al. *Anesth Analg*. 2018;126:725.
- 232i. Formenti P, et al. *Intensive Care Med*. 2011;37:561.
- 232j. Chiumello D, Gattinoni L. *Intensive Care Med*. 2011;37:561.
- 232k. Henzler D, et al. *Anesth Analg*. 2007;105(1072). table of contents.
233. Otis AB, et al. *J Appl Physiol*. 1956;8:427.
- 233a. Kaczka DW, et al. *Ann Biomed Eng*. 2011;39:1112.
- 233b. Suki B, Bates JHT. *J Appl Physiol* (1985). 2011;110:1111.
- 233c. Carvalho AR. *Crit Care*. 2007;11:R86.
- 233d. Dellacà RL. *Intensive Care Medicine*. 2011;37:1021.
- 233e. Zannin E, et al. *Crit Care*. 2012;16:R217.
- 233f. Writing Group for the Alveolar Recruitment for Acute Respiratory Distress Syndrome, Trial I, Cavalcanti AB, et al. *JAMA*. 2017;318:1335.
- 233g. Fumagalli J, et al. *Crit Care Med*. 2017;45(8):1374.
234. Mead J. *J Appl Physiol*. 1956;9:208.
235. Hager DN, et al. *Crit Care Med*. 2007;35:1522.
- 235a. Kaczka DW, et al. *Anesthesiology*. 2015;123:1394.
- 235b. Amini R, Kaczka DW. *Ann Biomed Eng*. 2013;41:2699.
236. Kaczka DW, et al. *Ann Biomed Eng*. 1995;23:135.
237. Peslin R, et al. *Eur Respir J*. 1992;5:871.
238. Ruiz-Ferron F, et al. *Intensive Care Med*. 2001;27:1487.
239. Kaczka DW, et al. *J Appl Physiol*. 2001;90:1833.
240. Kaczka DW, et al. *Ann Biomed Eng*. 2011;39:1112.
241. Downie JM, et al. *Am J Respir Crit Care Med*. 2004;169:957.
242. Lu Q, Rouby JJ. *Critical Care*. 2000;4:91.
243. Salazar E, Knowles JH. *J Appl Physiol*. 1964;19:97.
244. Venegas JG, et al. *J Appl Physiol*. 1998;84:389.
245. Mead J, et al. *J Appl Physiol*. 1957;10:191.
246. Bates JH, Irvin CG. *J Appl Physiol*. 2002;93:705.
247. Hildebrandt J. *J Appl Physiol*. 1970;28:365.
248. Otis AB, et al. *J Appl Physiol*. 1950;2:592.
249. Bates JHT, Milic-Emili J. *Ann Biomed Eng*. 1993;21:489.
- 249a. Moraes L, et al. *Front Physiol*. 2018;9:318.
- 249b. Cressoni M, et al. *Anesthesiology*. 2016;124:1100.
- 249c. Gattinoni L, et al. *Intensive Care Med*. 2016;42:1567.
- 249d. Santos RS, et al. *Anesthesiology*. 2018;128:1193.
250. Masselli GM, et al. *Conf Proc IEEE Eng Med Biol Soc*. 2006;1:5603.
251. Jensen A, Lutchen KR, Kaczka DW, et al. Estimation of respiratory dynamic mechanical properties during clinically used mechanical ventilation. In: *Proceedings of the first joint BMES/EMBS Conference*. Vol 1. Atlanta: IEEE; 1999;337.
252. Lancaster CT, Boyle PM, Kaczka DW. Delivered tidal volume from the Fabius GS depends upon breathing circuit configuration despite compliance compensation. In: *Proceedings of the American Society of Anesthesiologists 2005 Annual Meeting*. Atlanta, 2005, abstract A863.
253. Loring SH, et al. *J Appl Physiol*. 2010;108:512.
- 253a. Akoumianaki E, et al. *Am J Respir Crit Care Med*. 2014;189:520.
254. Schuessler TF, et al. *Ann Biomed Eng*. 1998;26:260.
255. Hager DN, Brower RG. *Crit Care Med*. 2006;34:1544.
256. Talmor D, et al. *N Engl J Med*. 2008;359:2095.
- 256a. Eichler L, et al. *Obes Surg*. 2018;28:122.
257. Schultz MJ, et al. *Anesthesiology*. 2007;106:1226.
- 257a. Mauri T, et al. *Intensive Care Med*. 2016;42:1360.
- 257b. Yoshida T, et al. *Am J Respir Crit Care Med*. 2018;197(1018).
- 257c. Amato MB, et al. *N Engl J Med*. 2015;372:747.
- 257d. Bugeo G, et al. *Crit Care*. 2017;21:199.
258. Ladha K, et al. *BMJ*. 2015;351:h3646.
259. Neto AS, et al. *Lancet Respir Med*. 2016;4:272.
260. Laghi F, Goyal A. *Minerva Anestesiol*. 2012;78:201.
261. Brochard L. *Intensive Care Med*. 2002;28:1552.
262. McCall CB, et al. *J Appl Physiol*. 1957;10:215.
263. Lutchen KR, et al. *J Appl Physiol*. 1993;75:2549.
264. Jackson AC, Vinegar A. *J Appl Physiol*. 1979;47:462.
265. Schuessler TF, Bates JHT. *IEEE Trans Biomed Eng*. 1995;42:860.
266. Schuessler TF, Bates JHT, Maksym GN. Estimating tracheal flow in small animals: Engineering in Medicine and Biology Society, 1993. In: *Proceedings of the 15th Annual International Conference of the IEEE*. 1993;560–561.
267. Simon BA, Mitzner W. *IEEE Trans Biomed Eng*. 1991;38:214.
268. Sullivan WJ, et al. *Respir Care*. 1984;29:736.
269. Yeh MP, et al. *J Appl Physiol*. 1982;53:280.
270. Renzi PE, et al. *J Appl Physiol*. 1990;68:382.
271. Jaffe MB. *IEEE Eng Med Biol Mag*. 2010;29:44.
272. Plakk P, et al. *Med Biol Eng Comput*. 1998;36(17).

273. Ligeza P. *Rev Sci Instrum*. 2008;79(096105).
274. Al-Salaymeh A, et al. *Med Eng Phys*. 2004;26:623.
275. Ligeza P. *Rev Sci Instrum*. 2007;78(075104).
276. Hager DN, et al. *Crit Care Med*. 2006;34:751.
- 276a. Mondonedo JR, et al. *J Clin Monit Comput*. 2017;31:1263.
- 276b. Farre R, et al. *Medical & Biological Engineering & Computing*. 1991;29:18.
- 276c. Jandre FC, et al. *Respir Physiol Neurobiol*. 2005;148:309–314.
277. Schmolzer GM, et al. *Arch Dis Child Fetal Neonatal Ed*. 2010;95: F295.
278. Wolf GK, Arnold JH. *Crit Care Med*. 2005;33:S163.
279. Stick SM, et al. *Pediatr Pulmonol*. 1992;14:187.
280. van Vonderen JJ, et al. *Arch Dis Child Fetal Neonatal Ed*. 2015; 100:F514.
281. Khemani RG, et al. *Am J Respir Crit Care Med*. 2016;193:198.
282. Atkins JH, et al. *Anesth Analg*. 2010;111:1168.
283. Greenstein YY, et al. *J Bronchology Interv Pulmonol*. 2017;24:206.
284. Mandel JE, Atkins JH. *Anesth Analg*. 2016;122:126.
285. Overdyk FJ, et al. *Anesth Analg*. 2007;105:412.
286. Walther-Larsen S, Rasmussen LS. *Acta Anaesthesiol Scand*. 2006;50:888.
287. Folke M, et al. *Med Biol Eng Comput*. 2003;41:377.
288. Al-Khalidi FQ, et al. *Pediatr Pulmonol*. 2011;46:523.
289. Wiklund L, et al. *J Clin Anesth*. 1994;6:182.
290. Lam T, et al. *Anesth Analg*. 2017;125:2019.
- 290a. Meade MO, et al. *Am J Respir Crit Care Med*. 2017;196:727.
291. Gaucher A, et al. *Br J Anaesth*. 2012;108:316.
292. Kasuya Y, et al. *Anesthesiology*. 2009;111:609.
293. Chang KC, et al. *J Clin Monit Comput*. 2016;30:169.
294. Cashman JN, Dolin SJ. *Br J Anaesth*. 2004;93(212).
295. Walder B, et al. *Acta Anaesthesiol Scand*. 2001;45:795.
296. Shapiro A, et al. *J Clin Anesth*. 2005;17:537.
297. Nassi N, et al. *Arch Dis Child*. 2008;93:126.
298. Lightdale JR, et al. *Pediatrics*. 2006;117:e1170.
299. Waisman D, et al. *Intensive Care Med*. 2011;37:1174.
300. Curry J, Lynn L. *APSF Newsletter*. 2011;26:32.
301. Gupta R, Edwards D. *APSF Newsletter*. 2018;32:70–72.
302. Gupta K, et al. *Curr Opin Anaesthesiol*. 2018;31:110.
303. Simon BA, et al. *J Appl Physiol*. 2012;113:647.
304. Harris RS, Schuster DP. *J Appl Physiol*. 2007;102:448.
305. Bodenstein M, et al. *Crit Care Med*. 2009;37:713.
306. Turner JP, Dankoff J. *Emerg Med Clin North Am*. 2012;30:451.
307. Volpicelli G, et al. *Intensive Care Med*. 2012;38:577.
308. Kruisselbrink R, et al. *Anesthesiology*. 2017;127:568.
309. Lichtenstein DA. *Chest*. 2015;147:1659.
310. Lichtenstein DA, et al. *Intensive Care Med*. 2004;30:276.
311. Lichtenstein D, et al. *Anesthesiology*. 2004;100:9.
312. Lichtenstein DA. *Crit Care Med*. 2007;35:S250.
313. Lichtenstein D. *Minerva Anestesiol*. 2009;75:313.
314. Lichtenstein D, et al. *Intensive Care Med*. 2000;26:1434.
315. Lichtenstein DA, Meziere GA. *Chest*. 2008;134:117.
316. Adler A, et al. *Physiol Meas*. 2012;33:679.
317. Costa EL, et al. *Curr Opin Crit Care*. 2009;15:18.
318. Hahn G, et al. *Physiol Meas*. 2006;27:S187.
319. Frerichs I, et al. *Thorax*. 2017;72:83.
320. Humphreys S, et al. *Paediatr Anaesth*. 2011;21:887.
321. Victorino JA, et al. *Am J Respir Crit Care Med*. 2004;169:791.
322. Radke OC, et al. *Anesthesiology*. 2012;116:1227.
323. Frerichs I, et al. *J Crit Care*. 2012;27:172.
324. Karsten J, et al. *Acta Anaesthesiol Scand*. 2011;55:878.
325. Costa EL, et al. *Intensive Care Med*. 2009;35:1132.
326. Nestler C, et al. *Br J Anaesth*. 2017;119:1194.
327. Costa EL, et al. *Crit Care Med*. 2008;36:1230.
328. Borges JB, et al. *J Appl Physiol*. 2012;112:225.
329. Kok J, et al. *Pathology*. 2015;47:405.
330. Leino A, Kurvinen K. *Clin Chem Lab Med*. 2011;49:1187.
331. Luukkonen AA, et al. *Clin Chem Lab Med*. 2016;54:585.
332. Hopfer SM, et al. *Ann Clin Lab Sci*. 2004;34:75.
333. Gayat E, et al. *Anesth Analg*. 2017;124:1820.
334. Allardet-Servent J, et al. *PLoS One*. 2017;12:e0169593.
335. Van de Louw A, et al. *Intensive Care Med*. 2007;33:355.
336. Seguin P, et al. *J Crit Care*. 2011;26:423.
337. Wax DB, Reich DL. *Anesth Analg*. 2007;105:1711.
338. Chang HK. *J Appl Physiol*. 1984;56:553.
339. Pillow JJ. *Crit Care Med*. 2005;33:S135.
340. Fredberg JJ. *J Appl Physiol*. 1980;49:232.
341. Hurst JM, et al. *Ann Surg*. 1990;211:486.
342. Venegas JG, et al. *J Appl Physiol*. 1986;60:1025.
- 343a. Herrmann J, et al. *J Appl Physiol* (1985). 2016;121:1306.
343. Pillow JJ. *Eur Respir J*. 2012;40:291.
344. Courtney SE, et al. *N Engl J Med*. 2002;347:643.
345. Johnson AH, et al. *N Engl J Med*. 2002;347:633.
- 345a. Ferguson ND, et al. *N Engl J Med*. 2013;368:795.
- 345b. Young D, et al. *N Engl J Med*. 2013;368:806.
346. Fessler HE, Brower RG. *Crit Care Med*. 2005;33:S223.
347. Fessler HE, et al. *Crit Care Med*. 2007;35:1649.
348. Krishman JA, Brower RG. *Chest*. 2000;118:795.
349. Ali S, Ferguson ND. *Crit Care Clin*. 2011;27:487.
350. Ip T, Mehta S. *Curr Opin Crit Care*. 2012;18:70.
351. Custer JW, et al. *Pediatr Crit Care Med*. 2011;12:e176.
352. Pillow JJ, et al. *Am J Respir Crit Care Med*. 2001;164:1019.
353. Kaczka DW, Lutchen KR. *Ann Biomed Eng*. 2004;32:596.
354. Biro P. *Anesth Clin*. 2010;28:397.
355. Hess DR, et al. *Respir Care Clin North Am*. 2001;7:577.
356. Kalenga M, et al. *J Appl Physiol*. 1998;84:1174.
357. Pillow JJ, et al. *Pediatr Crit Care Med*. 2004;5:172.
358. Pillow JJ, et al. *Pediatr Res*. 2002;52:538.
- 358a. Harcourt ER, et al. *Pediatr Crit Care Med*. 2014.
- 358b. Tingay DG, et al. *Neonatology*. 2015;108:220.
359. Hager DN. *Curr Opin Anaesthesiol*. 2012;25:17.
360. Lucangelo U, et al. Capnography and adjuncts of mechanical ventilation. In: Gravenstein JS, et al., ed. *Capnography*. 2nd ed. Cambridge: Cambridge University Press; 2011:169–181.
361. Kil HK, et al. *Yonsei Med J*. 2002;43:20.
362. Kugelman A, et al. *Pediatr Pulmonol*. 2012;47:876.
363. Frietsch T, et al. *Acta Anaesthesiol Scand*. 2000;44:391.
364. Nishimura M, et al. *Chest*. 1992;101:1681.
365. Biro P, et al. *Anesth Analg*. 1998;87:180.
- 365a. Herrmann J, et al. *J Appl Physiol* (1985). 2018;124:653.
- 365b. Mehta PP, et al. *Am J Gastroenterol*. 2016;111:395.
366. Evans KL, et al. *J Laryngol Otol*. 1994;108:23.
367. Miodownik S, et al. *Crit Care Med*. 1984;12:718.
368. Algorta-Weber A, et al. *Crit Care Med*. 1986;14:895.
369. Sehati S, et al. *Br J Anaesth*. 1989;63:47S.
370. Simon M, et al. *Acta Anaesthesiol Scand*. 2003;47:861.
371. Wallen E, et al. *Crit Care Med*. 1995;23:1588.
372. Waydhas C, et al. *Intensive Care Med*. 1995;21:784.
373. Bercault N, et al. *Crit Care Med*. 2005;33:2471.
374. Nakamura T, et al. *Chest*. 2003;123:159.
375. Kue R, et al. *Am J Crit Care*. 2011;20:153.
376. Prodhan P, et al. *Pediatr Crit Care Med*. 2010;11:227.
377. Szem JW, et al. *Crit Care Med*. 1995;23:1660.
378. Tobias JD, et al. *Pediatr Emerg Care*. 1996;12:249.
379. Ansermino JM, et al. *Anesth Analg*. 2009;108:873.
380. Lee J, et al. *Conf Proc IEEE Eng Med Biol Soc*. 2011;2011:8315.
381. Saeed M, et al. *Crit Care Med*. 2011;39:952.
382. Imhoff M, Kuhls S. *Anesth Analg*. 2006;102:1525.
383. Melek WW, et al. *IEEE Trans Biomed Eng*. 2005;52:639.
384. Simons DJ, Rensink RA. *Trends Cogn Sci*. 2005;9:16.
385. Dosani M, et al. *Br J Anaesth*. 2009;102:686.
386. Schadler D, et al. *Am J Respir Crit Care Med*. 2012;185:637.
387. Blount M, et al. *IEEE Eng Med Biol Mag*. 2010;29:110.
388. Chatburn RL, Mireles-Cabodevila E. *Respir Care*. 2011;56:85.
389. Epstein RH, Dexter F. *Anesth Analg*. 2012;115:929.
390. Chiumello D, et al. *Crit Care*. 2008;12:R150.
391. Dellamonica J, et al. *Crit Care*. 2011;15:R294.
392. Pillow JJ, et al. *Pediatr Pulmonol*. 2006;41:105.
393. Tobias JD. *Paediatr Anaesth*. 2009;19:434.
394. Sorensen LC, et al. *Scand J Clin Lab Invest*. 2011;71:548.
395. Sandberg KL, et al. *Acta Paediatr*. 2011;100:676.
396. Xue Q, et al. *Anesth Analg*. 2010;111:417.
397. Klopstein CE, et al. *Acta Anaesthesiol Scand*. 2008;52:700.
398. De Oliveira GS Jr, et al. *Br J Anaesth*. 2010;104:774.
399. Chakravarthy M, et al. *J Cardiothorac Vasc Anesth*. 2010;24:451.
400. Kelly AM, Klim S. *Respir Med*. 2011;105:226.
401. Spelten O, et al. *J Clin Monit Comput*. 2017;31:153.
402. Yu M, et al. *Shock*. 2007;27:615.
403. Chakravarthy M, et al. *J Clin Monit Comput*. 2009;23:363.
404. He HW, et al. *Shock*. 2012;37:152.
405. Yu M, et al. *Shock*. 2006;26:450.

406. Michard F. *J Clin Monit Comput*. 2018.
407. Pistolesi M, Giuntini C. *Radiol Clin North Am*. 1978;16:551.
408. Rubenfeld GD, et al. *Chest*. 1999;116:1347.
409. Meade MO, et al. *Am J Respir Crit Care Med*. 2000;161:85.
410. Sakka SG, et al. *Intensive Care Med*. 2000;26:180.
411. Isakow W, Schuster DP. *Am J Physiol Lung Cell Mol Physiol*. 2006;291:L1118.
412. Martin GS, et al. *Crit Care*. 2005;9:R74.
413. Kuzkov VV, et al. *Crit Care Med*. 2006;34:1647.
414. Phillips CR, et al. *Crit Care Med*. 2008;36:69.
415. Fernandez-Mondejar E, et al. *J Trauma*. 2005;59:1420. discussion 1424.
416. Assaad S, et al. *J Cardiothorac Vasc Anesth*. 2017;31:1471.
417. Stephan F, et al. *Crit Care Med*. 2017;45:e409–e417.
418. Pottecher J, et al. *Transplantation*. 2017;101:112.
419. Michelet P, et al. *Anesthesiology*. 2006;105:911.
420. Mitchell JP, et al. *Am Rev Respir Dis*. 1992;145:990.
421. Mutoh T, et al. *Stroke*. 2009;40:2368.
422. von Spiegel T, et al. *Anesthesiology*. 2002;96:827.
423. Perkins GD, et al. *Am J Respir Crit Care Med*. 2006;173:281.
424. Licker M, et al. *Chest*. 2008;133:845.
425. Effros RM, et al. *Am J Physiol Lung Cell Mol Physiol*. 2008;294:L1023.
426. Easley RB, et al. *Anesthesiology*. 2009;111:1065.
427. de Prost N, et al. *J Appl Physiol*. 2011;111:1249.
428. Roch A, et al. *Crit Care Med*. 2004;32:811.
429. Carlile PV, Gray BA. *J Appl Physiol*. 1984;57:680.
430. Kuntscher MV, et al. *J Burn Care Rehabil*. 2003;24:142.
431. Saugel B, et al. *Scand J Trauma Resusc Emerg Med*. 2011;19:31.
432. Saugel B, et al. *J Clin Monit Comput*. 2018.
433. Rossi P, et al. *Crit Care Med*. 2006;34:1437.

References

1. American Society of Anesthesiologists. *Standards for Basic Anesthetic Monitoring*; 2011.
2. International Task Force on Anaesthesia Safety. *World Federation of Societies of Anaesthesiologists: International Standards for a Safe Practice of Anaesthesia 2010*; 2010.
3. Eichhorn JH, Cooper JB, Cullen DJ, Maier WR, Philip JH, Seeman RG. Standards for patient monitoring during anesthesia at Harvard Medical School. *JAMA*. 1986;256:1017–1020.
4. Botham KM, Mayes PA. Biologic oxidation, Harper's illustrated biochemistry. In: Murray RK, Rodwell VW, Bender D, Botham KM, Weil PA, Kennelly PJ, eds. *eBook Collection (EBSCOhost)*. 28th ed. McGraw-Hill Medical; 2009:98.
5. Severinghaus JW. Monitoring oxygenation. *J Clin Monit Comput*. 2011;25:155–161.
6. Severinghaus JW. Gadgeteering for health care: the John W. Severinghaus lecture on translational science. *Anesthesiology*. 2009;110:721–728.
7. Campbell S, Wilson G, Engelhardt T. Equipment and monitoring—what is in the future to improve safety? *Paediatr Anaesth*. 2011;21:815–824.
8. Kenzaka T, Okuyama M, Kuroki S, et al. Importance of vital signs to the early diagnosis and severity of sepsis: association between vital signs and sequential organ failure assessment score in patients with sepsis. *Intern Med*. 2012;51:871–876.
9. Welsby PD, Earis JE. Some high pitched thoughts on chest examination. *Postgrad Med J*. 2001;77:617–620.
10. Epstein O, Perkin G G, et al. The respiratory system, clinical examination. In: *Anonymous*. 4th ed. Elsevier Health Sciences; 2008.
11. Thomas C, Lumb AB. Physiology of haemoglobin. *Cont Ed Anaesth Crit Care Pain*. 2012;12:251–256.
12. Severinghaus JW. Nomenclature of oxygen saturation. *Adv Exp Med Biol*. 1994;345:921–923.
13. Tremper KK, Barker SJ. Pulse oximetry. *Anesthesiology*. 1989;70:98–108.
14. Severinghaus JW, Honda Y. Pulse oximetry. *Int Anesthesiol Clin*. 1987;25:205–214.
- 14a. Pulse Oximeters - Premarket Notification Submissions [510(k)s]: Guidance for Industry and Food and Drug Administration Staff - Document issued on: March 4, 2013. <https://www.fda.gov/RegulatoryInformation/Guidances/ucm341718.htm>. Accessed April 7, 2019.
15. Milner QJ, Mathews GR. An assessment of the accuracy of pulse oximeters. *Anaesthesia*. 2012;67:396–401.
16. Polge JA. Pulse oximetry: technical aspects of machine design. *Int Anesthesiol Clin*. 1987;25:137–153.
17. Merry AF, Cooper JB, Soyannwo O, Wilson IH, Eichhorn JH. International standards for a safe practice of anesthesia 2010. *Can J Anaesth*. 2010;57:1027–1034.
18. Haynes AB, Weiser TG, Berry WR, et al. Safe Surgery Saves Lives Study Group. A surgical safety checklist to reduce morbidity and mortality in a global population. *N Engl J Med*. 2009;360:491–499.
19. Macknet MR, Allard M, Applegate 2nd RL, Rook J. The accuracy of noninvasive and continuous total hemoglobin measurement by pulse co-oximetry in human subjects undergoing hemodilution. *Anesth Analg*. 2010;111:1424–1426.
20. Barker SJ, Curry J, Redford D, Morgan S. Measurement of carboxyhemoglobin and methemoglobin by pulse oximetry: a human volunteer study. *Anesthesiology*. 2006;105:892–897.
21. Roth D, Herkner H, Schreiber W, et al. Accuracy of noninvasive multiwave pulse oximetry compared with carboxyhemoglobin from blood gas analysis in unselected emergency department patients. *Ann Emerg Med*. 2011;58:74–79.
22. Lamhaut L, Apriotesei R, Combes X, Lejay M, Carli P, Vivien B. Comparison of the accuracy of noninvasive hemoglobin monitoring by spectrophotometry (SpHb) and HemoCue(R) with automated laboratory hemoglobin measurement. *Anesthesiology*. 2011;115:548–554.
23. Frasca D, Dahyot-Fizelier C, Catherine K, Levrat Q, Debaene B, Mimoz O. Accuracy of a continuous noninvasive hemoglobin monitor in intensive care unit patients. *Crit Care Med*. 2011;39:2277–2282.
24. Berkow L, Rotolo S, Mirski E. Continuous noninvasive hemoglobin monitoring during complex spine surgery. *Anesth Analg*. 2011;113:1396–1402.
25. Morey TE, Gravenstein N, Rice MJ. Assessing point-of-care hemoglobin measurement: be careful we don't bias with bias. *Anesth Analg*. 2011;113:1289–1291.
26. Shamir MY, Avramovich A, Smaka T. The current status of continuous noninvasive measurement of total, carboxy, and methemoglobin concentration. *Anesth Analg*. 2012;114:972–978.
27. Maisel WH, Lewis RJ. Noninvasive measurement of carboxyhemoglobin: how accurate is accurate enough? *Ann Emerg Med*. 2010;56:389–391.
28. Caboot JB, Jawad AF, McDonough JM, et al. Non-invasive measurements of carboxyhemoglobin and methemoglobin in children with sickle cell disease. *Pediatr Pulmonol*. 2012;47:808–815.
29. Feiner JR, Rollins MD, Sall JW, Eilers H, Au P, Bickler PE. Accuracy of carboxyhemoglobin detection by pulse co-oximetry during hypoxemia. *Anesth Analg*. 2013;117:847–858.
30. Feiner JR, Bickler PE. Improved accuracy of methemoglobin detection by pulse co-oximetry during hypoxia. *Anesth Analg*. 2010;111:1160–1167.
31. Mahle WT, Newburger JW, Matherne GP, et al. American Heart Association Congenital Heart Defects Committee of the Council on Cardiovascular Disease in the Young, Council on Cardiovascular Nursing, and Interdisciplinary Council on Quality of Care and Outcomes Research, American Academy of Pediatrics Section on Cardiology and Cardiac Surgery, and Committee on Fetus and Newborn. Role of pulse oximetry in examining newborns for congenital heart disease: a scientific statement from the American Heart Association and American Academy of Pediatrics. *Circulation*. 2009;120:447–458.
32. Mahle WT, Martin GR, Beekman 3rd RH, Morrow WR. Section on Cardiology and Cardiac Surgery Executive Committee. Endorsement of Health and Human Services recommendation for pulse oximetry screening for critical congenital heart disease. *Pediatrics*. 2012;129:190–192.
33. Ewer AK, Middleton LJ, Furmston AT, et al. Pulse oximetry screening for congenital heart defects in newborn infants (PulseOx): a test accuracy study. *Lancet*. 2011;378:785–794.
34. Thangaratinam S, Brown K, Zamora J, Khan KS, Ewer AK. Pulse oximetry screening for critical congenital heart defects in asymptomatic newborn babies: a systematic review and meta-analysis. *Lancet*. 2012;379:2459–2464.
35. Dorlas JC, Nijboer JA. Photo-electric plethysmography as a monitoring device in anaesthesia. Application and interpretation. *Br J Anaesth*. 1985;57:524–530.
36. Cannesson M, Attof Y, Rosamel P, et al. Respiratory variations in pulse oximetry plethysmographic waveform amplitude to predict fluid responsiveness in the operating room. *Anesthesiology*. 2007;106:1105–1111.
37. Cannesson M, Delannoy B, Morand A, et al. Does the Pleth variability index indicate the respiratory-induced variation in the plethysmogram and arterial pressure waveforms? *Anesth Analg*. 2008;106(94):1189, table of contents.
38. Cannesson M, Sliker J, Desebbe O, et al. The ability of a novel algorithm for automatic estimation of the respiratory variations in arterial pulse pressure to monitor fluid responsiveness in the operating room. *Anesth Analg*. 2008;106(200):1195, table of contents.
39. Yin JY, Ho KM. Use of plethysmographic variability index derived from the Massimo(R) pulse oximeter to predict fluid or preload responsiveness: a systematic review and meta-analysis. *Anesthesia*. 2012;67:777–783.
40. Wu CY, Cheng YJ, Liu YJ, Wu TT, Chien CT, Chan KC. NTUH Center of Microcirculation Medical Research (NCMMR). Predicting stroke volume and arterial pressure fluid responsiveness in liver cirrhosis patients using dynamic preload variables: a prospective study of diagnostic accuracy. *Eur J Anaesthesiol*. 2016;33:645–652.
41. Sandroni C, Cavallaro F, Marano C, Falcone C, De Santis P, Antonelli M. Accuracy of plethysmographic indices as predictors of fluid responsiveness in mechanically ventilated adults: a systematic review and meta-analysis. *Intensive Care Med*. 2012;38:1429–1437.
42. Forget P, Lois F, de Kock M. Goal-directed fluid management based on the pulse oximeter-derived pleth variability index reduces lactate levels and improves fluid management. *Anesth Analg*. 2010;111:910–914.
43. Gothgen IH, Siggaard-Andersen O, Kokholm G. Variations in the hemoglobin-oxygen dissociation curve in 10079 arterial blood samples. *Scand J Clin Lab Invest Suppl*. 1990;203:87–90.

44. Perkins GD, McAuley DF, Giles S, Routledge H, Gao F. Do changes in pulse oximeter oxygen saturation predict equivalent changes in arterial oxygen saturation? *Crit Care*. 2003;7:R67.
45. Van de Louw A, Cracco C, Cerf C, et al. Accuracy of pulse oximetry in the intensive care unit. *Intensive Care Med*. 2001;27:1606–1613.
- 45a. Pedersen T, Nicholson A, Hovhannisyan K, et al. Pulse oximetry for perioperative monitoring. *Cochrane Database Syst Rev*. 2014;(3):CD002013.
- 45b. Moller JT, Johannessen NW, Espersen K, et al. Randomized evaluation of pulse oximetry in 20,802 patients: II. Perioperative events and postoperative complications. *Anesthesiology*. 1993;78(3):445–453.
- 45c. Ochroch EA, Russell MW, Hanson 3rd WC, et al. The impact of continuous pulse oximetry monitoring on intensive care unit admissions from a postsurgical care floor. *Anesth Analg*. 2006;102(3):868–875.
46. Mannheimer PD. The light-tissue interaction of pulse oximetry. *Anesth Analg*. 2007;105:S10–S17.
47. Feiner JR, Severinghaus JW, Bickler PE. Dark skin decreases the accuracy of pulse oximeters at low oxygen saturation: the effects of oximeter probe type and gender. *Anesth Analg*. 2007;105(23):S18. tables of contents.
48. Cox P. New pulse oximetry sensors with low saturation accuracy claims - a clinical evaluation. *Anesthesiology*. 2007;107:A1540.
49. Hinkelbein J, Genzweker HV, Fiedler F. Detection of a systolic pressure threshold for reliable readings in pulse oximetry. *Resuscitation*. 2005;64:315–319.
50. Barker SJ. "Motion-resistant" pulse oximetry: a comparison of new and old models. *Anesth Analg*. 2002;95(72):967. table of contents.
51. Shah N, Ragaswamy HB, Govindugari K, Estanol L. Performance of three new-generation pulse oximeters during motion and low perfusion in volunteers. *J Clin Anesth*. 2012;24:385–391.
52. Chan ED, Chan MM, Chan MM. Pulse oximetry: understanding its basic principles facilitates appreciation of its limitations. *Respir Med*. 2013;107:789–799.
53. Hampson NB. Pulse oximetry in severe carbon monoxide poisoning. *Chest*. 1998;114:1036–1041.
54. Eisenkraft JB. Pulse oximeter desaturation due to methemoglobinemia. *Anesthesiology*. 1988;68:279–282.
55. Jay GD, Hughes L, Renzi FP. Pulse oximetry is accurate in acute anemia from hemorrhage. *Ann Emerg Med*. 1994;24:32–35.
56. Severinghaus JW, Koh SO. Effect of anemia on pulse oximeter accuracy at low saturation. *J Clin Monit*. 1990;6:85–88.
57. Ortiz FO, Aldrich TK, Nagel RL, Benjamin IJ. Accuracy of pulse oximetry in sickle cell disease. *Am J Respir Crit Care Med*. 1999;159:447–451.
58. Rajadurai VS, Walker AM, Yu VY, Oates A. Effect of fetal haemoglobin on the accuracy of pulse oximetry in preterm infants. *J Paediatr Child Health*. 1992;28:43–46.
59. Ahmed S, Siddiqui AK, Sison CP, Shahid RK, Mattana J. Hemoglobin oxygen saturation discrepancy using various methods in patients with sickle cell vaso-occlusive painful crisis. *Eur J Haematol*. 2005;74:309–314.
60. Comber JT, Lopez BL. Evaluation of pulse oximetry in sickle cell anemia patients presenting to the emergency department in acute vaso-occlusive crisis. *Am J Emerg Med*. 1996;14:16–18.
61. Verhovsek M, Henderson MP, Cox G, Luo HY, Steinberg MH, Chui DH. Unexpectedly low pulse oximetry measurements associated with variant hemoglobins: a systematic review. *Am J Hematol*. 2010;85:882–885.
62. Scheller MS, Unger RJ, Kelner MJ. Effects of intravenously administered dyes on pulse oximetry readings. *Anesthesiology*. 1986;65:550–552.
63. Hinkelbein J, Genzweker HV, Sogl R, Fiedler F. Effect of nail polish on oxygen saturation determined by pulse oximetry in critically ill patients. *Resuscitation*. 2007;72:82–91.
64. Hinkelbein J, Koehler H, Genzweker HV, Fiedler F. Artificial acrylic finger nails may alter pulse oximetry measurement. *Resuscitation*. 2007;74:75–82.
65. Adler JN, Hughes LA, Vivilecchia R, Camargo CA Jr. Effect of skin pigmentation on pulse oximetry accuracy in the emergency department. *Acad Emerg Med*. 1998;5:965–970.
66. Bickler PE, Feiner JR, Severinghaus JW. Effects of skin pigmentation on pulse oximeter accuracy at low saturation. *Anesthesiology*. 2005;102:715–719.
67. Amar D, Neidzwski J, Wald A, Finck AD. Fluorescent light interferes with pulse oximetry. *J Clin Monit*. 1989;5:135–136.
68. Trivedi NS, Ghouri AF, Shah NK, Lai E, Barker SJ. Effects of motion, ambient light, and hypoperfusion on pulse oximeter function. *J Clin Anesth*. 1997;9:179–183.
69. Fluck RR Jr, Schroeder C, Frani G, Kropf B, Engbretson B. Does ambient light affect the accuracy of pulse oximetry? *Respir Care*. 2003;48:677–680.
70. van Oostrom JH, Mahla ME, Gravenstein D. The stealth station image guidance system may interfere with pulse oximetry. *Can J Anaesth*. 2005;52:379–382.
71. Mathes AM, Kreuer S, Schneider SO, Ziegeler S, Grundmann U. The performance of six pulse oximeters in the environment of neuronavigation. *Anesth Analg*. 2008;107:541–544.
72. Kelleher JF, Ruff RH. The penumbra effect: vasomotion-dependent pulse oximeter artifact due to probe malposition. *Anesthesiology*. 1989;71:787–791.
73. Zoremka N, Brulls C, Thiel V, Rohl A, Rossaint R. Pulse oximetry during intraaortic balloon pump application. *Acta Anaesthesiol Scand*. 2011;55:322–327.
74. Oleyar M, Stone M, Neustein SM. Perioperative management of a patient with a nonpulsatile left ventricular-assist device presenting for noncardiac surgery. *J Cardiothorac Vasc Anesth*. 2010;24:820–823.
75. Mabadeje O, Agwu A, Passaretti K, Lehman H, Asiyambola B. Do disposable pulse oximeter sensors impact infection rates? A review of the literature. *J Hosp Infect*. 2010;76:93–94.
76. Evans ML, Geddes LA. An assessment of blood vessel vasoactivity using photoplethysmography. *Med Instrum*. 1988;22:29–32.
77. Sinex JE. Pulse oximetry: principles and limitations. *Am J Emerg Med*. 1999;17:59–67.
78. Berkenbosch JW, Tobias JD. Comparison of a new forehead reflectance pulse oximeter sensor with a conventional digit sensor in pediatric patients. *Respir Care*. 2006;51:726–731.
79. MacLeod DB, Cortinez LI, Keifer JC, et al. The desaturation response time of finger pulse oximeters during mild hypothermia. *Anesthesia*. 2005;60:65–71.
80. Kulcke A, Feiner J, Menn I, Holmer A, Hayoz J, Bickler P. The accuracy of pulse spectroscopy for detecting hypoxemia and coexisting methemoglobin or carboxyhemoglobin. *Anesth Analg*. 2016;122:1856–1865.
81. Smit M, Levin AI, Coetzee JF. Comparison of minimally and more invasive methods of determining mixed venous oxygen saturation. *J Cardiothorac Vasc Anesth*. 2016;30:379–388.
82. Jenstrup M, Ejlersen E, Mogensen T, Secher NH. A maximal central venous oxygen saturation (SvO2max) for the surgical patient. *Acta Anaesthesiol Scand Suppl*. 1995;107:29–32.
83. Harms MP, van Lieshout JJ, Jenstrup M, Pott F, Secher NH. Postural effects on cardiac output and mixed venous oxygen saturation in humans. *Exp Physiol*. 2003;88:611–616.
84. Ho KM, Harding R, Chamberlain J. The impact of arterial oxygen tension on venous oxygen saturation in circulatory failure. *Shock*. 2008;29:3–6.
85. Dahn MS, Lange MP, Jacobs LA. Central mixed and splanchnic venous oxygen saturation monitoring. *Intensive Care Med*. 1988;14:373–378.
86. Martin C, Auffray JP, Badetti C, Perrin G, Papazian L, Gouin F. Monitoring of central venous oxygen saturation versus mixed venous oxygen saturation in critically ill patients. *Intensive Care Med*. 1992;18:101–104.
87. Varpula M, Karlsson S, Ruokonen E, Pettila V. Mixed venous oxygen saturation cannot be estimated by central venous oxygen saturation in septic shock. *Intensive Care Med*. 2006;32:1336–1343.
88. Ho KM, Harding R, Chamberlain J, Bulsara M. A comparison of central and mixed venous oxygen saturation in circulatory failure. *J Cardiothorac Vasc Anesth*. 2010;24:434–439.
89. Reinhart K, Rudolph T, Bredle DL, Hannemann L, Cain SM. Comparison of central-venous to mixed-venous oxygen saturation during changes in oxygen supply/demand. *Chest*. 1989;95:1216–1221.
90. Chawla LS, Zia H, Gutierrez G, Katz NM, Seneff MG, Shah M. Lack of equivalence between central and mixed venous oxygen saturation. *Chest*. 2004;126:1891–1896.
91. Dueck MH, Klimek M, Appenrodt S, Weigand C, Boerner U. Trends but not individual values of central venous oxygen saturation agree with mixed venous oxygen saturation during varying hemodynamic conditions. *Anesthesiology*. 2005;103:249–257.

92. Lorentzen AG, Lindskov C, Sloth E, Jakobsen CJ. Central venous oxygen saturation cannot replace mixed venous saturation in patients undergoing cardiac surgery. *J Cardiothorac Vasc Anesth*. 2008;22:853–857.
93. Grissom CK, Morris AH, Lanken PN, et al. National Institutes of Health/National Heart, Lung and Blood Institute Acute Respiratory Distress. Association of physical examination with pulmonary artery catheter parameters in acute lung injury. *Crit Care Med*. 2009;37:2720–2726.
94. Kopterides P, Bonovas S, Mavrou I, Kostadima E, Zakynthinos E, Armanagidis A. Venous oxygen saturation and lactate gradient from superior vena cava to pulmonary artery in patients with septic shock. *Shock*. 2009;31:561–567.
95. Dahmani S, Paugam-Burtz C, Gauss T, et al. Comparison of central and mixed venous saturation during liver transplantation in cirrhotic patients: a pilot study. *Eur J Anaesthesiol*. 2010;27:714–719.
96. Lequeux PY, Bouckaert Y, Sekkat H, et al. Continuous mixed venous and central venous oxygen saturation in cardiac surgery with cardiopulmonary bypass. *Eur J Anaesthesiol*. 2010;27:295–299.
97. Lamia B, Monnet X, Teboul JL. Meaning of arterio-venous PCO₂ difference in circulatory shock. *Minerva Anestesiol*. 2006;72:597–604.
98. Suter PM, Lindauer JM, Fairley HB, Schlobohm RM. Errors in data derived from pulmonary artery blood gas values. *Crit Care Med*. 1975;3:175–181.
99. Pond CG, Blessios G, Bowlin J, McCawley C, Lappas DG. Perioperative evaluation of a new mixed venous oxygen saturation catheter in cardiac surgical patients. *J Cardiothorac Vasc Anesth*. 1992;6:280–282.
100. Maddirala S, Khan A. Optimizing hemodynamic support in septic shock using central and mixed venous oxygen saturation. *Crit Care Clin*. 2010;26(3):323. table of contents.
101. Scuderi PE, MacGregor DA, Bowton DL, James RL. A laboratory comparison of three pulmonary artery oximetry catheters. *Anesthesiology*. 1994;81:245–253.
102. Baulig W, Dullenkopf A, Kobler A, Baulig B, Roth HR, Schmid ER. Accuracy of continuous central venous oxygen saturation monitoring in patients undergoing cardiac surgery. *J Clin Monit Comput*. 2008;22:183–188.
103. Baulig W, Bettex D, Burki C, et al. The PediaSat continuous central SvO₂ monitoring system does not reliably indicate state or course of central venous oxygenation. *Eur J Anaesthesiol*. 2010;27:720–725.
104. Schmidt CR, Frank LP, Forsythe SB, Estafanous FG. Continuous S-vO₂ measurement and oxygen transport patterns in cardiac surgery patients. *Crit Care Med*. 1984;12:523–527.
105. Routsis C, Vincent JL, Bakker J, et al. Relation between oxygen consumption and oxygen delivery in patients after cardiac surgery. *Anesth Analg*. 1993;77:1104–1110.
106. Polonen P, Hippelainen M, Takala R, Ruokonen E, Takala J. Relationship between intra- and postoperative oxygen transport and prolonged intensive care after cardiac surgery: a prospective study. *Acta Anaesthesiol Scand*. 1997;41:810–817.
107. Pearse R, Dawson D, Fawcett J, Rhodes A, Grounds RM, Bennett ED. Changes in central venous saturation after major surgery, and association with outcome. *Crit Care*. 2005;9:R694–R699.
108. Collaborative Study Group on Perioperative ScVO₂ Monitoring: Multicentre study on peri- and postoperative central venous oxygen saturation in high-risk surgical patients. *Crit Care*. 2006;10:R158.
109. Polonen P, Ruokonen E, Hippelainen M, Poyhonen M, Takala J. A prospective, randomized study of goal-oriented hemodynamic therapy in cardiac surgical patients. *Anesth Analg*. 2000;90:1052–1059.
110. Rivers E, Nguyen B, Havstad S, et al. Early Goal-Directed Therapy Collaborative Group. Early goal-directed therapy in the treatment of severe sepsis and septic shock. *N Engl J Med*. 2001;345:1368–1377.
111. Donati A, Loggi S, Preiser JC, et al. Goal-directed intraoperative therapy reduces morbidity and length of hospital stay in high-risk surgical patients. *Chest*. 2007;132:1817–1824.
112. Dellinger RP, Levy MM, Carlet JM, et al. American Association of Critical-Care Nurses, American College of Chest Physicians, American College of Emergency Physicians, Canadian Critical Care Society, European Society of Clinical Microbiology and Infectious Diseases, European Society of Intensive Care Medicine, European Respiratory Society, International Sepsis Forum, Japanese Association for Acute Medicine, Japanese Society of Intensive Care Medicine, Society of Critical Care Medicine, Society of Hospital Medicine, Surgical Infection Society, World Federation of Societies of Intensive and Critical Care Medicine. Surviving sepsis campaign: international guidelines for management of severe sepsis and septic shock: 2008. *Crit Care Med*. 2008;36:296–327.
113. Otero RM, Nguyen HB, Huang DT, et al. Early goal-directed therapy in severe sepsis and septic shock revisited: concepts, controversies, and contemporary findings. *Chest*. 2006;130:1579–1595.
114. Bellomo R, Reade MC, Warrillow SJ. The pursuit of a high central venous oxygen saturation in sepsis: growing concerns. *Crit Care*. 2008;12:130.
115. Peake SL, Bailey M, Bellomo R, et al. ARISE Investigators, for the Australian and New Zealand Intensive Care Society Clinical Trials Group. Australasian resuscitation of sepsis evaluation (ARISE): a multi-centre, prospective, inception cohort study. *Resuscitation*. 2009;80:811–818.
116. Jones AE, Shapiro NI, Trzeciak S, Arnold RC, Claremont HA, Kline JA. Emergency Medicine Shock Research Network (EMShockNet) Investigators. Lactate clearance vs central venous oxygen saturation as goals of early sepsis therapy: a randomized clinical trial. *JAMA*. 2010;303:739–746.
117. Suehiro K, Tanaka K, Matsuura T, et al. Discrepancy between superior vena cava oxygen saturation and mixed venous oxygen saturation can predict postoperative complications in cardiac surgery patients. *J Cardiothorac Vasc Anesth*. 2014;28:528–533.
118. Bickler P, Feiner J, Rollins M, Meng L. Tissue oximetry and clinical outcomes. *Anesth Analg*. 2017;124:72–82.
119. Ubbink R, Bettink MAW, Janse R, et al. A monitor for Cellular Oxygen METabolism (COMET): monitoring tissue oxygenation at the mitochondrial level. *J Clin Monit Comput*. 2017;31:1143–1150.
120. Wahr JA, Tremper KK, Samra S, Delpy DT. Near-infrared spectroscopy: theory and applications. *J Cardiothorac Vasc Anesth*. 1996;10:406–418.
121. Cui W, Wang N, Chance B. Study of photon migration depths with time-resolved spectroscopy. *Opt Lett*. 1991;16:1632–1634.
122. Schober P, Schwarte LA. From system to organ to cell: oxygenation and perfusion measurement in anesthesia and critical care. *J Clin Monit Comput*. 2012;26:255–265.
123. Jobsis FF. Noninvasive, infrared monitoring of cerebral and myocardial oxygen sufficiency and circulatory parameters. *Science*. 1977;198:1264–1267.
124. Watzman HM, Kurth CD, Montenegro LM, Rome J, Steven JM, Nicolson SC. Arterial and venous contributions to near-infrared cerebral oximetry. *Anesthesiology*. 2000;93:947–953.
125. Sakr Y, Gath V, Oishi J, et al. Characterization of buccal microvascular response in patients with septic shock. *Eur J Anaesthesiol*. 2010;27:388–394.
126. Holzle F, Rau A, Loeffelbein DJ, Mucke T, Kesting MR, Wolff KD. Results of monitoring fasciocutaneous, myocutaneous, osteocutaneous and perforator flaps: 4-year experience with 166 cases. *Int J Oral Maxillofac Surg*. 2010;39:21–28.
127. Karliczek A, Benaron DA, Baas PC, Zeebregts CJ, Wiggers T, van Dam GM. Intraoperative assessment of microperfusion with visible light spectroscopy for prediction of anastomotic leakage in colorectal anastomoses. *Colorectal Dis*. 2010;12:1018–1025.
128. Pham TH, Perry KA, Enestvedt CK, et al. Decreased conduit perfusion measured by spectroscopy is associated with anastomotic complications. *Ann Thorac Surg*. 2011;91:380–385.
129. Friedland S, Benaron D, Parachikov I, Soetikno R. Measurement of mucosal capillary hemoglobin oxygen saturation in the colon by reflectance spectrophotometry. *Gastrointest Endosc*. 2003;57:492–497.
130. Friedland S, Benaron D, Coogan S, Sze DY, Soetikno R. Diagnosis of chronic mesenteric ischemia by visible light spectroscopy during endoscopy. *Gastrointest Endosc*. 2007;65:294–300.
131. Bludau M, Holscher AH, Vallbohmer D, Gutschow C, Schroder W. Ischemic conditioning of the gastric conduit prior to esophagectomy improves mucosal oxygen saturation. *Ann Thorac Surg*. 2010;90:1121–1126.
132. Highton D, Elwell C, Smith M. Noninvasive cerebral oximetry: is there light at the end of the tunnel? *Curr Opin Anaesthesiol*. 2010;23:576–581.
133. Chan MJ, Chung T, Glassford NJ, Bellomo R. Near-infrared spectroscopy in adult cardiac surgery patients: a systematic review and meta-analysis. *J Cardiothorac Vasc Anesth*. 2017;31:1155–1165.
134. Murkin JM, Adams SJ, Novick RJ, et al. Monitoring brain oxygen saturation during coronary bypass surgery: a randomized, prospective study. *Anesth Analg*. 2007;104:51–58.

135. Slater JP, Guarino T, Stack J, et al. Cerebral oxygen desaturation predicts cognitive decline and longer hospital stay after cardiac surgery. *Ann Thorac Surg.* 2009;87(36):44, discussion 44-5.
136. Yao FS, Tseng CC, Ho CY, Levin SK, Illner P. Cerebral oxygen desaturation is associated with early postoperative neuropsychological dysfunction in patients undergoing cardiac surgery. *J Cardiothorac Vasc Anesth.* 2004;18:552-558.
137. Fischer GW, Lin HM, Krol M, et al. Noninvasive cerebral oxygenation may predict outcome in patients undergoing aortic arch surgery. *J Thorac Cardiovasc Surg.* 2011;141:815-821.
138. de Tournay-Jette E, Dupuis G, Bherer L, Deschamps A, Cartier R, Denault A. The relationship between cerebral oxygen saturation changes and postoperative cognitive dysfunction in elderly patients after coronary artery bypass graft surgery. *J Cardiothorac Vasc Anesth.* 2011;25:95-104.
139. Ghosal S, Trivedi J, Chen J, et al. Regional cerebral oxygen saturation level predicts 30-day mortality rate after left ventricular assist device surgery. *J Cardiothorac Vasc Anesth.* 2018;32:1185-1190.
140. Kirkpatrick PJ, Lam J, Al-Rawi P, Smielewski P, Czosnyka M. Defining thresholds for critical ischemia by using near-infrared spectroscopy in the adult brain. *J Neurosurg.* 1998;89:389-394.
141. Grubhofer G, Plochl W, Skolka M, Czerny M, Ehrlich M, Lassnigg A. Comparing Doppler ultrasonography and cerebral oximetry as indicators for shunting in carotid endarterectomy. *Anesth Analg.* 2000;91:1339-1344.
142. Vets P, ten Broecke P, Adriaensen H, Van Schil P, De Hert S. Cerebral oximetry in patients undergoing carotid endarterectomy: preliminary results. *Acta Anaesthesiol Belg.* 2004;55:215-220.
143. Al-Rawi PG, Kirkpatrick PJ. Tissue oxygen index: thresholds for cerebral ischemia using near-infrared spectroscopy. *Stroke.* 2006;37:2720-2725.
144. Moritz S, Kasprzak P, Arlt M, Taeger K, Metz C. Accuracy of cerebral monitoring in detecting cerebral ischemia during carotid endarterectomy: a comparison of transcranial Doppler sonography, near-infrared spectroscopy, stump pressure, and somatosensory evoked potentials. *Anesthesiology.* 2007;107:563-569.
145. de Letter JA, Sie HT, Thomas BM, et al. Near-infrared reflected spectroscopy and electroencephalography during carotid endarterectomy—in search of a new shunt criterion. *Neurol Res.* 1998;20(suppl 1):S23-S27.
146. Hirofumi O, Otone E, Hiroshi I, et al. The effectiveness of regional cerebral oxygen saturation monitoring using near-infrared spectroscopy in carotid endarterectomy. *J Clin Neurosci.* 2003;10:79-83.
147. Rigamonti A, Scandroglio M, Minicucci F, Magrin S, Carozzo A, Casati A. A clinical evaluation of near-infrared cerebral oximetry in the awake patient to monitor cerebral perfusion during carotid endarterectomy. *J Clin Anesth.* 2005;17:426-430.
148. Yamamoto K, Miyata T, Nagawa H. Good correlation between cerebral oxygenation measured using near infrared spectroscopy and stump pressure during carotid clamping. *Int Angiol.* 2007;26:262-265.
149. Jonsson M, Lindstrom D, Wanhainen A, Djavani Gidlund K, Gillgren P. Near infrared spectroscopy as a predictor for shunt requirement during carotid endarterectomy. *Eur J Vasc Endovasc Surg.* 2017;53:783-791.
150. Samra SK, Dy EA, Welch K, Dorje P, Zelenock GB, Stanley JC. Evaluation of a cerebral oximeter as a monitor of cerebral ischemia during carotid endarterectomy. *Anesthesiology.* 2000;93:964-970.
151. Mille T, Tachimiri ME, Klersy C, et al. Near infrared spectroscopy monitoring during carotid endarterectomy: which threshold value is critical? *Eur J Vasc Endovasc Surg.* 2004;27:646-650.
152. Boezeman RP, van Dongen EP, Morshuis WJ, et al. Spinal near-infrared spectroscopy measurements during and after thoracoabdominal aortic aneurysm repair: a pilot study. *Ann Thorac Surg.* 2015;99:1267-1274.
153. Casati A, Fanelli G, Pietropaoli P, et al. Continuous monitoring of cerebral oxygen saturation in elderly patients undergoing major abdominal surgery minimizes brain exposure to potential hypoxia. *Anesth Analg.* 2005;101(7):740. table of contents.
154. Tang L, Kazan R, Taddei R, Zaouter C, Cyr S, Hemmerling TM. Reduced cerebral oxygen saturation during thoracic surgery predicts early postoperative cognitive dysfunction. *Br J Anaesth.* 2012;108:623-629.
155. Murphy GS, Szokol JW, Marymont JH, et al. Cerebral oxygen desaturation events assessed by near-infrared spectroscopy during shoulder arthroscopy in the beach chair and lateral decubitus positions. *Anesth Analg.* 2010;111:496-505.
156. Moerman AT, De Hert SG, Jacobs TF, De Wilde LF, Wouters PF. Cerebral oxygen desaturation during beach chair position. *Eur J Anaesthesiol.* 2012;29:82-87.
157. Tange K, Kinoshita H, Minonishi T, et al. Cerebral oxygenation in the beach chair position before and during general anesthesia. *Minerva Anestesiol.* 2010;76:485-490.
158. Crookes BA, Cohn SM, Bloch S, et al. Can near-infrared spectroscopy identify the severity of shock in trauma patients? *J Trauma.* 2005;58(13):806. discussion 813-6.
159. Cohn SM, Nathens AB, Moore FA, et al. StO₂ in Trauma Patients Trial Investigators. Tissue oxygen saturation predicts the development of organ dysfunction during traumatic shock resuscitation. *J Trauma.* 2007;62(54):44. discussion 54-5.
160. Ilkossi DG, Knudson MM, Morabito DJ, et al. Continuous muscle tissue oxygenation in critically injured patients: a prospective observational study. *J Trauma.* 2006;61(8):780. discussion 788-90.
161. Yu Y, Zhang K, Zhang L, Zong H, Meng L, Han R. Cerebral near-infrared spectroscopy (NIRS) for perioperative monitoring of brain oxygenation in children and adults. *Cochrane Database Syst Rev.* 2018;1:CD010947.
162. Sun X, Ellis J, Corso PJ, Hill PC, Chen F, Lindsay J. Skin pigmentation interferes with the clinical measurement of regional cerebral oxygen saturation. *Br J Anaesth.* 2015;114:276-280.
163. Bohr C. Ueber die Lungenathmung. *Skandinavisches Archiv Für Physiologie.* 1891;2:236-268.
164. Mogue LR, Rantala B. Capnometers. *J Clin Monit.* 1988;4:115-121.
165. Bhavani-Shankar K, Kumar AY, Moseley HS, Ahyee-Hallsworth R. Terminology and the current limitations of time capnography: a brief review. *J Clin Monit.* 1995;11:175-182.
166. Gravenstein JS, Paulus DA, Hayes TJ. *Capnography in Clinical Practice.* 1st ed. Boston: Butterworth Publishers; 1989.
167. Gravenstein JS, Paulus DA, Hayes TJ. *Gas Monitoring in Clinical Practice.* Boston: Butterworth-Heinemann; 1995.
168. Jaffe MB. Infrared measurement of carbon dioxide in the human breath: "breath-through" devices from Tyndall to the present day. *Anesthesia and Analgesia.* 2008;107:890-904.
169. Raemer DB, Calalang I. Accuracy of end-tidal carbon dioxide tension analyzers. *J Clin Monit.* 1991;7:195-208.
170. Hess D. Capnometry and capnography: Technical aspects, physiologic aspects, and clinical applications. *Respiratory Care.* 1990;35:557-576.
171. Brunner JX, Westenskow DR. How the rise time of carbon dioxide analysers influences the accuracy of carbon dioxide measurements. *Br J Anaesth.* 1988;61:628-638.
172. Jaffe MB. *Mainstream or Sidestream Capnography? Technical Considerations.* Wallingford, CT: Respiration Novametric, Inc; 2002.
173. Kaczka DW, Lutchen KR, Hantos Z. Emergent behavior of regional heterogeneity in the lung and its effects on respiratory impedance. *J Appl Physiol.* 2011;110:1473-1481.
174. Bhavani-Shankar K, Philip JH. Defining segments and phases of a time capnogram. *Anesth Analg.* 2000;91:973-977.
175. Moon RE, Camporesi EM. Respiratory monitoring. In: Miller RD, ed. *Miller's anesthesia.* New York: Elsevier; 2005: 1255,1295; 33.
- 175a. Mondoñedo JR, McNeil JS, Herrmann J, Simon BA, Kaczka DW. Targeted versus continuous delivery of volatile anesthetics during cholinergic bronchoconstriction. *ASME J of Medical Diagnostics.* 2018;1(031003):031003-031012.
176. Fletcher R, Jonson B, Cumming G, Brew J. The concept of deadspace with special reference to the single breath test for carbon dioxide. *Br J Anaesth.* 1981;53:77-88.
177. McKenzie DC. Respiratory physiology: adaptations to high-level exercise. *Br J Sports Med.* 2012;46:381-384.
178. Grocott MP, Martin DS, Levett DZ, McMorrow R, Windsor J, Montgomery HE. Caudwell Xtreme Everest Research Group. Arterial blood gases and oxygen content in climbers on Mount Everest. *N Engl J Med.* 2009;360:140-149.
179. Wagner PD, Laravuso RB, Uhl RR, West JB. Continuous distributions of ventilation-perfusion ratios in normal subjects breathing air and 100 per cent O₂. *J Clin Invest.* 1974;54:54-68.

180. Ravin MB, Epstein RM, Malm JR. Contribution of thebesian veins to the physiologic shunt in anesthetized man. *J Appl Physiol*. 1965;20:1148–1152.
181. Brismar B, Hedenstierna G, Lundquist H, Strandberg A, Svensson L, Tokics L. Pulmonary densities during anesthesia with muscular relaxation—a proposal of atelectasis. *Anesthesiology*. 1985;62:422–428.
182. Rothen HU, Sporre B, Engberg G, Wegenius G, Hedenstierna G. Airway closure, atelectasis and gas exchange during general anaesthesia. *Br J Anaesth*. 1998;81:681–686.
183. Riley RL, Cournand A. Ideal alveolar air and the analysis of ventilation-perfusion relationships in the lungs. *J Appl Physiol*. 1949;1:825–847.
184. Whiteley JP, Gavaghan DJ, Hahn CE. Variation of venous admixture, SF6 shunt, PaO₂, and the PaO₂/FIO₂ ratio with FIO₂. *Br J Anaesth*. 2002;88:771–778.
185. Gould MK, Ruoss SJ, Rizk NW, Doyle RL, Raffin TA. Indices of hypoxemia in patients with acute respiratory distress syndrome: reliability, validity, and clinical usefulness. *Crit Care Med*. 1997;25:6–8.
186. McCahon RA, Columb MO, Mahajan RP, Hardman JG. Validation and application of a high-fidelity, computational model of acute respiratory distress syndrome to the examination of the indices of oxygenation at constant lung-state. *Br J Anaesth*. 2008;101:358–365.
187. Kathirgamanathan A, McCahon RA, Hardman JG. Indices of pulmonary oxygenation in pathological lung states: an investigation using high-fidelity, computational modelling. *Br J Anaesth*. 2009;103:291–297.
188. Lilenthal JL Jr, Riley RL. An experimental analysis in man of the oxygen pressure gradient from alveolar air to arterial blood during rest and exercise at sea level and at altitude. *Am J Physiol*. 1946;147:199–216.
189. Mellegaard K. The alveolar-arterial oxygen difference: its size and components in normal man. *Acta Physiol Scand*. 1966;67:10–20.
190. Gowda MS, Klocke RA. Variability of indices of hypoxemia in adult respiratory distress syndrome. *Crit Care Med*. 1997;25:41–45.
191. Ranieri VM, Rubenfeld GD, Thompson BT, et al. Acute respiratory distress syndrome: the Berlin definition. *JAMA*. 2012;307:2526–2533.
192. Rice TW, Wheeler AP, Bernard GR, Hayden DL, Schoenfeld DA, Ware LB, for the National Institutes of Health, National Heart, Lung, and Blood Institute ARDS Network. Comparison of the SpO₂/FIO₂ ratio and the PaO₂/FIO₂ ratio in patients with acute lung injury or ARDS. *Chest*. 2007;132:410–417.
193. Khemani RG, Thomas NJ, Venkatachalam V, et al. Pediatric Acute Lung Injury and Sepsis Network Investigators (PALISI). Comparison of SpO₂ to PaO₂ based markers of lung disease severity for children with acute lung injury. *Crit Care Med*. 2012;40:1309–1316.
194. DesPrez K, McNeil JB, Wang C, Bastarache JA, Shaver CM, Ware LB. Oxygenation saturation index predicts clinical outcomes in ARDS. *Chest*. 2017;152:1151–1158.
195. Villar J, Blanco J, del Campo R, et al. Spanish Initiative for Epidemiology, Stratification & Therapies for ARDS (SIESTA) Network. Assessment of PaO₂/FIO₂ for stratification of patients with moderate and severe acute respiratory distress syndrome. *BMJ Open*. 2015;5: e006812.
196. Balzer F, Menk M, Ziegler J, et al. Predictors of survival in critically ill patients with acute respiratory distress syndrome (ARDS): an observational study. *BMC Anesthesiol*. 2016;16:108.
197. Ortiz RM, Cilley RE, Bartlett RH. Extracorporeal membrane oxygenation in pediatric respiratory failure. *Pediatr Clin North Am*. 1987;34:39–46.
198. Trachsse D, McCrindle BW, Nakagawa S, Bohn D. Oxygenation index predicts outcome in children with acute hypoxic respiratory failure. *Am J Respir Crit Care Med*. 2005;172:206–211.
199. Gajic O, Afessa B, Thompson BT, et al. Second International Study of Mechanical Ventilation and ARDS-net Investigators. Prediction of death and prolonged mechanical ventilation in acute lung injury. *Crit Care*. 2007;11:R53.
200. Kaczka DW, Herrmann J, Zonneveld CE, et al. Multifrequency oscillatory ventilation in the premature lung: effects on gas exchange, mechanics, and ventilation distribution. *Anesthesiology*. 2015;123:1394–1403.
201. Christiansen J, Douglas CG, Haldane JS. The absorption and dissociation of carbon dioxide by human blood. *J Physiol*. 1914;48:244–271.
202. Severinghaus JW, Astrup PB. History of blood gas analysis. IV. Leland Clark's oxygen electrode. *J Clin Monit*. 1986;2:125–139.
203. Severinghaus JW. The invention and development of blood gas analysis apparatus. *Anesthesiology*. 2002;97:253–256.
204. Andritsch RF, Muravchick S, Gold MI. Temperature correction of arterial blood-gas parameters: a comparative review of methodology. *Anesthesiology*. 1981;55:311–316.
205. Kern FH, Greeley WJ, Pro: pH-stat management of blood gases is not preferable to alpha-stat in patients undergoing brain cooling for cardiac surgery. *J Cardiothorac Vasc Anesth*. 1995;9:215–218.
206. Burrows FA, Con: pH-stat management of blood gases is preferable to alpha-stat in patients undergoing brain cooling for cardiac surgery. *J Cardiothorac Vasc Anesth*. 1995;9:219–221.
207. Patel RL, Turtle MR, Chambers DJ, James DN, Newman S, Venn GE. Alpha-stat acid-base regulation during cardiopulmonary bypass improves neuropsychologic outcome in patients undergoing coronary artery bypass grafting. *J Thorac Cardiovasc Surg*. 1996;111:1267–1279.
208. Engelhardt W, Dierks T, Pause M, Hartung E. Early cerebral functional outcome after coronary artery bypass surgery using different acid-base management during hypothermic cardiopulmonary bypass. *Acta Anaesthesiol Scand*. 1996;40:457–465.
209. du Plessis AJ, Jonas RA, Wypij D, et al. Perioperative effects of alpha-stat versus pH-stat strategies for deep hypothermic cardiopulmonary bypass in infants. *J Thorac Cardiovasc Surg*. 1997;114(1000):991, discussion 1000–1.
210. Bellinger DC, Wypij D, du Plessis AJ, et al. Developmental and neurologic effects of alpha-stat versus pH-stat strategies for deep hypothermic cardiopulmonary bypass in infants. *J Thorac Cardiovasc Surg*. 2001;121:374–383.
211. Kiziltan HT, Baltali M, Bilen A, et al. Comparison of alpha-stat and pH-stat cardiopulmonary bypass in relation to jugular venous oxygen saturation and cerebral glucose-oxygen utilization. *Anesth Analg*. 2003;96(50):644, table of contents.
212. Piccioni MA, Leirner AA, Auler JO Jr. Comparison of pH-stat versus alpha-stat during hypothermic cardiopulmonary bypass in the prevention and control of acidosis in cardiac surgery. *Artif Organs*. 2004;28:347–352.
213. Sakamoto T, Kurosawa H, Shin'oka T, Aoki M, Isomatsu Y. The influence of pH strategy on cerebral and collateral circulation during hypothermic cardiopulmonary bypass in cyanotic patients with heart disease: results of a randomized trial and real-time monitoring. *J Thorac Cardiovasc Surg*. 2004;127:12–19.
214. Hoover LR, Dinavahi R, Cheng WP, et al. Jugular venous oxygenation during hypothermic cardiopulmonary bypass in patients at risk for abnormal cerebral autoregulation: influence of alpha-stat versus pH-stat blood gas management. *Anesth Analg*. 2009;108:1389–1393.
215. Nagy ZL, Collins M, Sharpe T, et al. Effect of two different bypass techniques on the serum troponin-T levels in newborns and children: does pH-Stat provide better protection? *Circulation*. 2003;108:577–582.
216. Murkin JM, Martzke JS, Buchan AM, Bentley C, Wong CJ. A randomized study of the influence of perfusion technique and pH management strategy in 316 patients undergoing coronary artery bypass surgery. II. Neurologic and cognitive outcomes. *J Thorac Cardiovasc Surg*. 1995;110:349–362.
217. Svyatets M, Tolani K, Zhang M, Tulman G, Charchaflej J. Perioperative management of deep hypothermic circulatory arrest. *J Cardiothorac Vasc Anesth*. 2010;24:644–655.
218. Biswas CK, Ramos JM, Agroyannis B, Kerr DN. Blood gas analysis: effect of air bubbles in syringe and delay in estimation. *Br Med J (Clin Res Ed)*. 1982;284:923–927.
219. Kaczka DW, Colletti AA, Tawhai MH, Simon BA. Computational analyses of airway flow and lung tissue dynamics, image-based computational modeling of the human circulatory and pulmonary systems: methods and applications. In: *Image-based computational modeling of the human circulatory and pulmonary systems: Methods and applications*. Chandran KB, Udaykumar HS, Reinhardt JM, eds. 1st ed. New York: Springer; 2011:375. 402; 10.

220. Kaczka DW, Smallwood JL. Constant-phase descriptions of canine lung, chest wall, and total respiratory viscoelasticity: effects of distending pressure. *Respir Physiol Neurobiol*. 2012;183:75–84.
221. Warner DO. So you want to be a pulmonary mechanic: a clinical guide. *J Clin Monit Comput*. 2000;16:417–423.
222. Bates JHT. *Lung Mechanics: An Inverse Modeling Approach*. Cambridge: Cambridge University Press; 2009:220.
223. Pedley TJ, Schroter RC, Sudlow MF. The prediction of pressure drop and variation of resistance within the human bronchial airways. *Respiration Physiology*. 1970;9:387–405.
224. Rohrer F. Der Strömungswiderstand in den menschlichen Atemwegen und der Einfluss der unregelmässigen Verzweigung des Bronchialsystems auf den Atmungsverlauf in verschiedenen Lungenbezirken. *Pfluegers Arch Gesamte Physiol Menschen Tiere*. 1915;162:225–299.
225. Mora R, Arold S, Marzan Y, Suki B, Ingenito EP. Determinants of surfactant function in acute lung injury and early recovery. *Am J Physiol Lung Cell Mol Physiol*. 2000;279:L342–L349.
226. Fredberg JJ, Stamenovic D. On the imperfect elasticity of lung tissue. *J Appl Physiol*. 1989;67:2408–2419.
227. Fredberg JJ, Inouye D, Miller B, et al. Airway smooth muscle, tidal stretches, and dynamically determined contractile states. *Am J Respir Crit Care Med*. 1997;156:1752–1759.
228. McIlroy MB, Mead J, Selverstone NJ, Radford EP Jr. Measurement of lung tissue viscous resistance using gases of equal kinematic viscosity. *J Appl Physiol*. 1955;7:485–490.
229. Bachofen H. Lung tissue resistance and pulmonary hysteresis. *J Appl Physiol*. 1968;24:296–301.
230. Hantos Z, Daroczy B, Suki B, Nagy S, Fredberg JJ. Input impedance and peripheral inhomogeneity of dog lungs. *J Appl Physiol*. 1992;72:168–178.
231. Kaczka DW, Ingenito EP, Suki B, Lutchen KR. Partitioning airway and lung tissue resistances in humans: effects of bronchoconstriction. *J Appl Physiol*. 1997;82:1531–1541.
232. Hoppin FG Jr, Hildebrandt J. *Mechanical Properties of the Lung, Biomechanical Aspects of the Lung*. West JB, ed. New York: M. Dekker; 1977:83–162.
- 232a. Kano S, Lanteri CJ, Duncan AW, Sly PD. Influence of nonlinearities on estimates of respiratory mechanics using multilinear regression analysis. *J Appl Physiol* (1985). 1994;77:1185–1197.
- 232b. Amini R, Herrmann J, Kaczka DW. Intratidal overdistension and derecruitment in the injured lung: a simulation study. *IEEE Trans Biomed Eng*. 2017;64:681–689.
- 232c. Carvalho AR, Spieth PM, Pelosi P, et al. Ability of dynamic airway pressure curve profile and elastance for positive end-expiratory pressure titration. *Intensive Care Medicine*. 2008;34:2291–2299.
- 232d. Carvalho AR, Pacheco SA, de Souza Rocha PV, et al. Detection of tidal recruitment/overdistension in lung-healthy mechanically ventilated patients under general anesthesia. *Anesth Analg*. 2013;116:677–684.
- 232e. D'Antini D, Huhle R, Herrmann J, et al. Respiratory system mechanics during low versus high positive end-expiratory pressure in open abdominal surgery: a substudy of PROVHILO randomized controlled trial. *Anesth Analg*. 2018;126:143–149.
- 232f. Ranieri VM, Zhang H, Mascia L, et al. Pressure-time curve predicts minimally injurious ventilatory strategy in an isolated rat lung model. *Anesthesiology*. 2000;93:1320–1328.
- 232g. Motulsky H, Christopoulos A. *Fitting Models to Biological Data using Linear and Nonlinear Regression. A Practical Guide to Curve Fitting*. New York: Oxford University Press; 2004:351.
- 232h. Huhle R, D'Antini D, Herrmann J, et al. Intratidal analysis of intraoperative respiratory system mechanics: keep it simple. *Anesth Analg*. 2018;126:725–726.
- 232i. Formenti P, Graf J, Santos A, et al. Non-pulmonary factors strongly influence the stress index. *Intensive Care Med*. 2011;37:594–600.
- 232j. Chiumello D, Gattinoni L. Stress index in presence of pleural effusion: does it have any meaning? *Intensive Care Med*. 2011;37:561–563.
- 232k. Henzler D, Hochhausen N, Dembinski R, Orfao S, Rossaint R, Kuhlen R. Parameters derived from the pulmonary pressure volume curve, but not the pressure time curve, indicate recruitment in experimental lung injury. *Anesth Analg*. 2007;105:1072–1078. table of contents.
233. Otis AB, McKerrow CB, Bartlett RA, et al. Mechanical factors in the distribution of pulmonary ventilation. *J Appl Physiol*. 1956;8:427–443.
- 233a. Kaczka DW, Cao K, Christensen GE, Bates JHT, Simon BA. Analysis of regional mechanics in canine lung injury using forced oscillations and 3D image registration. *Ann Biomed Eng*. 2011;39:1112–1124.
- 233b. Suki B, Bates JHT. Lung tissue mechanics as an emergent phenomenon. *J Appl Physiol* (1985). 2011;110:1111–1118.
- 233c. Carvalho AR, Jandre FC, Pino AV, et al. Positive end-expiratory pressure at minimal respiratory elastance represents the best compromise between mechanical stress and lung aeration in oleic acid induced lung injury. *Crit Care*. 2007;11:R86.
- 233d. Dellacà RL, Zannin E, Kostic P, et al. Optimisation of positive end-expiratory pressure by forced oscillation technique in a lavage model of acute lung injury. *Intensive Care Med*. 2011;37:1021–1030.
- 233e. Zannin E, Dellaca RL, Kostic P, et al. Optimizing positive end-expiratory pressure by oscillatory mechanics minimizes tidal recruitment and distension: an experimental study in a lavage model of lung injury. *Crit Care*. 2012;16:R217.
- 233f. Cavalcanti AB, Suzumura EA, et al. Effect of lung recruitment and titrated positive end-expiratory pressure (PEEP) vs low PEEP on mortality in patients with acute respiratory distress syndrome: a randomized clinical trial. *JAMA*. 2017;318:1335–1345.
- 233g. Fumagalli J, Berra L, Zhang C, et al. Transpulmonary pressure describes lung morphology during decremental positive end-expiratory pressure trials in obesity. *Crit Care Med*. 2017;45(8):1374–1381.
234. Mead J. Measurement of inertia of the lungs at increased ambient pressure. *J Appl Physiol*. 1956;9:208–212.
235. Hager DN, Fessler HE, Kaczka DW, et al. Tidal volume delivery during high-frequency oscillatory ventilation in adults with acute respiratory distress syndrome. *Crit Care Med*. 2007;35:1522–1529.
- 235a. Kaczka DW, Herrmann J, Zonneveld CE, et al. Multifrequency oscillatory ventilation in the premature lung: effects on gas exchange, mechanics, and ventilation distribution. *Anesthesiology*. 2015;123:1394–1403.
- 235b. Amini R, Kaczka DW. Impact of ventilation frequency and parenchymal stiffness on flow and pressure distribution in a canine lung model. *Ann Biomed Eng*. 2013;41:2699–2711.
236. Kaczka DW, Barnas GM, Suki B, Lutchen KR. Assessment of time-domain analyses for estimation of low-frequency respiratory mechanical properties and impedance spectra. *Ann Biomed Eng*. 1995;23:135–151.
237. Peslin R, Felicio de Silva J, Chabot F, Duvivier C. Respiratory mechanics studied by multiple linear regression in unsedated ventilated patients. *Eur Respir J*. 1992;5:871–878.
238. Ruiz-Ferron F, Rucabado Aguilar L, Ruiz Navarro S, Ramirez Puerta R, Parra Alonso S, Munoz Munoz JL. Results of respiratory mechanics analysis in the critically ill depend on the method employed. *Intensive Care Med*. 2001;27:1487–1495.
239. Kaczka DW, Ingenito EP, Body SC, et al. Inspiratory lung impedance in COPD: effects of PEEP and immediate impact of lung volume reduction surgery. *J Appl Physiol*. 2001;90:1833–1841.
240. Kaczka DW, Cao K, Christensen GE, Bates JHT, Simon BA. Analysis of regional mechanics in canine lung injury using forced oscillations and 3D image registration. *Ann Biomed Eng*. 2011;39:1112–1124.
241. Downie JM, Nam AJ, Simon BA. Pressure-volume curve does not predict steady-state lung volume in canine lavage lung injury. *Am J Respir Crit Care Med*. 2004;169:957–962.
242. Lu Q, Rouby JJ. Measurement of pressure-volume curves in patients on mechanical ventilation: methods and significance. *Critical Care*. 2000;4:91–100.
243. Salazar E, Knowles JH. An analysis of pressure-volume characteristics of the lungs. *J Appl Physiol*. 1964;19:97–104.
244. Venegas JG, Harris RS, Simon BA. A comprehensive equation for pulmonary pressure-volume curve. *J Appl Physiol*. 1998;84:389–395.
245. Mead J, Whittenberger JL, Radford EP Jr. Surface tension as a factor in pulmonary hysteresis. *J Appl Physiol*. 1957;10:191–196.

246. Bates JH, Irvin CG. Time dependence of recruitment and derecruitment in the lung: a theoretical model. *J Appl Physiol*. 2002;93:705–713.
247. Hildebrandt J. Pressure-volume data of the cat determined by a plastic elastic, linear viscoelastic model. *J Appl Physiol*. 1970;28:365–372.
248. Otis AB, Fenn WO, Rahn H. Mechanics of breathing in man. *J Appl Physiol*. 1950;2:592–607.
249. Bates JHT, Milic-Emili J. Influence of the viscoelastic properties of the respiratory system on the energetically optimum breathing frequency. *Ann Biomed Eng*. 1993;21:489–499.
- 249a. Moraes L, Silva PL, Thompson A, et al. Impact of different tidal volume levels at low mechanical power on ventilator-induced lung injury in rats. *Front Physiol*. 2018;9:318.
- 249b. Cressoni M, Gotti M, Chiurazzi C, et al. Mechanical power and development of ventilator-induced lung injury. *Anesthesiology*. 2016;124:1100–1108.
- 249c. Gattinoni L, Tonetti T, Cressoni M, et al. Ventilator-related causes of lung injury: the mechanical power. *Intensive Care Med*. 2016;42:1567–1575.
- 249d. Santos RS, Maia LA, Oliveira MV, et al. Biologic impact of mechanical power at high and low tidal volumes in experimental mild acute respiratory distress syndrome. *Anesthesiology*. 2018;128:1193–1206.
250. Masselli GM, Silvestri S, Sciuto SA, Cappa P. Circuit compliance compensation in lung protective ventilation. *Conf Proc IEEE Eng Med Biol Soc*. 2006;1:5603–5606.
251. Jensen A, Lutchen KR, Kaczka DW, Sanborn W, Isaza F. Estimation of respiratory dynamic mechanical properties during clinically used mechanical ventilation. *Proceedings of the First Joint BMES/EMBS Conference*, 1999. 1999;1:337.
252. Lancaster CT, Boyle PM, Kaczka DW. Delivered tidal volume from the fabius gs depends upon breathing circuit configuration despite compliance compensation. *Proceedings of the American Society of Anesthesiologist 2005 Annual Meeting*. 2005;A863.
253. Loring SH, O'Donnell CR, Behazin N, et al. Esophageal pressures in acute lung injury: do they represent artifact or useful information about transpulmonary pressure, chest wall mechanics, and lung stress? *J Appl Physiol*. 2010;108:512–522.
- 253a. Akoumianaki E, Maggiore SM, Valenza F, et al. The application of esophageal pressure measurement in patients with respiratory failure. *Am J Respir Crit Care Med*. 2014;189:520–531.
254. Schuessler TF, Gottfried SB, Goldberg P, Kearney RE, Bates JHT. An adaptive filter to reduce cardiogenic oscillations on esophageal pressure signals. *Ann Biomed Eng*. 1998;26:260–267.
255. Hager DN, Brower RG. Customizing lung-protective mechanical ventilation strategies. *Critical Care Med*. 2006;34:1544–1555.
256. Talmor D, Sarge T, Malhotra A, et al. Mechanical ventilation guided by esophageal pressure in acute lung injury. *N Engl J Med*. 2008;359:2095–2104.
- 256a. Eichler L, Truskowska K, Dupree A, Busch P, Goetz AE, Zollner C. Intraoperative ventilation of morbidly obese patients guided by transpulmonary pressure. *Obes Surg*. 2018;28:122–129.
257. Schultz MJ, Haitsma JJ, Slutsky AS, Gajic O. What tidal volumes should be used in patients without acute lung injury? *Anesthesiology*. 2007;106:1226–1231.
- 257a. Mauri T, Yoshida T, Bellani G, et al. Esophageal and transpulmonary pressure in the clinical setting: meaning, usefulness and perspectives. *Intensive Care Med*. 2016;42:1360–1373.
- 257b. Yoshida T, Amato MBP, Grieco DL, et al. Esophageal manometry and regional transpulmonary pressure in lung injury. *Am J Respir Crit Care Med*. 2018;197:1018–1026.
- 257c. Amato MB, Meade MO, Slutsky AS, et al. Driving pressure and survival in the acute respiratory distress syndrome. *N Engl J Med*. 2015;372:747–755.
- 257d. Bugeo G, Retamal J, Bruhn A. Driving pressure: a marker of severity, a safety limit, or a goal for mechanical ventilation? *Crit Care*. 2017;21:199.
258. Ladha K, Vidal Melo MF, McLean DJ, et al. Intraoperative protective mechanical ventilation and risk of postoperative respiratory complications: hospital based registry study. *BMJ*. 2015;351:h3646.
259. Neto AS, Hemmes SN, Barbas CS, et al. PROVE Network Investigators. Association between driving pressure and development of postoperative pulmonary complications in patients undergoing mechanical ventilation for general anaesthesia: a meta-analysis of individual patient data. *Lancet Respir Med*. 2016;4:272–280.
260. Laghi F, Goyal A. Auto-PEEP in respiratory failure. *Minerva Anestesiol*. 2012;78:201–221.
261. Brochard L. Intrinsic (or auto-) positive end-expiratory pressure during spontaneous or assisted ventilation. *Intensive Care Med*. 2002;28:1552–1554.
262. McCall CB, Hyatt RE, Noble FW, Fry DL. Harmonic content of certain respiratory flow phenomena of normal individuals. *J Appl Physiol*. 1957;10:215–218.
263. Lutchen KR, Kaczka DW, Suki B, Barnas G, Cevenini G, Barbini P. Low-frequency respiratory mechanics using ventilator-driven forced oscillations. *J Appl Physiol*. 1993;75:2549–2560.
264. Jackson AC, Vinegar A. A technique for measuring frequency response of pressure, volume, and flow transducers. *J Appl Physiol*. 1979;47:462–467.
265. Schuessler TF, Bates JHT. A computer-controlled research ventilator for small animals: design and evaluation. *IEEE Trans Biomed Eng*. 1995;42:860–866.
266. Schuessler TF, Bates JHT, Maksym GN. Estimating tracheal flow in small animals. *Engineering in Medicine and Biology Society*, 1993. *Proceedings of the 15th Annual International Conference of the IEEE*. 1993:560–561.
267. Simon BA, Mitzner W. Design and calibration of a high-frequency oscillatory ventilator. *IEEE Trans Biomed Eng*. 1991;38:214–218.
268. Sullivan WJ, Peters GM, Enright PL. Pneumotachographs: theory and clinical application. *Respiratory Care*. 1984;29:736–749.
269. Yeh MP, Gardner RM, Adams TD, Yanowitz FG. Computerized determination of pneumotachometer characteristics using a calibrated syringe. *J Appl Physiol*. 1982;53:280–285.
270. Renzi PE, Giurdanella CA, Jackson AC. Improved frequency response of pneumotachometers by digital compensation. *J Appl Physiol*. 1990;68:382–386.
271. Jaffe MB. Continuous monitoring of respiratory flow and CO₂: challenges of on-airway measurements. *IEEE Eng Med Biol Mag*. 2010;29:44–52.
272. Plakk P, Liik P, Kingisepp PH. Hot-wire anemometer for spirometry. *Med Biol Eng Comput*. 1998;36:17–21.
273. Ligeza P. Construction and experimental testing of the constant-bandwidth constant-temperature anemometer. *Rev Sci Instrum*. 2008;79:096105.
274. Al-Salaymeh A, Jovanović J, Durst F. Bi-directional flow sensor with a wide dynamic range for medical applications. *Med Eng Phys*. 2004;26:623–637.
275. Ligeza P. Constant-bandwidth constant-temperature hot-wire anemometer. *Rev Sci Instrum*. 2007;78:075104.
276. Hager DN, Fuld M, Kaczka DW, Fessler HE, Brower RG, Simon BA. Four methods of measuring tidal volume during high-frequency oscillatory ventilation. *Critical Care Med*. 2006;34:751–757.
- 276a. Mondonedo JR, Herrmann J, McNeil JS, Kaczka DW. Comparison of pneumotachography and anemometry for flow measurement during mechanical ventilation with volatile anesthetics. *J Clin Monit Comput*. 2017;31:1263–1271.
- 276b. Farre R, Rotger M, Navajas D. Time-domain digital filter to improve signal-to-noise ratio in respiratory impedance measurements. *Med Biol Eng Comput*. 1991;29:18–24.
- 276c. Jandre FC, Carvalho ARS, Pino AV, Giannella-Neto A. Effects of filtering and delays on the estimates of a nonlinear respiratory mechanics model. *Respir Physiol Neurobiol*. 2005;148:309–314.
277. Schmolzer GM, Kamlin OC, Dawson JA, te Pas AB, Morley CJ, Davis PG. Respiratory monitoring of neonatal resuscitation. *Arch Dis Child Fetal Neonatal Ed*. 2010;95:F295–303.
278. Wolf GK, Arnold JH. Noninvasive assessment of lung volume: respiratory inductance plethysmography and electrical impedance tomography. *Crit Care Med*. 2005;33:S163–S169.
279. Stick SM, Ellis E, LeSouef PN, Sly PD. Validation of respiratory inductance plethysmography ("Respirtrace") for the measurement of tidal breathing parameters in newborns. *Pediatr Pulmonol*. 1992;14:187–191.
280. van Vonderen JJ, Lista G, Cavigioli F, Hooper SB, te Pas AB. Effectivity of ventilation by measuring expired CO₂ and RIP during stabilisation of preterm infants at birth. *Arch Dis Child Fetal Neonatal Ed*. 2015;100:F514–F518.

281. Khemani RG, Hotz J, Morzov R, et al. Evaluating risk factors for pediatric post-extubation upper airway obstruction using a physiology-based tool. *Am J Respir Crit Care Med.* 2016;193:198–209.
282. Atkins JH, Mandel JE, Weinstein GS, Mirza N. A pilot study of respiratory inductance plethysmography as a safe, noninvasive detector of jet ventilation under general anesthesia. *Anesth Analg.* 2010;111:1168–1175.
283. Greenstein YY, Shakespeare E, Doelken P, Mayo PH. Defining a ventilation strategy for flexible bronchoscopy on mechanically ventilated patients in the medical intensive care unit. *J Bronchology Interv Pulmonol.* 2017;24:206–210.
284. Mandel JE, Atkins JH. Hilbert-Huang transform yields improved minute volume estimates from respiratory inductance plethysmography during transitions to paradoxical breathing. *Anesth Analg.* 2016;122:126–131.
285. Overdyk FJ, Carter R, Maddox RR, Callura J, Herrin AE, Henriquez C. Continuous oximetry/capnometry monitoring reveals frequent desaturation and bradypnea during patient-controlled analgesia. *Anesth Analg.* 2007;105:412–418.
286. Walther-Larsen S, Rasmussen LS. The former preterm infant and risk of post-operative apnoea: recommendations for management. *Acta Anaesthesiol Scand.* 2006;50:888–893.
287. Folke M, Cernerud L, Ekstrom M, Hok B. Critical review of non-invasive respiratory monitoring in medical care. *Med Biol Eng Comput.* 2003;41:377–383.
288. Al-Khalidi FQ, Saatchi R, Burke D, Elphick H, Tan S. Respiration rate monitoring methods: a review. *Pediatr Pulmonol.* 2011;46:523–529.
289. Wiklund L, Hok B, Stahl K, Jordeby-Jonsson A. Postanesthesia monitoring revisited: frequency of true and false alarms from different monitoring devices. *J Clin Anesth.* 1994;6:182–188.
290. Lam T, Nagappa M, Wong J, Singh M, Wong D, Chung F. Continuous pulse oximetry and capnography monitoring for postoperative respiratory depression and adverse events: a systematic review and meta-analysis. *Anesth Analg.* 2017;125:2019–2029.
- 290a. Meade MO, Young D, Hanna S, et al. Severity of hypoxemia and effect of high-frequency oscillatory ventilation in acute respiratory distress syndrome. *Am J Respir Crit Care Med.* 2017;196:727–733.
291. Gaucher A, Frasca D, Mimoz O, Debaene B. Accuracy of respiratory rate monitoring by capnometry using the Capnomask(R) in extubated patients receiving supplemental oxygen after surgery. *Br J Anaesth.* 2012;108:316–320.
292. Kasuya Y, Akca O, Sessler DL, Ozaki M, Komatsu R. Accuracy of postoperative end-tidal Pco_2 measurements with mainstream and sidestream capnography in non-obese patients and in obese patients with and without obstructive sleep apnea. *Anesthesiology.* 2009;111:609–615.
293. Chang KC, Orr J, Hsu WC, et al. Accuracy of CO_2 monitoring via nasal cannulas and oral bite blocks during sedation for esophagogastroduodenoscopy. *J Clin Monit Comput.* 2016;30:169–173.
294. Cashman JN, Dolin SJ. Respiratory and haemodynamic effects of acute postoperative pain management: evidence from published data. *Br J Anaesth.* 2004;93:212–223.
295. Walder B, Schafer M, Henzi I, Tramer MR. Efficacy and safety of patient-controlled opioid analgesia for acute postoperative pain. A quantitative systematic review. *Acta Anaesthesiol Scand.* 2001;45:795–804.
296. Shapiro A, Zohar E, Zaslansky R, Hoppenstein D, Shabat S, Friedman B. The frequency and timing of respiratory depression in 1524 postoperative patients treated with systemic or neuraxial morphine. *J Clin Anesth.* 2005;17:537–542.
297. Nassi N, Piumelli R, Lombardi E, Landini L, Donzelli G, de Martino M. Comparison between pulse oximetry and transthoracic impedance alarm traces during home monitoring. *Arch Dis Child.* 2008;93:126–132.
298. Lightdale JR, Goldmann DA, Feldman HA, Newburg AR, DiNardo JA, Fox VL. Microstream capnography improves patient monitoring during moderate sedation: a randomized, controlled trial. *Pediatrics.* 2006;117:e1170–e1178.
299. Waisman D, Levy C, Faingersh A, et al. A new method for continuous monitoring of chest wall movement to characterize hypoxic episodes during HFOV. *Intensive Care Med.* 2011;37:1174–1181.
300. Curry J, Lynn L. Threshold monitoring, alarm fatigue, and the patterns of unexpected hospital death. *APSF Newsletter.* 2011;26:32–35.
301. Gupta R, Edwards D. Monitoring for opioid-induced respiratory depression. *APSF Newsletter.* 2018;32:70–72.
302. Gupta K, Prasad A, Nagappa M, Wong J, Abrahamyan L, Chung FF. Risk factors for opioid-induced respiratory depression and failure to rescue: a review. *Curr Opin Anaesthesiol.* 2018;31:110–119.
303. Simon BA, Kaczka DW, Bankier AA, Parraga G. What can computed tomography and magnetic resonance imaging tell us about ventilation? *J Appl Physiol.* 2012;113:647–657.
304. Harris RS, Schuster DP. Visualizing lung function with positron emission tomography. *J Appl Physiol.* 2007;102:448–458.
305. Bodenstein M, David M, Markstaller K. Principles of electrical impedance tomography and its clinical application. *Crit Care Med.* 2009;37:713–724.
306. Turner JP, Dankoff J. Thoracic ultrasound. *Emerg Med Clin North Am.* 2012;30(451):73–ix.
307. Volpicelli G, Elbarbary M, Blaivas M, et al. International Liaison Committee on Lung Ultrasound (ILC-LUS) for International Consensus Conference on Lung Ultrasound (ICC-LUS). International evidence-based recommendations for point-of-care lung ultrasound. *Intensive Care Med.* 2012;38:577–591.
308. Kruisselbrink R, Chan V, Cibinel GA, Abrahamson S, Goffi A. I-AIM (Indication, Acquisition, Interpretation, Medical Decision-making) framework for point of care lung ultrasound. *Anesthesiology.* 2017;127:568–582.
309. Lichtenstein DA. BLUE-protocol and FALLS-protocol: two applications of lung ultrasound in the critically ill. *Chest.* 2015;147:1659–70.
310. Lichtenstein DA, Lascols N, Meziere G, Gepner A. Ultrasound diagnosis of alveolar consolidation in the critically ill. *Intensive Care Med.* 2004;30:276–281.
311. Lichtenstein D, Goldstein I, Mourgeon E, Cluzel P, Grenier P, Rouby JJ. Comparative diagnostic performances of auscultation, chest radiography, and lung ultrasonography in acute respiratory distress syndrome. *Anesthesiology.* 2004;100:9–15.
312. Lichtenstein DA. Ultrasound in the management of thoracic disease. *Crit Care Med.* 2007;35:S250–S261.
313. Lichtenstein D. Lung ultrasound in acute respiratory failure an introduction to the BLUE-protocol. *Minerva Anestesiol.* 2009;75:313–317.
314. Lichtenstein D, Meziere G, Biderman P, Gepner A. The “lung point”: an ultrasound sign specific to pneumothorax. *Intensive Care Med.* 2000;26:1434–1440.
315. Lichtenstein DA, Meziere GA. Relevance of lung ultrasound in the diagnosis of acute respiratory failure: the BLUE protocol. *Chest.* 2008;134:117–125.
316. Adler A, Amato MB, Arnold JH, et al. Whither lung EIT: where are we, where do we want to go and what do we need to get there? *Physiol Meas.* 2012;33:679–694.
317. Costa EL, Lima RG, Amato MB. Electrical impedance tomography. *Curr Opin Crit Care.* 2009;15:18–24.
318. Hahn G, Just A, Dudykevych T, et al. Imaging pathologic pulmonary air and fluid accumulation by functional and absolute EIT. *Physiol Meas.* 2006;27:S187–S198.
319. Frerichs I, Amato MB, van Kaam AH, et al. TRENDS study group. Chest electrical impedance tomography examination, data analysis, terminology, clinical use and recommendations: consensus statement of the TRAnslational EIT developmeNt stuDy group. *Thorax.* 2017;72:83–93.
320. Humphreys S, Pham TM, Stocker C, Schibler A. The effect of induction of anesthesia and intubation on end-expiratory lung level and regional ventilation distribution in cardiac children. *Paediatr Anaesth.* 2011;21:887–893.
321. Victorino JA, Borges JB, Okamoto VN, et al. Imbalances in regional lung ventilation: a validation study on electrical impedance tomography. *Am J Respir Crit Care Med.* 2004;169:791–800.
322. Radke OC, Schneider T, Heller AR, Koch T. Spontaneous breathing during general anesthesia prevents the ventral redistribution of ventilation as detected by electrical impedance tomography: a randomized trial. *Anesthesiology.* 2012;116:1227–1234.
323. Frerichs I, Achtzehn U, Pechmann A, et al. High-frequency oscillatory ventilation in patients with acute exacerbation of chronic obstructive pulmonary disease. *J Crit Care.* 2012;27:172–181.
324. Karsten J, Luepschen H, Grossherr M, et al. Effect of PEEP on regional ventilation during laparoscopic surgery monitored by electrical impedance tomography. *Acta Anaesthesiol Scand.* 2011;55:878–886.

325. Costa EL, Borges JB, Melo A, et al. Bedside estimation of recruitable alveolar collapse and hyperdistension by electrical impedance tomography. *Intensive Care Med.* 2009;35:1132–1137.
326. Nestler C, Simon P, Petroff D, et al. Individualized positive end-expiratory pressure in obese patients during general anaesthesia: a randomized controlled clinical trial using electrical impedance tomography. *Br J Anaesth.* 2017;119:1194–1205.
327. Costa EL, Chaves CN, Gomes S, et al. Real-time detection of pneumothorax using electrical impedance tomography. *Crit Care Med.* 2008;36:1230–1238.
328. Borges JB, Suarez-Sipmann F, Bohm SH, et al. Regional lung perfusion estimated by electrical impedance tomography in a piglet model of lung collapse. *J Appl Physiol.* 2012;112:225–236.
329. Kok J, Ng J, Li SC, et al. Evaluation of point-of-care testing in critically unwell patients: comparison with clinical laboratory analysers and applicability to patients with Ebolavirus infection. *Pathology.* 2015;47:405–409.
330. Leino A, Kurvinen K. Interchangeability of blood gas, electrolyte and metabolite results measured with point-of-care, blood gas and core laboratory analyzers. *Clin Chem Lab Med.* 2011;49:1187–1191.
331. Luukkonen AA, Lehto TM, Hedberg PS, Vaskivuo TE. Evaluation of a hand-held blood gas analyzer for rapid determination of blood gases, electrolytes and metabolites in intensive care setting. *Clin Chem Lab Med.* 2016;54:585–594.
332. Hopfer SM, Nadeau FL, Sundra M, Makowski GS. Effect of protein on hemoglobin and hematocrit assays with a conductivity-based point-of-care testing device: comparison with optical methods. *Ann Clin Lab Sci.* 2004;34:75–82.
333. Gayat E, Imbert N, Roujansky A, Lemasle L, Fischler M. Influence of fraction of inspired oxygen on noninvasive hemoglobin measurement: parallel assessment of 2 monitors. *Anesth Analg.* 2017;124:1820–1823.
334. Allardet-Servent J, Lebsir M, Dubroca C, et al. Point-of-care versus central laboratory measurements of hemoglobin, hematocrit, glucose, bicarbonate and electrolytes: a prospective observational study in critically ill patients. *PLoS One.* 2017;12:e0169593.
335. Van de Louw A, Lasserre N, Drouhin F, et al. Reliability of HemoCue in patients with gastrointestinal bleeding. *Intensive Care Med.* 2007;33:355–358.
336. Seguin P, Kleiber A, Chanavaz C, Morcet J, Maledant Y. Determination of capillary hemoglobin levels using the HemoCue system in intensive care patients. *J Crit Care.* 2011;26:423–427.
337. Wax DB, Reich DL. Changes in utilization of intraoperative laboratory testing associated with the introduction of point-of-care testing devices in an academic department. *Anesth Analg.* 2007;105(3):1711. table of contents.
338. Chang HK. Mechanisms of gas transport during ventilation by high-frequency oscillation. *J Appl Physiol.* 1984;56:553–563.
339. Pillow JJ. High-frequency oscillatory ventilation: mechanisms of gas exchange and lung mechanics. *Critical Care Med.* 2005;33:S135–S141.
340. Fredberg JJ. Augmented diffusion in the airways can support pulmonary gas exchange. *J Appl Physiol.* 1980;49:232–238.
341. Hurst JM, Branson RD, Davis K, Barrette RR, Adams KS. Comparison of conventional mechanical ventilation and high-frequency ventilation: a prospective, randomized trial in patients with respiratory failure. *Ann Surg.* 1990;211:486–491.
342. Venegas JG, Hales CA, Strieder DJ. A general dimensionless equation of gas transport by high-frequency ventilation. *Journal of Applied Physiology.* 1986;60:1025–1030.
- 342a. Herrmann J, Tawhai MH, Kaczka DW. Regional gas transport in the heterogeneous lung during oscillatory ventilation. *J Appl Physiol (1985).* 2016;121:1306–1318.
343. Pillow JJ. Tidal volume, recruitment and compliance in HFOV: same principles, different frequency. *Eur Respir J.* 2012;40:291–293.
344. Courtney SE, Durand DJ, Asselin JM, Hudak ML, Aschner JL, Shoemaker CT. High-frequency oscillatory ventilation versus conventional mechanical ventilation for very-low-birth-weight infants. *N Engl J Med.* 2002;347:643–652.
345. Johnson AH, Peacock JL, Greenough A, et al. Group United Kingdom Oscillation Study. High-frequency oscillatory ventilation for the prevention of chronic lung disease of prematurity. *N Engl J Med.* 2002;347:633–642.
- 345a. Ferguson ND, Cook DJ, Guyatt GH, et al. High-frequency oscillation in early acute respiratory distress syndrome. *N Engl J Med.* 2013;368:795–805.
- 345b. Young D, Lamb SE, Shah S, et al. High-frequency oscillation for acute respiratory distress syndrome. *N Engl J Med.* 2013;368:806–813.
346. Fessler HE, Brower RG. Protocols for lung protective ventilation. *Critical Care Med.* 2005;33:S223–S227.
347. Fessler HE, Derdak S, Ferguson ND, et al. A protocol for high-frequency oscillatory ventilation in adults: results from a round-table discussion. *Critical Care Med.* 2007;35:1649–1654.
348. Krishman JA, Brower RG. High-frequency ventilation for acute lung injury and ARDS. *Chest.* 2000;118:795–807.
349. Ali S, Ferguson ND. High-frequency oscillatory ventilation in ALI/ARDS. *Crit Care Clin.* 2011;27:487–499.
350. Ip T, Mehta S. The role of high-frequency oscillatory ventilation in the treatment of acute respiratory failure in adults. *Curr Opin Crit Care.* 2012;18:70–79.
351. Custer JW, Ahmed A, Kaczka DW, et al. In vitro performance comparison of the Sensormedics 3100A and B high-frequency oscillatory ventilators. *Pediatr Crit Care Med.* 2011;12.
352. Pillow JJ, Wilkinson MH, Neil HL, Ramsden CA. In vitro performance characteristics of high-frequency oscillatory ventilators. *Am J Respir Crit Care Med.* 2001;164:1019–1024.
353. Kaczka DW, Lutchen KR. Servo-controlled pneumatic pressure oscillator for respiratory impedance measurements and high frequency ventilation. *Ann Biomed Eng.* 2004;32:596–608.
354. Biro P. Jet ventilation for surgical interventions in the upper airway. *Anesthesia Clinics.* 2010;28:397–409.
355. Hess DR, Mason S, Branson R. High-frequency ventilation : design and equipment issues. *Respir Care Clin N Am.* 2001;7:577–598.
356. Kalenga M, Battisti O, François A, Langhendries JP, Gerstmann DR, Bertrand JM. High-frequency oscillatory ventilation in neonatal RDS: initial volume optimization and respiratory mechanics. *J Appl Physiol.* 1998;84:1174–1177.
357. Pillow JJ, Sly PD, Hantos Z. Monitoring of lung volume recruitment and derecruitment using oscillatory mechanics during high-frequency oscillatory ventilation in the preterm lamb. *Pediatr Crit Care Med.* 2004;5:172–180.
358. Pillow JJ, Sly PD, Hantos Z, Bates JHT. Dependence of intrapulmonary pressure amplitudes on respiratory mechanics during high-frequency oscillatory ventilation in preterm lambs. *Pediatric Research.* 2002;52:538–544.
- 358a. Harcourt ER, John J, Dargaville PA, Zannin E, Davis PG, Tingay DG. Pressure and flow waveform characteristics of eight high-frequency oscillators. *Pediatr Crit Care Med.* 2014.
- 358b. Tingay DG, John J, Harcourt ER, et al. Are all oscillators created equal? In vitro performance characteristics of eight high-frequency oscillatory ventilators. *Neonatology.* 2015;108:220–228.
359. Hager DN. High-frequency oscillatory ventilation in adults with acute respiratory distress syndrome. *Curr Opin Anesthesiol.* 2012;25:17–23.
360. Lucangelo U, Bernabe F, Blanch L. Capnography and adjuncts of mechanical ventilation. In: Gravenstein JS, Jaffe MB, Gravenstein N, Paulus DA, eds. *Capnography.* 2nd ed. Cambridge: Cambridge University Press; 2011:169, 181; 19.
361. Kil HK, Kim WO, Choi HS, Nam YT. Monitoring of PETCO₂ during high frequency jet ventilation for laryngomicrosurgery. *Yonsei Med J.* 2002;43:20–24.
362. Kugelman A, Riskin A, Shoris I, Ronen M, Stein IS, Bader D. Continuous integrated distal capnography in infants ventilated with high frequency ventilation. *Pediatr Pulmonol.* 2012;47:876–883.
363. Frietsch T, Kraft P, Becker HD, Buelzebruck H, Wiedemann K. Intermittent capnography during high-frequency jet ventilation for prolonged rigid bronchoscopy. *Acta Anaesthesiol Scand.* 2000;44:391–397.
364. Nishimura M, Imanaka H, Tashiro C, Taenaka N, Yoshiya I. Capnometry during high-frequency oscillatory ventilation. *Chest.* 1992;101:1681–1683.
365. Biro P, Eyrich G, Rohling RG. The efficiency of CO₂ elimination during high-frequency jet ventilation for laryngeal microsurgery. *Anesth Analg.* 1998;87:180–184.
- 365a. Herrmann J, Tawhai MH, Kaczka DW. Parenchymal strain heterogeneity during oscillatory ventilation: why two frequencies are better than one. *J Appl Physiol (1985).* 2018;124:653–663.

- 365b. Mehta PP, Kochhar G, Albeldawi M, et al. Capnographic monitoring in routine egd and colonoscopy with moderate sedation: a prospective, randomized, controlled trial. *Am J Gastroenterol*. 2016;111:395–404.
366. Evans KL, Keene MH, Bristow AS. High-frequency jet ventilation—a review of its role in laryngology. *J Laryngol Otol*. 1994;108:23–25.
367. Miodownik S, Ray C Jr, Carlon GC, Groeger JS, Howland WS. High-frequency jet ventilation: technical implications. *Crit Care Med*. 1984;12:718–720.
368. Algorta-Weber A, Rubio JJ, Dominguez de Villota E, Cortes JL, Gomez D, Mosquera JM. Simple and accurate monitoring of end-tidal carbon dioxide tensions during high-frequency jet ventilation. *Crit Care Med*. 1986;14:895–897.
369. Sehati S, Young JD, Sykes MK, McLeod CN. Monitoring of end-tidal carbon dioxide partial pressure during high frequency jet ventilation. *Br J Anaesth*. 1989;63:47S–52S.
370. Simon M, Gottschall R, Gugel M, Fritz H, Mohr S, Klein U. Comparison of transcutaneous and endtidal CO₂-monitoring for rigid bronchoscopy during high-frequency jet ventilation. *Acta Anaesthesiol Scand*. 2003;47:861–867.
371. Wallen E, Venkataraman ST, Grosso MJ, Kiene K, Orr RA. Intrahospital transport of critically ill pediatric patients. *Crit Care Med*. 1995;23:1588–1595.
372. Waydhas C, Schneck G, Duswald KH. Deterioration of respiratory function after intra-hospital transport of critically ill surgical patients. *Intensive Care Med*. 1995;21:784–789.
373. Bercault N, Wolf M, Runge I, Fleury JC, Boulain T. Intrahospital transport of critically ill ventilated patients: a risk factor for ventilator-associated pneumonia—a matched cohort study. *Crit Care Med*. 2005;33:2471–2478.
374. Nakamura T, Fujino Y, Uchiyama A, Mashimo T, Nishimura M. Intrahospital transport of critically ill patients using ventilator with patient-triggering function. *Chest*. 2003;123:159–164.
375. Kue R, Brown P, Ness C, Scheulen J. Adverse clinical events during intrahospital transport by a specialized team: a preliminary report. *Am J Crit Care*. 2011;20(15):61, quiz 162.
376. Prodhan P, Fiser RT, Cenac S, et al. Intrahospital transport of children on extracorporeal membrane oxygenation: indications, process, interventions, and effectiveness. *Pediatr Crit Care Med*. 2010;11:227–233.
377. Szem JW, Hydo LJ, Fischer E, Kapur S, Klemperer J, Barie PS. High-risk intrahospital transport of critically ill patients: safety and outcome of the necessary “road trip”. *Crit Care Med*. 1995;23:1660–1666.
378. Tobias JD, Lynch A, Garrett J. Alterations of end-tidal carbon dioxide during the intrahospital transport of children. *Pediatr Emerg Care*. 1996;12:249–251.
379. Ansermino JM, Daniels JP, Hewgill RT, et al. An evaluation of a novel software tool for detecting changes in physiological monitoring. *Anesth Analg*. 2009;108:873–880.
380. Lee J, Scott DJ, Villarreal M, Clifford GD, Saeed M, Mark RG. Open-access MIMIC-II database for intensive care research. *Conf Proc IEEE Eng Med Biol Soc*. 2011;2011:8315–8318.
381. Saeed M, Villarreal M, Reisner AT, et al. Multiparameter Intelligent Monitoring in Intensive Care II: a public-access intensive care unit database. *Crit Care Med*. 2011;39:952–960.
382. Imhoff M, Kuhls S. Alarm algorithms in critical care monitoring. *Anesth Analg*. 2006;102:1525–1537.
383. Melek WW, Lu Z, Kapps A, Fraser WD. Comparison of trend detection algorithms in the analysis of physiological time-series data. *IEEE Trans Biomed Eng*. 2005;52:639–651.
384. Simons DJ, Rensink RA. Change blindness: past, present, and future. *Trends Cogn Sci*. 2005;9:16–20.
385. Dosani M, Lim J, Yang P, et al. Clinical evaluation of algorithms for context-sensitive physiological monitoring in children. *Br J Anaesth*. 2009;102:686–691.
386. Schadler D, Engel C, Elke G, et al. Automatic control of pressure support for ventilator weaning in surgical intensive care patients. *Am J Respir Crit Care Med*. 2012;185:637–644.
387. Blount M, Ebling MR, Eklund JM, et al. Real-time analysis for intensive care: development and deployment of the artemis analytic system. *IEEE Eng Med Biol Mag*. 2010;29:110–118.
388. Chatburn RL, Mireles-Cabodevila E. Closed-loop control of mechanical ventilation: description and classification of targeting schemes. *Respir Care*. 2011;56:85–102.
389. Epstein RH, Dexter F. Implications of resolved hypoxemia on the utility of desaturation alerts sent from an anesthesia decision support system to supervising anesthesiologists. *Anesth Analg*. 2012.
390. Chiumello D, Cressoni M, Chierichetti M, et al. Nitrogen washout/washin, helium dilution and computed tomography in the assessment of end expiratory lung volume. *Crit Care*. 2008;12:R150.
391. Dellamonica J, Leroille N, Sargentini C, et al. Accuracy and precision of end-expiratory lung-volume measurements by automated nitrogen washout/washin technique in patients with acute respiratory distress syndrome. *Crit Care*. 2011;15:R294.
392. Pillow JJ, Frerichs I, Stocks J. Lung function tests in neonates and infants with chronic lung disease: global and regional ventilation inhomogeneity. *Pediatr Pulmonol*. 2006;41:105–121.
393. Tobias JD. Transcutaneous carbon dioxide monitoring in infants and children. *Paediatr Anaesth*. 2009;19:434–444.
394. Sorensen LC, Brage-Andersen L, Greisen G. Effects of the transcutaneous electrode temperature on the accuracy of transcutaneous carbon dioxide tension. *Scand J Clin Lab Invest*. 2011;71:548–552.
395. Sandberg KL, Brynjarsdóttir H, Hjalmarsson O. Transcutaneous blood gas monitoring during neonatal intensive care. *Acta Paediatr*. 2011;100:676–679.
396. Xue Q, Wu X, Jin J, Yu B, Zheng M. Transcutaneous carbon dioxide monitoring accurately predicts arterial carbon dioxide partial pressure in patients undergoing prolonged laparoscopic surgery. *Anesth Analg*. 2010;111:417–420.
397. Klopstein CE, Schiffer E, Pastor CM, et al. Laparoscopic colon surgery: unreliability of end-tidal CO₂ monitoring. *Acta Anaesthesiol Scand*. 2008;52:700–707.
398. De Oliveira GS Jr, Ahmad S, Fitzgerald PC, McCarthy RJ. Detection of hypoventilation during deep sedation in patients undergoing ambulatory gynaecological hysteroscopy: a comparison between transcutaneous and nasal end-tidal carbon dioxide measurements. *Br J Anaesth*. 2010;104:774–778.
399. Chakravarthy M, Narayan S, Govindarajan R, Jawali V, Rajeev S. Weaning mechanical ventilation after off-pump coronary artery bypass graft procedures directed by noninvasive gas measurements. *J Cardiothorac Vasc Anesth*. 2010;24:451–455.
400. Kelly AM, Klim S. Agreement between arterial and transcutaneous PCO₂ in patients undergoing non-invasive ventilation. *Respir Med*. 2011;105:226–229.
401. Spelten O, Fiedler F, Schier R, Wetsch WA, Hinkelbein J. Transcutaneous PTCCO₂ measurement in combination with arterial blood gas analysis provides superior accuracy and reliability in ICU patients. *J Clin Monit Comput*. 2017;31:153–158.
402. Yu M, Chapital A, Ho HC, Wang J, Takanishi D Jr. A prospective randomized trial comparing oxygen delivery versus transcutaneous pressure of oxygen values as resuscitative goals. *Shock*. 2007;27:615–622.
403. Chakravarthy M, Narayan S, Govindarajan R, Jawali V. Improvement in accuracy of transcutaneous measurement of oxygen with resumption of spontaneous ventilation in mechanically ventilated patients after off pump coronary artery bypass procedure: a prospective study. *J Clin Monit Comput*. 2009;23:363–368.
404. He HW, Liu DW, Long Y, Wang XT, Chai WZ, Zhou X. The transcutaneous oxygen challenge test: a noninvasive method for detecting low cardiac output in septic patients. *Shock*. 2012;37:152–155.
405. Yu M, Morita SY, Daniel SR, Chapital A, Waxman K, Severino R. Transcutaneous pressure of oxygen: a noninvasive and early detector of peripheral shock and outcome. *Shock*. 2006;26:450–456.
406. Michard F. Lung water assessment: from gravimetry to wearables. *J Clin Monit Comput*. 2018.
407. Pistolesi M, Giuntini C. Assessment of extravascular lung water. *Radiol Clin North Am*. 1978;16:551–574.
408. Rubenfeld GD, Caldwell E, Granton J, Hudson LD, Matthay MA. Interobserver variability in applying a radiographic definition for ARDS. *Chest*. 1999;116:1347–1353.
409. Meade MO, Cook RJ, Guyatt GH, et al. Interobserver variation in interpreting chest radiographs for the diagnosis of acute respiratory distress syndrome. *Am J Respir Crit Care Med*. 2000;161:85–90.

410. Sakka SG, Ruhl CC, Pfeiffer UJ, et al. Assessment of cardiac preload and extravascular lung water by single transpulmonary thermodilution. *Intensive Care Med*. 2000;26:180–187.
411. Isakow W, Schuster DP. Extravascular lung water measurements and hemodynamic monitoring in the critically ill: bedside alternatives to the pulmonary artery catheter. *Am J Physiol Lung Cell Mol Physiol*. 2006;291:L1118–L1131.
412. Martin GS, Eaton S, Mealer M, Moss M. Extravascular lung water in patients with severe sepsis: a prospective cohort study. *Crit Care*. 2005;9:R74–82.
413. Kuzkov VV, Kirov MY, Sovershaev MA, et al. Extravascular lung water determined with single transpulmonary thermodilution correlates with the severity of sepsis-induced acute lung injury. *Crit Care Med*. 2006;34:1647–1653.
414. Phillips CR, Chesnutt MS, Smith SM. Extravascular lung water in sepsis-associated acute respiratory distress syndrome: indexing with predicted body weight improves correlation with severity of illness and survival. *Crit Care Med*. 2008;36:69–73.
415. Fernandez-Mondejar E, Rivera-Fernandez R, Garcia-Delgado M, Touma A, Machado J, Chavero J. Small increases in extravascular lung water are accurately detected by transpulmonary thermodilution. *J Trauma*. 2005;59(3):1420. discussion 1424.
416. Assaad S, Shelley B, Perrino A. Transpulmonary thermodilution: its role in assessment of lung water and pulmonary edema. *J Cardiothorac Vasc Anesth*. 2017;31:1471–1480.
417. Stephan F, Mazeraud A, Laverdure F, Camous J, Fadel E. Evaluation of reperfusion pulmonary edema by extravascular lung water measurements after pulmonary endarterectomy. *Crit Care Med*. 2017;45:e409–e417.
418. Potticher J, Roche AC, Degot T, Groupe de Transplantation Pulmonaire des Hopitaux Universitaires de Strasbourg. Increased extravascular lung water and plasma biomarkers of acute lung injury precede oxygenation impairment in primary graft dysfunction after lung transplantation. *Transplantation*. 2017;101:112–121.
419. Michelet P, D'Journo XB, Roch A, et al. Protective ventilation influences systemic inflammation after esophagectomy: a randomized controlled study. *Anesthesiology*. 2006;105:911–919.
420. Mitchell JP, Schuller D, Calandino FS, Schuster DP. Improved outcome based on fluid management in critically ill patients requiring pulmonary artery catheterization. *Am Rev Respir Dis*. 1992;145:990–998.
421. Mutoh T, Kazumata K, Ishikawa T, Terasaka S. Performance of bedside transpulmonary thermodilution monitoring for goal-directed hemodynamic management after subarachnoid hemorrhage. *Stroke*. 2009;40:2368–2374.
422. von Spiegel T, Giannaris S, Wietasch GJ, et al. Effects of dexamethasone on intravascular and extravascular fluid balance in patients undergoing coronary bypass surgery with cardiopulmonary bypass. *Anesthesiology*. 2002;96:827–834.
423. Perkins GD, McAuley DF, Thickett DR, Gao F. The beta-agonist lung injury trial (BALTI): a randomized placebo-controlled clinical trial. *Am J Respir Crit Care Med*. 2006;173:281–287.
424. Licker M, Tschopp JM, Robert J, Frey JG, Diaper J, Ellenberger C. Aerosolized salbutamol accelerates the resolution of pulmonary edema after lung resection. *Chest*. 2008;133:845–852.
425. Effros RM, Pornsuriyasak P, Porszasz J, Casaburi R. Indicator dilution measurements of extravascular lung water: basic assumptions and observations. *Am J Physiol Lung Cell Mol Physiol*. 2008;294:L1023–L1031.
426. Easley RB, Mulreany DG, Lancaster CT, et al. Redistribution of pulmonary blood flow impacts thermodilution-based extravascular lung water measurements in a model of acute lung injury. *Anesthesiology*. 2009.
427. de Prost N, Costa EL, Wellman T, et al. Effects of surfactant depletion on regional pulmonary metabolic activity during mechanical ventilation. *J Appl Physiol*. 2011;111:1249–1258.
428. Roch A, Michelet P, Lambert D, et al. Accuracy of the double indicator method for measurement of extravascular lung water depends on the type of acute lung injury. *Crit Care Med*. 2004;32:811–817.
429. Carlile PV, Gray BA. Type of lung injury influences the thermal-dye estimation of extravascular lung water. *J Appl Physiol*. 1984;57:680–685.
430. Kuntscher MV, Czermak C, Blome-Eberwein S, Dacho A, Germann G. Transcardiopulmonary thermal dye versus single thermodilution methods for assessment of intrathoracic blood volume and extravascular lung water in major burn resuscitation. *J Burn Care Rehabil*. 2003;24:142–147.
431. Saugel B, Holzapfel K, Stollfuss J, et al. Computed tomography to estimate cardiac preload and extravascular lung water. A retrospective analysis in critically ill patients. *Scand J Trauma Resusc Emerg Med*. 2011;19:31.
432. Saugel B, Wildgruber M, Staudt A, et al. Quantitative computed tomography in comparison with transpulmonary thermodilution for the estimation of pulmonary fluid status: a clinical study in critically ill patients. *J Clin Monit Comput*. 2018.
433. Rossi P, Wanecek M, Rudehill A, Konrad D, Weitzberg E, Oldner A. Comparison of a single indicator and gravimetric technique for estimation of extravascular lung water in endotoxemic pigs. *Crit Care Med*. 2006;34:1437–1443.

KATHLEEN D. LIU, DANIEL H. BURKHARDT III, and RUPERT M. PEARSE

KEY POINTS

- The incidence of perioperative acute kidney injury (AKI) (previously referred to as acute renal failure) varies, depending on the definition used.
- Although uncommon, AKI requiring dialysis is associated with extremely high morbidity and mortality rates.
- The mechanism for perioperative AKI is complex and commonly involves multiple factors including ischemia-reperfusion injury, inflammation, and toxins.
- Repeated direct perioperative assessments of renal hemodynamics or tubular function are impractical; therefore indirect assessments, such as trends of serum creatinine concentrations, are the best practical perioperative tools to assess renal function.
- Intraoperative urine formation depends on many factors and is not validated as a measure of the risk of postoperative renal dysfunction. Yet postoperatively, patients with low intraoperative urine output may develop renal dysfunction. Therefore urine output should be carefully monitored in the intraoperative setting.
- Early biochemical markers for kidney injury may soon become new tests that can provide prompt clinical information.
- As part of preoperative risk assessment, both serum creatinine and proteinuria can provide important and useful information.
- Intraoperative hypotension and hypovolemia are significant risk factors for AKI.
- With regard to fluid management, the use of balanced salt solutions may reduce the risk of AKI. Volume overload is a risk factor for adverse outcomes in patients with AKI and may influence concentrations of conventional markers of kidney function such as serum creatinine.
- Renal replacement therapy may be indicated for severe AKI: at present, data does not support the use of one modality over another.

Introduction and Acute Kidney Injury Definitions

Acute kidney injury (AKI) (previously known as acute renal failure) is characterized by rapid decline in the glomerular filtration rate (GFR) and the accumulation of nitrogenous waste products (blood urea nitrogen [BUN] and creatinine). AKI occurs in approximately 5% to 25% of all hospitalized patients, depending on the precise definition used for AKI, and with more frequent rates in patients who are critically ill in the intensive care unit (ICU) (also see [Chapter 17](#)). AKI is also a serious perioperative complication for patients undergoing major surgery.¹⁻⁴ As the incidence of AKI varies by the definition used, the mortality of AKI ranges from 10% to 35% for mild AKI, whereas AKI in the ICU setting is associated with a 50% to 80% mortality rate. However, supportive care with dialysis has reduced mortality from AKI. Whereas the mortality rate of oliguric AKI was 91% during

World War II, mortality declined to 53% during the Korean War with the provision of dialysis.⁵ AKI requiring dialysis develops in 1% to 7% of patients after cardiac or major vascular surgery and is strongly associated with morbidity and mortality in this context.⁶⁻⁹

Perioperative renal failure was long defined as a requirement for postoperative dialysis. However, this concept has evolved during the past several years. First, because the implications of requiring postoperative dialysis are quite different for a patient starting with a normal baseline renal function compared with one starting with advanced chronic kidney disease and because the criteria for the use of dialysis are not standardized, the usefulness of dialysis alone to define AKI has been questioned. Second, studies are difficult to compare because of the use of nonstandard definitions for AKI. For example, in one review of 28 studies,¹⁰ definitions for perioperative AKI varied. Third, consensus definitions that focus on small changes in serum creatinine and on

TABLE 42.1 Comparison of the RIFLE, AKIN, and KDIGO Consensus Criteria for Acute Kidney Injury

RIFLE		AKIN		KDIGO	
Class	SCr	Stage	SCr	Stage	SCr
Risk	Increase in SCr to $>1.5 \times$ baseline	1	Increase in SCr $\geq 0.3 \text{ mg/dL}$ or to $\geq 1.5 \times 2 \times$ baseline	1	Increase in SCr $\geq 0.3 \text{ mg/dL}$ within 48 h or to $\geq 1.5 \times 2 \times$ baseline, which is known or presumed to have occurred within the past 7 days
Injury	Increase in SCr to $>2 \times$ baseline	2	Increase in SCr to $>2 \times 3 \times$ baseline	2	Increase in SCr to $>2 \times 3 \times$ baseline
Failure	Increase in SCr to $>3 \times$ baseline, or increase of $\geq 0.5 \text{ mg/dL}$ to absolute value of $\geq 4 \text{ mg/dL}$, or need for RRT	3	Increase in SCr to $>3 \times$ baseline, or increase of $\geq 0.5 \text{ mg/dL}$ to absolute value of $\geq 4 \text{ mg/dL}$, or need for RRT	3	Increase in SCr to $>3 \times$ baseline, or increase to absolute value of $\geq 4 \text{ mg/dL}$, or need for RRT; in pediatric patients eGFR $<35 \text{ mL/min/1.73 m}^2$
Loss	Need for RRT >4 weeks				
End stage	Need for RRT >3 months				

^aIs common to all three consensus criteria.

The three consensus criteria use the same urine output criteria, but slight differences in the creatinine criteria are used to define AKI.

AKI, Acute kidney injury; AKIN, acute kidney injury network; eGFR, estimated glomerular filtration rate; KDIGO, kidney disease: improving global outcomes; RIFLE, risk, injury, failure, loss, end-stage disease; RRT, renal replacement therapy; SCr, serum creatinine.

changes in urine output to define AKI have received widespread adoption. This last conclusion is based on the recognition that small changes in renal function directly relate to an increased risk of death.¹¹

As a result, recent consensus criteria are being used to define AKI in both the perioperative and other medical settings. The first proposed consensus criteria were the RIFLE (Risk, Injury, Failure, Loss, End-stage) kidney disease criteria developed by the Acute Dialysis Quality Initiative (Table 42.1).¹² These have subsequently undergone two modifications by the Acute Kidney Injury Network¹³ and in the Kidney Disease: Improving Global Outcomes (KDIGO) AKI guidelines.¹⁴ As detailed in Table 42.1, the central components of these criteria are the focus on relative and absolute changes in creatinine from a baseline value and the definition of several degrees of AKI severity. Consequently, milder AKI (e.g., KDIGO, stage 1 disease) will be more common than stage 3 disease and will also be associated with a lower mortality rate. These criteria have also proposed definitions for AKI based on urine output. Overall, although there are studies demonstrating that AKI defined based on urine output is associated with adverse outcomes in the critical care setting and is more common than AKI defined based on creatinine,¹⁵ the urine output criteria are not as well validated. At present, there is no clear method to correct urine output for morbid obesity; in addition, urine output may be unmeasurable if a urinary bladder catheter is not present.¹⁶ Not surprisingly, AKI by urine output criteria is substantially more common than AKI by creatinine-based criteria; in a study of more than 4000 subjects undergoing major noncardiac surgery, the incidence of AKI increased from 8% to 64% when urine output criteria were incorporated.¹⁷ Although each AKI stage was associated with an increased risk of death, the association with mortality was attenuated in this analysis when urine output criteria for AKI were used. Finally, it should be noted that the importance of oliguria ($<0.5 \text{ mL/kg/h}$) as a predictor of creatinine-based AKI is less well established in the perioperative setting than in other clinical settings.^{18,19} In a recent large

single-center observational study, urine output of less than 0.3 mL/kg/h during major abdominal surgery was associated with an increased risk of perioperative AKI (defined as a 0.3 mg/dL rise in serum creatinine within 48 hours or a 50% increase over 7 days from baseline).²⁰ However, urine output within the 0.3 to 0.5 mL/kg/h range was not associated with creatinine-based AKI.

Additional challenges for the identification of AKI in the intraoperative setting include large blood volume loss and fluid shifts, which may artificially dilute serum creatinine. Unlike the postoperative or critical care setting where renal monitoring can involve periodic evaluation of kidney function under relatively stable conditions, intraoperative renal monitoring involves a briefer unstable period, often involving significant blood loss, major fluid shifts, wide hemodynamic fluctuations, and even direct compromise to renal artery blood flow. Therefore the anesthesia provider is likely the first monitor (in a sense) required for preserving renal function by recognizing and treating factors that may contribute to or exacerbate AKI; for example, the toxic effects of aminoglycosides and iodinated contrast materials are exacerbated by intravascular volume depletion.

As medical populations shift toward older and more critically ill patients undergoing increasingly high-risk procedures, patients are at an increased risk of AKI in the perioperative setting, and the role of the anesthesia provider becomes even more critical. Indeed, a recent study of dialysis after elective major surgery suggests that the incidence of dialysis-requiring AKI is rising from 0.2% in 1995 to 0.6% in 2009, with the majority of the increase occurring after vascular and cardiac surgery.²¹ Although ischemic causes may be primarily responsible for perioperative AKI,^{22,23} the successful development of renoprotective strategies has not occurred. Furthermore, other pathophysiologic contributors to perioperative AKI may include contrast-induced nephropathy, pigment nephropathy (e.g., hemoglobin, myoglobin), cholesterol emboli (e.g., atheroembolic renal disease), aminoglycoside toxicity, and sepsis. Animal studies of such pure nephropathies treated

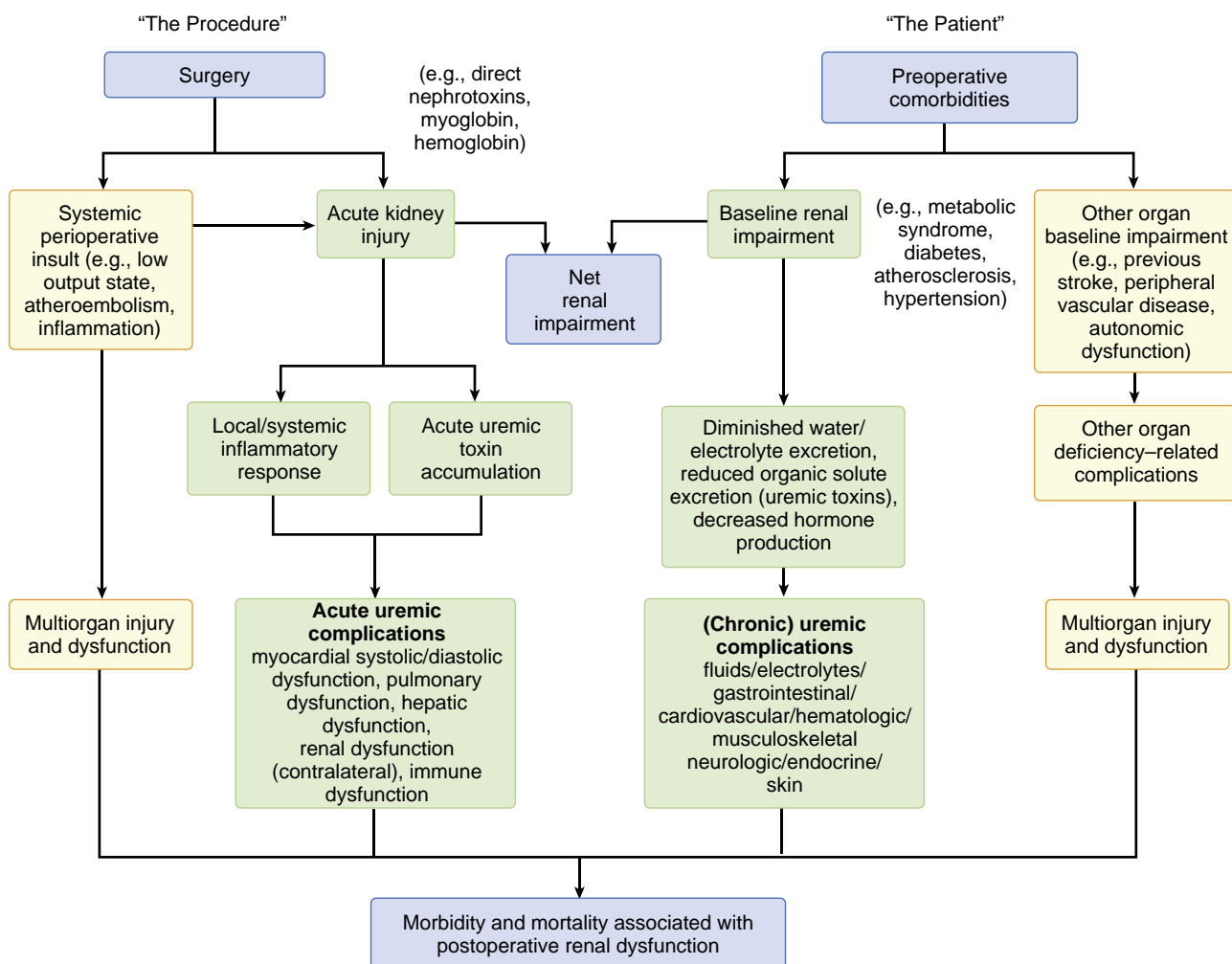


Fig. 42.1 Procedural and patient factors related to surgery contributing to the risk of perioperative acute kidney injury (AKI) and postoperative morbidity and mortality. Of note, although AKI contributes to the risk of morbidity and mortality, a significant part of this association must also be attributed to other very serious conditions, such as sepsis, that can cause injury and are also major sources of adverse outcomes. (Modified from Stafford-Smith M, Patel U, Phillips-Bute B, et al. Acute kidney injury and chronic kidney disease after cardiac surgery. *Adv Chronic Kid Dis*. 2008;15:157–177. Used with permission.)

with logical renoprotective interventions often demonstrate success; unfortunately, this success has not extended to equivalent renoprotection in humans. It may not be surprising that a specific treatment for a pure nephropathy nonselectively applied to a mixture of nephropathies, variably expressed in different patients, would be unsuccessful. Postoperative AKI, rather than being a single entity, is likely a mosaic of several pure nephropathies, each of varying importance for a particular patient and procedure (Fig. 42.1).

Pathophysiologic Processes of Ischemic Acute Kidney Injury

In general, the causes for AKI can be divided into prerenal, intrinsic renal, and postrenal sources. In the perioperative setting, patients may be at increased risk for prerenal AKI, either attributable to volume depletion or to exacerbation of associated chronic prerenal physiologic conditions, such as congestive heart failure, which may be exacerbated by volume overload. Intraoperatively, hypotension due to vasodilation and negative inotropy/chronotropy from anesthetic

agents may lead to prerenal physiology. Depending on the nature of the surgical procedure, the patient may also be at increased risk of postrenal AKI attributable to obstruction of the ureters, bladder, or urethra. However, the primary cause of perioperative AKI is *acute tubular necrosis* (ATN). Defining the cause of AKI is also critical because treatment of the underlying cause is critical for the reversal of AKI and potential renal recovery.

The two primary mechanisms of ATN are ischemia-reperfusion and nephrotoxic effects, with three sources of insult common to many surgical procedures during which postoperative AKI is prevalent: hypoperfusion, inflammation, and atheroembolism. Other sources of renal insult in selected patients may include rhabdomyolysis and specific drug-related effects. Certain classes of medications may also contribute to hypoperfusion by virtue of their hemodynamic effects (notably angiotensin-converting enzyme [ACE] inhibitor 1, angiotensin-receptor blockers [ARBs], and nonsteroidal antiinflammatory drugs [NSAIDs]), and, consequently, the risk of ATN.

Ischemic renal failure related to shock or severe dehydration is always preceded by an early compensatory phase of normal renal adaptation (e.g., pre-prerenal failure),

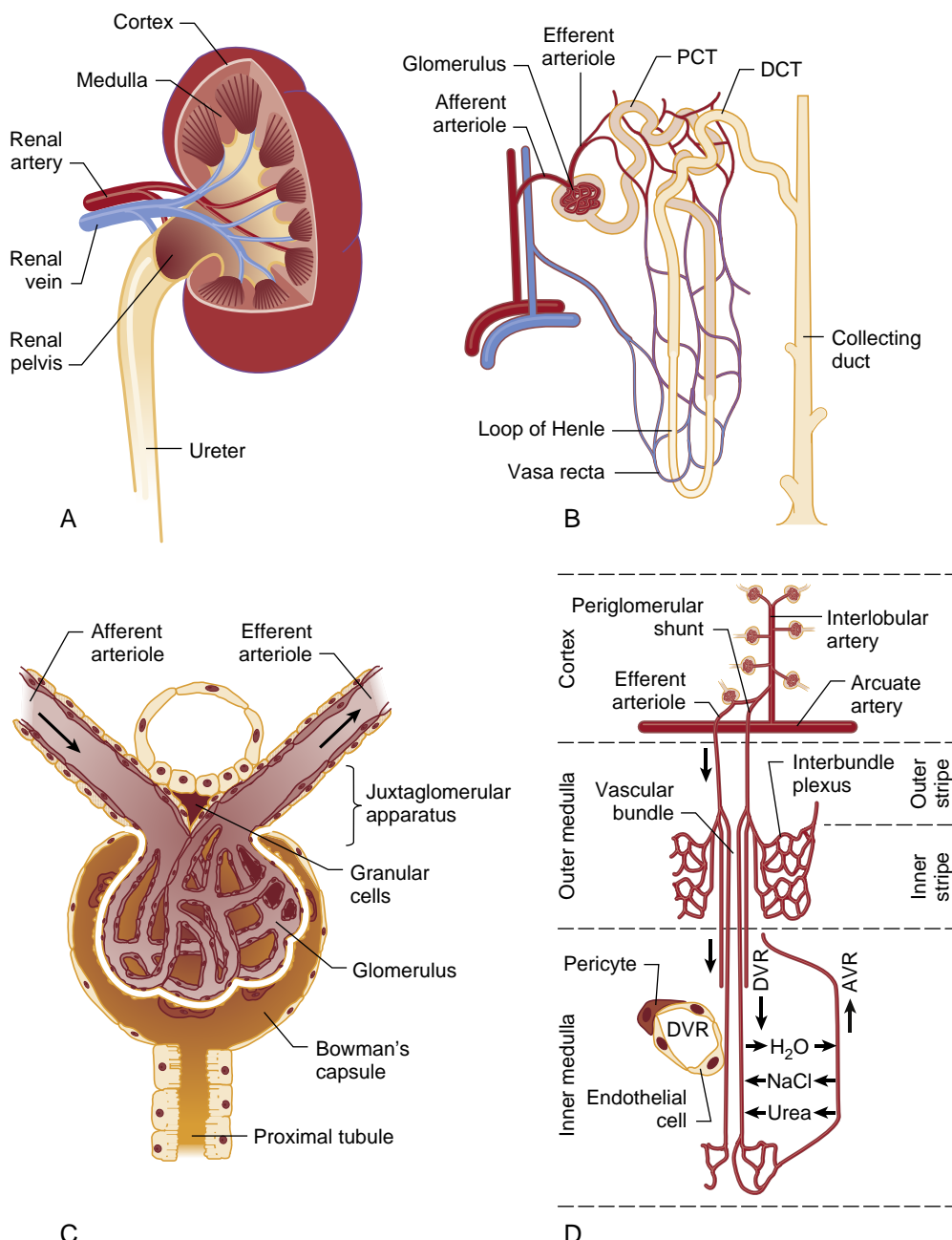


Fig. 42.2 (A) The internal structure of the kidney includes the vasculature, cortex and medulla regions, and urinary tract structures. (B) The functional unit of the kidney is the nephron. (C) The glomerulus is the site where plasma filtration occurs; approximately 20% of plasma entering the glomerulus will pass through the specialized capillary wall into the Bowman capsule and enter the tubule to be processed and to generate urine. (D) The vascular anatomy of the kidney is highly organized, and the medullary microcirculation is part of the mechanism that permits countercurrent exchange.⁴² AVR, Ascending vasa recta; DCT, distal convoluted tubule; DVR, descending vasa recta; NaCl, sodium chloride; PCT, proximal convoluted tubule. (A, From <http://www.niddk.nih.gov/consequences/kidney/>. Accessed February 17, 2008. B, From <http://cnx.org/content/m44809/1.8/>. Accessed February 24, 2014. C, From <http://www.cixip.com/index.php/page/content/id/422/>. Accessed June 26, 2014. D, From Pallone TL, Zhang Z, Rhinehart K. Physiology of the renal medullary microcirculation. *Am J Physiol Renal Physiol*. 2003;284:F253–F266. Used with permission.)

followed by a condition termed *prerenal azotemia* during which the kidney maximizes activities at the expense of the retention of nitrogenous end-products to preserve the internal environment through retention of solutes and water (Fig. 42.2). In studies of community-acquired AKI, the incidence of prerenal azotemia may be as frequent as 70%.²⁴ In contrast, in a classic study of hospital-acquired AKI, although hypoperfusion accounted for 42% of cases of AKI, only 41% of these cases of hypoperfusion were attributable to inadequate intravascular volume.²⁵

Although prerenal azotemia is ominous and typically accompanied by oliguria (<0.5 mL/kg/h), it is reversible. At a critical tilting point, as conditions go beyond the compensatory mechanisms that maintain renal perfusion, ischemia leads to irreversible renal cell necrosis or ATN.²⁶ This represents the pure form of ischemic AKI. Other forms of ATN are due to toxins, including medications (e.g., aminoglycosides, cisplatin), pigments (e.g., hemoglobin, myoglobin), and iodinated contrast dye. These forms of ATN do not involve the typical pattern of preceding prerenal azotemia with

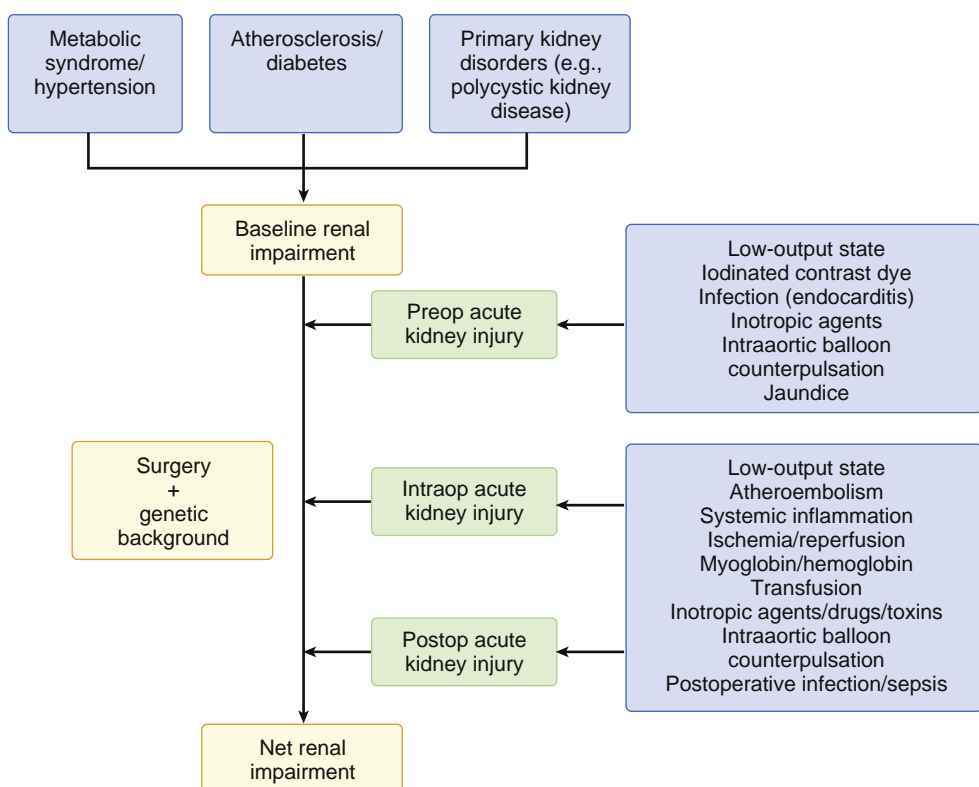


Fig. 42.3 Perioperative clinical risk factors associated with postoperative kidney injury.

associated oliguria, since the insult is sudden. Importantly, most cases of perioperative AKI are the result of numerous renal insults, rather than being attributable to one pure source (Fig. 42.3). In particular, patients with prerenal azotemia are likely at increased risk for toxic ATN.

Interruption of blood flow to the kidneys for more than 30 to 60 minutes results in ATN and irreversible cell damage. The kidneys receive 1000 to 1250 mL/min of blood or 3 to 5 mL/min/g of tissue for the average adult, and this amount far exceeds what is needed to provide the kidney's intrinsic oxygen requirement. Intracortical blood flow may not be evenly distributed.²⁷ Because the renal cortex contains most of the glomeruli and depends on oxidative metabolism for energy, ischemic hypoxia injures the renal cortical structures, particularly the pars recta of the proximal tubules. As ischemia persists, the supply of glucose and substrates continues to decrease; glycogen is consumed, and the medulla, which depends to a great extent on glycolysis for its energy sources, becomes more adversely affected. Early cell changes are reversible, such as the swelling of cell organelles, especially the mitochondria. As ischemia progresses, a lack of adenosine triphosphate interferes with the sodium pump mechanism, water and sodium accumulate in the endoplasmic reticulum of tubular cells, and the cells begin to swell. Onset of tubular damage usually occurs within 25 minutes of ischemia as the microvilli of the proximal tubular cell brush borders begin to change. Within an hour, they slough off into the tubular lumen, and membrane bullae protrude into the straight portion of the proximal tubule. After a few hours, intratubular pressure rises, and tubular fluid passively backflows. Within 24 hours, obstructing casts appear in the distal tubular lumen.

RENAL RESPONSE TO HYPOPERFUSION: AUTOREGULATION AND DISTRIBUTION OF CARDIAC OUTPUT TO THE KIDNEYS

A common intraoperative stress that puts patients at risk for AKI is hypoperfusion due to hypotension and/or hypovolemia. The fraction of cardiac output perfusing the kidneys depends on the ratio of renal vascular resistance to systemic vascular resistance.²⁶ In general, the response to renal hypoperfusion involves three major regulatory mechanisms that support renal function: (1) afferent arteriolar dilation increases the proportion of cardiac output that perfuses the kidney; (2) efferent arteriolar resistance increases the filtration fraction and preserves GFR; and (3) hormonal and neural responses improve renal perfusion by increasing intravascular volume, thereby indirectly increasing cardiac output.

The kidney produces vasodilator prostaglandins to counteract the effects of systemic vasoconstrictor hormones such as angiotensin II. In a state of low cardiac output when systemic blood pressure is preserved by the action of systemic vasopressors, RBF is not depressed because the effect of the vasopressors is blunted within the kidney. Studies using specific inhibitors of angiotensin II have shown that efferent arteriolar resistance largely results from the action of angiotensin II.²⁸ At low concentrations, norepinephrine has a vasoconstricting effect on efferent arterioles, indicating that the adrenergic system may also be important for maintaining the renal compensatory response.²⁹

Reductions in cardiac output are accompanied by the release of vasopressin and by increased activity of the

sympathetic nervous system and the renin-angiotensin-aldosterone system. These regulatory mechanisms to preserve RBF conserve salt and water. One study reported the normal response to hemorrhage in otherwise healthy patients, describing a 30% reduction in RBF with a decrease in mean perfusion pressure from 80 to 60 mm Hg.³⁰ Changes known to occur at the initiation of cardiopulmonary bypass (CPB) surgery include greater reduction in renal perfusion than systemic perfusion, loss of RBF autoregulation, and stress hormone and inflammatory responses known to be harmful to the kidney.^{31,32} These effects may explain why the duration of CPB surgery independently predicts postcardiac surgery renal impairment.

Detection of Acute Kidney Injury

LABORATORY TESTS OF SERUM AND URINE AS MARKERS OF RENAL FUNCTION

Standard serum and urine markers of renal function are discussed in [Chapter 17](#). It should be emphasized that at present, repeated serum creatinine determinations (relative or absolute changes), are most often used to identify AKI. An inherent limitation of almost all currently available tools to detect AKI is the obligate delay between the *onset* of AKI and the *diagnosis* of AKI. One striking difference between the management of AKI and acute myocardial infarction is the lack of early biomarkers for AKI in routine clinical practice to guide prompt recognition and intervention when tissue is threatened. Thus significant ongoing efforts are testing the value of early AKI biomarkers and of real-time measurement of GFR.

NOVEL (EARLY) BIOMARKERS OF ACUTE KIDNEY INJURY

Limited progress in the care for AKI has fueled an enormous interest in new early biomarkers.³³⁻³⁶ Although a few of the new tools represent attempts to find a filtration marker that is better than creatinine (e.g., cystatin C), most novel AKI biomarkers take advantage of one of the three early consequences of AKI: (1) tubular cell damage, (2) tubular cell dysfunction, and (3) adaptive stress response of the kidney. The hope is that such biomarkers will allow timely AKI identification, diagnosis (e.g., prerenal azotemia vs. ATN), and prognosis. Some of the more promising biomarkers are presented here ([Box 42.1](#)).

New Filtration-Based Markers of Renal Dysfunction

Of the most novel filtration-based markers of renal dysfunction, the most advanced is cystatin C, a member of the cystatin superfamily of cysteine-proteinase inhibitors that is produced by all nucleated cells at a constant rate. Cystatin C has been clinically available for longer than 15 years and can be rapidly determined. Similar to creatinine, cystatin C accumulates in the circulation with renal impairment and can be used as a marker of glomerular filtration. Serum cystatin C has theoretical advantages over creatinine, particularly as an indicator of mild chronic kidney disease and its sequelae.³⁸ Several GFR estimating equations have been

BOX 42.1 Early Biomarkers of Acute Kidney Injury

Filtration-Based Markers of Renal Dysfunction

Cystatin C
 β -trace protein
 β -2 microglobulin

Biomarkers Reflecting Renal Tubular Cell Damage (Tubular Enzymuria)

α -Glutathione S-transferase
 π -Glutathione S-transferase
 β -N-Acetyl- β -D-glucosaminidase
 γ -Glutamyl transpeptidase
Alkaline phosphatase
Sodium hydrogen exchanger isoform 3

Biomarkers Reflecting Renal Tubular Cell Dysfunction (Tubular Proteinuria)

α_1 -Microglobulin
 β_2 -Microglobulin
Albumin
Retinol-binding protein
Immunoglobulin G
Transferrin
Ceruloplasmin
Lambda and kappa light chains

Biomarkers Reflecting Renal Tubular Cell Response to Stress

Neutrophil gelatinase-associated lipocalin
Urinary interleukin-18
Kidney injury molecule-1
Liver fatty acid-binding protein
Insulin-like growth factor binding protein 7
Tissue inhibitor of metallo-proteinase 2

proposed, based on cystatin C alone or cystatin C and creatinine for use in chronic kidney disease.^{39,40} Although these are commonly used in clinical research studies, in general these are not in widespread clinical use at present.

Although cystatin C outperformed creatinine in detecting AKI after cardiac surgery in some small studies,⁴¹ this sensitivity has not consistently been the case. Indeed, a large multicenter prospective observational study of AKI after cardiac surgery suggested that serum cystatin C was less, not more, sensitive for the detection of AKI. This study, conducted by the Translational Research Investigating Biomarker Endpoints in Acute Kidney Injury (TRIBE-AKI) Consortium, prospectively enrolled more than 1200 adults undergoing cardiac surgery and has rapidly advanced the field of novel biomarkers in this context. Of note, the subset of patients who had AKI by cystatin C and creatinine had more frequent risk of dialysis and death than those who had AKI by creatinine alone.⁴² Conditions such as malignancy, human immunodeficiency viral infection, or corticosteroidal or thyroid hormone therapy are associated with increased serum levels of cystatin C without changes in renal function. Other novel markers of filtration include β -trace protein and β -2-microglobulin; these markers may be novel markers of mortality in the general population, compared with creatinine-based eGFR.⁴² However, the additional utility of these markers in estimating GFR above and beyond creatinine and cystatin C is unknown.

Biomarkers Reflecting Renal Tubular Cell Damage (Tubular Enzymuria)

Renal tubular cells contain enzymes that are highly specific to their location within the kidney and even tubule region. Under conditions of cellular stress, these enzymes are shed into the urine, making these potentially appealing markers of kidney dysfunction. These markers include α and π isomers of glutathione s-transferase (GST), which are cytosolic enzymes from proximal and distal tubular cells, respectively, and N-acetyl- β -D-glucosaminidase, a proximal tubule lysosomal enzyme. Of note, although enhanced urinary excretion of tubular enzymes can signal damaged tubular cells, it can also reflect an increased turnover of tubular cells or some other metabolic disturbance; thus the use of these markers may need to be applied with caution.

Biomarkers Reflecting Renal Tubular Cell Dysfunction (Tubular Proteinuria)

When small proteins are filtered by the glomerulus, binding and endocytic reuptake in the proximal tubule normally returns these substances to the body through a megalin-mediated transport system. So-called tubular proteinuria results from functional impairment of this process and the escape of small proteins into the urine. Endogenous low molecular weight proteins that are normally taken up in this way include β_2 - and α_1 -microglobulin, retinol-binding protein, lysozyme, ribonuclease, IgG, transferrin, ceruloplasmin, and lambda (λ) and kappa (κ) light chains. Appearance of any of these substances in the urine heralds abnormal proximal nephron function consistent with AKI. However, lysine and its analog (e.g., ϵ -aminocaproic acid, tranexamic acid) can cause a profound but reversible inhibition of low molecular weight protein reuptake⁴³ that is transient and apparently benign due to blocking renal-binding sites.^{44,45}

Biomarkers Reflecting Renal Tubular Cell Response to Stress

Examples of markers that assess the response of the kidney to stress include neutrophil gelatinase-associated lipocalin (NGAL), kidney injury molecule-1 (KIM-1), liver fatty acid-binding protein, and interleukin-18 (IL-18). These have each been extensively reviewed in detail in recent literature.³³⁻³⁶ Two markers of G1-cell cycle arrest have been shown to be upregulated in AKI, insulin-like growth factor-binding protein 7 (IGFBP-7) and tissue inhibitor of metalloproteinases-2 (TIMP-2).⁴⁶ A test that combines levels of IGFBP-7 and TIMP-2 has received U.S. Food and Drug Administration (FDA) clearance as a biomarker for the identification of patients at high risk of AKI.

NGAL is a protein with a critical role in iron scavenging. A transcriptome-wide interrogation for genes induced very early after renal ischemia identified NGAL as a protein generated by ischemic renal tubular cells.⁴⁷ Administration of exogenous NGAL in animal models attenuates renal injury.⁴⁸ Enthusiasm for NGAL as a biomarker of AKI was fueled by a study in pediatric patients who underwent cardiac surgery, suggesting that plasma and urinary NGAL could predict AKI before elevations in serum creatinine (Fig. 42.4).⁴⁹ Although increased NGAL levels are associated with adverse

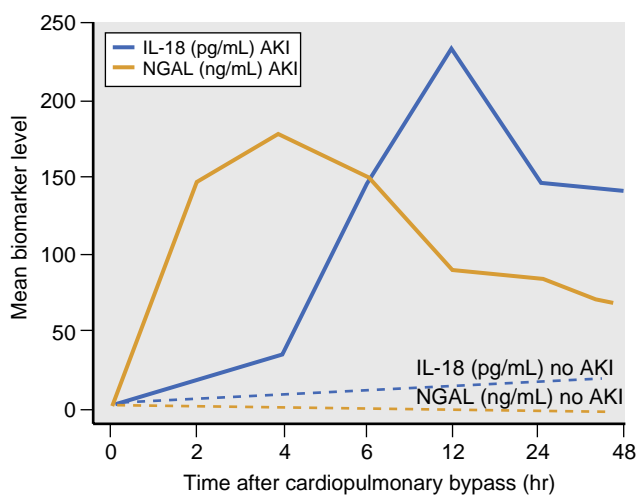


Fig. 42.4 Pattern of early biomarkers for urinary interleukin (IL)-18 and neutrophil gelatinase-associated lipocalin (NGAL) after cardiopulmonary bypass surgery in 55 patients with and without criteria for acute kidney injury (AKI) diagnosed 48 to 72 hours postoperatively (defined as a peak rise in serum creatinine concentration to >150% of baseline). (From Parikh CR, Mishra J, Thiessen-Philbrook H, et al. Urinary IL-18 is an early predictive biomarker of acute kidney injury after cardiac surgery. *Kidney Int*. 2006;70:199–203. Used with permission.)

outcomes,^{50,51} studies in the adult perioperative literature have not consistently shown NGAL to predict AKI before elevations in serum creatinine.

KIM-1 is a transmembrane protein expressed at low levels under normal conditions that is significantly upregulated in proximal renal tubular cells in response to ischemic or nephrotoxic AKI.⁵² In studies conducted by the Predictive Testing Safety Consortium, an academic-industrial partnership that has worked closely with the FDA to develop novel biomarkers of kidney injury for use in the preclinical setting (in particular, as markers of drug toxicity), KIM-1 outperformed a number of traditional markers of kidney injury in a variety of preclinical models.⁵³ More recently, assays have been developed to detect plasma KIM-1, which appears to correlate with urinary KIM-1 in the setting of both acute and chronic kidney disease.⁵⁴

Finally, cell cycle arrest has been implicated in models of AKI; more recently, two proteins that induce cell cycle arrest, IGFBP-7 and TIMP-2, have both been shown in a multicenter study to predict the development of KDIGO stage 2 and 3 AKI in critically ill patients. In a validation cohort, these biomarkers had an impressive area under the ROC curve of 0.80 for subsequent AKI.⁵⁵ There has been tremendous interest in the use of these biomarkers for perioperative risk stratification,^{56,57} with clinical trials enrolling patients based on elevated levels of IGFBP-7 and TIMP-2 (typically expressed as the product of these two biomarkers).⁵⁸

Preoperative Evaluation of Renal Function and Risk Stratification

The greater the magnitude and duration of the surgical insult and the number of acute and chronic risk factors, the greater the likelihood of perioperative renal compromise and hence the need for preoperative identification of

high-risk individuals.⁵⁸⁻⁶¹ Common risk factors for AKI include intravascular volume depletion, aminoglycoside use, radiocontrast dye exposure, use of NSAIDs, septic shock, and pigmenturia. ACE inhibitors and ARBs, respectively, may contribute to intraoperative hypotension and may exacerbate AKI in the setting of impaired hemodynamics (volume depletion, NSAID use). Patients with pre-existing renal insufficiency are clearly at increased risk for AKI and should be identified in the perioperative evaluation through measurement of serum creatinine and urinalysis (to evaluate for albuminuria/proteinuria). Chronic kidney disease affects more than 10% of the United States population. Common risk factors for chronic kidney disease include advanced age, diabetes, and hypertension. The potential value of understanding the genetic makeup of patients has yet to be fully explored and is likely to be important. For example, several genetic polymorphisms known to affect inflammation and vasoconstriction demonstrate strong associations with AKI after cardiac surgery,⁶² including the IL-6 572C and angiotensinogen 842C polymorphisms. In the future, identification of such polymorphisms may improve perioperative risk stratification.

Large multicenter epidemiologic studies have identified a relationship between markers of abnormal central aortic compliance, such as preoperative isolated systolic hypertension (>160 mm Hg) and wide pulse pressure hypertension (>40 mm Hg),^{63,64} and postoperative AKI and dialysis, in particular in patients undergoing cardiac surgery. Pulse pressure is an index of the effects of large artery stiffness and the rate of pressure on propagation and reflection within the arterial tree. Early return of reflected arterial waves during late systolic rather than early diastolic pressure (from increased propagation velocity in stiff vessels) increases systolic blood pressure (i.e., afterload) and decreases diastolic blood pressure (i.e., perfusion pressure). Perfusion pressure and the risk of perioperative renal dysfunction are linked by the preexisting capacity of the vasculature to compensate for low pressure as it determines flow. Those with a predisposition to low flow attributable to abnormal central aortic compliance (e.g., those with wide pulse pressure) may represent patients who require higher pressure to maintain adequate flow and minimize renal risk compared with normotensive patients.

In the context of specific surgery types (e.g., cardiac surgery), perioperative risk prediction tools have been developed. In general, these tend to effectively identify low-risk populations, but discrimination for higher risk patients is more modest. This may reflect the fact that intraoperative factors play a major role in the pathogenesis of AKI in a vulnerable patient. In addition, a number of these risk prediction tools focus on dialysis-requiring AKI, which is only the “tip of the iceberg” with regard to disease burden.

Perioperative Acute Kidney Injury: Mechanisms and Treatment

As described in Chapter 17, anesthesia and surgery influence normal renal function primarily through changes in GFR and urine flow that are attributable to changes in

blood pressure and cardiac output. Fluctuations in blood pressure have a major effect on RBF and glomerular filtration.^{19,31,65} Here, we will briefly discuss considerations for several anesthetic techniques, followed by several specific perioperative considerations.

REGIONAL ANESTHESIA

Regional anesthetics and the kidneys interact in a complex manner that varies according to the underlying cardiovascular, renal, fluid, and electrolyte status of the patient.⁶⁶ In general, epidural and spinal anesthesia reduce systemic and renal vascular sympathetic tone.⁶⁷ Spinal cord segments T4 through L1 contribute to the sympathetic innervation of the renal vasculature, which is mediated by sympathetic fibers from the celiac and renal plexus.^{67,68} Autonomic blockade above the fourth thoracic level also blocks cardioaccelerator sympathetic innervation to the heart. If neuraxial blockade reduces arterial blood pressure and cardiac output, then the RBF will be decreased with matching reductions in glomerular filtration and urine output.

Although controversial, intraoperative neuraxial blockade and postoperative epidural analgesia decrease rates of AKI. Rodgers and colleagues conducted a systematic review of 107 randomized clinical trials of intraoperative neuraxial blockade and demonstrated a 30% reduction in the odds of postoperative mortality.⁶⁹ This reduction was associated with decreases in the incidence of deep venous thrombosis, pulmonary embolism, transfusion, pneumonia, and respiratory depression, as well as renal failure, although the confidence limits for the renal failure estimates were very wide, in part due to the small number of cases of renal failure observed. Moraca and associates conducted a meta-analysis and reported on the association of thoracic epidural anesthesia with improved surgical outcomes attributable, in part, to a reduction of perioperative morbidity, including reductions in infection, ileus, blood loss, and AKI.⁷⁰ Other studies have examined the impact of epidural anesthesia during cardiac surgery and have suggested a benefit with regards to renal failure, although the confidence intervals were wide.⁷¹ Unfortunately, renal failure was not an outcome of several recently published meta-analyses focused on epidural anesthesia during cardiac surgery.^{72,73} Finally, with regard to postoperative analgesia, a recent Cochrane meta-analysis that focused on abdominal aortic surgery suggested better postoperative analgesia and a reduction in other complications including myocardial infarction and respiratory with epidural analgesia but no effect on AKI or postoperative mortality.⁷⁴

EFFECTS OF INHALED ANESTHETICS

From a historic perspective, older volatile inhaled anesthetics including methoxyflurane and enflurane (no longer clinically used) when used for prolonged periods lead to significant generation of inorganic fluoride⁷⁴⁻⁷⁷ and were associated with polyuric renal insufficiency. However, despite significant fluoride generation with sevoflurane and the generation of compound A (a metabolite associated with renal injury in experimental models), there is no reported association with AKI.⁷⁶ This may be due to the shorter

duration of elevated fluoride levels with sevoflurane and the site of metabolism (intrarenal metabolism of methoxyflurane is fourfold greater than that of sevoflurane).

EFFECTS OF INTRAVENOUS ANESTHETICS

Propofol and dexmedetomidine may have antiinflammatory effects that are renoprotective. Propofol increases production of bone morphogenetic protein-7 (BMP-7), which suppresses the tumor necrosis factor α -induced inflammatory cascade during sepsis-induced AKI,⁷⁸ as well as decreased injury during ischemia-reperfusion^{79,80} and unilateral ureteral obstruction.⁸¹ Similarly, in addition to altering RBF and sodium and water handling, the α_2 -adrenoreceptor agonists such as dexmedetomidine may stimulate BMP-7 production in the setting of sepsis and ischemia-reperfusion.⁸¹⁻⁸⁴ There has been significant interest in the use of dexmetomidine, in particular in the setting of cardiac surgery, with a recent meta-analysis suggesting a reduction in postoperative AKI with the use of dexmetomidine (OR 0.65; 95% confidence interval [CI], 0.45-0.92, $P = .02$).⁸⁵

SPECIFIC PERIOPERATIVE PERTURBATIONS AND RENAL FUNCTION

Several surgical interventions can affect RBF and, consequently, renal function. Whereas aortic cross-clamping above the renal arteries has obvious influence on glomerular filtration, infrarenal aortic cross-clamping and unclamping also have significant indirect effects on glomerular filtration and urine formation through changes in myocardial function, sympathetic activity, neuronal and hormonal activity (e.g., renin and angiotensin production), intravascular volume, and systemic vascular resistance.⁸⁶ During standard CPB surgery, cardiorenal relationships are approximately as expected; RBF decreases to 12% to 13% of total pump flow and is predicted by flow rate and perfusion pressure; however, only mean pressure correlates with urine output.^{31,87}

AKI after aortocoronary bypass surgery continues to be a devastating complication that is associated with multorgan dysfunction, increased resource utilization, high cost, and increased mortality. Annually, approximately 350,000 patients in the United States undergo coronary artery bypass graft (CABG) surgery. In a multicenter observational study focused on AKI after cardiac surgery, 5% of participants developed AKI as defined by the need for acute dialysis or a doubling of serum creatinine from baseline.⁸⁸ The mechanism of perioperative AKI during cardiac surgery is multifactorial. Significant risk factors for AKI include underlying patient characteristics, such as age older than 75 years, history of diabetes, hypertension, pulse pressure, ventricular dysfunction, myocardial infarction, renal disease, perioperative medication exposures (e.g., aprotinin, hetastarch), and surgical characteristics such as intraoperative use of multiple inotropes, insertion of intraaortic balloon pump, and extended duration of the CPB surgery.^{63,89-92}

The role of CPB surgery in postoperative AKI remains controversial. In their comprehensive guidelines on AKI, KDIGO reviewed the literature on postoperative AKI between patients undergoing off-pump and on-pump coronary revascularization surgeries and ultimately recommended

that “off-pump CABG surgery not be selected solely for the purpose of reducing perioperative AKI or need for renal replacement therapy (RRT).”¹⁴ However, patients with chronic kidney disease, who are at the highest risk for AKI after CPB surgery, have often been excluded from randomized clinical trials of off-pump versus on-pump CABG. For example, in the Randomized On/Off Bypass (ROOBY) trial, in which 2303 patients were randomized to off-pump versus on-pump CABG, approximately 7.5% of patients had a preoperative serum creatinine level ≥ 1.5 mg/dL.⁹³

A large observational study of 742,909 nonemergent, isolated CABG cases (including 158,561 off-pump cases) from the Society of Thoracic Surgery Database suggests a benefit to off-pump CABG in those with chronic kidney disease.⁹⁴ Propensity methods were used to adjust for patient- and center-level imbalances. The primary endpoint was death or dialysis. In those with lower estimated GFR (eGFR), the risk difference (i.e., number of patients with the outcome per 100 patients in those who underwent CPB minus the number with the outcome in those who underwent off-pump CABG) for the primary endpoint was 0.66 (95% CI, 0.45-0.87) for eGFR 30 to 59 mL/min/1.73 m² and 3.66 (95% CI, 2.14-5.18) for eGFR 15 to 29 mL/min/1.73 m². Both component endpoints followed the same trend. Highlighting the importance of chronic kidney disease as a risk factor for AKI after cardiac surgery, whereas slightly less than 1% of the overall cohort received dialysis after cardiac surgery, 2% of those with eGFR 30 to 59 mL/min/1.73 m² and 12.5% of those with eGFR 15 to 29 mL/min/1.73 m² required dialysis. The risk difference for dialysis alone in the same groups was 0.47 (95% CI, 0.31-0.62) and 2.79 (95% CI, 1.37-4.20) with on-pump versus off-pump CABG, respectively (Fig. 42.5). Along the same lines, a 2932 patient-substudy of the CORONARY clinical trial followed patients after off- or on-pump CABG surgery and demonstrated an interaction between preoperative chronic kidney disease (defined as eGFR < 60 mL/min/1.73 m²) and AKI (defined as a 50% increase in serum creatinine from prerandomization baseline within 30 days). In those with chronic kidney disease, 19.2% of those in the off-pump arm had AKI, compared to 30.2% in those who had on-pump surgery. However, there was no difference in sustained renal dysfunction, defined as a 20% or greater loss in eGFR at 1 year between the two study arms (17.1% vs. 15.3% in the off- vs. on-pump arms, $P = .23$). However, when those with AKI were compared to those who did not have AKI (regardless of treatment arm), AKI was independently associated with an increased risk of sustained renal dysfunction, with an adjusted odds ratio of 3.37 (95% CI, 2.65-4.28, $P < .001$).⁹⁵ This study highlights the fact that in the setting of chronic kidney disease, AKI is only one of many risk factors for chronic kidney disease progression.

In the setting of CABG, there has been tremendous interest in prevention of AKI, and numerous pharmacologic interventions have been tested. As stated previously, one of the major challenges for AKI prevention is that both pre- and intraoperative factors impact the risk of AKI, so it is difficult to identify *a priori* those who are at highest risk of AKI. Interventions of recent interest where there is not a sufficient evidence base for wide-spread adoption include remote ischemic preconditioning, atrial natriuretic peptide, and fenoldopam, among others.^{96,97}

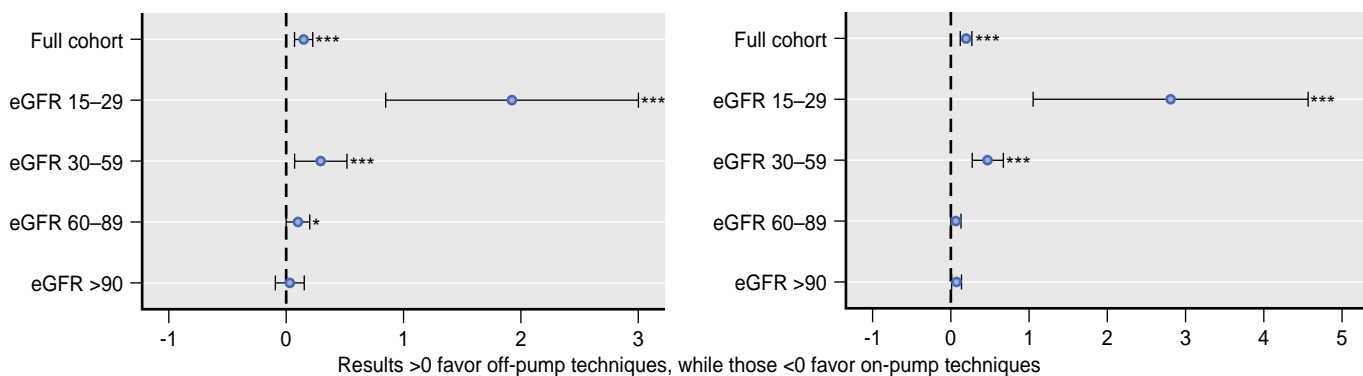


Fig. 42.5 Estimates of adverse outcomes associated with on-pump versus off-pump coronary artery bypass grafting by baseline estimated glomerular filtration rate (eGFR). For both mortality (left panel) and renal replacement therapy (right panel), off-pump CABG techniques appear to confer a benefit in those with lower eGFR. * $P < .05$, ** $P < .01$, *** $P < .001$. (Redrawn from Chawla LS, Zhao Y, Lough FC, et al. Off-pump versus on-pump coronary artery bypass grafting outcomes stratified by preoperative renal function. *J Am Soc Nephrol*. 2012;23:1389-1397.)

INTRAOPERATIVE MANAGEMENT FOR AKI PREVENTION: OXYGEN DELIVERY: BLOOD GAS, ACID-BASE BALANCE, AND HEMATOCRIT

Severe arterial hypoxemia to a partial arterial pressure of oxygen (PaO_2) value of less than 40 mm Hg is associated with decreased RBF and renal vasoconstriction.^{98,99} Inequalities in oxygen supply and demand are exaggerated and medullary hypoxia is extreme during CPB, effects that last well beyond separation from circulatory support in experimental models.¹⁰⁰

The effects of anemia on the kidney have been studied mostly in the context of CPB management. When crystalloid and colloid solutions are used to prime an extracorporeal circuit, the initiation of CPB surgery obligates an acute decrease of approximately 30% in oxygen-carrying capacity. Animal studies endorse moderate hemodilution (hematocrit 20% to 30%) as renoprotective during CPB surgery through a reduction of blood viscosity and improved regional blood flow.¹⁰¹ However, although hematocrit values less than 20% during CPB surgery are commonly accepted clinically (extreme hemodilution), very low hematocrit values are linked with adverse outcomes, including AKI.¹⁰²⁻¹⁰⁴ The Society of Thoracic Surgeons and the Society of Cardiovascular Anesthesiologists guidelines suggest that transfusion triggers should be lower during CPB surgery and that a transfusion trigger of 6 g/dL is reasonable, except in those at risk for end-organ ischemia, in whom a higher trigger may be reasonable.¹⁰⁵ More recently, the European Association for Cardio-Thoracic Surgery and the European Association of Cardiothoracic Anesthesia have developed comprehensive guidelines and suggest that a target hematocrit of 21% to 24% during cardiopulmonary bypass is reasonable.¹⁰⁶

The solution may not be as simple as transfusion because blood transfusions themselves have been linked to AKI. In a systematic review, Karkouti found 22 studies that examined the association between blood transfusions and AKI postcardiac surgery. An independent association between transfusions and AKI was found in 18 of the 22 studies.¹⁰⁷ The association of perioperative anemia with AKI was further examined in 14 studies, and 9 of the studies found an independent association of perioperative anemia with AKI. Proposed mechanisms for transfusion-associated AKI

include exacerbation of inflammation and oxidative stress, which occur during the CPB surgery.

There has been tremendous interest in the impact of the age of stored blood on the risk of AKI. Old blood may result in higher circulating levels of free hemoglobin and free iron, and there has been interest in the impact of the “storage lesion” on AKI. However, at present, data does not support the selective use of fresh blood in the perioperative setting to reduce the risk of AKI.¹⁰⁸⁻¹¹⁰

Perioperative Blood Pressure and Fluid Management

There has been significant interest in perioperative blood pressure targets and the impact on AKI. Several large observational cohort studies have suggested that even transient hypotension was associated with postoperative AKI.¹¹¹⁻¹¹⁵ One prospective randomized trial compared an individualized blood pressure management strategy targeted at maintaining systolic blood pressure within 10% of baseline versus a standard management strategy (treatment of systolic blood pressure <80 mm Hg or lower than 40% from baseline) and demonstrated a significant reduction in the primary composite endpoint (systemic inflammatory response and at least one organ dysfunction within 7 days). This modest sized clinical trial demonstrated a nonsignificant trend toward reduced postoperative AKI in the individualized blood pressure management arm.¹¹⁶ Thus blood pressure targets, in particular in patients with chronic kidney disease, need to take into consideration preoperative blood pressure.

Intravascular volume depletion, which commonly occurs in fasting patients undergoing surgery, is a risk factor for AKI. For example, the combination of diabetes mellitus and intravascular volume depletion increases the chance of developing AKI by 100-fold.¹¹⁷ The most practical preoperative methods to assess volume status are with preoperative patient history and physical examination and by assessing changes in arterial blood pressure in response to changing conditions and dynamic maneuvers. For example, an awake patient normally does not have significant orthostatic changes in arterial blood pressure unless an

autonomic or intravascular volume deficit exists. During anesthesia, a similarly dehydrated patient may demonstrate paradoxical arterial pulse changes with positive-pressure inspiration. Nonetheless, there has been tremendous interest in the use of intravascular monitoring techniques in the perioperative setting to reduce the risk of AKI.

The decision to use any monitor should depend on the patient's functional cardiac reserve status and the extent of the proposed surgical insult. Although maintaining adequate cardiac output is necessary for maintaining adequate RBF, adequate flow may still not occur. The use of intravascular volume monitoring techniques must include cautious identification of physiologic conditions that influence their validity as a reflection of preload in a particular patient. For example, monitoring central venous pressure to assess preload involves assumptions about normal left and right ventricular function; pulmonary vascular resistance; and mitral, pulmonary, and tricuspid valve function. Similarly, monitoring pulmonary artery pressure or pulmonary capillary wedge pressure assumes normal left ventricular compliance, mitral valve function, and normal airway pressure.

Direct measurements of left atrial pressure may offer insight into the kidney pressure-flow relationship because left atrial hypotension is a powerful stimulus for renal vasoconstriction. Despite equivalent reductions in cardiac output and arterial blood pressure, RBF decreases significantly more when left atrial pressure is decreased (e.g., hemorrhagic shock), compared with left atrial pressure when it is increased (e.g., cardiogenic shock).¹¹⁸ Left atrial pressure receptors modulate renal vasoconstriction through the release of ANP, a hormone secreted by the cardiac atria in response to intravascular volume expansion.¹¹⁹ ANP acts on the arterial and venous systems, the adrenal glands, and the kidneys to reduce intravascular volume and decrease blood pressure.¹²⁰ Within the kidney, the hormone increases hydraulic pressure in the glomerular capillaries through afferent arteriolar dilation and efferent arteriolar vasoconstriction. ANP reduces arterial blood pressure by relaxing smooth muscle and reducing sympathetic vascular stimulation and also inhibits renin and aldosterone secretion, causing renal vasodilation, natriuresis, and diuresis.

Despite the direct relationship of left atrial pressure and renal vasoconstriction, static monitors of intravascular volume status are gradually being replaced by echocardiographic and dynamic monitors of intravascular volume status. Intraoperatively, one of the most direct ways to monitor intravascular volume may be by direct assessment of the left ventricular end-diastolic area with transesophageal echocardiography. However, monitoring with invasive devices, such as pulmonary artery catheters, arterial cannulas, and transesophageal echocardiography, has not been demonstrated to reduce the incidence of AKI.

Guided fluid optimization has recently garnered significant interest as a step beyond traditional, somewhat unreliable guides to fluid administration (e.g., central venous pressure).^{121,122} The principle behind fluid optimization is to maximize tissue-oxygen delivery by achieving a maximum stroke volume. Intravascular fluid management is typically guided by the physiologic response to dynamic measures;

proposed measures include systolic pressure variation, pulse pressure variation, continuous cardiac output monitoring, and esophageal Doppler ultrasonography fluid boluses.¹²³ Some maneuvers to assess fluid responsiveness may be feasible in the critical care setting but not in the perioperative setting (e.g., passive leg raise).

Given the improved outcomes in patients who are critically ill with the acute respiratory distress syndrome and are managed with a restrictive fluid management strategy,¹²⁴ fluid restriction in the perioperative setting has gained attention. A meta-analysis of seven randomized clinical trials in the setting of intraabdominal surgery suggested a restrictive fluid strategy offered no benefit; however, there was also no evidence of harm, including AKI.¹²⁵ In some studies, excessive fluid restriction was associated with harm, including an increased risk of anastomotic breakdown and sepsis, and should clearly be avoided.¹²⁶ However, more recently, the RELIEF clinical trial randomized 3000 patients undergoing major abdominal surgery to a restrictive or liberal fluid strategy during surgery and up to 24 hours afterward; the restrictive fluid strategy was designed to provide a net even fluid balance.¹²⁷ There was no difference in the primary endpoint of disability-free survival at 1 year. However, the restrictive fluid strategy was associated with an increased rate of AKI (8.6% vs. 5.0%, $P < .001$) and surgical site infections (16.5% vs. 13.6%, unadjusted $P = .02$), though the comparison for surgical site infections was not considered significant after adjustment for multiple comparisons. Thus at present, fluid management strategies should avoid markedly positive fluid balance, but also need to be wary of underresuscitation.

There has been considerable interest in the use of balanced salt solutions instead of chloride-rich solutions to prevent AKI; the rationale is that chloride-rich solutions reduce renal perfusion in animal models.¹²⁸ Subsequently, a pre-post study of chloride-rich versus balanced salt solutions demonstrated a reduced incidence of stage 2 and 3 AKI during the balanced salt solution period.¹²⁹ Similarly, a propensity-matched study of patients undergoing major abdominal surgery suggested that patients who received balanced salt solutions had fewer postoperative complications, including postoperative dialysis.¹³⁰ However, a subsequent clinical trial, the SPLIT trial, suggested that there was no decrease in AKI with the use of Plasma-Lyte 148 in ICU patients.¹³¹ Of note, 72% of the trial population was enrolled after surgery, with 49% enrolled after cardiac surgery. More recently, the SALT-ED and SMART trials were pragmatic clinical trials that randomized patients to receive balanced salt solutions or normal saline in alternating months in the Emergency Department and Intensive Care Units, respectively, at a single clinical center.^{132,133} Both studies demonstrated a statistically significant reduction in the rate of major adverse kidney events at 30 days, a composite endpoint of death, dialysis, and persistent doubling of creatinine. In SMART, approximately 20% of subjects were admitted in the postoperative setting; there was no evidence of an interaction between treatment effect and type of ICU, but the study was underpowered to observe a difference within this subgroup.

Finally, are these solutions safe in patients who are prone to hyperkalemia? Because balanced salt solutions contain a physiologic amount of potassium, there has been concern

that the administration of balanced salt solutions might lead to hyperkalemia in patients with reduced renal function. However, in two randomized clinical trials of intraoperative fluid selection in end-stage kidney disease patients undergoing kidney transplantation, there was no increase in the incidence of hyperkalemia.¹³⁴ The median volume of intravenous solution administered in a trial that compared normal saline to an acetate based buffer was 2625 mL (IQR 2000-3001 mL);¹³⁵ in a trial comparing normal saline to lactated Ringers, mean fluid volumes were 6.1 ± 1.2 L and 5.6 ± 1.4 L, respectively.¹³⁶ Thus at reasonable doses, balanced salt solutions appear safe across a wide variety of patient populations and are associated with a decreased risk of AKI.

EXCESSIVE INTRAVASCULAR VOLUME AND THE ABDOMINAL COMPARTMENT SYNDROME

The abdominal compartment syndrome was first defined in 1985; since then, it has been progressively recognized as a common contributor to renal dysfunction in the setting of excessive intravascular volume.¹³⁷⁻¹³⁹ Not surprisingly, excessive intravascular volume and mechanical ventilation with high airway pressures are significant contributors to the abdominal compartment syndrome. Abdominal compartment syndrome is defined as a sustained increase in intraabdominal pressures to greater than 20 mm Hg that causes organ dysfunction; in contrast, intraabdominal hypertension is typically defined as intraabdominal pressures ≥ 12 mm Hg without organ dysfunction. This increase in intraabdominal pressure decreases abdominal perfusion pressure (which is mean arterial pressure – intraabdominal pressure), and results in a functional prerenal state attributable to reduced renal perfusion.

The intraabdominal pressure can easily be measured using an indwelling Foley catheter and the same pressure tubing setup used for arterial line blood pressure monitoring.¹⁴⁰ The Foley catheter is clamped distal to the instillation port, and up to 25 mL of saline is instilled into the bladder. The transducer should be zeroed at the midaxillary line, and the pressure should be measured at end-expiration approximately 30 to 60 seconds after fluid is instilled into the bladder to allow for detrusor muscle relaxation. Of note, intraabdominal pressure may be chronically elevated to as high as 12 mm Hg in the obese adult but is not associated with end-organ dysfunction in this context.¹⁴¹ Prompt recognition of the abdominal compartment syndrome and treatment via decompression in the appropriate clinical context is critical.

Nephrotoxins and Acute Kidney Injury

Recently, there has been significant controversy regarding the impact of iodinated contrast on AKI, with a number of observational studies suggesting that at a population level, iodinated contrast is not associated with an increased risk of AKI.^{142,143} However, iodinated contrast is associated with intense renal vasoconstriction and causes significant AKI in the vulnerable subject. There has been significant

interest in pharmacologic prevention of contrast-associated AKI. Clinical trials have demonstrated that pharmacologic interventions, including fenoldopam, n-acetyl-cysteine, and sodium bicarbonate, do not reduce the incidence of contrast-associated AKI.^{144,145} Volume depletion and concomitant exposure to other nephrotoxins are key, preventable risk factors for AKI.

Other nephrotoxins commonly encountered in the perioperative setting include aminoglycosides and NSAIDs. In addition, there has been increasing interest in antibiotic nephrotoxicity. Specifically, the combination of vancomycin and piperacillin-tazobactam has been associated with an increased rate of AKI.¹⁴⁶ When possible, avoiding combinations of nephrotoxins is likely beneficial for AKI prevention.¹⁴⁷

Renal Replacement Therapy

Despite best supportive care, at times, AKI progresses, and RRT is indicated. Conventional indications for dialysis include acidosis, electrolyte abnormalities (in particular, hyperkalemia), ingestions, volume overload, and uremia. There has been considerable interest in the optimal timing of dialysis initiation in critically ill and postoperative patients. A provocative, single-center study suggested that after cardiac surgery, there was significant benefit to initiation of dialysis for stage 2 AKI (doubling of sCr from baseline or urine output <0.5 mL/kg/h for 12 hours) versus waiting until stage 3 AKI (tripling of sCr from baseline, sCr ≥ 4 mg/dL with an acute rise of ≥ 0.5 mg/dL, or urine output <0.3 mL/kg/h for 24 hours).¹⁴⁸ Early RRT was associated with a lower incidence of death (39.3% vs. 54.7%, $P = .03$) and a greater rate of renal recovery at 90 days (53.6% vs. 38.7%, $P = 0.02$). It should be noted 90% of patients in the delayed arm received RRT, and the median difference in time to dialysis initiation was only 21 hours, so this is a remarkably large effect size that should be interpreted with caution. This study is in marked contrast to two large randomized clinical trials in critically ill patients suggesting that dialysis can be safely delayed in a number of patients.^{149,150} In these clinical trials, patients were randomized to receive dialysis when they met criteria for stage 3 AKI or to initiate dialysis only after prespecified electrolyte/metabolic criteria were met or after AKI exceeded a prespecified duration. There was no difference in mortality between the two treatment arms; in addition, a significant proportion of subjects in the delayed therapy arm recovered and never required dialysis (29% in the IDEAL-ICU trial). Additional clinical trials are ongoing to further test the hypothesis that in critically ill patients, dialysis can be safely delayed.¹⁵¹

There has also been considerable interest in dialysis modality and the impact on outcomes. At present, four modalities of dialysis are possible in the ICU. Peritoneal dialysis requires placement of a catheter in the intraabdominal space; this is typically performed laparoscopically, but can be inserted at the bedside if needed. Dextrose-containing fluids drive fluid and solute removal. Thus a significant risk of peritoneal dialysis is infection (e.g., peritonitis). Furthermore, this modality cannot be used in patients who have had recent intraabdominal surgery, so in general, its role is quite limited in the perioperative setting, with the exception

of patients who are maintained on this therapy for end-stage renal disease preoperatively. With regard to hemodialysis, modalities are typically divided into: intermittent hemodialysis (IHD), prolonged intermittent RRT (PIRRT)/ slow low efficiency dialysis (SLED), and continuous renal replacement therapies (CRRT). As the name implies, IHD is typically performed over a 3- to 4-hour period, 3 to 6 days/week. PIRRT/SLED is typically performed over 6 to 12 hours/day, 3 to 6 days/week; there is no standard dialysis machine for PIRRT/SLED so dialysis programs may use this therapy quite differently. CRRT is performed on a continuous, 24 hours/day basis.

With regard to modality and outcomes, it has been specifically hypothesized that intradialytic hypotension might prolong AKI and delay renal recovery. However, no randomized clinical trials have demonstrated clear benefit to continuous RRT with regards to mortality or renal recovery.¹⁵² Clinical trials have also examined the impact of dialysis dose and membrane on outcomes. These studies have established that there is a minimum dose of dialysis that should likely be measured and delivered,^{153,154} and that modern dialysis membranes are all relatively biocompatible and there is no benefit of one membrane over another.

To maintain circuit patency, anticoagulation is often needed. At present, the two most common forms of anticoagulation are low-dose heparin (100 to 500 units/h) and regional citrate. In both cases, the anticoagulant is infused prefilter to minimize systemic effects. Even though the goal of heparin anticoagulation is to not affect systemic coagulation parameters such as partial thromboplastin time, there is a small increase in bleeding risk.^{155,156} The goal of regional citrate anticoagulation is to reduce the ionized calcium concentration in the dialysis filter, since calcium is a required cofactor in the coagulation cascade. Thus citrate is infused prefilter and titrated to maintain a low postfilter ionized calcium. One of the challenges in the United States to the routine use of citrate anticoagulation is the lack of a citrate solution approved by the Food and Drug Administration for use with RRT; thus each center typically has developed its own protocol for titration and monitoring. That said, regional citrate anticoagulation is typically recommended in favor of other forms of anticoagulation.^{14,155,156}

Occasionally, RRT is indicated in the operating room, typically during prolonged cases with significant blood product transfusion (e.g., liver transplantation). Close coordination between the nephrologist and the anesthesiologist is needed.

Summary

In patients with or at risk for developing AKI, perioperative management continues to be challenging. Numerous factors contribute to the heterogeneous condition referred to as perioperative AKI, but insults collectively combine through ischemic and toxic mechanisms. Recent research efforts directed to the investigation of AKI will likely lead to rapid developments in the field of renal function monitoring. At present, serum creatinine continues to be the mainstay of most renal function monitoring strategies, along with urine output. Best supportive care for perioperative AKI includes preoperative risk stratification with quantitation of serum

creatinine and proteinuria/albuminuria for moderate-high risk surgeries, avoidance of hypotension and hypovolemia, along with judicious use of nephrotoxins. In the setting of severe AKI, support with RRT may be needed. At present, the timing of dialysis initiation is controversial, but early initiation does not appear to be associated with improved outcomes in critically ill patients.

Acknowledgment

The editors, publisher, and authors, Drs. Kathleen D. Liu, Daniel H. Burkhardt III, and Rupert M. Pearse, would like to thank Drs. Mark Stafford-Smith and Andrew Shaw for their contribution to this chapter in the prior edition of this work. It has served as the foundation for the current chapter.

 Complete references available online at expertconsult.com.

References

1. Thakar CV. *Adv Chronic Kidney Dis.* 2013;20(67).
2. Chaudery H, et al. *Anesth Analg.* 2018. <https://doi.org/10.1213/ANE.0000000000003923>.
3. O'Connor ME, et al. *Br J Surg.* 2017;104:868.
4. Zarbock A, et al. *Anesth Analg.* 2018;127:1236.
5. Smith Jr LH, et al. *Am J Med.* 1955;18:187.
6. Gaffney AM, Sladen RN. *Curr Opin Anaesthesiol.* 2015;28:50.
7. Hoste EAJ, Vandenberghe W. *Best Pract Res Clin Anaesthesiol.* 2017;31:299.
8. Fuhrman DY, Kellum JA. *Curr Opin Anaesthesiol.* 2017;30:60.
9. Hobson C, et al. *J Vasc Surg.* 2018;68:916.
10. Novis BK, et al. *Anesth Analg.* 1994;78(143).
11. Chertow GM, et al. *Am J Med.* 1998;104:343.
12. Bellomo R, et al. *Crit Care.* 2004;8:R204.
13. Mehta RL, et al. *Crit Care.* 2007;11:R31.
14. Group KDIGO KAKIW. *Kidney Int Suppl.* 2012;2(1).
15. Kellum JA, et al. *J Am Soc Nephrol.* 2015;26:2231.
16. Palevsky PM, et al. *Am J Kidney Dis.* 2013;61:649.
17. Quan S, et al. *Nephrol Dial Transplant.* 2016;31:2049.
18. Alpert RA, et al. *Surgery.* 1984;95:707.
19. Knos GB, et al. *J Clin Anesth.* 1989;1:181.
20. Mizota T, et al. *Br J Anaesth.* 2017;119:1127–1134.
21. Siddiqui NF, et al. *CMAJ.* 2012;184(1237).
22. Myers BD, Moran SM. *N Engl J Med.* 1986;314:97.
23. Myers BD, et al. *J Clin Invest.* 1984;73:329.
24. Kaufman J, et al. *Am J Kidney Dis.* 1991;17:191.
25. Hou SH, et al. *Am J Med.* 1983;74:243.
26. Badr KF, Ichikawa I. *N Engl J Med.* 1988;319:623.
27. Barger A, Herd J, In: Orlaff J, Berliner R, eds. *Handbook of Physiology.* Baltimore, MD: Williams and Wilkins; 1973.
28. Packer M, et al. *Circulation.* 1986;74:766.
29. Edwards RM. *Am J Physiol.* 1983;244:F526.
30. Stone AM, Stahl WM. *Am Surg.* 1970;17:825.
31. Andersson LG, et al. *Eur J Cardiothorac Surg.* 1994;8:597.
32. Laffey JG, et al. *Anesthesiology.* 2002;97:215.
33. McMahon G, Waikar S. *Am J Kidney Dis.* 2013;61:165.
34. Parikh CR, Mansouri SG. *J Am Soc Nephrol.* 2017;28:1677.
35. Waikar SS, Bonventre JV. *Nephron Clin Pract.* 2008;109:c192.
36. Chen L-X,C, Koyner JL. *Crit Care Clin.* 2015;31:633–648.
37. Shlipak MG, et al. *Am J Kidney Dis.* 2013;62:595–603.
38. Inker LA, et al. *N Engl J Med.* 2012;367:20.
39. Stevens LA, et al. *Am J Kidney Dis.* 2008;51:395.
40. Zhu J, et al. *Clin Chim Acta.* 2006;374:116.
41. Spahillari A, et al. *Am J Kidney Dis.* 2012;60:922.
42. Foster MC, et al. *Am J Kidney Dis.* 2013;62:42.
43. Mogensen CE, Solling. *Scand J Clin Lab Invest.* 1977;37:477.
44. Smith MS. *Anesthesiology.* 1999;90:928.
45. Stafford-Smith M. *Am J Kidney Dis.* 2011;57:960; author reply, p1.
46. Kashani K, et al. *Crit Care.* 2013;17:R25.

47. Mishra J, et al. *J Am Soc Nephrol*. 2003;14:2534.
48. Mishra J, et al. *J Am Soc Nephrol*. 2004;15:3073.
49. Mishra J, et al. *Lancet*. 2005;365:1231.
50. Haase-Fielitz A, et al. *Ann Clin Biochem*. 2014;51:335.
51. Haase M, et al. *J Am Coll Cardiol*. 2011;57:1752.
52. Ichimura T, et al. *Am J Physiol Renal Physiol*. 2004;286:F552.
53. Vaidya VS, et al. *Nat Biotechnol*. 2010;28:478.
54. Sabbisetti VS, et al. *J Am Soc Nephrol*. 2014;25(2177).
55. Bihorac A, et al. *Am J Respir Crit Care Med*. 2014;189:932.
56. Gunnerson KJ, et al. *J Trauma Acute Care Surg*. 2016;80:243.
57. Meersch M, et al. *PLoS One*. 2014;9:e93460. 3968141.
58. Meersch M, et al. *Intensive Care Med*. 2017;43:1151.
59. Wang Y, Bellomo R. *Nat Rev Nephrol*. 2017;13:697.
60. Wilson T, et al. *Nephrol Dial Transplant*. 2016;31:231.
61. Hobson C, et al. *Crit Care Clin*. 2017;33(379).
62. Stafford-Smith M, et al. *Am J Kidney Dis*. 2005;45:519.
63. Aronson S, et al. *Circulation*. 2007;115:733.
64. Chertow GM, et al. *Circulation*. 1997;95:878.
65. Everett GB, et al. *Anesth Analg*. 1973;52:470.
66. Mark JB, Steele SM. *Int Anesthesiol Clin*. 1989;27:31.
67. Kennedy Jr WF, et al. *Anesthesiology*. 1969;31:414.
68. Kennedy Jr WF, et al. *Acta Anaesthesiol Scand Suppl*. 1969;37:163.
69. Rodgers A, et al. *BMJ*. 2000;321:1493.
70. Moraca RJ, et al. *Ann Surg*. 2003;238:663.
71. Bignami E, et al. *J Cardiothorac Vasc Anesth*. 2010;24:586.
72. Landoni G, et al. *Br J Anaesth*. 2015;115:25.
73. Svircevic V, et al. *Cochrane Database Syst Rev*. 2013;6:CD006715.
74. Guay J, Kopp S. *Cochrane Database Syst Rev*. 2016;1:CD005059.
75. Cousins MJ, Mazze RI. *JAMA*. 1973;225:1611.
76. Mazze RI. *Anesthesiology*. 2006;105:843.
77. Mazze RI, et al. *Anesthesiology*. 1977;46:265.
78. Hsing CH, et al. *Nephrol Dial Transplant*. 2011;26:1162.
79. Yuzbasioglu MF, et al. *Renal Fail*. 2010;32(578).
80. Sanchez-Conde P, et al. *Anesth Analg*. 2008;106:371; table of contents.
81. Dikmen B, et al. *J Anesth*. 2010;24:73.
82. Hsing CH, et al. *Am J Physiol Renal Physiol*. 2012;303:F1443.
83. Sugita S, et al. *J Nippon Med Sch*. 2013;80:131.
84. Gu J, et al. *Crit Care*. 2011;15:R153.
85. Liu Y, et al. *BMC Anesthesiol*. 2018;18(7).
86. Gamulin Z, et al. *Anesthesiology*. 1984;61:394.
87. Szabo G, et al. *Injury*. 1977;9(146).
88. Parikh CR, et al. *J Am Soc Nephrol*. 2011;22(1748):3171945.
89. Rioux JP, et al. *Crit Care Med*. 2009;37:1293.
90. Myburgh JA, et al. *N Engl J Med*. 2012;367:1901.
91. Rosner MH, Okusa MD. *Clin J Am Soc Nephrol*. 2006;1(19).
92. Mangano DT, et al. *N Engl J Med*. 2006;354:353.
93. Shroyer AL, et al. *N Engl J Med*. 2009;361:1827.
94. Chawla LS, et al. *J Am Soc Nephrol*. 2012;23:1389.
95. Garg AX, et al. *JAMA*. 2014;311:2191.
96. Deferrari G, et al. *Nephrol Dial Transplant*. 2018;33:813.
97. Romagnoli S, et al. *Curr Opin Anaesthesiol*. 2017;30:92.
98. Kilburn KH, Dowell AR. *Arch Intern Med*. 1971;127:754.
99. Pelletier CL, Shepherd JT. *Am J Physiol*. 1975;228:331.
100. Stafford-Smith M, et al. *Am J Kidney Dis*. 2005;45:519.
101. Utley JR, et al. *Ann Thorac Surg*. 1981;31:121.
102. Karkouti K, et al. *J Thorac Cardiovasc Surg*. 2005;129:391.
103. Swaminathan M, et al. *Ann Thorac Surg*. 2003;76(784):92; discussion.
104. Mehta RH, et al. *Ann Thorac Surg*. 2013;96:133.
105. Ferraris VA, et al. *Ann Thorac Surg*. 2011;91:944.
106. Pagano D, et al. *Eur J Cardiothorac Surg*. 2018;53(79).
107. Karkouti K. *Br J Anaesth*. 2012;109(suppl 1):i29.
108. Hovaguimian F, Myles PS. *Anesthesiology*. 2016;125:46.
109. Curley GF. *Crit Care Med*. 2014;42:2611.
110. Mazer CD, et al. *N Engl J Med*. 2017;377:2133.
111. Walsh M, et al. *Anesthesiology*. 2013;119(507).
112. Sun LY, et al. *Anesthesiology*. 2015;123:515.
113. Salmasi V, et al. *Anesthesiology*. 2017;126:47.
114. Hallqvist L, et al. *Eur J Anaesthesiol*. 2018;35:273.
115. Vernooy LM, et al. *Br J Anaesth*. 2018;120:1080.
116. Futier E, et al. *JAMA*. 2017;318(1346).
117. Shusterman N, et al. *Am J Med*. 1987;83:65.
118. Gorfinkel HJ, et al. *Am J Physiol*. 1972;222:1260.
119. Kahl FR, et al. *Am J Physiol*. 1974;226:240.
120. Cogan MG. *Annu Rev Physiol*. 1990;52:699.
121. Bednarczyk JM, et al. *Crit Care Med*. 2017;45(1538).
122. Vincent JL, et al. *Crit Care*. 2015;19(224).
123. Busse L, et al. *Adv Chronic Kidney Dis*. 2013;20:21.
124. Wiedemann HP, et al. *N Engl J Med*. 2006;354:2564.
125. Boland MR, et al. *World J Surg*. 2013;37:1193.
126. Futier E, et al. *Arch Surg*. 2010;145:1193.
127. Myles PS, et al. *N Engl J Med*. 2018;378:2263.
128. Wilcox CS. *J Clin Invest*. 1983;71(726).
129. Yunos NM, et al. *Crit Care*. 2010;14:226.
130. Shaw AD, et al. *Ann Surg*. 2012;255:821.
131. Young P, et al. *JAMA*. 2015;314:1701.
132. Self WH, et al. *N Engl J Med*. 2018;378:819.
133. Semler MW, et al. *N Engl J Med*. 2018;378:829.
134. Wan S, et al. *Cochrane Database Syst Rev*. 2016;CD010741.
135. Potura E, et al. *Anesth Analg*. 2015;120(123).
136. O'Malley CM, et al. *Anesth Analg*. 2005;100(1518); table of contents.
137. Mohmand H, Goldfarb S. *J Am Soc Nephrol*. 2011;22:615.
138. Carr JA. *J Am Coll Surg*. 2013;216:135.
139. Rogers WK, Garcia L. *Chest*. 2018;153:238.
140. Malbrain ML, et al. *Intensive Care Med*. 2006;32:1722.
141. Lambert D, et al. *Obes Surg*. 2005;15:1225.
142. Wilhelm-Leen E, et al. *J Am Soc Nephrol*. 2017;28:653.
143. Luk L, et al. *Adv Chronic Kidney Dis*. 2017;24:169.
144. Weisbord SD, et al. *Clin J Am Soc Nephrol*. 2013;8:1618.
145. Weisbord SD, et al. *N Engl J Med*. 2018;378:603.
146. Luther MK, et al. *Crit Care Med*. 2018;46(12).
147. Goldstein SL, et al. *Kidney Int*. 2016;90:212.
148. Zarbock A, et al. *JAMA*. 2016;315:2190.
149. Gaudry S, et al. *N Engl J Med*. 2016;375:122.
150. Barbar SD, et al. *N Engl J Med*. 2018;379:1431.
151. Wald R, et al. *Kidney Int*. 2015;88:897.
152. Nash DM, et al. *J Crit Care*. 2017;41:138.
153. Palevsky PM, et al. *N Engl J Med*. 2008;359(7).
154. Bellomo R, et al. *N Engl J Med*. 2009;361:1627.
155. Oudemans-van Straaten HM. *Semin Thromb Hemost*. 2015;41:91.
156. Brandenburger T, et al. *Best Pract Res Clin Anaesthesiol*. 2017;31:387.

References

1. Thakar CV. Perioperative acute kidney injury. *Adv Chronic Kidney Dis.* 2013;20:67–75.
2. Chaudery H, MacDonald N, Ahmad T, et al. International Surgical Outcomes Study, G: acute kidney injury and risk of death after elective surgery: prospective analysis of data from an international cohort study. *Anesth Analg.* 2018.
3. O'Connor ME, Hewson RW, Kirwan CJ, Ackland GL, Pearse RM, Prowle JR. Acute kidney injury and mortality 1 year after major non-cardiac surgery. *Br J Surg.* 2017;104:868–876.
4. Zarbock A, Koyner JL, Hoste EAJ, Kellum JA. Update on perioperative acute kidney injury. *Anesth Analg.* 2018;127:1236–1245.
5. Smith Jr LH, Post RS, Teschan PE, et al. Post-traumatic renal insufficiency in military casualties. II. Management, use of an artificial kidney, prognosis. *Am J Med.* 1955;18:187–198.
6. Gaffney AM, Sladen RN. Acute kidney injury in cardiac surgery. *Curr Opin Anaesthesiol.* 2015;28:50–59.
7. Hoste EAJ, Vandenberghe W. Epidemiology of cardiac surgery-associated acute kidney injury. *Best Pract Res Clin Anaesthesiol.* 2017;31:299–303.
8. Fuhrman DY, Kellum JA. Epidemiology and pathophysiology of cardiac surgery-associated acute kidney injury. *Curr Opin Anaesthesiol.* 2017;30:60–65.
9. Hobson C, Lysak N, Huber M, Scali S, Bihorac A. Epidemiology, outcomes, and management of acute kidney injury in the vascular surgery patient. *J Vasc Surg.* 2018;68:916–928.
10. Novis BK, Roizen MF, Aronson S, Thisted RA. Association of pre-operative risk factors with postoperative acute renal failure. *Anesth Analg.* 1994;78:143–149.
11. Chertow GM, Burdick E, Honour M, Bonventre JV, Bates DW. Acute kidney injury, mortality, length of stay, and costs in hospitalized patients. *J Am Soc Nephrol.* 2005;16:3365–3370.
12. Bellomo R, Ronco C, Kellum J, Mehta R, Palevsky P. Acute renal failure - definition, outcome measures, animal models, fluid therapy and information technology needs: the Second International Consensus Conference of the Acute Dialysis Quality Initiative Group. *Crit Care.* 2004;8:R204–212.
13. Mehta RL, Kellum JA, Shah SV, et al. Acute kidney injury network: report of an initiative to improve outcomes in acute kidney injury. *Crit Care.* 2007;11:R31.
14. The KDIGO AKI Workgroup. KDIGO clinical practice guideline for acute kidney injury. *Kidney Int Suppl.* 2012;2:1–138.
15. Kellum JA, Sileanu FE, Murugan R, Lucko N, Shaw AD, Clermont G. Classifying AKI by urine output versus serum creatinine level. *J Am Soc Nephrol.* 2015;26:2231–2238.
16. Palevsky PM, Liu KD, Brophy PD, et al. KDOQI US commentary on the 2012 KDIGO clinical practice guideline for acute kidney injury. *Am J Kidney Dis.* 2013;61:649–672.
17. Quan S, Pannu N, Wilson T, et al. Prognostic implications of adding urine output to serum creatinine measurements for staging of acute kidney injury after major surgery: a cohort study. *Nephrol Dial Transplant.* 2016;31:2049–2056.
18. Alpert RA, Roizen MF, Hamilton WK, et al. Intraoperative urinary output does not predict postoperative renal function in patients undergoing abdominal aortic revascularization. *Surgery.* 1984;95:707–711.
19. Knos GB, Berry AJ, Isaacson JJ, Weitz FI. Intraoperative urinary output and postoperative blood urea nitrogen and creatinine levels in patients undergoing aortic reconstructive surgery. *J Clin Anesth.* 1989;1:181–185.
20. Mizota T, Yamamoto Y, Hamada M, Matsukawa S, Shimizu S, Kai S. Intraoperative oliguria predicts acute kidney injury after major abdominal surgery. *Br J Anaesth.* 2017;119:1127–1134.
21. Siddiqui NF, Coca SG, Devereaux PJ, et al. Secular trends in acute dialysis after elective major surgery--1995 to 2009. *CMAJ.* 2012;184:1237–1245. 3414596.
22. Myers BD, Miller DC, Mehigan JT, et al. Nature of the renal injury following total renal ischemia in man. *J Clin Invest.* 1984;73:329–341. 425022.
23. Myers BD, Moran SM. Hemodynamically mediated acute renal failure. *N Engl J Med.* 1986;314:97–105.
24. Kaufman J, Dhakal M, Patel B, Hamburger R. Community-acquired acute renal failure. *Am J Kidney Dis.* 1991;17:191–198.
25. Hou SH, Bushinsky DA, Wish JB, Cohen JJ, Harrington JT. Hospital-acquired renal insufficiency: a prospective study. *Am J Med.* 1983;74:243–248.
26. Badr KF, Ichikawa I. Prerenal failure: a deleterious shift from renal compensation to decompensation. *N Engl J Med.* 1988;319:623–629.
27. Barger A, Herd J. Renal vascular anatomy and distribution of blood flow. In: Orlaff J, Berliner R, eds. *Handbook of Physiology.* Baltimore, MD: Williams and Wilkins; 1973.
28. Packer M, Lee WH, Kessler PD. Preservation of glomerular filtration rate in human heart failure by activation of the renin-angiotensin system. *Circulation.* 1986;74:766–774.
29. Edwards RM. Segmental effects of norepinephrine and angiotensin II on isolated renal microvessels. *Am J Physiol.* 1983;244:F526–534.
30. Stone AM, Stahl WM. Renal effects of hemorrhage in normal man. *Annals of Surgery.* 1970;172:825–836.
31. Andersson LG, Bratteby LE, Ekroth R, et al. Renal function during cardiopulmonary bypass: influence of pump flow and systemic blood pressure. *Eur J Cardiothorac Surg.* 1994;8:597–602.
32. Laffey JG, Boylan JF, Cheng DC. The systemic inflammatory response to cardiac surgery: implications for the anesthesiologist. *Anesthesiology.* 2002;97:215–252.
33. McMahon G, Waikar S. Biomarkers in nephrology: core curriculum 2013. *Am J Kidney Dis.* 2013;61:165–178.
34. Parikh CR, Mansour SG. Perspective on clinical application of biomarkers in AKI. *J Am Soc Nephrol.* 2017;28:1677–1685.
35. Waikar SS, Bonventre JV. Biomarkers for the diagnosis of acute kidney injury. *Nephron Clin Pract.* 2008;109:c192–197. 2713682.
36. Chen L-X, Koyner JL. Biomarkers in acute kidney injury. *Crit Care Clin.* 2015;31:633–648.
37. Shlipak MG, Mattes MD, Peralta CA. Update on cystatin C: incorporation into clinical practice. *Am J Kidney Dis.* 2013;62:595–603.
38. Inker LA, Schmid CH, Tighiouart H, et al. Estimating glomerular filtration rate from serum creatinine and cystatin C. *N Engl J Med.* 2012;367:20–29.
39. Stevens LA, Coresh J, Schmid CH, et al. Estimating GFR using serum cystatin C alone and in combination with serum creatinine: a pooled analysis of 3,418 individuals with CKD. *Am J Kidney Dis.* 2008;51:395–406. 2390827.
40. Zhu J, Yin R, Wu H, et al. Cystatin C as a reliable marker of renal function following heart valve replacement surgery with cardiopulmonary bypass. *Clin Chim Acta.* 2006;374:116–121.
41. Spahillari A, Parikh CR, Sint K, et al. Serum cystatin C- versus creatinine-based definitions of acute kidney injury following cardiac surgery: a prospective cohort study. *Am J Kidney Dis.* 2012;60:922–929. 3496012.
42. Foster MC, Inker LA, Levey AS, et al. Novel filtration markers as predictors of all-cause and cardiovascular mortality in US adults. *Am J Kidney Dis.* 2013;62:42–51.
43. Mogensen CE, Solling. Studies on renal tubular protein reabsorption: partial and near complete inhibition by certain amino acids. *Scand J Clin Lab Invest.* 1977;37:477–486.
44. Smith MS. Antifibrinolytic agents make alpha1- and beta2-microglobulinuria poor markers of postcardiac surgery renal dysfunction. *Anesthesiology.* 1999;90:928–929.
45. Stafford-Smith M. Antifibrinolytic use during cardiac and hepatic surgery makes tubular proteinuria-based early biomarkers poor tools to diagnose perioperative acute kidney injury. *Am J Kidney Dis.* 2011;57(960):960–961; author reply.
46. Kashani K, Al-Khafaji A, Ardiles T, et al. Discovery and validation of cell cycle arrest biomarkers in human acute kidney injury. *Crit Care.* 2013;17:R25.
47. Mishra J, Ma Q, Prada A, et al. Identification of neutrophil gelatinase-associated lipocalin as a novel early urinary biomarker for ischemic renal injury. *J Am Soc Nephrol.* 2003;14:2534–2543.
48. Mishra J, Mori K, Ma Q, et al. Amelioration of ischemic acute renal injury by neutrophil gelatinase-associated lipocalin. *J Am Soc Nephrol.* 2004;15:3073–3082.
49. Mishra J, Dent C, Tarabishi R, et al. Neutrophil gelatinase-associated lipocalin (NGAL) as a biomarker for acute renal injury after cardiac surgery. *Lancet.* 2005;365:1231–1238.
50. Haase-Fielitz A, Haase M, Devarajan P. Neutrophil gelatinase-associated lipocalin as a biomarker of acute kidney injury: a critical evaluation of current status. *Ann Clin Biochem.* 2014;51:335–351.
51. Haase M, Devarajan P, Haase-Fielitz A, et al. The outcome of neutrophil gelatinase-associated lipocalin-positive subclinical acute kidney